CHALMERS

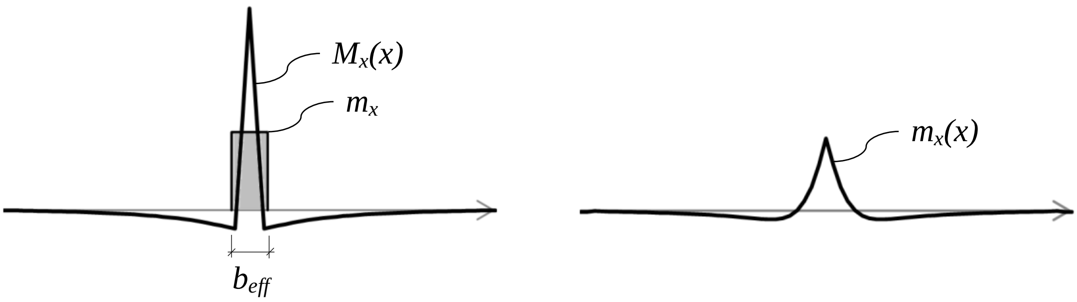

FE-modelling of a typical trough bridge with regard to distribution of load effects

Master of Science Thesis in the Master’s Programme Structural Engineering and Building Technology

JENNY AXELSSON
ANNA WERNER

Department of Civil and Environmental Engineering
Division of Structural Engineering
Concrete Structures
CHALMERS UNIVERSITY OF TECHNOLOGY
Göteborg, Sweden 2013
Master’s Thesis 2013:92

MASTER’S THESIS 2013:92

FE-modelling of a typical trough bridge with regard to distribution of load effects

Master of Science Thesis in the Master’s Programme Structural Engineering and Building Technology

JENNY AXELSSON

ANNA WERNER

Department of Civil and Environmental Engineering
Division of Structural Engineering
Concrete Structures
CHALMERS UNIVERSITY OF TECHNOLOGY

Göteborg, Sweden 2013

FE-modelling of a typical trough bridge with regard to distribution of load effects

Master of Science Thesis in the Master's Programme Structural Engineering and Building Technology

JENNY AXELSSON
ANNA WERNER

Examensarbete / Institutionen för bygg- och miljöteknik,
Chalmers tekniska högskola 2013:92

Department of Civil and Environmental Engineering
Division of Structural Engineering
Concrete Structures
Chalmers University of Technology
SE-412 96 Göteborg
Sweden
Telephone: + 46 (0)31-772 1000

Cover:
Bending moment distributions in the beam grillage model (to the left) and the combined model (to the right). Distribution of peak values in the beam grillage model over an effective width.

Chalmers Reproservice
Göteborg, Sweden 2013

FE-modelling of a typical trough bridge with regard to distribution of load effects

Master of Science Thesis in the Master's Programme Structural Engineering and Building Technology

JENNY AXELSSON
ANNA WERNER
Department of Civil and Environmental Engineering
Division of Structural Engineering
Concrete Structures
Chalmers University of Technology

ABSTRACT

Until recently, simplified 2D-models have been used in design and analysis of concrete trough bridges. Today structural analysis is often performed in three dimensions and this project investigated if and how the transverse and longitudinal responses can be coupled in one simplified linear elastic 3D-model. For that purpose, two different FE-models of a two span trough bridge were created; a beam grillage model and a combined beam-shell model, where the latter was considered as reference model.

The sectional forces of a model subjected to a modified load application that accounts for distribution of load effects within rails, sleepers and ballast was compared to that of a model subjected to the trivial concentrated load. The results indicate that it is necessary to use the modified load application in order to achieve coupling, as the concentrated load cannot be used in design of the slab.

While transverse distribution of load effects occurs naturally in the slab of the combined model, the beam grillage model needed to be modified to account for this distribution. The sectional forces in the slab were thus distributed over effective widths recommended in codes. It was shown that the effective widths differ significantly from the transverse distributions of the combined model, resulting in different maximum unit sectional forces. When influence line values computed from one load are superimposed for several loads the effective widths need to be decreased as the distributions of adjacent loads may overlap. In addition, the transverse distributions in the combined model were significantly smaller near the mid support section which cannot be accounted for when applying effective widths onto the beam grillage model output.

The end walls were modelled either with shell elements or beam elements concurrent with the model concept. It was noted that the element type of the slab to a large extent affects the structural response of the end walls. The torsional moment distributions of the girders when including the end walls in the models were compared to that of a model where the end walls were instead simplified into prescribed boundary conditions at end supports. In both the beam grillage and combined models, the differences in all section between the mid support and mid-span sections were negligible while considerable differences could be found near end wall sections. It was also found that the supports influence the torsional moment distribution locally both when supports are pinned-pinned and pinned-roller in the transverse direction of the bridge.

Key words: FEM, trough bridge, distribution of load effects, effective width, end walls, torsional resistance, beam elements, shell elements

FE-modellering av en typisk trågbalkbro med avseende på fördelning av lasteffekter

Examensarbete inom mastersprogrammet Structural Engineering and Building Technology
JENNY AXELSSON
ANNA WERNER
Institutionen för bygg- och miljöteknik
Avdelningen för konstruktionsteknik
Betongbyggnad
Chalmers tekniska högskola

SAMMANFATTNING

Förenklade 2D-modeller har tidigare använts vid utformning och analys av trågbalkbroar av betong. Idag utförs ofta strukturanalys i tre dimensioner och detta projekt undersökte om och hur tvärgående och längsgående respons kan kopplas i en förenklad linjär-elastisk 3D-modell. Två olika FE-modeller av en trågbalkbro i två spann togs därför fram; en balkrostmodell och en kombinerad balk-skalmodell, där den senare ansågs vara referensmodell.

Snittkrafter i en modell belastad med en modifierad last, motsvarande fördelningen av lasteffekter inom räler, sliprar och ballast, jämfördes med de som uppstod i en modell med en koncentrerad last. Resultaten visar att det är nödvändigt att använda den modifierade lasten för att uppnå koppling eftersom den koncentrerade lasten inte kan användas för dimensionering av plattan.

Fördelning av lasteffekter i tvärled sker automatiskt i plattan i den kombinerade modellen men balkrostmodellen behövde modifieras för att erhålla en liknande fördelning. Snittkrafterna i plattan fördelades därför över medverkande bredder från normer. Det visade sig att dessa medverkande bredder skilde sig avsevärt från motsvarande utbredning i referensmodellen, vilket resulterade i olika maximala snittkrafter. Vid superponering av värden i influenslinjer beräknade utifrån en last behöver de medverkande bredderna reduceras eftersom fördelningar från näraliggande laster kan sammanfalla. Spridningen av lasteffekter i tvärled var dessutom betydligt mindre vid mittstöd i referensmodellen, vilket inte kan beaktas vid tillämpning av en medverkande bredd på balkrostmodellens resultat.

Ändskärmarna modellerades med skal- eller balkelement i enlighet med modellernas uppbyggnad. Det noterades att elementtypen i plattan hade stor påverkan på verkningssättet i ändskärmarna. Vridmomentsfördelningen i balkarna jämfördes mellan en modell där ändskärmar inkluderades och en modell där ändskärmarna istället förenklades till randvillkor vid ändstöd. I både balkrost- och den kombinerade modellen påvisades försumbara skillnader i snitt mellan mittstöd och fältmitt medan skillnaderna var avsevärda i snitt nära ändskärmarna. Det konstaterades också att stöden påverkar vridmomentsfördelningen lokalt, både när de utfördes med fasta lager i brons tvärriktning och när brons ena sida var upplåst för förskjutning i detta led.

Nyckelord: FEM, trågbalkbro, fördelning av lasteffekter, medverkande bredd, ändskärmar, vridmotstånd, balkelement, skalelement

Contents

Preface

In this master's thesis project two FE-models of a typical trough bridge have been studied with the intent to couple the transversal and longitudinal structural response. The project was carried out at REINERTSEN between January 2013 and June 2013 and is a continuation of a project from 2012. The previous project evaluated different element types and boundary conditions with regard to the longitudinal response of a trough bridge.

During the project we have obtained supervision by Ginko Georgiev at REINERTSEN on a weekly basis and continuous meetings with Björn Engström at Chalmers. Björn was also the examiner of the project. We would like to thank both our supervisors for their highly appreciated support and feedback.

An equal ambition level and a shared curiosity have facilitated our working process and made us investigate several aspects further. Modelling, analyses and report writing have been evenly distributed between the two of us.

Göteborg, June 2013

Jenny Axelsson & Anna Werner

Notations

Roman upper case letters

E	Modulus of elasticity
F	Nodal force
F_j	Nodal force in j-direction
H	Height
L	Length
M	Bending moment
M_i	Bending moment in node i
M_j	Nodal moment around j-axis
M_T	Concentrated applied torsional moment
N	Normal force
Q	Concentrated applied load
T	Torsional moment
V	Shear force
V_i	Shear force in node i

Roman lower case letters

b_{eff}	Effective width
b	Width
c	Spacing
d	Minimum effective height of slab
h	Thickness
k_θ	Rotational stiffness
m	Unit bending moment
m_T	Distributed applied torsional moment
q	Distributed applied load
r	r-coordinate
s	s-coordinate
t	t-coordinate
u	Displacement in x-direction
v	Unit shear force
w	Displacement in z-direction

x	x-coordinate
y	y-coordinate
z	z-coordinate

Greek lower case letters

γ	Rotation of beam section due to shear
θ	Rotation around i-axis
ν	Poisson's ratio
τ	Shear stress
φ	Total rotation of beam section

1 Introduction

1.1 Background

Finite element analysis is an approximate numerical method that can be used to determine the structural response of various structures. The extent of the FE-model and what type of elements is used affect the accuracy and complexity of the analysis.

Ideally, analysis should be carried out in three dimensions using non-linear material response and solid elements. However, both non-linear analysis and the use of solid elements demand much time and resources and are not rational in practice. The common procedure is therefore to design on the basis of linear elastic analysis. It is not possible to simulate the response of the structure during loading using linear elastic analysis, but the sectional forces are assumed to reach the calculated distribution in the ultimate limit state. In design in general, simplifications are necessary in order to obtain a reasonable work effort, but the response of the model must not deviate too much from reality.

The subject of this Master's project is a concrete trough bridge, which is a common type of railway bridge. The trough cross-section can be divided into a slab and two main girders. The slab mainly distributes the load in the transverse direction to the main girders that thereafter distributes the load to the supports. The track is placed upon sleepers and ballast between the girders, which results in eccentric loading of and hence torsion in the girders. Commonly, design of transversal and longitudinal members is separated, using a combination of the maximum values from the two cases. As a result this method leads to conservative reinforcement amounts with regard to sectional forces.

Until recently, simplified 2D models have been used in design of concrete trough bridges but today the FE-modelling is often performed in three dimensions in order to capture a more accurate linear elastic response of the structure. This offers the possibility to increase the accuracy regarding load application and boundary conditions and to establish a coupling between the components of the trough cross-section. When coupling exists, it is also possible to obtain a more accurate linear elastic torsional moment distribution and hence more economic structures can be designed.

FE-modelling is also used in assessment of existing structures, where both environmental and economic savings can be made by reducing the conservative sectional forces to realistic values and thereby enabling a longer lifetime of bridges.

Some of the issues regarding 3D-modelling of trough bridges were treated in a previous Master's project (Lundin & Magnander, 2012). In those analyses, the train loading was simplified into one concentrated load applied directly onto the concrete slab. In reality, the effect of the load applied on the rails will be distributed within the sleepers and ballast and bending moment and shear force distributions transverse to the load-carrying direction will occur in the slab. The use of a more distributed load is expected to even out peaks in the distribution of sectional forces, leading to decreased design values.

In FE-modelling, a number of different element types can be used to represent the behaviour of the model. Available element types and the amount of post-processing required to obtain sectional forces depend on the software. In the previous Master's project, the most appropriate combination of beam and/or shell elements to represent the different components of the cross-section was investigated. It was found that a combined model, where the slab and the girders consist of shell elements and beam elements respectively, is acceptable as a reference model but that shell elements require extensive post-processing. Another investigated model was the beam grillage model, where the slab is instead represented by parallel transversal beams. This model demands less work effort but the transversal beams are limited to distribution of load effects in one direction only.

1.2 Aim

This project aimed to investigate if and how the transverse and longitudinal responses of a trough bridge can be coupled in one linear elastic 3D-model in order to obtain a more accurate linear elastic response. It was also studied if the output of a beam grillage model can be adjusted to simulate the behaviour of a combined beam-shell model. The following questions were identified:

- How should the distribution of load effects within rails, sleepers and ballast be taken into account in a combined model and a beam grillage model respectively? Can a more accurate load application be motivated by a significant reduction of sectional forces in relation to modelling with a simplified load?
- How should the transverse distributions of bending moment and shear force in the slab be considered in the beam grillage model?
- How is torsion resisted in supports and end walls and how should these be modelled in order to obtain a realistic linear elastic response with regard to torsion?

1.3 Limitations

Analyses should be executed assuming linear elastic response, uncracked sections (state I) and constant stiffness during loading. The influence of varying reinforcement amount along the bridge should be neglected as the reinforcement has little contribution to the stiffness in state I.

The geometry of the cross-section and the length of the spans should be kept constant during analyses as this study mainly focused on the comparison between different methods of FE modelling.

Loading should be limited to the variable load of a train. Permanent loads, such as the self-weight from the bridge itself and the ballast, sleepers and rails should be neglected. Also, the walkway extension at the outer side of the girders should be neglected both in the cross-section geometry and with regard to load. All neglected loads are uniformly distributed along the bridge and the responses of these loads in both models can therefore be assumed to be equal. Any positive influence from the ballast on the torsion of the girders should also be omitted to simplify the model.

The modelling techniques and comparisons are primarily valid for the studied FE-software.

1.4 Method

The composition of trough bridges and possible support conditions were investigated through interviews with a bridge engineer at REINERTSEN and by studying regulations in codes such as Broprojektering (Banverket, 2007), TRVK Bro 11 (Trafikverket, 2011) and BVS 583:11 (Trafikverket, 2012).

Requirements regarding distribution of load effects within railway components were checked in the codes mentioned above as well as Eurocode 1 (CEN, 2003) and Eurocode 2 (CEN, 2005). The distribution was chosen according to Eurocode 1, which provided the most conservative result of the studied codes. Based on the distribution within rails, sleepers and ballast; the area of the slab subjected to the distributed load from one wheel axle could be computed.

Two different finite element models of a typical trough bridge were created; a combined beam-shell model and a beam grillage model. The main difference between the models is the constitution of the slab, which consists of either shell elements or transversal beam elements. A literature study on structural finite elements was performed to obtain an understanding of how to make appropriate choices in modelling based on the theories the elements are formulated from.

The distribution of load effects in the slab was a key feature in establishing a coupling between the longitudinal and transverse response of the structure. While in-plane distribution of load effects occurs naturally in the slab of the combined model, the beam grillage model needed to be modified to account for distribution in the longitudinal direction of the bridge.

The sectional response of models subjected to a distributed load was compared to that of models subjected to a concentrated centrically placed load in order to study how much can be gained by modelling a more realistic load application.

The output data of the slab in the beam grillage model was adjusted by distributing sectional forces over a certain effective width, which was calculated according to current regulations. These unit sectional forces were thereafter compared to the reference model in order to establish if the adjustment resulted in conservative and reasonable results.

Sectional force diagrams were produced for both models to verify that the linear elastic response was consistent between the models. Furthermore, influence lines were created for both models in order to study the response of the bridge when subjected to a moving load. It was investigated if influence lines created considering transverse distribution from one wheel axle can be superimposed and used to determine the sectional response of the bridge when loaded with several wheel axles. Sectional forces for a typical train load combination of four wheel axles were found by superposition of influence lines and compared to those found in a model subjected to the loads from four wheel axles.

Torsion theory was studied in literature to provide an understanding of how torsional moments arise in structures and how they are resisted. In the previous Master’s project (Lundin & Magnander, 2012), the torsional resistance of the model originated from a fixed twisting boundary condition defined at the end supports. In this project however, the FE-models were developed further and provided with end walls to simulate a more realistic response. It was investigated if it can be motivated to include end walls in the model or if a model with fixed twisting obtains satisfactory results to be a valid simplification.

The FE analyses were executed in ADINA, where all analyses were performed in a version of the software with a maximum of 900 nodes. The FE models were verified with simple hand calculations and convergence studies were carried out in the 900 node version as well as in the full version to minimize the effect of mesh density.

2 Composition of trough bridges

The finite element models established and studied in this project were based on the geometry of a typical trough bridge. However, trough bridges in reality differ in geometry and it was of interest to study how much variation there is with regard to the cross-section, span and support conditions. The content of this chapter is, when nothing else is stated, based on an interview with a bridge engineer (Lidemar, 2013-01-30).

The load-carrying system is what defines a trough bridge and separates it from other types of bridge structures. Visually, the cross-section may resemble both a slab bridge and a girder bridge, but the function and thereby also the proportions of the components differs from these bridge types. A typical trough bridge and its parts are illustrated in Figure 2.1. The main function of the slab is to distribute the applied train load in the transverse direction of the bridge out to the main girders, and so it does not significantly contribute to the longitudinal distribution of the load. The main girders transfer the load to the supports in the longitudinal direction.

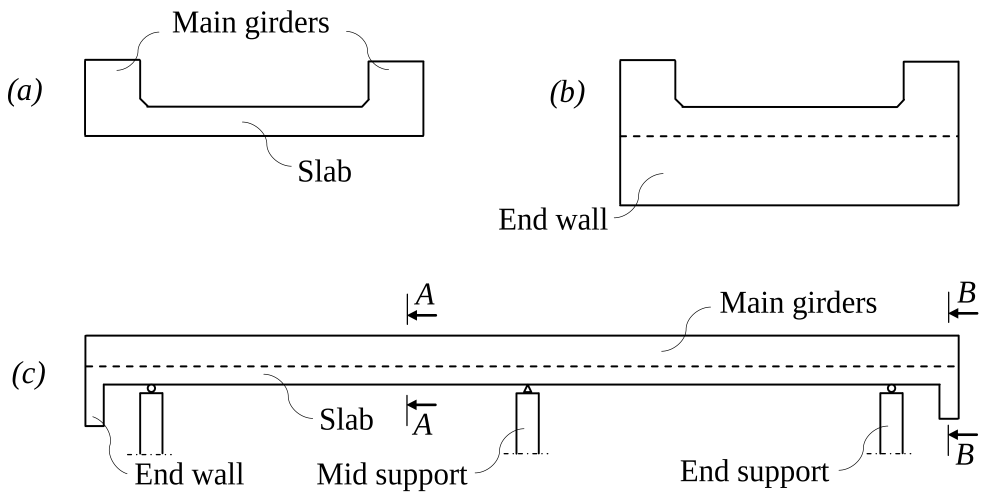

Figure 2.1 Schematic drawing of a typical trough bridge. a) Cross-section in section A-A, b) cross-section in section B-B and c) elevation.

The superstructure is placed on supports that transfer the load down to the foundation. Bearings are placed in between support and superstructure and these can be fixed with regard to in-plane displacements. Different types of supports and bearings are discussed further in Section 2.2.

New concrete trough bridges are often provided with end walls that reach down into the soil, as illustrated in Figure 2.1c. The function of the end walls is to resist horizontal loads, e.g. braking loads, through passive earth pressure. They also resist torsional moments that are transferred through the main girders.

2.1 Cross-section and span

A typical cross-section of a trough bridge is shown in Figure 2.2. The dimensions vary for bridges with different spans and depending on which design code it is based on. The requirements today do not fully agree with older codes and regulations and thus the dimensions of existing bridges may differ from the current standard.

The width of the main girders is typically around 700-1000 mm, which is needed to achieve required capacity. To allow for enough space for maintenance vehicles, the current code (Banverket, 2007) requests a free spacing between the girders of 4200 mm, which is more than can be found in existing bridges.

The thickness of the slab differs between old existing bridges and new designs. According to Lidemar, new bridges have an approximate thickness of 450 mm, while slabs in old bridges generally are more slender; from 300 mm and upwards. Naturally, the thickness of the slab is highly dependent on the distance between the girders. It is required that the inner corners of the cross-section should be chamfered, see Figure 2.2, as this section is critical with regard to shear force. The chamfering, with an additional reinforcement arrangement underneath, prevents extensive shear cracking as well as simplifies the removal of formwork and improves the durability of the structure.

The thickness of the ballast is measured from the top of the sleepers to the top of the concrete slab and should be at least 600 mm deep within a certain distance from the track. The sleepers have a height and width of 200 mm, a length of 2500 mm and are placed with a spacing of 650 mm. The height of the rails themselves is normally either 192 mm or 172 mm.

A free space sideways is required from 750 mm above the top of the rail and upwards as shown in Figure 2.2, thus limiting the top face of the girder (Banverket, 2007). However, Lidemar states that this requirement is seldom critical with regard to the height of the beam and the use of the maximum height may result in a clumsy and aesthetically non-pleasing structure. If the required height of the structure interferes with the free space, the girders may be lowered in relation to the bottom face of the slab.

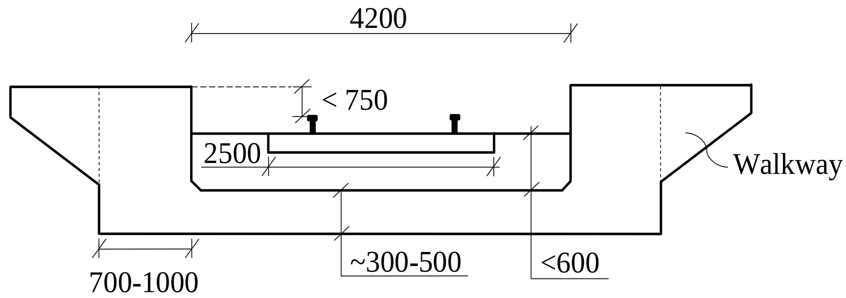

Figure 2.2 Typical cross-sectional dimensions [mm] of a trough bridge.

Railway bridges are required to be fitted with a walkway on the sides of the main track in order to allow for inspections, placement of cables etc. Any positive influence from this extension on the bearing and torsional capacity of the girder should be neglected in design as it should be possible to replace the walkway. However, the additional load of the walkway must be considered in the design of the main girders.

Trough bridges are always limited to contain one railway track, in order to maintain the load-carrying system where the slab mainly distributes the load in the transverse direction of the bridge. If another track was to be added within the girders, the slab thickness would have to be increased and hence the function of the structure approaches that of a slab bridge. It is also rare that two trough cross-sections are placed adjacent to each other to enable two tracks to cross. The normal centre spacing of tracks on land is approximately 4.5 m; a spacing that exceeds the minimum required dimensions of the trough cross-section. In such cases, bridges are instead designed as slab bridges or girder bridges. When more than two tracks need to bridge a crossing, frame bridges or slab frame bridges are the most common.

As the available height for the structure is almost always limited at intersections of railway and other infrastructure, it is appropriate to shorten the spans and thereby achieve a lower cross-section. However, there is often a limited choice of possible support positions, which may mean that a relatively long span is still required. Reinforced trough bridges can span approximately 10-30 m (Banverket, 2007). For spans larger than 30 m trough bridges are designed as prestressed.

2.2 Support conditions and end wall dimensions

The interior supports are recommended to consist of circular columns centrically placed under the main girders so that the column reinforcement can be continued up into the upper part of the girders (Banverket, 2007). Furthermore, trough bridges are normally provided with cross-beams between column supports.

According to Lidemar, bridges can also be designed with interior supports in the shape of walls, either rectangular or tapered closer to the ground at the long side of the support. A wall support is especially suitable when the support is placed in water, as it withstands ice pressure better than columns (Banverket, 2007), or when large collision loads need to be considered. Column supports are sometimes placed eccentrically to the bridge cross-section, especially when a bridge is to be replaced and the traffic interruption needs to be minimised. When eccentrically placed, the supports need to be connected to rather robust cross-beams.

The superstructure is often placed upon bearings that are resting on the supports. These bearings can be fixed in either one or two directions in the horizontal plane depending on what movement of the bridge that should be allowed.

Vertical loads will be transferred into the supports in a straight-forward manner, disregarding what types of supports and bearings are used. However, horizontal loads, such as brake loads, can be resisted in various ways. End walls are often used in new bridges to resist these loads by passive earth pressure acting on the outer side of the end wall, see Figure 2.3. To avoid too large horizontal forces in the end wall, longer bridges need to be equipped with fixed bearings on at least one interior support. The use of earth pressure is also present when the end support consists of an abutment with fixed bearings.

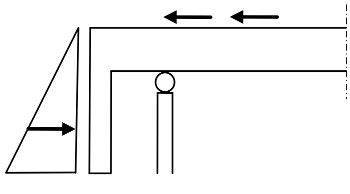

Figure 2.3 Forces acting on end wall (earth pressure and brake forces).

An alternative way of resisting horizontal loads, typically when there is not enough room for an end wall or abutment is to only use fixed bearings on supports. However, this approach gives rise to large horizontal forces that need to be resisted in supports and piles, if such are used, leading to large material use and expensive piling. Fixed bearings may also induce restraint forces in the structure that are caused by thermal change, concrete shrinkage or need for deformation due to loading.

Most existing bridges do not have end walls. Short bridges are instead often supported on rubber bearings. Due to the self-weight of the superstructure and friction in the interface, these can resist horizontal forces up to a certain limit. The horizontal forces are then transferred to the foundation according to Figure 2.4.

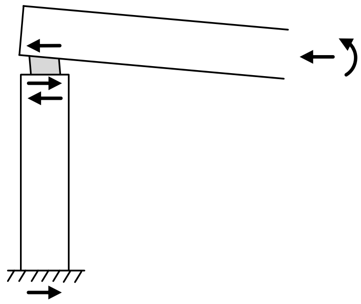

Figure 2.4 Horizontal loads are transferred to the foundations through the rubber bearings and the support.

Lift of the bearings is not permitted and hence the simply supported nature of the interior and end supports can only to some extent contribute to the resistance against torsion. The torsion resistance at interior and end supports also depends on the fixation in the transverse direction of the beam. This is further explained in Section 3.2.4. When end walls are used, the static system differs with regard to the different sectional forces, see Figure 2.5.

Figure 2.5 Schematic static system of a continuous trough bridge with end walls with regard to a) torsion of main girders, b) bending moment and shear force and c) normal force.

Banverket (2007) recommends that at least one of the bearings should be fixed in the longitudinal direction of the bridge when roller bearings are used at some supports. The fixed bearing is normally placed in one of the interior supports of the bridge. If the pinned support is placed closer to the end of the bridge, the movements in the other end of the bridge may exceed what the rails can tolerate. Rails may be constructed so that some dilatation is possible, but this requires maintenance that is both difficult and expensive and should therefore be avoided.

The end wall is cast together with slab and girder at each end and extends downwards into the soil. The height of the end wall is determined by the length of the bridge, i.e. the magnitude of the brake force, and how deep into the soil it needs to reach to allow for potential settlements during the service life. It is not unusual that the end wall reaches 2-2.5 m in height. Its thickness is normally around 0.5 m and the width corresponds to the distance between the walkway extensions, see Figure 2.6.

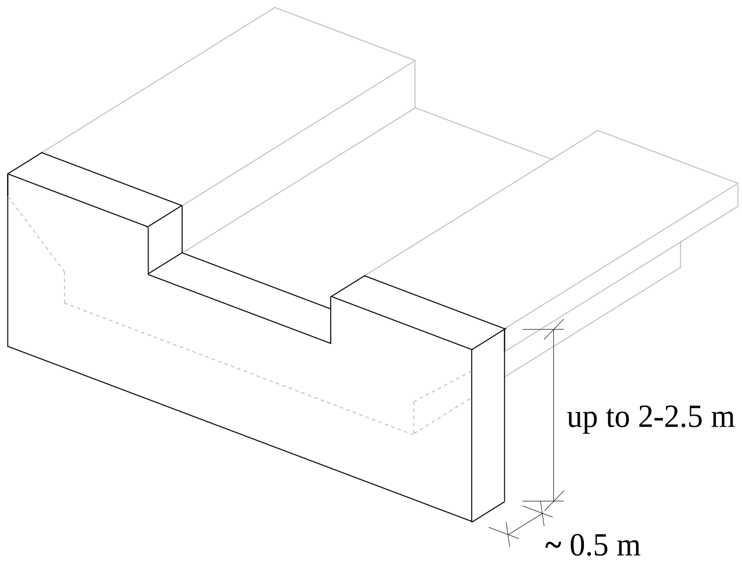

Figure 2.6 Layout and typical dimensions of an end wall.

The distance between the end support and the end wall depends on the required space for inspection and the deflection of the cantilevering part of the bridge. The deflection must be kept to a minimum in order to keep the rails straight. Lidemar estimates the typical distance to vary between 1 and 2 m.

3 Theoretical models and practical applications

This section aims to put the FE-modelling and analyses of this Master's project into a context and enable understanding of modelling choices and results. The reader is assumed to possess a basic knowledge of the finite element method. The theories and applications regarding this subject are therefore limited to the behaviour of and difference between beam and shell elements. These two element types are used in the studied models and constitute the main issue when distribution of load effects is considered.

The rise, distribution and resistance of torsion in general cases as well as the specific case of a trough bridge are also treated in this section as torsion represents one of the main concerns in design and analysis of this bridge type. Additionally, torsion was rarely mentioned during the courses that preceded this Master's project and a theoretical overview was needed for the authors and presumably also for many readers.

In order to define a reasonable and permitted load distribution, regulations and recommendations regarding transverse and longitudinal distribution of load effects within the rails, sleepers, ballast and concrete slab are presented. The load from a train is rarely static but moves along the bridge. A common way of treating this in practice is the use of influence lines, which may at first glance resemble sectional force diagrams but represent another way of thinking. Influence lines are briefly described at the end of this section as an aid for readers unfamiliar with this technique.

3.1 Finite elements in structural design

FE-models consist of elements that aim to describe the behaviour of the real structure. Different types of element are based on different theories and assumptions and the use of two different element types may cause drastically different behaviour of the model. The FE models analysed in this project consist of shell elements and/or beam elements and the theories behind these two types as well as software-specific considerations are presented in this section.

3.1.1 Beam elements

A beam subjected to loading normal to its main axis distributes the load longitudinally and as a result extends only in the axial direction. The deformation of beam elements is based on beam theory. The most commonly used beam theories are Euler-Bernoulli, often denoted classical beam theory, and Timoshenko beam theory. The latter has been developed from Euler-Bernoulli with the addition that shear deformations are taken into account and is therefore preferable in design and analysis of deep beams. The Euler-Bernoulli beam theory is valid for slender beams with high aspect ratio, i.e. $L/H > 5$-10 (Ottosen & Petersson), where L is the span and H represents the height of the beam cross-section.

Both theories assume that plane sections normal to the longitudinal axis of the beam remain plane when the beam is deforming. However, the Euler-Bernoulli beam theory also assumes that the plane sections remain normal to the beam axis while the Timoshenko beam theory allows the plane section to rotate around the y-axis. The angle between the normal of the undeformed beam and the rotated plane section consists of one contribution due to bending and one due to shear, which are denoted dw_0 / dx and γ in Figure 3.1.

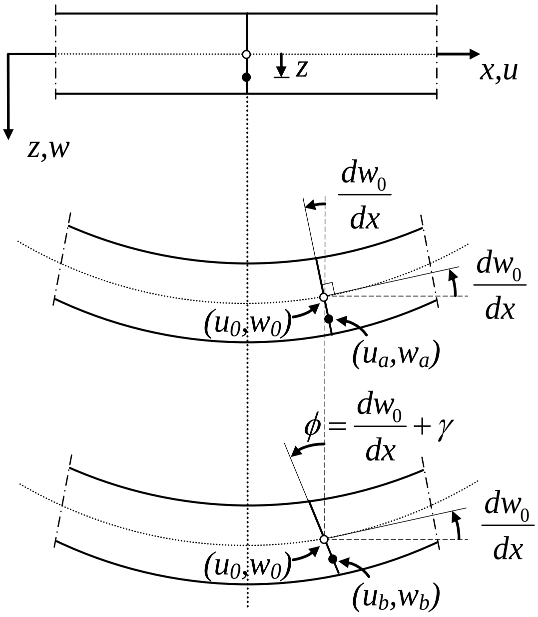

Figure 3.1 Schematic drawing of the deformation of a beam according to a) Euler-Bernoulli beam theory and b) Timoshenko beam theory. Adapted from Wang et al. (2000).

There are two different types of beam finite elements available in ADINA; Hermitian beam elements and iso-parametric beam elements (ADINA, 2010). The Hermitian beam element is formulated based on Euler-Bernoulli beam theory, but can if necessary be modified to account for shear deformations. A constant cross-section is assigned to the beam element that consists of 2 nodes, each with 6 degrees of freedom.

The most common Hermitian beam element is the linear beam element, where the elastic-isotropic material model is used and displacements, rotations and strains are assumed to be infinitesimally small. The element stiffness matrix is obtained through analytical integration, which implies that sectional forces can be obtained directly in ADINA. Sectional forces in a linear beam element are illustrated in Figure 3.2.

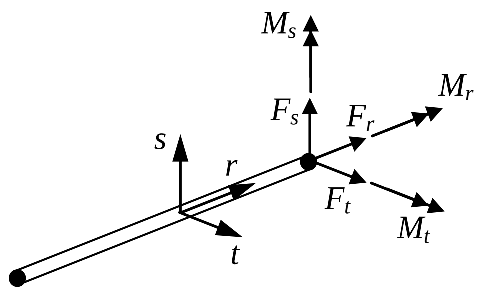

Figure 3.2 Local coordinate system and sectional forces for a linear beam element, adapted from ADINA (2010).

Other Hermitian beam element types include large displacement elastic beam elements, suitable for large displacement analyses only, warping beam elements intended for thin-walled open sections and nonlinear elasto-plastic beam elements for nonlinear analyses. It is also possible to define the behaviour of the elements by the moment-curvature relationship or the relationship between torsional moment and angle of twist. This is conducted using moment-curvature beam elements and is especially suitable in nonlinear analyses where the cross-section has an arbitrary shape.

Iso-parametric beam elements can be defined as plane stress or plane strain 2D-beam elements, axisymmetric shell elements or a general 3D-beam. The latter has six degrees of freedom whereas the other ones have three. Iso-parametric beam elements may have 2, 3 or 4 nodes. When assigned with internal nodes, i.e. nodes that are not placed on the edges, the elements may be curved. The elements are based on Timoshenko beam theory and shear deformations are therefore considered directly in the model, assuming a constant shear across the cross-section.

Iso-parametric beam elements are limited when it comes to cross-sectional shape and its variation along the beam. The shape needs to be rectangular and all element types except the axisymmetric shell element need to be assigned a constant cross-section along the beam. The iso-parametric beam elements are suitable for both thick and thin beams and shells and are mainly used for curved beams, beams in large displacement analysis, stiffeners to shells and axisymmetric shells subjected to axisymmetric loading.

The most common type of iso-parametric beam element is linear and it is based on the same assumptions regarding displacements and material model as the linear Hermitian beam element. The main difference, however, is that the element stiffness matrix is obtained by iso-parametric interpolation and numerical integration, using either Gauss or Newton-Cotes approach (ADINA, 2010). For 2D and axisymmetric shell elements, the numerical integration is limited to one plane, which reduces the analysis time significantly compared to the 3D beam element. The use of numerical integration makes the iso-parametric beam elements less effective than Hermitian beam elements in linear elastic analysis of straight beams. It has also been shown that it may be more effective to use several small straight 2-node Hermitian beam elements when analysing curved beams (ADINA, 2010).

3.1.2 Shell elements

Shell finite elements are developed from plate elements, based on plate theory, and plane stress elements that take membrane action into account. Shell elements are defined as mid-plane surfaces assigned a certain thickness.

A plate is defined by its small height in comparison with the in-plane dimensions and that loading is applied perpendicular to the plane. The out-of-plane loading results in bending moments about in-plane axes and shear force in the out-of-plane direction, as is illustrated in Figure 3.3a.

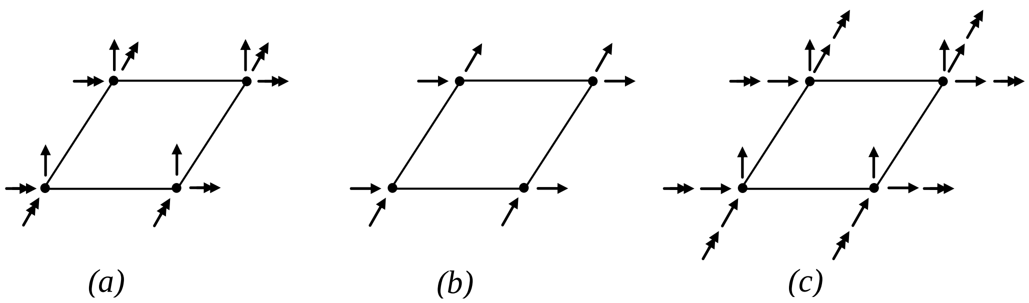

Figure 3.3 Degrees of freedom for a) plate element, b) plane stress element and c) shell element.

Similarly to beam theories, the classical approach according to Kirchhoff neglects shear deformation while more developed theories, such as the Mindlin plate theory, take shear deformation into account. Kirchhoff and Mindlin plate theories correspond to the Euler-Bernoulli and Timoshenko beam theories respectively and rely on the same assumptions regarding plane section deformation.

Membrane action occurs when a plate is loaded in its plane. Due to the small thickness of the plate, any out-of-plane stresses can be assumed to be insignificant and are neglected, leading to a plane stress state. Thus, each node has two degrees of freedom as the loading results in forces in the *xy*-plane, see Figure 3.3b.

The combined effect of the plate element and the plane stress element is achieved in shell elements with generally 5 degrees of freedom in each node, as shown in Figure 3.3c. In some cases a sixth degree of freedom should be assigned to a node, for example if shell elements are coupled to other types of structural elements or to rigid links, or if there are imposed rotational moments or boundary conditions at the node.

Different types of shell elements can be constructed through various methods. The simplest element, referred to as a flat shell element, is obtained by superimposing the contribution from membrane action in plane stress elements and bending in plate elements into the element stiffness matrix. The flat shell elements generally have low accuracy and are therefore only suitable for small elements. A more advanced and commonly used shell element type is the iso-parametric shell element. Here, a 3D solid element is reduced into its mid-plane in order to obtain shell behaviour. In the reduction, the assumption according to Mindlin that plane sections remain plane during deformation applies. Further, the stress in the *z*-direction should be zero (ADINA, 2010).

Unlike beam elements, shell elements have isotropic behaviour and distribute the load uniformly in all in-plane directions, provided that the stiffness and support conditions are the same in all directions.

Three types of shell finite elements can be chosen in ADINA; plate/shell elements, iso-parametric shell-elements and 3D shell elements. The latter are only suitable when varying thickness is of importance, e.g. in large strain analysis, and is not treated further in this section.

The plate/shell element is a triangular flat shell element, as described above, consisting of 3 nodes, each with 6 degrees of freedom. The bending is based on Kirchhoff plate theory and thus any shear deformation is neglected. This limits the recommended use of this element type to thin plates and shells.

Iso-parametric shell elements, which are often denoted only shell elements, can consist of 4 to 32 nodes. The 4-node element is the element type most frequently used and recommended by the software manufacturer (ADINA, 2010). However, Ekström (2009) found that these elements might result in an unsatisfactory description of bending due to increased stiffness if the mesh is too coarse. This is a result of low polynomial order of the FE-approximation. When the number of elements is increased, the results approach the analytical solution.

As the reduction from 3D is based on Mindlin plate theory, shear deformations are taken into account and the shell element is applicable for both thick and thin shell structures. Shear deformations are assumed to be constant over the thickness of the shell element but can be corrected if desired in linear elastic and linear orthotropic models.

The element stiffness matrix is obtained by numerical integration, using Gauss integration in the plane and either Gauss or Newton-Cotes integration through the shell thickness. A difference between these two integration schemes is that all of the Gauss integration points are located within the thickness of the shell, whereas Newton-Cotes integration points are located through the whole shell thickness with the two outer points placed at the upper and lower boundary of the element.

3.2 Torsion in structures

Torsion of a structural member occurs when eccentric loading induces twisting moments around the longitudinal axis of the member. Different types of torsion and the structural response of girders with regard to torsion are described in this section. The possibility of failure due to torsion, compatibility with adjacent members and appropriate design measures differs for the case of statically determinate and indeterminate systems respectively, which is also treated further in this section.

In design with linear elastic analysis it is assumed that the reinforced concrete remains uncracked but the structural response when cracked and the effect of cracking are also described to enhance the understanding of torsion. Further, the twisting moments need to be resisted by a torque in the opposite direction somewhere along the structure, e.g. at supports or end walls and possible means to obtain torsional resistance are presented.

3.2.1 Torsional response of girders

Torsion is generally divided into two categories; circulatory and warping torsion. Circulatory torsion, often denoted St Venant torsion, is characterised by a circular shear flow in the cross-section. The rate of twist is constant over the length of the member for a constant applied torsional moment, due to a lack of restraint over the cross-section at end supports. This allows warping and deformation in the longitudinal direction.

Warping torsion occurs when warping is prevented due to restraints over the cross-section at end supports, causing the rate of twist to vary over the length of the member. As a result, normal stresses arise and different sectional components will be subjected to bending in opposite directions. Warping torsion is mainly limited to open thin-walled cross-sections, e.g. I-beams, due to their low torsional stiffness. In the open trough cross-section studied in this project, only the solid main girders are subjected to torsion and warping torsion is therefore not an issue.

In linear elastic response, the shear stress varies from the centre of the cross-section towards the edges, as illustrated in Figure 3.4a. The shear stress in the corners of a rectangular cross-section subjected to torsion is therefore zero, resulting in a circularly shaped effective area (Lundh, 2000), as illustrated in Figure 3.4b. The part of the cross-section that contributes to the torsional stiffness is confined within this circular area, which depends on the geometry of the cross-section. As the shear stresses are the largest near the outer edges of the cross-section, solid cross-sections are often simplified into a tube with the same outer dimensions as the beam but with thin wall thickness, see Figure 3.4c.

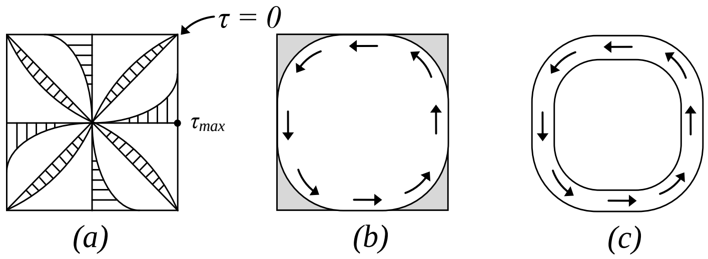

Figure 3.4 a) Shear stress distribution in a rectangular cross-section. b) Shear flow in a rectangular cross section. c) Shear flow in a simplified tube.

The torsional moment distribution in a fixed end beam subjected to an applied distributed torsional moment is obtained in analogy with the shear force distribution from a distributed load applied on a simply supported beam, see Figure 3.5a. The same coupling holds for an applied concentrated torsional moment, as shown in Figure 3.5b

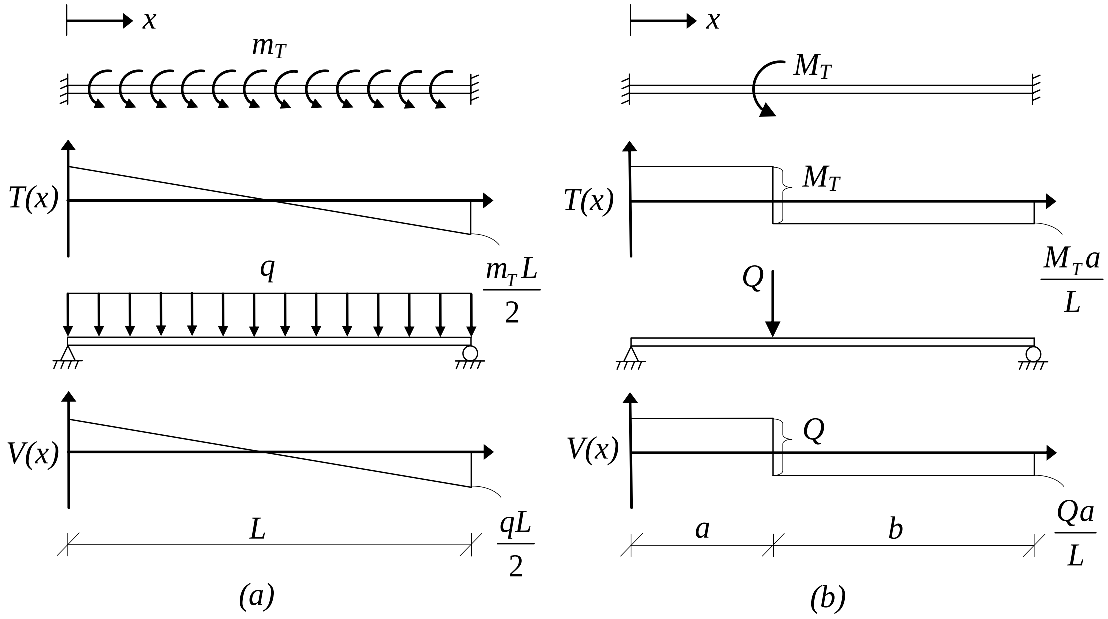

Figure 3.5 Analogy between applied torsional moment on a fixed end beam and applied load on a simply supported beam for a) distributed action, and b) concentrated action.

3.2.2 Compatibility and equilibrium torsion

In design with regard to torsion, it is appropriate to distinguish between equilibrium and compatibility torsion. Equilibrium torsion occurs in statically determinate problems, where an eccentrically applied load needs to be resisted by torsion, see Figure 3.6a. The torsional response is then governed by equilibrium conditions as the structural member is free to rotate except at supports. If the torsional moment capacity of the member is insufficient, a mechanism will develop and failure occurs.

Equilibrium torsion is rare as structural members are often connected to other members, with a limited ability to twist as a result. In such cases, compatibility between adjacent members gives rise to torsion. When one member is subjected to loading, it will deform and cause the adjacent member to twist, as illustrated in Figure 3.6b. This problem, known as compatibility torsion, is statically indeterminate as the torsional moments depend on static equilibrium, the stiffness of the twisted member and continuity conditions. The torsional moment in the beam depends on the torsional stiffness, but if the beam cracks due to torsion, the torsional stiffness decreases and the torsional moment can be ignored. Thus, if torsion is inadequately considered, extensive cracking may occur but failure is not necessarily reached due to the possibility of redistribution.

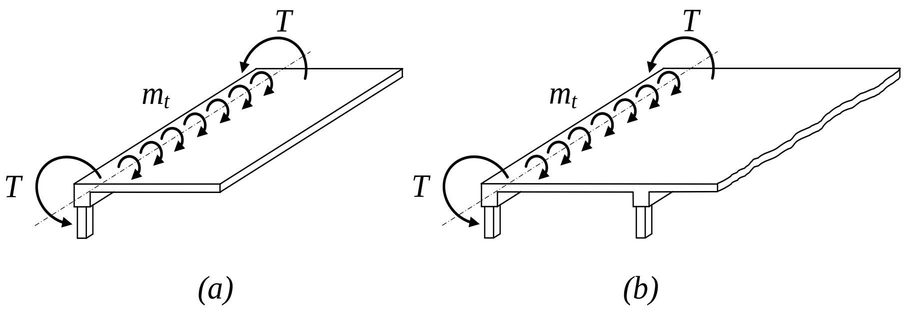

Figure 3.6 Examples of a) equilibrium torsion (statically determinate), and b) compatibility torsion (statically indeterminate), adapted from Nilson & Winter (1991).

The connection between the structural members, their stiffness and the stiffness of the supports will influence the magnitude of the torsional moment and its distribution along the twisted member. Systems where compatibility torsion occur are therefore rather complex, which is evident by examining the relationship between the members at the connection, discussed by Engström (2008). The deformation of the loaded member will induce its end to rotate and thereby cause twisting of the supporting member. At the same time, the end rotation may be reduced by the rotational stiffness of the supporting member. The connection in a compatibility torsion system is normally assumed to be rigid, as full continuity between members is expected.

The main girders in the studied trough cross-section are subjected to compatibility torsion in the linear elastic analysis. When the concrete slab is subjected to train loading, it deflects transverse to the main direction of the bridge. Due to compatibility between the deformation of the slab and the girders, the girders account for the deformation of the slab by twisting, which is illustrated in Figure 3.7.

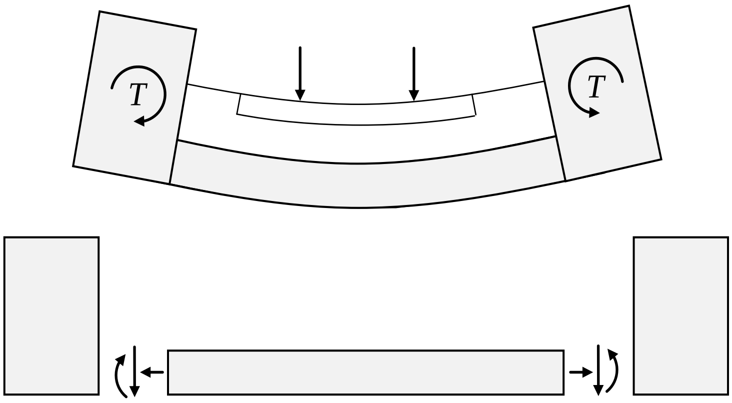

Figure 3.7 a) Rise of torsion in the main girders of a trough bridge due to deflection of the slab. b) Sectional forces at slab edge that induce torsion of girders.

Before cracking, the slab is partially fixed to the girders, which act as rotational springs in the statically indeterminate system of the slab. The rotational stiffness of the girders determines the degree of fixation. The fixed end bending moment, shear force and axial force at the slab edge induce torsion in the main girder. The axial force arises due to the deformation of the slab and the need for elongation under load. In the statically indeterminate problem, continuity needs to be fulfilled along the connection between slab and girder along the entire length of the structure. The torsional moment distribution of the girders is therefore highly dependent on the distribution of bending moment along the slab edge.

3.2.3 Influence of cracking

Uncracked concrete resists torsion without any influence of the reinforcement. This is however unlikely since the shear stress over the cross-section due to applied torsion normally reaches the tensile strength of the concrete, resulting in shear cracking. In BVS 583:11 (Trafikverket, 2012), uncracked concrete is defined exclusively as prestressed concrete. A reinforced concrete structure, such as the bridge studied in this project, should therefore be assumed to be cracked. However, the structural analysis including calculations of the torsional moment distribution should be carried out according to the theory of linear elasticity. Cracking is instead taken into account in design by reducing the torsional stiffness of the girders by a factor of 0.3.

The following theories are mainly adapted from Collins & Mitchell (1990). When the principal tensile stress reaches the cracking strength of concrete, diagonal shear cracks appear in a spiral pattern along the beam. Inclined compressive concrete stresses, concentrated to the uncracked areas between the diagonal cracks, resist the shear flow induced by torsion.

These compressive struts are balanced by tensile stresses in the longitudinal reinforcement, see Figure 3.8. The transverse reinforcement is needed to transfer the compressive stresses along the beam. The principle is the same as for shear resistance, which is illustrated in Figure 3.9, although for shear force cracks only occur along the vertical sides of the beam.

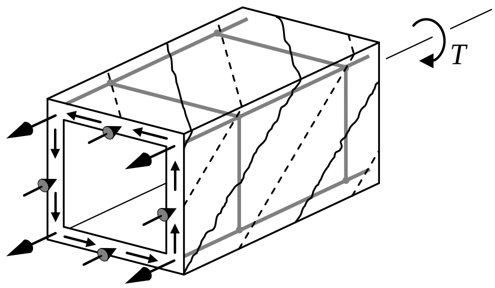

Figure 3.8 Truss model for torsion resistance in cracked reinforced concrete, adapted from Collins & Mitchell (1990).

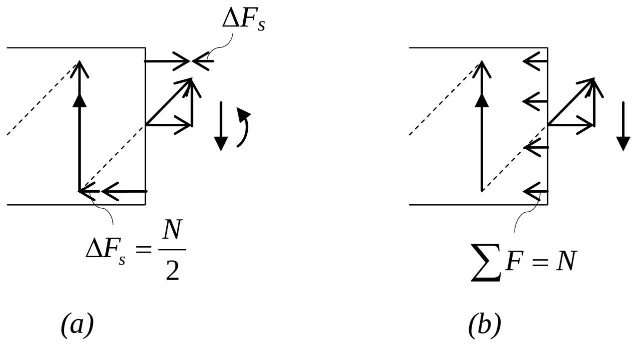

Figure 3.9 Analogy between a) shear force resistance and b) torsion resistance in a reinforced concrete beam.

The magnitude of the torsion in a member subjected to compatibility torsion is proportional to its torsional stiffness. After cracking due to torsion, the torsional stiffness is reduced significantly, thus leading to a lower torsional moment in the member. Testing has been conducted where the relation between applied loading on a floor beam and the torsional moment in the supporting beam was investigated. In Figure 3.10 these test results are compared with results using analytical values of the torsional stiffness for uncracked and cracked reinforced concrete respectively. The torsional stiffness for cracked sections is estimated based on the deformation of the reinforcement. For full derivations, the reader is referred to Collins & Mitchell (1990).

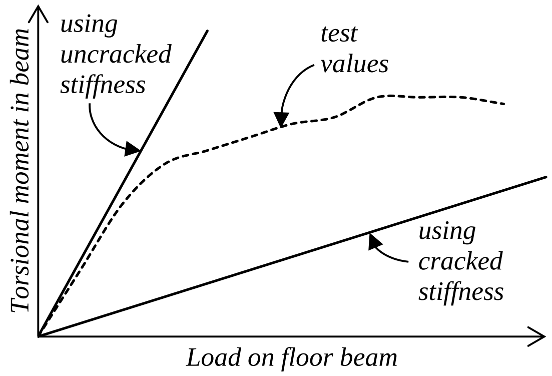

Figure 3.10 Relationship between applied load on floor beam and torsional moment in the supporting beam, adapted from Collins & Mitchell (1990).

It can be noticed from the figure above that the test results correspond well to the predicted values using uncracked torsional stiffness when the magnitude of the loading was small. As loading was increased, the test values approached the predicted values with cracked stiffness, a sign of extensive cracking in the tested member. It is apparent that the magnitude of the torsion did not change significantly when the load was increased after cracking. This is due to the proportional relationship between torsional moment and torsional stiffness.

Bending cracks may appear in the connection between the slab and the girders of a trough bridge. This is often prevented by adding a chamfer in the inner corner, see Section 2.1. If cracking does appear, the reinforcement alone transfers sectional forces from the slab to the girders. However, the stiffness of the connection is significantly reduced.

3.2.4 Torsion resistance in supports and end wall

If a structural member without any restraints is subjected to eccentric loading, free twisting of the member will occur without reaching a stable state of equilibrium. Torsional moments arise when the member is fully or partially restricted from twisting. Torsion is resisted and transferred to other structural members in supports and the rotational stiffness of the supports affects the distribution of torsional moment to a large extent.

The torsion in wide beams subjected to a small torsional moment may be resisted by an eccentric reaction force, see Figure 3.11a. However, this induces small deformations in the connection and minor tilting may occur (Engström (Ed.), 2008). An eccentric reaction force may not be sufficient for narrower beams or larger torsional moment. A force couple must then be enabled in the support to balance the torque, see Figure 3.11b.

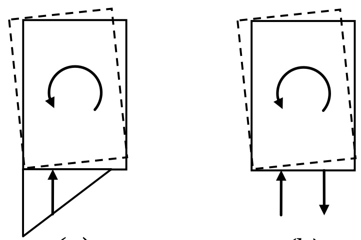

(a) *(b)*

Figure 3.11 Torsional resistance at support by a) an eccentric reaction force and b) a force couple. Adapted from Engström (Ed.) (2008).

If bearings at supports are fixed in the transverse direction of a trough bridge, the bottom of the slab is prevented from elongation when loaded. This results in horizontal reaction forces that balance each other and induce a torque of opposite direction to that induced by the sectional forces at the slab edge. The torsional moment distribution is therefore affected as twisting is partially or fully prevented for the trough cross-section at supports. Note that this effect should be eliminated if one bearing is free to translate in the transverse direction of the bridge.

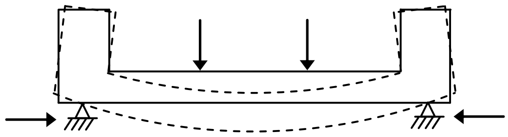

Figure 3.12 Horizontal reaction forces at bearings fixed in the transverse direction due to prevented need for deformation.

End walls function as deep beams with high bending stiffness and therefore provide high rotational stiffness around the longitudinal axis of the girders. The circular shear flow in each main girder is transferred in a spiral pattern to the end wall where it can be resisted by a force couple. Figure 3.13 illustrates the torsion resistance in one side of an end wall when the load is applied away from the end wall section, i.e. torsion in the girder is the only applied load in the considered section. The struts and ties that might be expected in the upper left corner in the girder are excluded as the forces in this position can be assumed to be zero. Static equilibrium is fulfilled by the presented configuration as each node in the three-dimensional strut-and-tie model is in equilibrium.

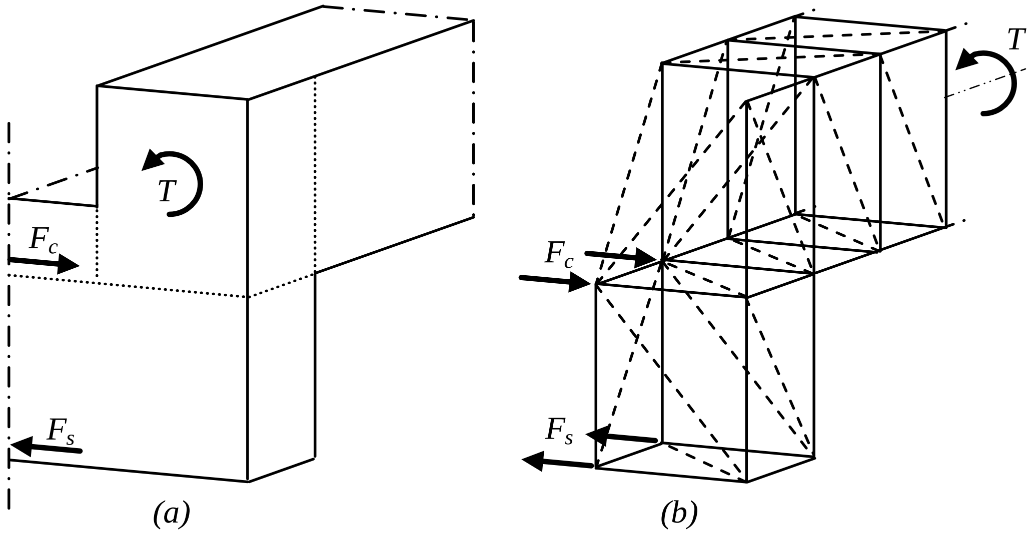

Figure 3.13 Torsion resistance in one side of an end wall when load is applied away from the end wall. a) Geometry of end wall and connecting girder. b) 3D strut-and-tie model of end wall and girder. Compressive struts are represented by dashed lines and tensile ties by solid lines. The torsion is transferred in a spiral pattern through the girder to the end wall where it is resisted by a force couple.

When the load is applied close to or above the end wall, the structural response will differ from that when load is subjected far away. The load effect then needs to be transferred from the bottom of the end wall to the main girders, which is achieved with the same type of reinforcement that is used to resist torsion.

In design, both load cases need to be considered as the bridge normally is subjected to a load combination. The combined effect from loads applied directly above the end wall and loads applied at some distance from the end wall will subject the end wall for both bending and torsion.

3.3 Distribution of load effects

The distribution of load effects is one of the key steps in the unification of the longitudinal and transversal load-carrying systems of a trough bridge. Distribution occurs within the railway components, i.e. the rails, sleepers and ballast, and in the concrete slab.

When considering the distribution of load effects, it is important to distinguish between loads and internal forces. Loads are acting on the structure while internal forces and moments occur within the structure and can be studied in each section. For the trough cross-section studied in this project, the train load is applied on the rails and the normal stress is then distributed through the rails, sleepers and ballast before it reaches the concrete slab. These internal forces within the ballast can therefore be seen as a load effect applied onto the slab face.

3.3.1 Distribution of load effects in railway components

In the previous Master's project (Lundin & Magnander, 2012), the two concentrated wheel loads applied on the rails were simplified into one concentrated force applied directly onto the concrete slab in the middle of the cross-section. In reality, the effect of the train load will be distributed both longitudinally and transversally through the rails, sleepers and ballast. This results in a distribution of vertical normal stresses over a certain area of the slab face, as shown in Figure 3.14.

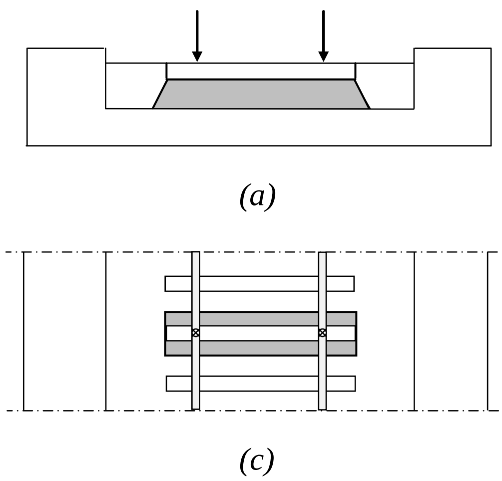

Figure 3.14 Schematic drawing of normal stress distribution in ballast (shaded areas) in a) transverse and b) longitudinal direction of the bridge. c) Plan view showing both transverse and longitudinal normal stress distribution in ballast.

The normal stress distribution that occurs in the ballast beneath the load application is often treated by choosing an angle of load distribution. This angle is prescribed in design codes, but varies between different codes. With this approach, the stress is assumed to be uniform within the area. In reality, the stress distribution is more complex and is affected by factors such as the weight and friction angle of the material. As the focus in this project was to develop a model that is appropriate to use in practice, the study of distribution of load effects through rails, ballast and sleepers was limited to a comparison between the approaches prescribed in different codes.

In Eurocode 1 (CEN, 2003), which is used for design of new structures, the concentrated load is assumed to be distributed through the rail into the underlying sleeper and the closest adjacent sleeper on each side, with a distribution according to Figure 3.15a. This specific distribution is also mentioned in the Swedish code for analysis of the bearing capacity of existing structures BVS 583:11 (Trafikverket, 2012). In the first code, another less favourable distribution is also shown, illustrated in Figure 3.15b.

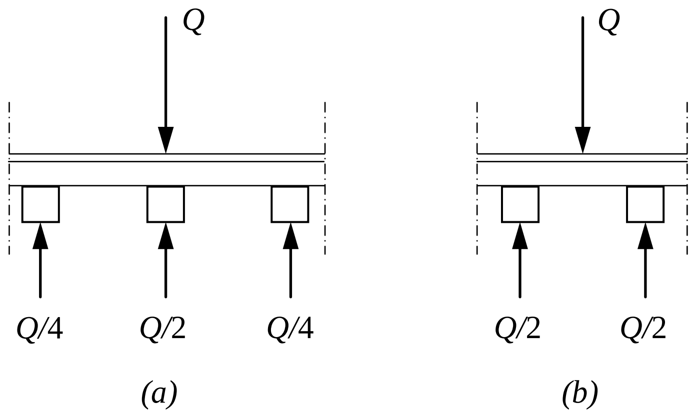

Figure 3.15 Assumed load distributions through rail according to a) Eurocode 1 and BVS 583:11 and b) Eurocode 1.

The distribution of load effect in the sleepers and ballast is in both codes assumed to be distributed both in transverse and longitudinal direction with a certain slope. However, the slope differs between the codes, as is illustrated in Figure 3.16. For design of new structures, Eurocode 1 prescribes a slope of 4:1 whereas BVS 583:11 urges a slope of 2:1. Note that the distribution within the sleeper is treated differently in the two codes.

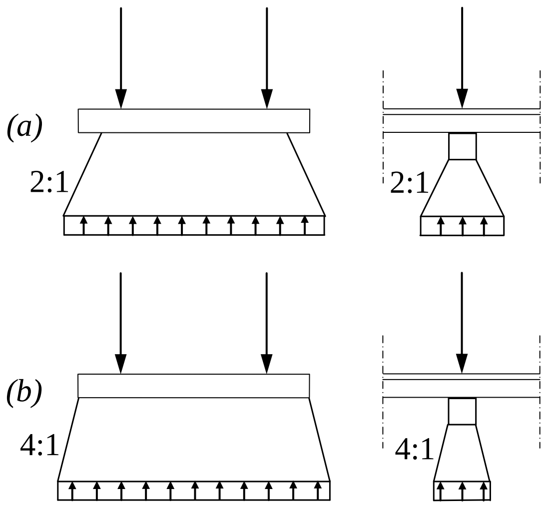

Figure 3.16 Load distribution assumptions according to a) BVS 583:11 and b) Eurocode 1.

3.3.2 Distribution of load effects in concrete slabs

According to Eurocode 2 (CEN, 2005), slabs that have two parallel free edges and are subjected to concentrated loads are considered to carry load in only one direction. This is also valid for the centre region of slabs supported on four edges with a length to width ratio larger than two. The latter condition applies for the slab in the studied trough bridge. The slab can then be divided into strips with behaviour similar to beams. However, when the load is concentrated or distributed onto a limited area, the slab strips subjected to the load cannot deflect freely due to compatibility with adjacent strips. As a result, the load effect is distributed in the transverse direction and a wider part of the slab contributes to the resistance, given that the slab is provided with minimum secondary reinforcement. This behaviour can also be compared with the distribution of load effect when a wide beam is subjected to a concentrated load and the stress flow is expanded within the width of the member.

Each structure has a specific transverse distribution of bending moment and shear force, which are statically indeterminate problems that depends on the design, i.e. the development of cracking and the reinforcement amount. It is possible to determine the exact transverse distributions through non-linear analysis but this approach is hardly efficient in practice. Instead simplified formulas for the transverse distribution width, often referred to as the effective width, have been developed to enable a rational design process with linear elastic analysis.

The formulas differ between codes but are based on a common approach. The distributions transverse to the load-carrying direction of the slab are considered as a unit bending moment or shear force per unit length, spread over an effective width, see example in Figure 3.17. This is based on the fact that redistribution occurs when the concrete slab cracks and the reinforcement yields. The distributions in the ultimate limit state will therefore correspond to what was assumed in design based on linear elastic analysis after redistribution due to cracking and yielding. Hence, the designer can control the magnitude of the transverse distribution by varying the reinforcement amounts. Thus, if a one-way behaviour is desired in a slab subjected to concentrated loads, the designer may choose to place the reinforcement almost entirely in one direction.

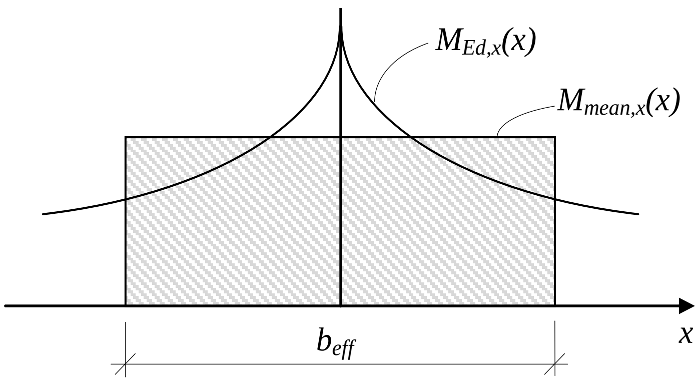

Figure 3.17 Bending moment distribution transverse to the load-carrying direction of the slab and the application of a uniform moment over an effective width b_{eff} in codes.

The effective width, with regard to distribution of load effects, varies when considering bending moment and shear force due to compatibility requirements and possible collapse mechanisms. Effective widths in codes are presented for each response below.

3.3.2.1 Effective width for transverse distribution of bending moment

The variation of bending moment perpendicular to the primary load direction depends on the slab's need for deformation in order to maintain compatibility. In the Swedish handbook BBK 04 (Boverket, 2004), the effective width on each side of the applied load is calculated as

$$b_{eff} = \min\left(3h, \frac{l}{10}\right) \tag{3-1}$$

where h = height of cross-section

l = theoretical span length

The values $3h$ and $l/10$ refer to the distance within which adjacent reinforcement bars interact with each other.

Another recommendation, still in use for classification of existing road bridges, origins from the Swedish handbook 'BYGG' (Wahlström (Ed.), 1969). Here, the effective width for road bridges should be calculated according to Equation (3-2), see also Figure 3.18.

$$b_{eff} = b_x + t_{coat} + t_{fill} + \min(0.75l, 2.5m) \tag{3-2}$$

where b_x = width of concentrated load (wheel load)

t_{coat} = thickness of coating

t_{fill} = thickness of fill

The thickness of coating and fill does not apply to railway bridges and the original formula is therefore modified to only consider the width of the load when this type of bridge is treated, see Equation (3-3).

$$b_{eff} = b_x + \min(0.75l, 2.5m) \tag{3-3}$$

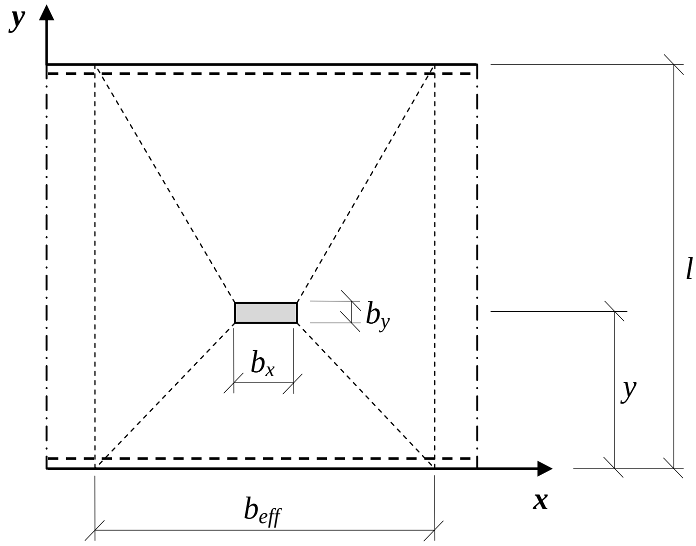

Figure 3.18 Effective width with regard to bending moment, adapted from 'BYGG' (Wahlström (Ed.), 1969).

In 'BYGG' the maximum value of 2.5 m represents half of the width of one traffic lane. This is valid for road bridges but it is stated that a similar limitation should be used for railway bridges. However, it is not specified if the same maximum width applies or whether this value should be adjusted to suit the width of the track. For short span bridge slabs, such as the one studied in this thesis, the difference between Equations (3-1) and (3-3) is significant, and it is questionable if the same maximum value is appropriate.

Notice that both equations above are only applicable for a single concentrated load and also disregard the load position. When two or more wheel loads are applied in close proximity, their individual distributed load effects may intersect. The equations must then be adjusted to account for the combined load effect and in this case, the load spacing needs to be considered. It is therefore questionable if superposition of adjacent loads is applicable. In 'BYGG', the total effective width for two wheel loads is calculated as in Equation (3-4). No specification regarding effective width for multiple wheel loads are given in BBK 04.

$$b_{eff} = 2b_x + \min\left(1.5l, 2.5 + c_x - b_x, 0.75l + c_x - b_x\right) \tag{3-4}$$

where c_x = distance between the two wheel loads (c/c)

Furthermore, the distance between the load and the line support is not considered in the two approaches. Davidsson (2003) has analysed the effect of different load positions on the effective width by a linear elastic FE-analysis. It was found that the effective width decreased significantly in the FE-model when the wheel load was located close to the support. This implies that the theoretical equations should be used with caution for this load application.

It is further not stated whether the approaches above are valid when the slab is fixed at supports or when the load application area is prolonged in the span direction, i.e. b_y is larger.

Note that no regulations or guidelines regarding the transverse distribution in slabs are given in Eurocode 2 (CEN, 2005).

3.3.2.2 Effective width for transverse distribution of shear force

For a beam, a possible failure mode due to shear force consists of a part of the beam sheared off along an inclined crack. When it comes to slabs it is more difficult to predict a collapse mechanism. In fact, the only realistic mechanism in slabs caused by shear force from a concentrated load is punching, where a cone-shaped part of the slab is pushed away from the rest of the slab. This is however closely related to column supports and other large concentrated forces.

Shear forces will occur in both the longitudinal and transverse directions of the slab. The distribution of shear force per unit width depends on the crack pattern and equilibrium must be fulfilled between all sections. The recommendations regarding transverse distribution of shear force differ within the studied literature. With regard to shear force, there is a clear distinction between point supports and line supports and the equations listed in this section are only valid for the latter. In BBK 04 (Boverket, 2004), the effective width is calculated as

$$b_{eff} = \max\left(7d + b_x + t, 10d + 1{,}3y\right) \tag{3-5}$$

where d = minimum effective height of slab

b_x = width of load

t = thickness of coating etc.

y = distance from centre of load to studied section

Notice that only the latter of the considered sums in Equation (3-5) takes the load position and the non-uniformity of the transverse shear distribution into account, where the distribution of shear force propagates further away from the position of the load, see Figure 3.19.

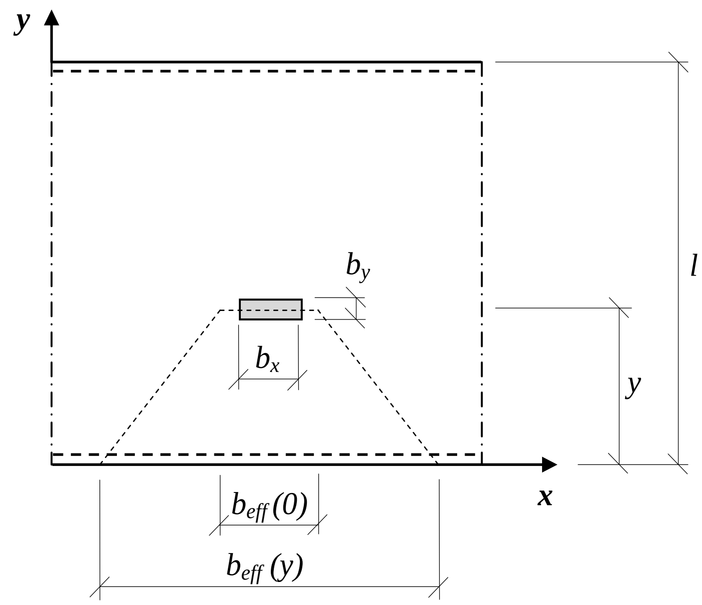

Figure 3.19 Effective width with regard to shear force according to BBK 04 (Boverket, 2004), the second sum of Equation (3-5).

When considering railway bridges, the formula is simplified by excluding the thickness of coating and only considering the width of the load in line with the procedure described in the previous section. Using the same variables as defined in Equation (3-5), the effective width is then computed as

$$b_{eff} = \max(7d + b_x, 10d + 1{,}3y) \tag{3-6}$$

In 'BYGG' (Wahlström (Ed.), 1969), the width of the transverse shear distribution is calculated in two steps, as illustrated in Figure 3.20. Firstly, the transverse distribution at the line support is computed according to Equation (3-7). The distribution in the section of load application is then computed as in Equation (3-8).

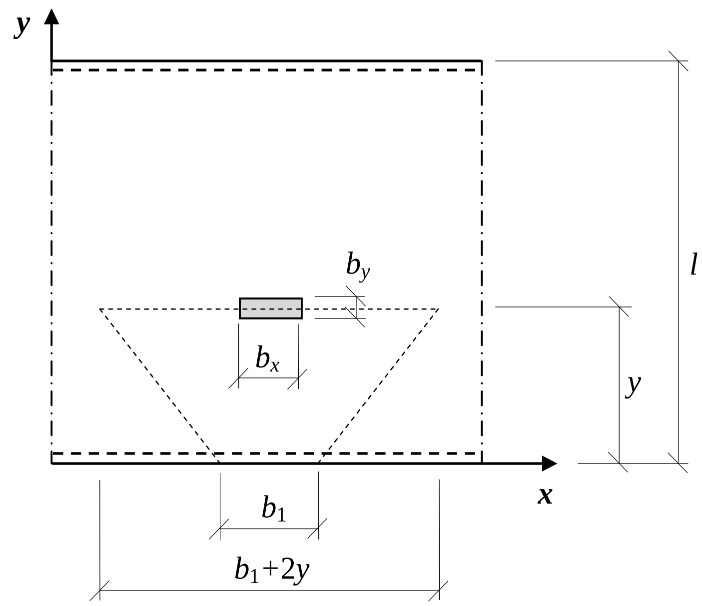

Figure 3.20 Effective width with regard to shear force according to 'BYGG' (Wahlström (Ed.), 1969).

$$b_1 = \max\left(b_x + 2\left(t_{coat} + t_{fill} + h_{\min}\right), 5h_{\min}\right) \tag{3-7}$$

$$b_{eff} = \frac{1}{f}\left(b_1 + 2y\right) \tag{3-8}$$

where $h_{\min}$ = minimum height of cross-section

y = longitudinal distance to centre of load

$f = \dfrac{4 + y/d}{8}$ for $y \leq 4d$ and $f = 1$ $y > 4d$ for

d = effective height of cross-section

As for BBK 04 the thickness of coating and fill is neglected when calculating the transverse distribution of shear force in railway bridges. Using the same two-step approach as above, the effective width according to 'BYGG' is then computed as in (3-8) but with the difference that

$$b_1 = \max\left(b_x + 2h_{\min}, 5h_{\min}\right) \tag{3-9}$$

A recently published study (Pacoste et al., 2012) recommends that the distribution width regarding shear force should not exceed five times the thickness of the slab in the considered section. The effective width according to 'BYGG' in Equation (3-8) is very likely to exceed this value and a concern is therefore raised that this code may lead to effective widths that allow too extensive distribution.

Similarly to the transverse distribution of bending moment, the effective width needs to be adjusted with regard to multiple nearby loads. This is not described explicitly in any of the codes but it is treated further in Appendix D.2. It is not mentioned if the formulas should be adjusted when the loading is distributed in the *y*-direction. Unlike the bending moment distribution, no influence of the boundary conditions is expected.

3.4 Influence lines

In linear elastic analysis, the structural members of a bridge need to be designed for the maximum sectional forces in each section. The variable loads for a bridge are typically moving loads and hence the most critical load location needs to be determined. An effective way of finding this location in linear elastic analysis is to create influence lines for the section that is to be designed. An influence line is a diagram that represents the variation in sectional forces in one studied section for all load positions along the structure.

Simply supported structural members have linearly varying influence lines that can easily be determined, see A.1 for derivation and example. Influence lines for statically indeterminate structures, e.g. continuous beams, can be derived by analytical solutions but this approach leads to complex and lengthy calculations. Influence lines may also be determined iteratively by successively applying a unit load in a number of sections along the structure. The response is calculated for each location and gathered into an influence line. This is also the method used when finding the influence line for torsional moment.

Independently of how the influence line is created, the sectional force at the studied section is gathered in the same manner. In the case of a concentrated load, the sectional force is found by multiplying the value of the influence line at the loaded section by the applied load. For distributed loads the sectional force is obtained by multiplying the applied load with the area under the load under the influence line, see example in Figure 3.21.

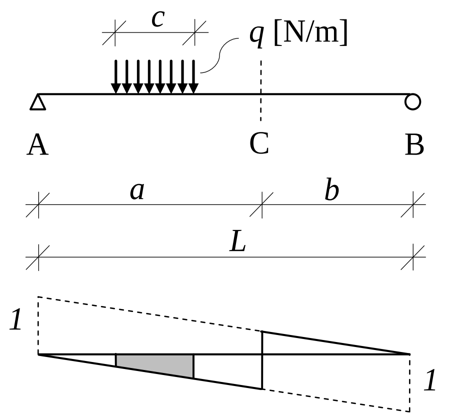

Figure 3.21 Influence line for the shear force at section C for a uniformly distributed load. The shear force is found as the shaded area under the influence line multiplied with the applied load.

Once an influence line is created for the section, superposition of several loads is easily performed by summation of the sectional forces that each load position induces.

In a typical bridge design task it is appropriate to collect the maximum value of a specific sectional force in all sections into one diagram as it indicates how the reinforcement should be curtailed efficiently. This is achieved in so called envelope diagrams, where the maximum values of the influence line for a number of selected sections are compiled into the same diagram.

In the studied FE-software ADINA necessary outputs for influence lines can be obtained by creating one time step for each load application along the member, resulting in a moving load as time progresses. This will further on be denoted load stepping.

4 Description of FE-modelling

The analyses of the combined model and the beam grillage model were preceded by a preliminary study of a simplified model corresponding to one span of the bridge. This study aimed to investigate how the transverse distribution of load effects in a slab consisting of shell elements is influenced by the boundary conditions and the type of load application. The results for the cases of fixed ends and simply supported ends constitute the upper and lower boundary for the sectional forces in the slab in the trough bridge model, which is partially fixed to the main girders. The distribution widths and sectional forces obtained in this model were also compared to analytical values spread over effective widths computed according to the codes presented in Section 3.3.2.

The dimensions and properties of the studied trough bridge defined in Section 4.3 are based on typical dimensions and code regulations. The constitutions of the combined and beam grillage trough bridge models are presented in Section 4.3.1 and 4.3.2 respectively. Modified models were created in cases where analyses of the influence of e.g. load type or boundary conditions were of interest. All modified models are described in Section 4.3.3.

Common for all studied FE-models is the area of the applied load, which is described in detail in Section 4.1.2. However, the application of the distributed load differed somewhat between the models depending on what type of elements was used in the slab. The modelling procedure of distributed load is described in Section 4.1.1.

Sectional forces in the beam grillage model can be obtained directly while the models containing shell elements require post-processing. However, when creating influence lines and envelope diagrams, the output data from all models required some processing. All post-processing procedures are described in further detail in Section 4.4.

4.1 Load application

The load that was applied in the FE-models was obtained from the distribution of load effects from the two concentrated loads of one wheel axle within rails, sleepers and ballast. This distribution was calculated according to the codes presented in Section 3.3.1, which resulted in a certain loaded area. The practical application of distributed load in finite element software is described in the section below.

4.1.1 Modelling of distributed load in ADINA

In ADINA distributed load can be represented by pressure load acting on a surface or distributed load acting along a line (ADINA, 2010). In both approaches, ADINA converts the distributed load into corresponding consistent nodal load vectors based on the principle of virtual work. These load vectors are thereafter assembled into an external load vector. The methodology differs between beam and shell elements and is explained further for each element type below.

For beam elements distributed load is applied on the neutral axis. The distributed line load is transformed into equivalent nodal forces and moments as illustrated in Figure 4.1. These nodal forces are computed using shape functions and have the same magnitude as fixed-end reaction forces and moments of the beam element. Note however that the directions differ from the fixed-end forces. When considering only nodal actions, the numerical solution inside the element will however differ from the analytical solution according to beam theory, as can be seen in Figure 4.2.

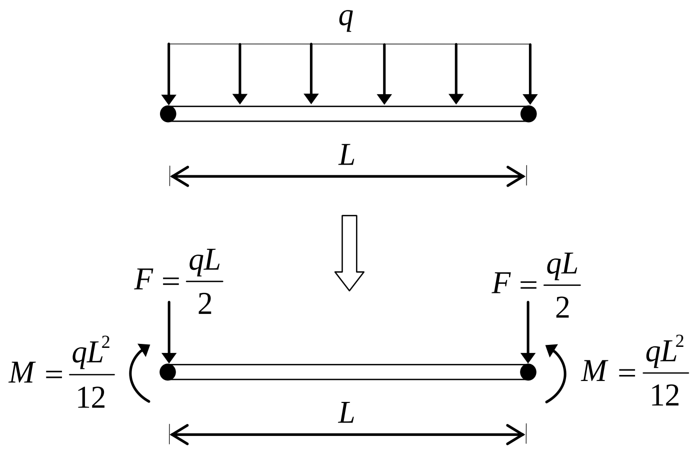

Figure 4.1 Transformation of distributed load on a beam element into equivalent nodal forces, adapted from ADINA (2010).

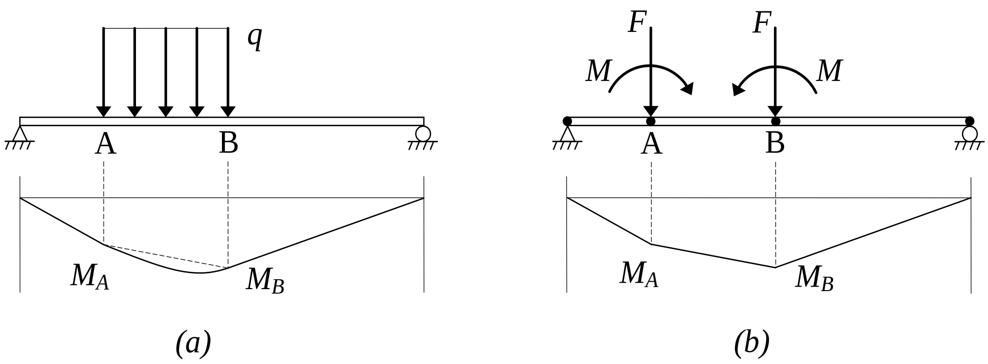

Figure 4.2 Schematic bending moment distribution in a beam subjected to distributed load. a) Analytical result. b) Numerical result using three beam elements and equivalent nodal forces, adapted from ADINA (2010).

Distributed load on shell elements can be applied as pressure load on the mid-plane surface or distributed line load along the mid-plane edges. The latter will not be described further as it is not relevant for the considered distributed effect of the train load. The load can either be applied on geometry surfaces, prior to or after meshing, or on elements after meshing by defining one or several element-face sets. The geometry of a model is always constant while the element numbering depends on the chosen mesh density. Thus, a load application defined on the geometry of the model is more generally applicable than the use of element-face sets, as the latter approach is dependent on the meshing and the element numbering.

Similar to beam elements, the load is transformed into equivalent nodal forces acting in the nodes of the element. Translation and rotation are found independently of each other; resulting in an equivalent nodal load vector without any moment, i.e. consisting of forces only, see Figure 4.3.

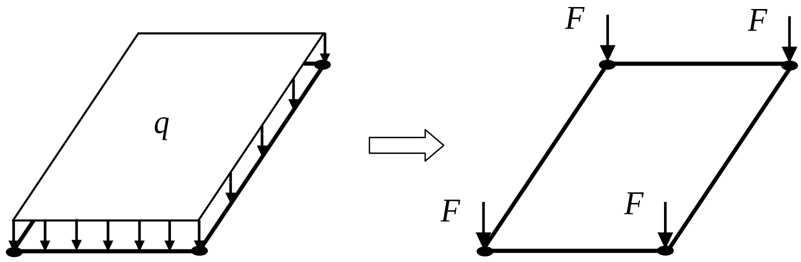

Figure 4.3 Transformation of pressure load on a shell element into equivalent nodal forces.

Note that the transformation into equivalent nodal forces only applies to distributed loading. Concentrated loads are always applied in one point and hence only one node of an element is directly subjected by the load.

4.1.2 Slab area subjected to train load

In modelling, the train load was simplified into a distributed load corresponding to the distribution of load effects within the rails, sleepers and ballast, as illustrated in Figure 4.4. The loaded area was calculated according to Eurocode 1 (CEN, 2003), see Equations (4-1) and (4-2), as the distribution prescribed in this design code induced the maximum sectional forces of the two studied regulations. See Section 3.3.1 where regulated distributions are described. The width of the distributed load was determined for a load application between two sleepers as this application generated the smallest distribution area, i.e. the most conservative result.

$$L_{load} = L_{sleeper} + \frac{1}{4} \cdot (h_{ballast} - h_{sleeper}) \cdot 2 = 2.7\,\mathrm{m}$$

$$= 2.5 + \frac{1}{4} \cdot (0.6 - 0.2) \cdot 2 = 2.7\,\mathrm{m} \tag{4-1}$$

$$b_{load} = cc_{sleeper} + \left(\frac{b_{sleeper}}{2} + \frac{1}{4} \cdot (h_{ballast} - h_{sleeper}) \right) \cdot 2 = 1.05\,\mathrm{m}$$

$$= 0.65 + \left(\frac{0.2}{2} + \frac{1}{4} \cdot (0.6 - 0.2) \right) \cdot 2 = 1.05\,\mathrm{m} \tag{4-2}$$

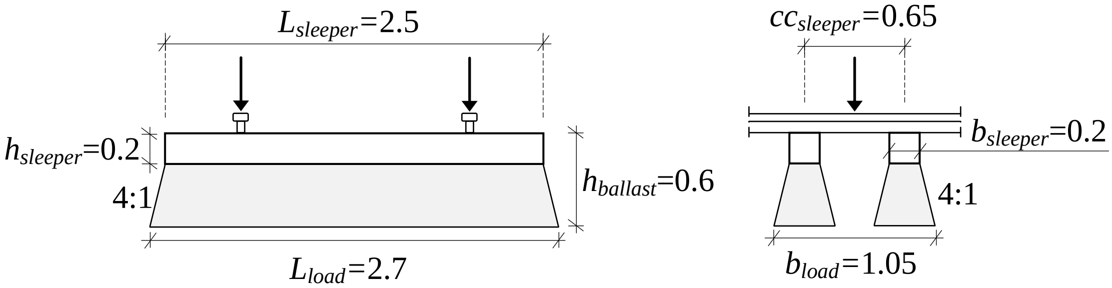

Figure 4.4 Length and width [m] of the distributed load effect within rails, sleepers and ballast calculated based on Eurocode 1 regulations.

A simplification of the distributed load in the models was that the unloaded part between the distributions from each sleeper was included in the distribution width in the longitudinal direction of the bridge. This approach was considered to be reasonable as the further distribution of load effects in the reinforced concrete slab most likely will coincide. Also, the normal force in the ballast would in reality vary over the loaded area but was simplified as a uniform pressure in the model.

The calculated length and width of the distributed load effect was 2.7 and 1.05 m respectively. However, as the load was applied on geometry surfaces or lines that were connected to the size of the elements in the slab the width of the distributed load effect was modified slightly to fit to these dimensions. The new width was 1 m, which reduced the area with approximately 5%. This modification was on the safe side as the pressure, and thereby also the sectional forces, increased slightly.

4.2 Study of distribution of load effects in shell elements

Beam elements distribute load in the longitudinal direction only according to analytical formulations from beam theory. Shell elements on the other hand distribute load in both in-plane directions. This built-in transverse distribution was studied in a shell model of a slab and compared to analytically derived sectional forces distributed over the code regulated effective widths presented in Section 3.3.2.

Traditionally, the design of a slab strip of a trough bridge is based on two different static systems. As described in Section 3.2.2, the main girders act as rotational springs with a fixity degree between fully fixed ends and simply supported ends. The top reinforcement of the slab can be designed conservatively assuming a one-way slab strip with fixed ends and length equal to the free distance between the girders, which is illustrated in Figure 4.5a. The bottom reinforcement is then designed assuming a simply supported one-way slab between the system lines of the main girders; as this induces the maximum field moment, see Figure 4.5b.

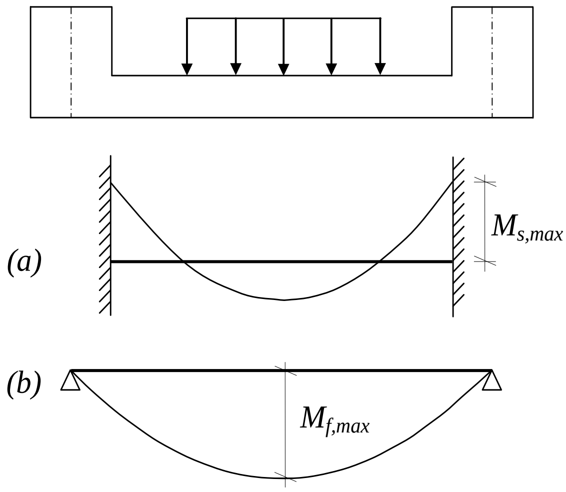

Figure 4.5 Bending moment distribution in a trough bridge slab subjected to a distributed load. Static systems in design of a) top reinforcement and b) bottom reinforcement of a slab strip in a trough bridge.

A simple and effective way of applying the static systems with the different lengths described above on the same geometry is to introduce stiff parts at the ends of the slab. The stiff parts represent the part of the girders between the slab edge and the girder system line. As shown in Figure 4.6, this should induce the sought deformation and thereby also the correct bending moment distribution in both the simply supported and the fixed-end slab. As this geometry is valid for these two extreme cases, it is also applicable for the real fixation degree in the slab-to-girder connection in the trough cross-section. It is natural to assume that this fixation degree is the greatest at support sections where the girders are prevented from free deformation. The rotational stiffness of the girders can then be expected to decrease closer to the mid-span section where the cross-section is the most free to deform.

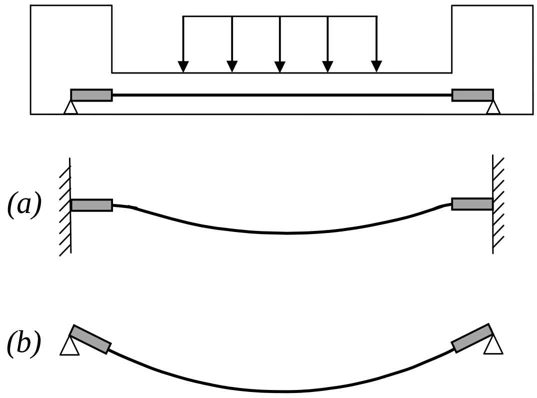

Figure 4.6 Deformed shape of a a) fixed-end, and b) simply supported trough bridge slab with rigid links subjected to a distributed load.

In the shell model the stiff parts were represented by rigid links, which were used to connect the slab edge to a line of beam elements where boundary conditions were applied. Rigid links act like infinitely stiff members between a master and a slave node that constrain the deformation of the slave node. As the rigid link is prevented from any form of deformation, the distance between the master and slave node is kept constant during deformation. Rigid links are appropriate to use when structural elements need to be connected or when boundary conditions need to be applied eccentrically from the centre line of a structural element. Note that boundary conditions must be defined in master nodes. A master node may be part of several rigid links but a slave node must naturally be connected to one rigid link only. Also, a node cannot be both slave and master at the same time.

Two models were created to study the influence of the fixity at the boundaries and the type of load application, i.e. concentrated or distributed load. Schematic drawings of the different boundary conditions and the centre of load applications are shown in Figure 4.7, as well as the global *xyz*-coordinate system and the dimensions of the studied slab. The dimensions of the FE-model correspond to those of one span of the trough bridge models presented later in this report. The models were created using ADINA IN-files (*.in) and the script of one of the models can be found in Appendix E.1.

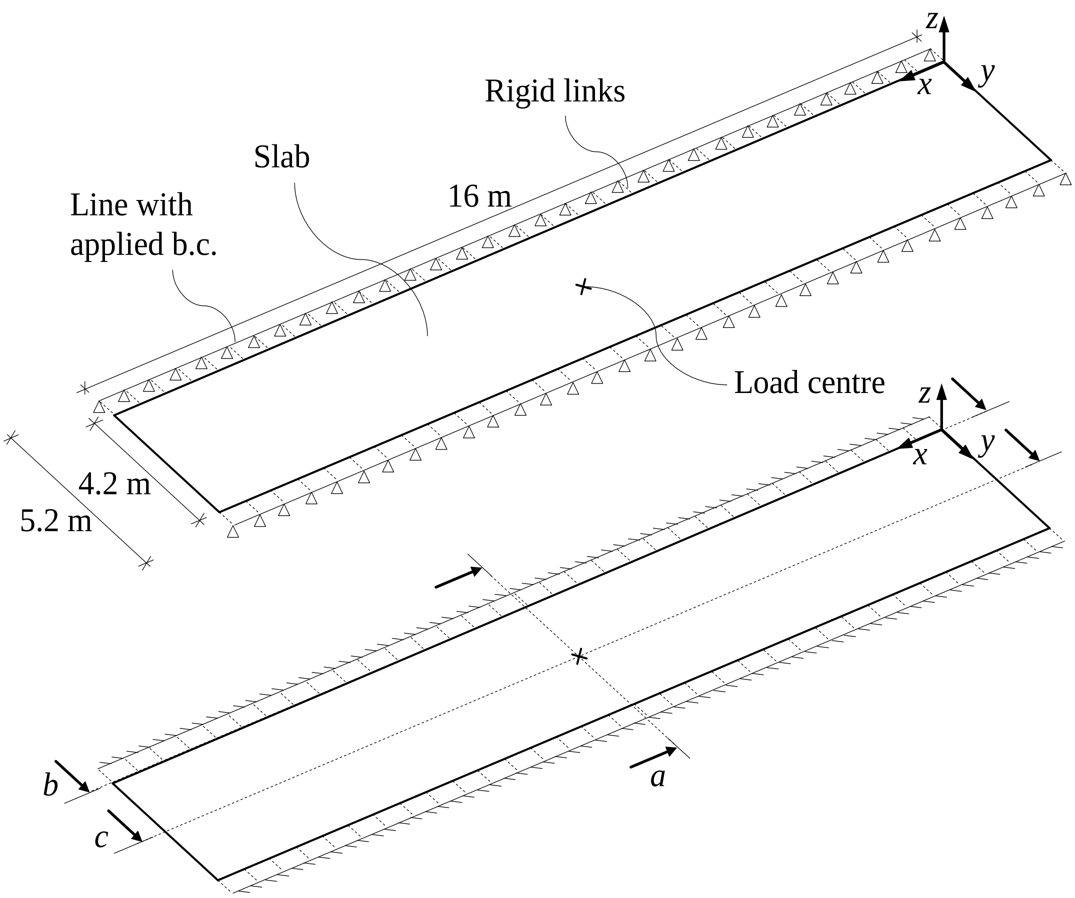

Figure 4.7 Model of slab represented by shell elements with dimensions and studied sections a) transverse mid-section b) edge section and c) mid-span section. Rigid links (represented by dashed lines) connect slab and adjacent beams where boundary conditions are defined as either pinned (top) or fixed (bottom).

The load was applied as pressure onto a geometry surface, as defined in Section 4.1, with its centre as shown in Figure 4.7. A comparison was also made with a centrically placed concentrated load with a magnitude that corresponds to the total load of the pressure load.

Bending moments and shear forces were studied along the transverse mid-section, the edge section and the mid-span section marked in Figure 4.7. The sectional forces were computed according to procedures presented in Section 4.4.1. The transverse distribution of load effects in the slab is of interest as it determines how large area of the concrete slab that is engaged in resisting the load and the maximum bending moments used in design of the slab. In addition, the distribution width at the slab edge is interesting as it affects the distance over which sectional forces that induce torsional moments in the girders of the trough bridge cross-section are introduced.

A convergence study was carried out in order to verify the chosen mesh, which is presented in Appendix C.1. It was assessed that a mesh with 6x32 elements, with element sizes of 0.675x0.5 m and 0.75x0.5 m, achieves a sufficient result with regard to the analyses performed in this project. This mesh density was used for all the studies described in this section.

4.3 FE-models of the trough bridge

The dimensions of the studied trough bridge can be seen in Figure 4.8. The dimensions of the cross-section were chosen with regard to regulations (Banverket, 2007) and typical dimensions, which are presented in Section 2.1. The chosen span is within reasonable limits and corresponds to spans of existing bridges. The bridge was assumed to have no inclination or curvature in order to simplify the model.

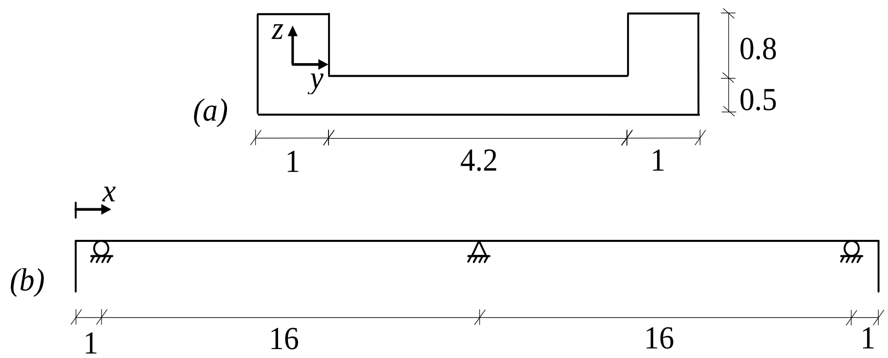

Figure 4.8 a) Cross-section and b) spans [m] of the studied bridge model.

Note that the walkway extensions on each side of the main girders described in Section 2.1 were excluded in the model. This was done to simplify the modelling procedure and also to account for the scenario when walkways are being replaced, as the bridge then only consists of the trough cross-section illustrated in the figure above. It was also considered reasonable since the neglected influence from the self-weight of the walkways on the torsional moment in the girders leads to a more rigorous load case.

Properties of the trough bridge models are presented in Table 4.1. The concrete was assigned isotropic linear elastic behaviour. Poisson’s ratio was chosen to 0.0 as Ekström (2009) found that non-zero values of this constant influence the deflections, stress distributions and sectional forces within the elements in ADINA. The load application differed between the models, as described further in Section 4.3.1 and 4.3.2, but the total magnitude was constant.

Table 4.1 Properties of the trough bridge models.

Modulus of elasticity, E	30 GPa
Poisson’s ratio, v	0.0
Total magnitude of load	1 kN
Span length	16 m
Total length	34 m

Ideally, FE-models should consist of solid elements to simulate the real linear elastic response of the structure. However, this approach is not rational in practice, as it demands more time and resources than what is probable to be gained by the accuracy of the model. Instead, simplified models were used and analysed to enable reasonable results with less modelling and post-processing effort.

Two models, similar to some of those studied in Lundin & Magnander (2012), were investigated; a combined model and a beam grillage model. The latter generates less post-processing and the output should preferably be modified so that it imitates the response of the first, which is considered as a reference model. Shell elements are considered to sufficiently describe the linear elastic response of a structure and the combined model was found to achieve the most reasonable structural response of a number of different FE-models investigated in the previous Master's project. It is therefore assumed in this project that the combined model can be used as a reference when studying the response of the beam grillage model. Model-specific components and inputs for both models are described further in separate sections below.

Similarly to the slab models in the study of distribution of load effects in shell elements, rigid links were used to connect the slab and girders, with the difference that the rigid links were inclined in the trough bridge models to account for the vertical and horizontal eccentricities between the slab edge and the girders. The nodes along the girder were defined as master nodes and the nodes at the slab edge as slave nodes.

Supports were modelled as prescribed displacements. All support nodes were fixed for translations in *y*- and *z*-direction and rotations around the *z*-axis, in line with the degrees of freedom of a bridge superstructure placed upon bearings. The mid support nodes were also fixed for translation in *x*-direction. The global coordinate system is defined in Figure 4.8.

In order to apply the boundary conditions on the bottom edge of the girders, where the supports are located in reality, stiff elements were introduced between the girder centre line and the bottom of the girder cross-section. The stiff elements have the same material properties as the slab and girders, but the cross-section is defined by moments of inertia and area, all with comparably high values to achieve a very rigid behaviour. This approach was also used in the previous Master's project (Lundin & Magnander, 2012) in cases where a node would have needed to be connected to more than one rigid link and act as both master and slave node.

4.3.1 Combined beam-shell model

In the combined model the slab and girders were represented by 4-node shell elements and 2-node Hermitian linear beam elements respectively, see Figure 4.9. The beam elements were modelled in the centre line of the girders and the shell elements along the mid-surface of the slab. The beam elements were analysed in 5 section integration points along the mid axis of the element. The first and last section integration point coincides with the global nodes of the element. The model was created using an ADINA IN-file (*.in), which can be found in Appendix E.2.

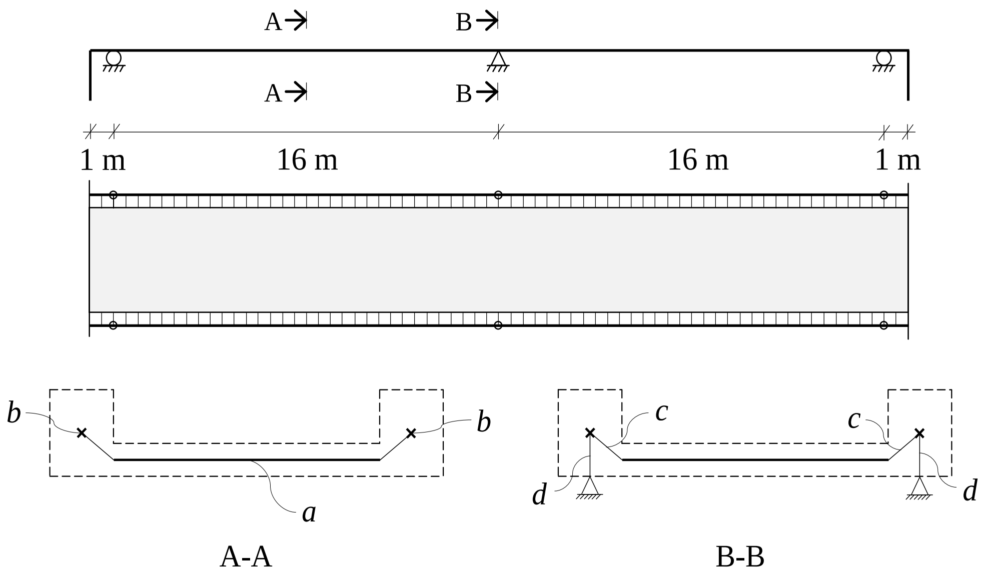

Figure 4.9 Elevation, plan view and cross-sections in section A-A and B-B of combined beam-shell model. a) Slab represented by shell elements b) main girders represented by beam elements c) rigid links connecting slab and main girders d) stiff elements.

The end walls were modelled as plates with 4-node shell elements, with dimensions according to Figure 4.10 and thickness 0.5 m. They were modelled as a vertical continuation of the slab edge, thus starting at the slab mid-plane. The part of the end wall above the slab mid-plane was therefore excluded and hence the height of the end wall was slightly reduced in order to simplify the model. The width of the end wall is equal to the width of the total cross-section and the part that extends beyond the slab is connected to the main girders with rigid links. Note again that the walkway extensions on the outer sides of the girders were neglected in the model, which resulted in a smaller width of the end wall.

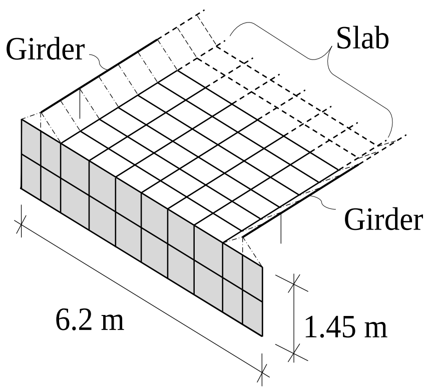

Figure 4.10 End wall (shaded area) represented by shell elements in the combined beam-shell model. Dash-dotted lines represent rigid links.

The distributed load was applied as pressure onto geometry surfaces corresponding to the area calculated in Section 4.1.2. This approach was convenient when using load stepping to create influence lines as all the surfaces were defined in the geometry of the model, hence making the load definition independent of the meshing and the element numbering. The load was constantly applied onto two adjacent surfaces, as illustrated in Figure 4.11. For each new time step the load moved to the next adjacent surface, resulting in load steps of 0.5 m. The time function (*.in) used in modelling can be found in Appendix E.3.

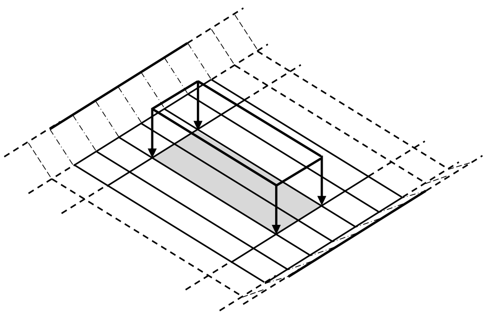

Figure 4.11 Pressure load in the combined model acting on two geometry surfaces for each time step.

A convergence study of the combined model was carried out for the mesh in order to ensure an adequate accuracy of the model. See Appendix C.2 for results. A mesh consisting of 6x68 elements in the slab and 68 elements in each girder was considered to give sufficient accuracy. This mesh was coarse enough to be analysed with the 900-node version of the software.

4.3.2 Beam grillage model

The main girders in the beam grillage model were modelled as in the combined model but the slab consisted instead of parallel transversal beams, also represented by 2-node Hermitian linear beam elements, see Figure 4.12. The ADINA IN-file (*.in) used to create the model is presented in Appendix E.4.

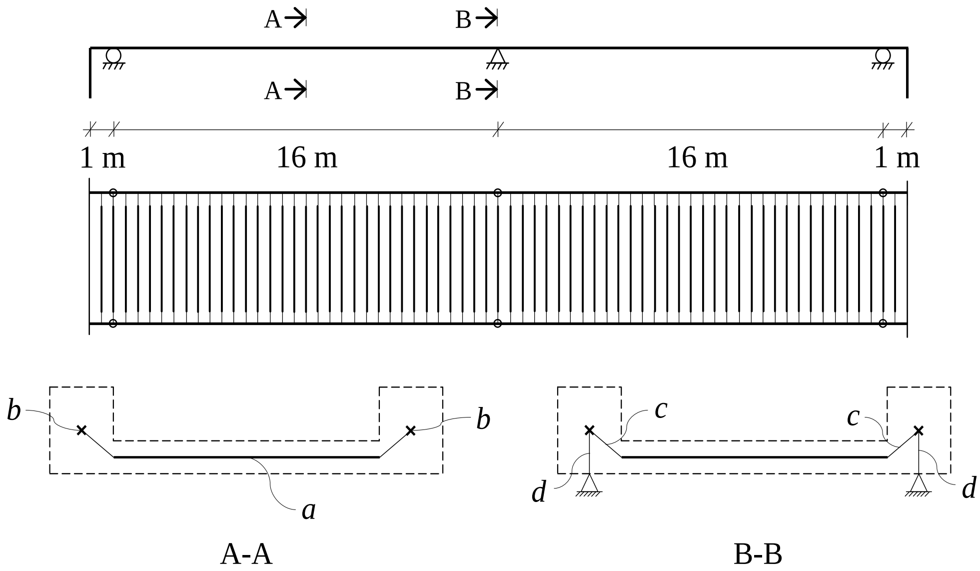

Figure 4.12 Elevation, plan view and cross-sections in section A-A and B-B of beam grillage model. a) Slab represented by transversal beam elements b) main

girders represented by beam elements c) rigid links connecting slab and main girders d) stiff elements.

The end wall was modelled with beam elements placed in the centre of gravity of the end wall, as illustrated in Figure 4.13. The beam elements were assigned a cross-section with dimensions corresponding to the end wall in the combined model, assuming a thickness of 0.5 m and height and width according to the figure below. The vertical eccentricity of the end wall required connections with the transversal beams and the main girders; all achieved by rigid links. The connections ensured that the end walls and the ends of the main girders and slab act together as plates.

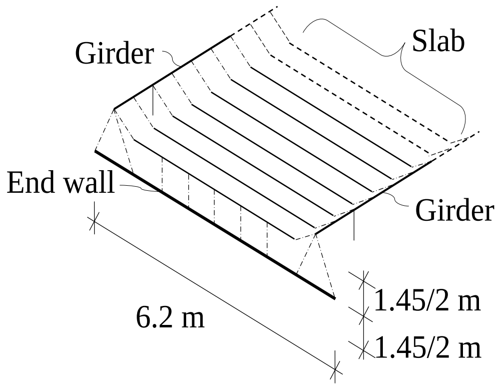

Figure 4.13 End wall represented by beam elements in the beam grillage model. Dash-dotted lines represent rigid links.

The distributed load effect within rails, sleepers and ballast was transformed into distributed line loads acting on several transversal beams within the area calculated in Section 4.1.2. The number of beams that were subjected to load varied as the load moved along the bridge. The load stepping was divided into 136 time steps. For every uneven time step, the load was uniformly distributed between two transversal beams, see Figure 4.14a. For the even time steps, the load was instead divided unevenly between three transversal beams, as indicated in Figure 4.14b. This resulted in load steps of 0.25 m. The latter time steps were added to enable centric load applications in the studied sections, which are both found in nodes along or in line with a transversal beam. The load stepping is defined in the script file (*.in) that is presented in Appendix E.5.

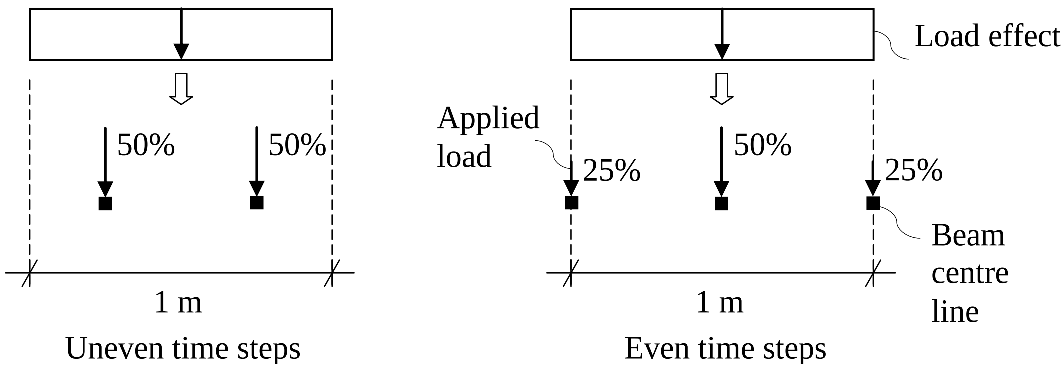

Figure 4.14 Load application in the beam grillage model for a) uneven time steps and b) even time steps.

4.3.3 Modified models

The combined and beam grillage models described in the previous sections were sometimes compared to models where either the load application or boundary conditions were slightly modified to enable comparisons or further studies. These modifications are presented and illustrated in this section.

4.3.3.1 Concentrated load application

In order to evaluate the consequences of modelling with a more accurate load, i.e. that account for the transverse and longitudinal distribution of load effects in rails, sleepers and ballast, models subjected to a concentrated load were created. As illustrated in Figure 4.15, the load was applied onto load points situated slightly above the slab and connected to the slab with rigid links. This was also the procedure of the previous Master's project as a concentrated load needs to be applied onto a point. Similarly to the original load modelling, load stepping was achieved with time steps. See Appendix 4.3.3.1 where changed model inputs are presented.

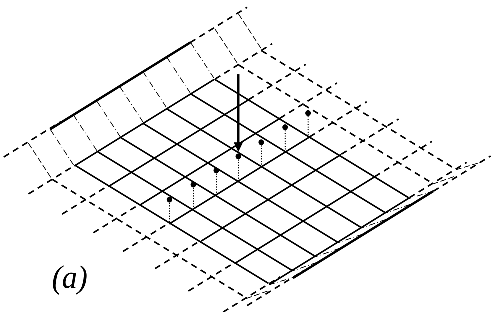

Figure 4.15 Application of a concentrated load in a) the combined model and b) the beam grillage model.

4.3.3.2 Application of concentrated applied torque

It was found of interest to investigate the rotational stiffness of the models as this indicates the degree of fixation in the slab-to-girder connection. This was performed by replacing the load applied on the slab by moving concentrated twisting moments along the girders, as illustrated for the beam grillage model in Figure 4.16. Modified model inputs and time function can be found in Appendix E.6 and 0 respectively.

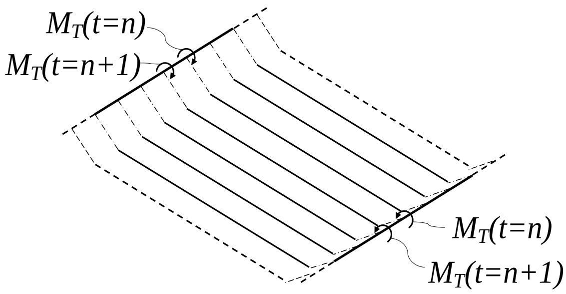

Figure 4.16 Moving concentrated moments M_T applied along the girders in the beam grillage model.

4.3.3.3 Load from four wheel axles

The project focuses on the load from one wheel axle but it was of interest to verify the adjusted beam grillage model outputs with a model subjected to several loads. The load applications at mid-span in the two models are presented in Figure 4.17a-b and were derived from a standard train load application where the concentrated loads are originally 1.6 m apart. The spacing was slightly reduced to fit with the element sizes of the models in this project. Normally, the load should not be element dependent but since this study was simply a verification of the original model it was assessed to be motivated. The load of four wheel axles at the mid support section was applied in analogy with Figure 4.17. The same geometry as in the models for one load application was used, which meant that the loads were placed slightly eccentrically in relation to the mid-span and mid support sections in order to fit with the defined geometry.

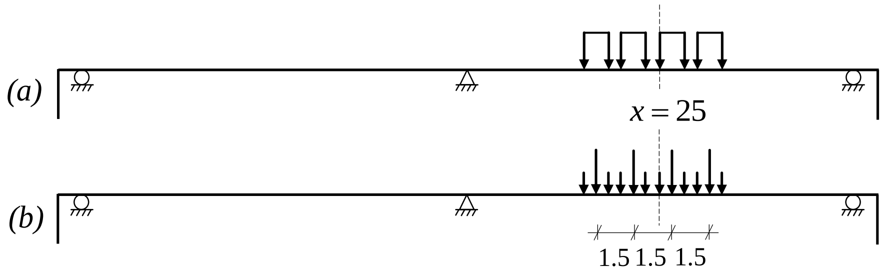

Figure 4.17 Application of the loads of four wheel axles in the mid-span section of a) the combined model and b) the beam grillage model. Distances in [m].

As solely the sectional response when load is placed in the mid-span and mid support sections was of interest, no load stepping was performed for this model.

4.3.3.4 Pinned-roller supports in transverse direction

Translations in *y*-direction were sometimes modelled as fixed below one girder and free below the other. The standard and modified support conditions are presented in Figure 4.18 and are from now on referred to as pinned-pinned and pinned-roller in *y*-direction respectively. Both these boundary conditions exist in real bridges and the use of one free side is applied to avoid restraint forces in the cross-section. When pinned-roller supports are used in this project, this is clearly stated.

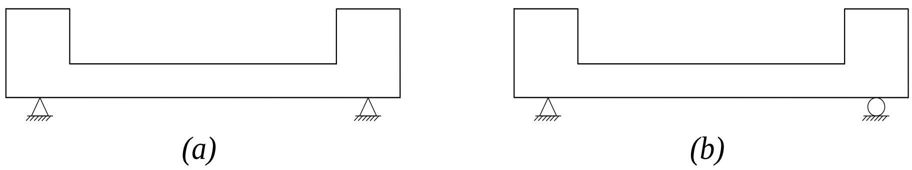

Figure 4.18 Studied support conditions in y-direction, i.e. the transversal direction of the bridge. a) Pinned-pinned supports in y-direction (standard models). b) Pinned-roller supports in y-direction (models used in comparisons where influence of supports is studied).

4.3.3.5 Fixed twisting boundary conditions

Complementary models that correspond to the choices regarding twisting fixation made in the previous Master's project were created as presented in Figure 4.19. Modified model inputs in the ADINA IN-file are presented in Appendix E.8.

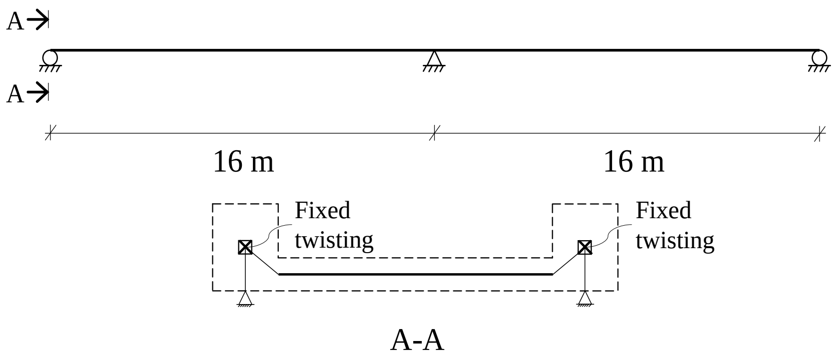

Figure 4.19 Modified model with fixed twisting at end supports replacing end walls.

4.4 Post-processing procedures

The two studied models include different element types and thus the available result output varies. Procedures necessary to obtain sectional forces in the various model components and necessary output processing in ADINA are presented in this section. The methodology when adjusting the beam grillage model with respect to transverse distribution is also described.

4.4.1 Integration of sectional forces

For shell elements sectional forces can be calculated at points on the mid-surface of the shell element where the integration points are projected and are presented with respect to the local coordinate system of the element. Forces and moments are found directly in ADINA by integration of shear stresses and normal stresses over the thickness of the element (Ekström, 2009). This output gives results per meter width of the shell element and in order to obtain the total shear force and bending moment over the whole cross-section the user has to integrate these results over the width of the member.

If results are sought in the global nodes of a structural member, nodal forces and moments about the global *x*-, *y*- and *z*-axes can be calculated. These are defined in the local nodes of each element and summation of nodal values from two elements is often needed in order to find the sectional forces in the global node. Note however that the sectional force in the global node computed in this way represents the total sectional force over the width of one element, as illustrated in Figure 4.20. The total sectional force in a section is therefore found by summation of the sectional force in all global nodes along that section. It is necessary to divide the values obtained from summation of element contributions with the element width in order to achieve sectional forces per unit width. Note that only half an element contributes to the nodal force and moment at the edge of the slab.

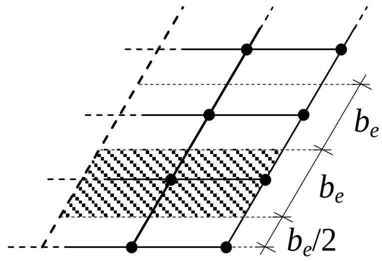

Figure 4.20 The summed up nodal forces and moments in a section are achieved per element width.

Figure 4.21a illustrates the directions of the vertical local nodal forces and the corresponding global sectional force, i.e. the shear force. The left value of the shear force is obtained by summation of the nodal force contributions from the two elements to the left of the node. In ADINA these values are all positive given that the local coordinate system of the shell elements is defined as in Figure 4.21. The same procedure applies for the right value of the shear force, with the difference that the nodal force contributions from the two elements to the right have the opposite sign as the shear force. In analogy bending moment in a global node is obtained by summation of the contributions of nodal moments of the elements to the left or right respectively, see Figure 4.21b.

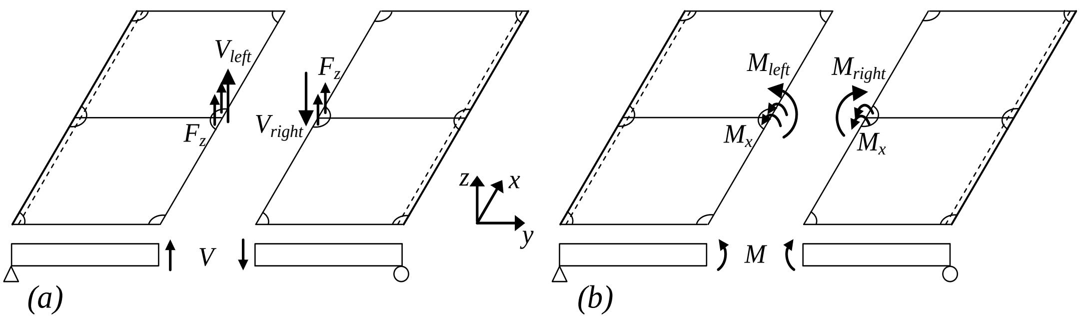

Figure 4.21 a) Nodal forces F_z are summed up to obtain sectional shear forces V_{left} and V_{right}. b) Nodal moments M_x are summed up to obtain sectional bending moments M_{left} and M_{right}.

It is important to account for the sign convention in ADINA, which is shown in Figure 4.21 and differs from the general convention with regard to shear force. In this report the values of the shear force diagrams are presented in accordance with the sign convention in ADINA, but the vertical axis has been inverted to simplify the understanding.

The nodal forces of nodes in elements subjected to distributed load include both the equivalent nodal force, described further in Section 4.1.1, and the vertical sectional force. Thus, when computing the shear force in these nodes, the value of the equivalent nodal force must be added or subtracted depending on the direction of the shear force.

For beam elements sectional forces can be obtained in the section integration points, which include the global nodes, directly in ADINA. No summation of nodal forces is therefore needed. It is however important to account for the equivalent nodal force and moment in nodes of elements subjected to distributed load. The bending moment varies linearly over the element, while the torsional moment and shear force remain constant over the element, which is illustrated in Figure 4.22.

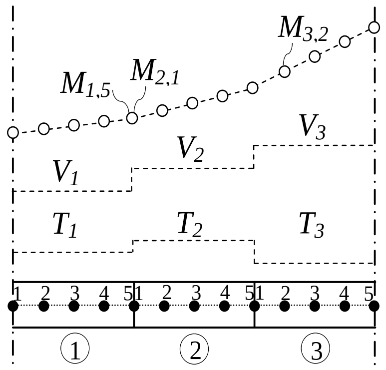

Figure 4.22 Schematic drawing of the bending moment, shear force and torsional moment distributions over three beam elements.

Similar to shell elements, the shear force and bending moment in beam elements are obtained per element width, which refers to the width of the cross-section that is assigned to the beam element. In order to achieve values per unit width the sectional forces need to be divided by the width of the cross-section, which is assigned to the element in the software.

4.4.2 Bending moment for the entire cross-section in the combined model

In the combined model bending moments can be obtained for the slab, as described in the previous section, and girders respectively. The longitudinal bending moment for the entire trough cross-section depends, in addition to the bending moment of the slab and the girders, on the membrane force F_x in the slab and the normal force N of the beam (Lundin & Magnander, 2012). The slab, girders and entire cross-section all have different gravity centres resulting in eccentricities of the two mentioned forces, as illustrated in Figure 4.23.

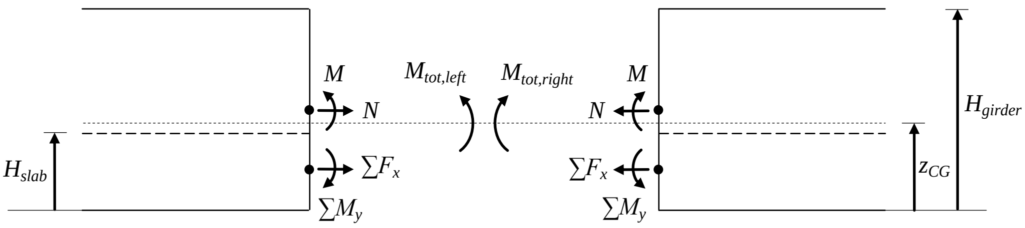

Figure 4.23 Longitudinal bending moment of the entire cross-section in the combined model based on contributions from the girders and the slab, adapted from Lundin & Magnander (2012).

The moment contribution of the slab is therefore derived as

$$M_{slab,left} = -\sum M_y + \sum F_x \cdot \left(z_{CG} - \frac{H_{slab}}{2} \right) \tag{4-3}$$

$$M_{slab,right} = -\sum M_y + \sum F_x \cdot \left(z_{CG} - \frac{H_{slab}}{2} \right) \tag{4-4}$$

Consequently, the moment contribution of the girder is

$$M_{girder,left} = M - N \cdot \left(\frac{H_{girder}}{2} - z_{CG} \right) \tag{4-5}$$

$$M_{girder,right} = M - N \cdot \left(\frac{H_{girder}}{2} - z_{CG} \right) \tag{4-6}$$

The bending moment of the entire cross-section is thus calculated as the summation of the two distributions above.

$$M_{tot,left} = M_{slab,left} + 2 \cdot M_{girder,left} \tag{4-7}$$

$$M_{tot,right} = M_{slab,right} + 2 \cdot M_{girder,right} \tag{4-8}$$

All summations above were executed in a MATLAB command-file that can be found in Appendix F.1.

The bending moment distribution of the entire cross-section in the combined model must correspond exactly to that of the girders in the beam grillage model as well as that of a 2D beam.

4.4.3 Integration of sectional forces in the end walls

The study of sectional forces in the end wall was limited to the width between the two girders. The outer parts of the end wall mainly transfer the applied torsional moment from the girders to the middle part where it is resisted through bending, as described in Section 3.2.4. Sectional forces are therefore only presented in the middle part of the end wall, as indicated in Figure 4.24.

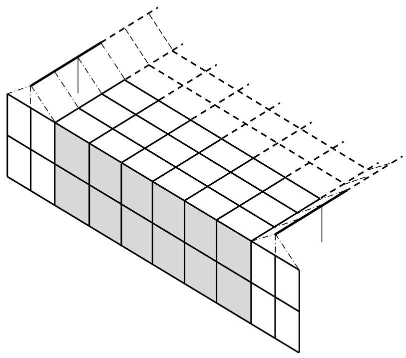

Figure 4.24 The shaded area represents the part of the end wall in the combined model where sectional forces are computed. The same length is considered in the beam grillage model.

For the end wall modelled with shell elements in the combined model, the bending moment for one section may be derived in any point along that section as the horizontal nodal forces in the end wall multiplied by their lever arms to the studied point plus the moment around x in each node of the section. This is presented in Figure 4.25 and Equation (4-9). Consequently, the shear force is computed as the sum of all vertical nodal forces in the studied section, as shown in Figure 4.25 and Equation (4-10). Note that the nodes along the top of the end wall also include the force and moment contributions from the end nodes of the slab, which must be considered.

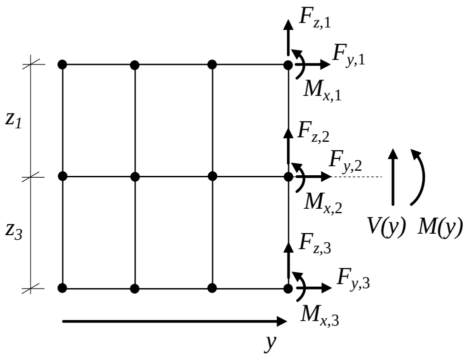

Figure 4.25 Nodal forces and moments that contribute to the bending moment and shear force of the end wall in the combined model at section y.

$$M_{comb}(y) = \sum_{i=1}^{3} \left(F_{y,i} \cdot z_i + M_{x,i} \right) \tag{4-9}$$

$$V_{comb}(y) = \sum_{i=1}^{3} F_{z,i} \tag{4-10}$$

In the beam grillage model the end walls are modelled with beam elements along their centre lines. Sectional forces can be obtained directly in the end wall elements, but due to the use of rigid links between the transversal beam at the slab edge and the end wall, the sectional forces of this beam also need to be considered. This is illustrated in Figure 4.26 and Equations (4-11) and (4-12).

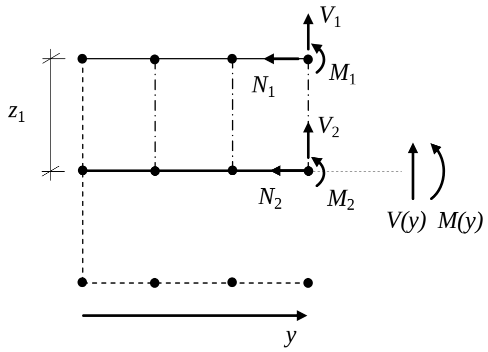

Figure 4.26 Sectional forces that contribute to the bending moment and shear force of the end wall in the beam grillage model at section y.

$$M_{bg}(y) = M_1 + M_2 + N_1 \cdot z_1 \tag{4-11}$$

$$V_{bg}(y) = V_1 + V_2 \tag{4-12}$$

4.4.4 Envelope line diagrams

It is appropriate to establish envelope diagrams to compile the maximum sectional forces for each section into one diagram. This has been described briefly in Section 3.4 in association with influence lines, as envelope diagrams may be created using the maximum value of the influence line for each section. However, for the simple load case in this project it was assumed that the maximum bending moment in each section of the slab occurs when the load is applied directly above that section. Envelope diagrams were therefore created by collecting the sectional forces in each node at the specific time step when load was applied at that node.

4.4.5 Transformation into unit sectional forces

In design of slabs it is of interest to establish the bending moment and shear force per unit width, also denoted unit sectional forces. As mentioned earlier it lies within the property of the isotropic shell finite elements in the combined model to distribute load effects in both directions. Modelling with shell elements hence results in a model that resembles the real linear elastic behaviour of the bridge slab better than the transversal beam elements in the beam grillage model that only transfer load in one direction. Transformation of the sectional forces in the transversal beams into unit sectional forces offers the possibility to distribute the sectional forces in the loaded transversal beams over a certain effective width and thus imitate the behaviour of the combined model.

The transformation into unit bending moments in the beam grillage model differed slightly for influence lines and envelope diagrams, but the common approach was to consider only the even time steps, i.e. when the load was applied onto three transversal beams. For envelope diagrams the unit bending moment was derived by summation of the bending moments in the loaded beams followed by division by the effective width. For influence lines the bending moments to be summed were instead constantly obtained in the three beams located at the studied section. The procedures are presented in Figure 4.27 and Equation (4-13) and were executed in MATLAB-command files, which can be found in Appendix F.3 and F.5 respectively.

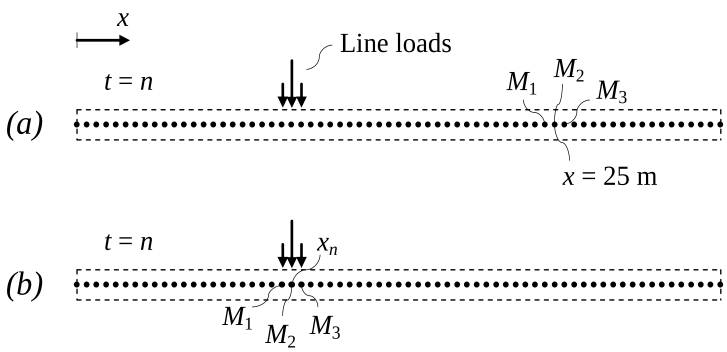

Figure 4.27 Procedure when creating a) influence lines for the mid-span section (x=25 m) and b) envelope diagrams of sectional forces (here illustrated by M) in the slab mid- and edge section in the beam grillage model.

$$m_{x.Ed.bg} = \frac{\sum_{i=1}^{3} M_i}{b_{eff,M}} \tag{4-13}$$

where i refers to the studied sections for influence lines and the loaded sections for envelope diagrams.

The effective width was the same for both envelope diagrams and influence lines. The effective widths valid for the studied trough bridge and its dimensions were derived from BBK 04 (Boverket, 2004) and 'BYGG' (Wahlström (Ed.), 1969) according to the formulas presented in Section 3.3.2. See Appendix D.1 for calculations.

Bending moments were analysed along the mid and edge sections of the slab, as these distributions affect the design support and field moments of the slab. The latter section also affects the distribution of torsional moments in the girders. Note that the equivalent nodal moment that arises due to the applied load, explained in Section 4.1.1, needs to be subtracted from the bending moment that ADINA gives at the slab mid-section. In the influence lines this needs to be taken into account when load is applied at one or several of the studied transversal beams, while in the envelope diagrams it needs to be considered for all load applications.

In the combined model transverse distribution takes place in the model automatically. It was assumed in both the envelope and influence lines that the bending moments within $3h_{slab}$ of the position of the maximum bending moment could be evenly distributed over that width, thus obtaining a unit bending moment. This width was derived from an assumed angle of distribution of normal forces of 45° over the thickness of the slab, see Figure 4.28.

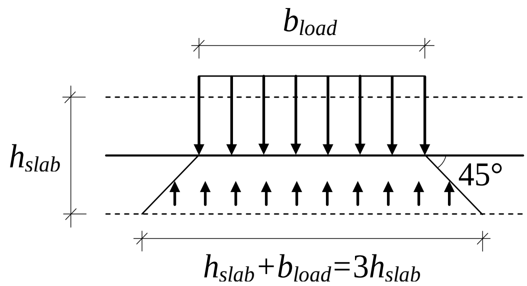

Figure 4.28 Assumption of the distribution of normal forces over the thickness of the slab.

The angle of distribution depends in reality on flexibility and varies for bending moment and shear force, but this variation was neglected to simplify the post-processing procedures. In the model, the load was applied on the shell elements in the slab mid-plane. The distribution of normal forces at the level of the bottom reinforcement is therefore h_{slab} + b_{load} which equals $3h_{slab}$. Selecting the distribution width to three times the height of the slab allowed three values to be summed. As the elements in the combined model had a length of 0.5 m this included the maximum bending moment and the bending moment of the two adjacent nodes. The unit bending moments were calculated as in Figure 4.29 and Equation (4-13) and the MATLAB-codes are found in Appendix F.2 and F.4.

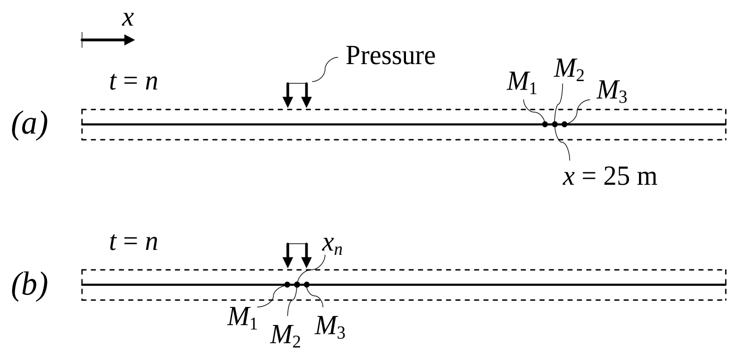

Figure 4.29 Procedure when creating a) influence lines for the mid-span section (x=25 m) and b) envelope diagrams of sectional forces (here illustrated by M) in the slab mid- and edge section in the combined model.

$$m_{x.Ed.comb} = \frac{\sum_{i=1}^{3} M_i}{3h_{slab}} \tag{4-14}$$

Note that it is never possible to obtain the bending moment around the y-axis, m_y, in the slab in the beam grillage model and this moment was therefore not investigated in the combined model either.

The same procedure was carried out for the shear force along the slab edge section only, as the shear force is zero along the mid-section when the slab is subjected to a distributed load. In the design of slabs it is in fact the shear force at 0.9d from the edge that is of interest, but it is the shear force at the edge that contributes to torsion of the main girders. Also, considering the way the models were built and load applied, it was only along the slab edge that the shear forces did not need to be corrected with respect to equivalent nodal forces from the distributed load.

The formulas for unit shear force naturally correspond to those for bending moment. The calculation procedure for the beam grillage and combined model is presented in Equations (4-15) and (4-16) respectively.

$$v_{x.Ed.bg} = \frac{\sum_{i=1}^{3} V_i}{b_{eff,V}} \tag{4-15}$$

$$v_{x.Ed.comb} = \frac{\sum_{i=1}^{3} V_i}{3h_{slab}} \tag{4-16}$$

4.4.6 Calculation of rotational stiffness

The rotational stiffness of the girder was investigated in the modified model with concentrated applied torques moving along the girder, described in Section 4.3.3.2. The rotational stiffness at a section was derived as the applied twisting moment at that section divided by the rotation around x in the girder in the same section, as shown in

Equation (4-17). In the project this was executed in MATLAB-codes and an example can be found in Appendix F.6.

$$k_\theta(x) = \frac{M_T}{\theta_x} \tag{4-17}$$

where $k_\theta(x)$ = rotational stiffness [Nm/rad] of girder in section x

M_T = applied torque [Nm] in the section

θ_x = rotation around x [rad] in the section

5 Results of FE-modelling

The initial study in Section 5.1 provides an understanding of the distribution of load effects within shell elements. All the following sections treat the trough bridge FE-models. An overview of the sectional response of the trough bridge models is given in Section 5.2. The difference in sectional forces generated by the application of a distributed and a concentrated load respectively was examined both in the initial study and in the combined trough bridge model; see Section 5.1 and Section 5.3 respectively. The aim of this study was to determine how much that can be gained by modelling the load application more accurately.

The output from the beam grillage model was adjusted with regard to effective widths to account for transverse distribution of load effects in the slab. These results were compared to the response of the combined model, both for a single load application and a load combination comprising of the load from four wheel axles. The two load cases were studied through influence lines and envelope diagrams and the results are presented in Section 5.4.

A disturbance in the torsional moment distribution in the girders was found in support sections. This local effect was investigated further and the results are presented in Section 5.5.

The structural response of the end walls was compared for the combined and the beam grillage models to evaluate the two modelling approaches and study their influence on the torsional moment distribution in the main girders. These results are presented in Section 5.6, as well as comparisons between the torsional moment of the main girders in models that included end walls and models where the end walls instead were replaced by prescribed fixed twisting at the end supports.

To simplify the interpretation of diagrams for the reader, studied sections of the trough bridge models and the simplified slab model are presented in Figure 5.1 and Figure 5.2 respectively.

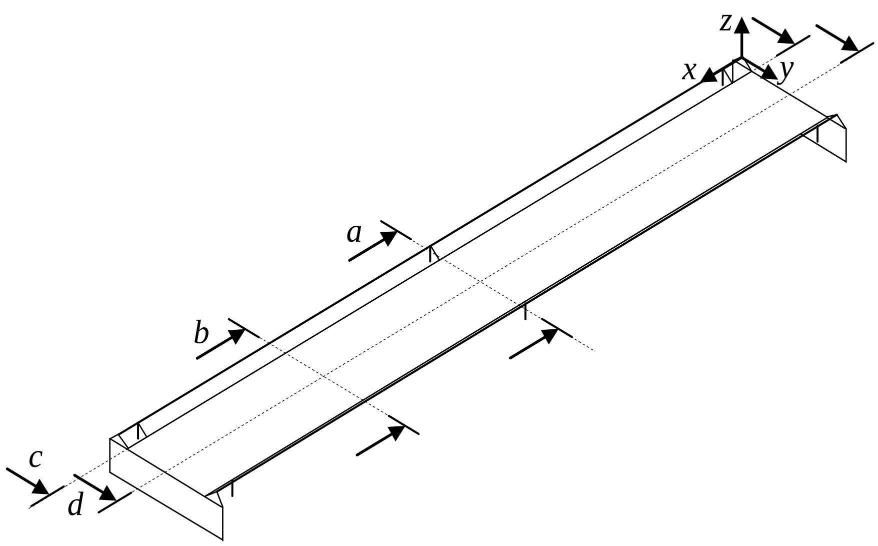

Figure 5.1 Schematic drawing of studied sections in the trough bridge models. a) Mid support section of bridge, b) Mid-span section of bridge, c) Slab edge section and d) Mid-span section of slab.

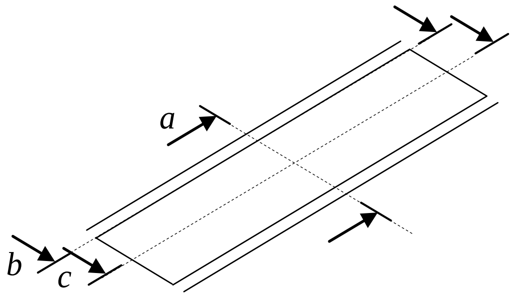

Figure 5.2 Schematic drawing of studied sections in the simplified slab model. a) Transverse mid-section, b) slab edge section and c) mid-span section.

5.1 Distribution of load effects in shell elements

The transverse distribution of load effects within shell elements was studied in the slab model described in Section 4.2. It was of interest to investigate the influence of the fixation degree along the slab edges, as the trough bridge that was the main focus of this project has a fixity in the slab-to-girder connection that lies somewhere in between fully fixed and simply supported.

A comparison was also made between a concentrated and a distributed load application to estimate how much that can be gained by modelling the load more accurately with regard to the distribution of load effects that occurs within rails, sleepers and ballast. The distribution widths that were found in the slab model were compared to analytical values of sectional forces derived for a beam, which were then distributed over effective widths. The aim of this was to examine the relation between the built-in transverse distribution of shell elements and the prescribed effective widths in codes.

All sectional forces are presented per meter, which was achieved according to the procedure described in Section 4.4.1.

5.1.1 Influence of the fixation degree at boundaries

The effect of fixity at boundaries was studied by modelling the slab either as simply supported or with fixed ends along the adjacent beams. The distributed load was applied as pressure on a geometry surface in the centre of the slab in both the longitudinal and transverse direction, according to Section 4.1.2.

The shear force distributions in the transverse mid-section presented in Figure 5.3 deviate from the expected analytical distribution for a beam subjected to loading over a certain length. The shear force distribution should then have a constant slope over the length subjected to load and be constant over non-loaded parts. This difference is believed to depend on the differing distribution of load effects in the transverse direction, i.e. along *x*, between the two models. The lower shear force in the simply supported model suggests a more extensive transverse distribution than in the fixed-end model.

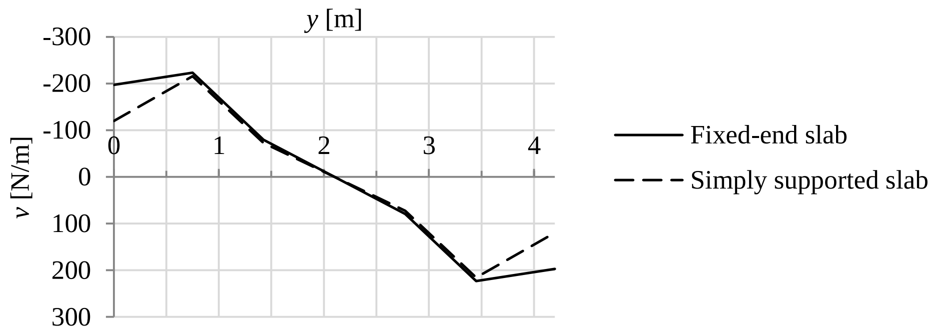

Figure 5.3 Shear force distribution at the transverse mid-section for different boundary conditions.

The distribution transverse to the load-carrying direction is obvious from Figure 5.4, where it can be seen that the shear force along the slab edge is distributed over a certain width. The figure below implies that the fixation degree at the boundary influences the distribution of shear force to a large extent, since the fixed-end model achieved much less transverse distribution than the simply supported. The fixed-end model therefore had a larger maximum shear force along the slab edge than the simply supported; however, a summation of the shear forces in all points along the edge resulted in equal reaction forces for both cases, as was expected. This sum from the FE model corresponds very well with the analytical reaction forces, which demonstrates that the analysis obtained reliable results. The total shear force at mid-span was found using the same summarising method. This value is naturally zero, as can also be found by inspection of the shear force distribution in the transverse mid-section, and was therefore not treated further.

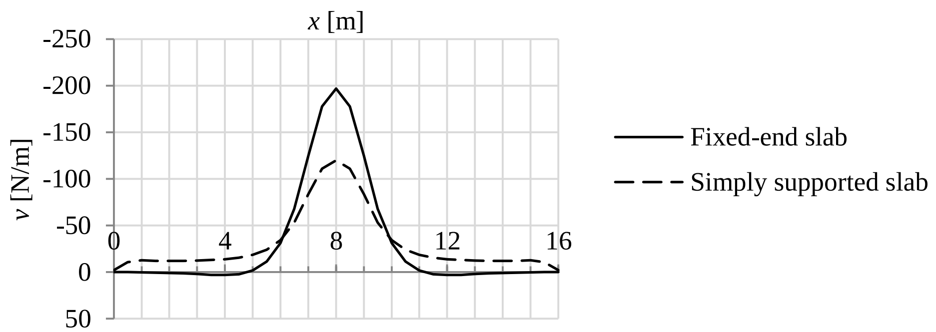

Figure 5.4 Shear force distribution transverse to the load-carrying direction along the slab edge section for different boundary conditions.

The bending moment distributions in the transverse mid-section are presented in Figure 5.5. The appearance of the curve for the fixed-end model corresponds to that of a fixed-end beam. However, the simply supported model gave a negative support moment at the edge of the section, which was not expected as simply supported members should obtain positive bending moments only. Note again that the boundary conditions were not defined along the slab edges at y = 0 m and y = 4.2 m, but along the centroid axis of adjacent beams at y = -0.5 m and y = 4.7 m.

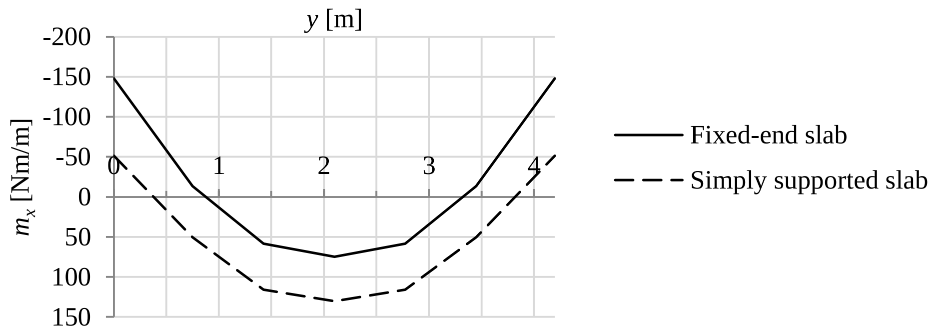

Figure 5.5 Bending moment distribution at mid-section for different boundary conditions.

The bending moment is distributed transversally over a certain width in analogy with the shear force, see Figure 5.6 and Figure 5.7. It can be noted that the bending moments in the middle of the edge section and the mid-span section correspond to the values at slab edge and mid-span in the transverse mid-section. From Figure 5.6 it is apparent that the negative edge moment in the simply supported model is concentrated to a width close to the load application. The rest of the edge moment is positive and a summation of all edge moments results in a positive moment. The occurrence of this local effect on the bending moment was assumed to be a 3D-effect that arises when adjacent nodes in the transversal direction constrain the deformation of nodes close to the load. It was however not studied further in this project. Note also that the bending moment is distributed over the whole length of the slab at both edge and mid sections in the simply supported model, while that of the fixed-end model is limited to a width of approximately half the length of the slab.

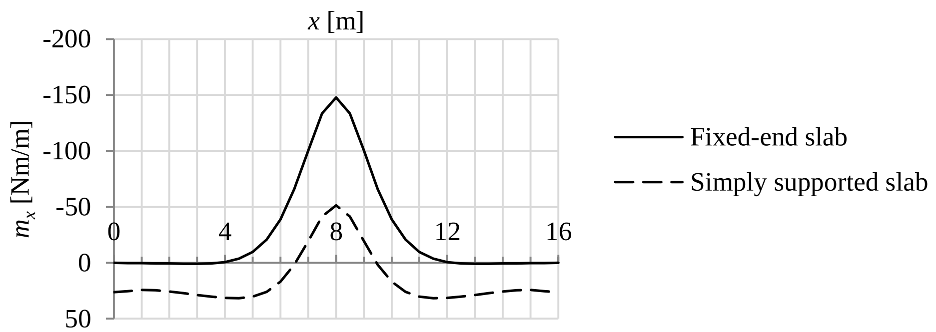

Figure 5.6 Bending moment distribution transverse to the load-carrying direction along the slab edge section for different boundary conditions.

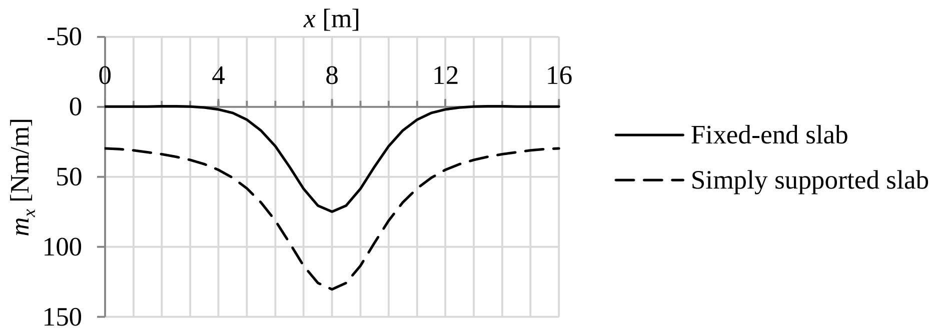

Figure 5.7 Bending moment distribution transverse to the load-carrying direction at mid-span section for different boundary conditions.

The summed bending moments along the mid-span and edge sections are listed in Table 5.1 and compared to analytical solutions for a beam. Since the load is distributed over a certain length, and not over the entire span, no explicit fundamental case exists for the fixed-end model. These analytical values were therefore calculated through superposition of two fundamental cases, as described in detail in Appendix B. Analytical bending moments were obtained both for the case of a span of 4.2 m, which is the slab length, and a span of 5.2 m, which corresponds to the distance between the girder system lines, in analogy with Section 4.2.

Table 5.1 Summations of bending moment along mid-span and edge sections of the slab[Nm] compared to analytical solutions for a beam of different lengths.

	Fixed-end slab			Simply supported slab		
	Mid-span	Edge	ΔM	Mid-span	Edge	ΔM
Analytical (5.2 m)	371.01	-341.25	712.25	961.54	249.75	711.79
Analytical (4.2 m)	259.55	-452.23	711.75	711.79	0.00	711.79
Model	268.59	-443.19	711.79	961.54	249.75	711.79
ΔM (5.2 m)	102.42	-101.94	0.46	0.00	0.00	0.00
ΔM (4.2 m)	-9.04	9.04	-0.04	-249.75	-249.75	0.00

The response of the fixed-end model corresponds rather well with that of a fixed-end beam of span length 4.2 m. Although the values at the edge and mid-span of the slab differ by a small amount from the analytical solution, the differences between the support and field moments are equal. This difference also corresponds to the field moment for the simply supported case, which is expected. The result of the simply supported model corresponds exactly to the analytical solution of a simply supported beam with a length of 5.2 m. These results imply that the use of rigid links is applicable in design of reinforcement in the slab of a trough bridge, which has a fixation degree somewhere in between fully fixed and simply supported.

5.1.2 Influence of type of load application

The slab was subjected to either a centrically placed concentrated load or a distributed load, as described in Section 4.1.2, and only the fixed-end slab was examined. Since both loads are of the same total magnitude, the reaction forces are equal but the edge moments differ.

The transverse distributions of shear force along the slab edge are presented in Figure 5.8 and Figure 5.9, where the latter is an enlargement of the distribution width near $v = 0$. From the zoomed-in graph it can be seen that the width of the slab that is engaged in resisting the load is the same disregarding the type of load. The maximum values differ slightly where the distributed load results in somewhat higher maximum shear force. The amount of transverse distribution is therefore slightly smaller in the slab subjected to a distributed load. The sum of all values along the edge is naturally the same for both load applications, as the total reaction force must be equal.

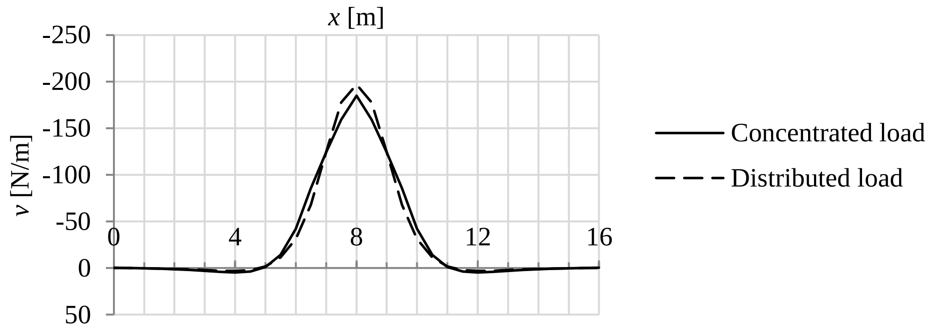

Figure 5.8 Shear force distribution transverse to the load-carrying direction along the slab edge section for different load types.

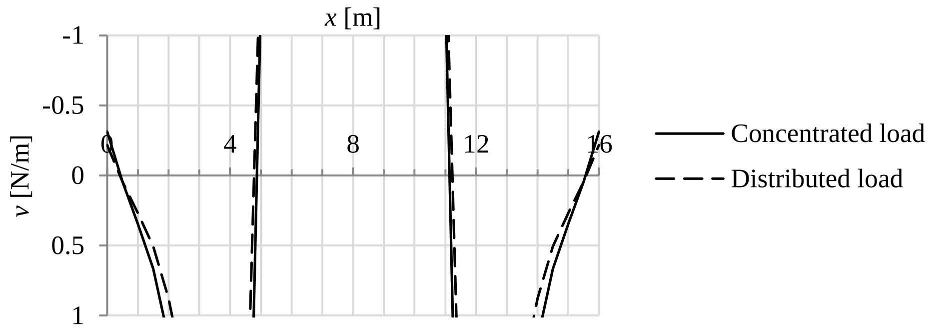

Figure 5.9 Zoomed-in graph of the shear force distribution transverse to the load-carrying direction along the slab edge section for different load types.

The shear force distribution along the mid-span section and the transverse mid-section of the slab are presented in Figure 5.10 and Figure 5.11 respectively. It is apparent that no transverse distribution of shear force due to the concentrated load application occurs in the mid-span section of the slab as the shear force is confined to the node subjected to load. The lack of distribution in this section may depend on that shell elements cannot describe the shear force in the loaded section in a correct way. As can be seen in Figure 5.11 the shear force is distributed in sections further away from the load application. The shear force distribution in this figure can be compared with that of a beam, where a concentrated load should give rise to a constant shear force on each side of the load application. This is not the case in the slab model as the transverse distribution of shear force in the slab results in lower values further away from the load. The distribution would be captured better if the mesh was more refined as this rather coarse mesh only gives the values in a few sections along the span.

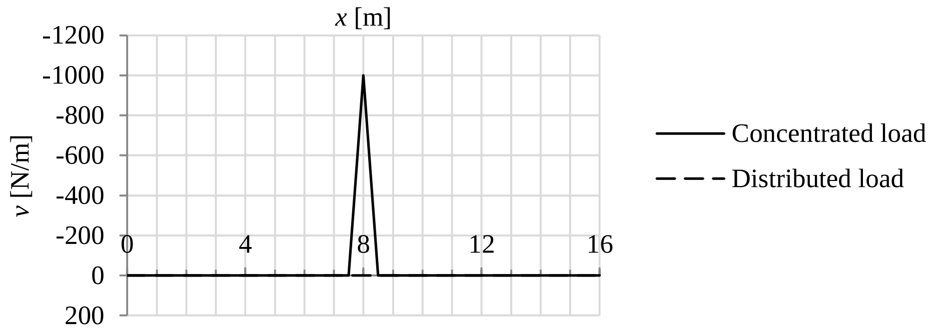

Figure 5.10 Shear force distribution transverse to the load-carrying direction along the slab mid-span section for different load types.

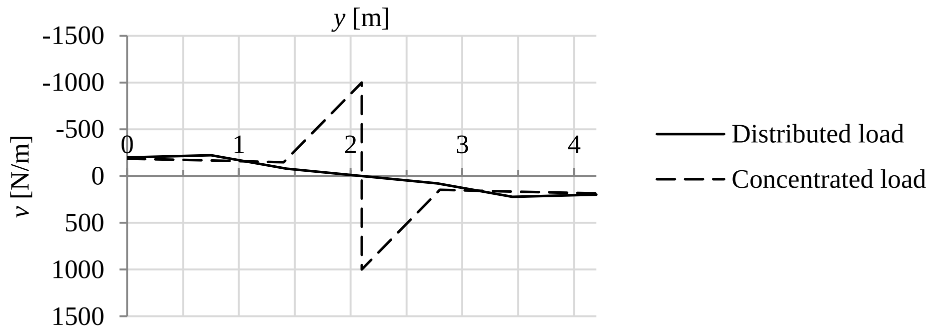

Figure 5.11 Shear force distribution at transverse mid-section for different load types.

In accordance with the shear force, the bending moment distributions along the slab edge transverse to the main direction of the slab and enlargements near $m_x = 0$ are shown in Figure 5.12 and Figure 5.13. Similarly, these results imply that the type of load application does not to a large extent affect the transverse distribution of bending moments along the slab edge in this finite element model as both graphs approach zero in the same sections. The maximum bending moment is however somewhat greater in the model subjected to concentrated load, hence less transverse distribution occurs for this model.

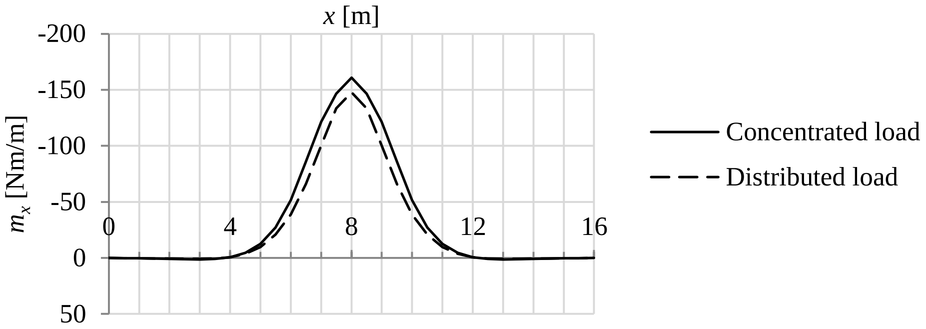

Figure 5.12 Bending moment distribution transverse to the load-carrying direction along the slab edge section for different load types.

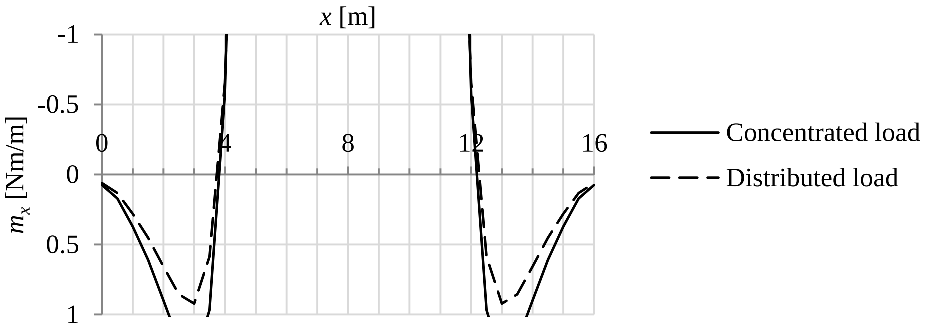

Figure 5.13 Zoomed-in graph of the bending moment distribution transverse to the load-carrying direction along the slab edge section for different load types.

The bending moment at mid-span differs greatly in magnitude, while no difference in the distribution width can be detected, see Figure 5.14. The difference in magnitude depends to a large extent on the type of load application and it is difficult to assess whether the transverse distribution differs. FE-models have difficulties with describing the structural response in sections close to a concentrated load application and the difference between the two load types is therefore expected. In fact, if the mesh was finer it would be seen that the bending moment generated by the concentrated load approaches infinity. This is of course not realistic but it is assumed that the concentrated load do result in larger bending moment than the distributed load as this agrees with the analytical solution for a beam.

Figure 5.15 illustrates the bending moment distribution at the transverse mid-section, where the difference at mid-span also is apparent. Note however the small difference between the different edge moments described earlier.

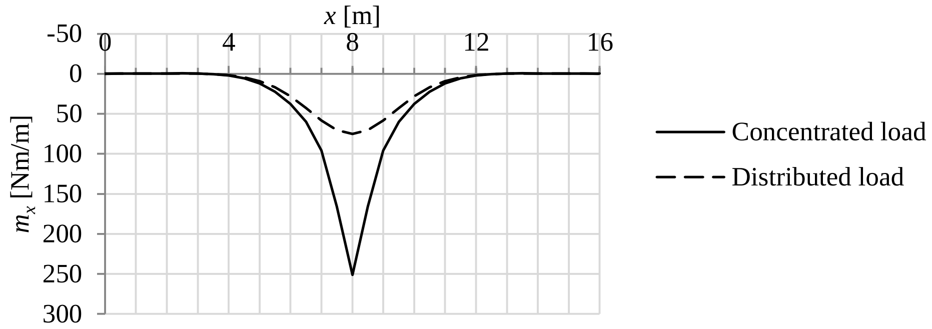

Figure 5.14 Bending moment distribution transverse to the load-carrying direction along the slab mid-span section for different load types.

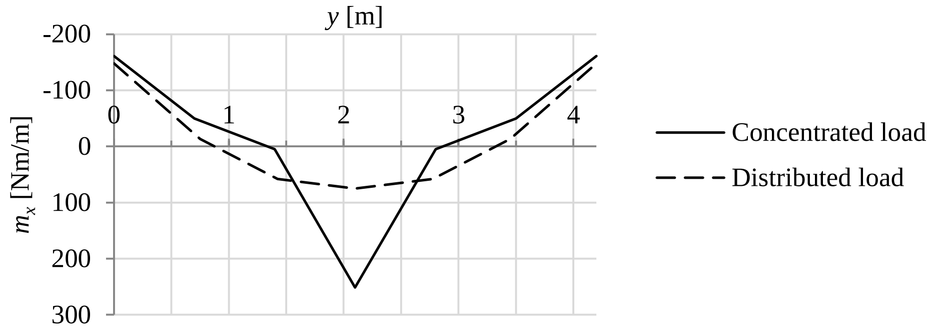

Figure 5.15 Bending moment distribution at transverse mid-section for different load types.

5.1.3 Comparison with effective widths in codes

If the slab had instead been modelled with beam elements no transverse distributions would have occurred within the model. One approach to manually distribute the load effects is to evenly distribute the edge and mid-section sectional forces over effective widths prescribed in codes, as described in Section 3.3.2. It was therefore considered to be of interest to compare the sectional forces of the shell elements of the simplified slab model with those obtained analytically and distributed over the effective widths derived from BBK 04 (Boverket, 2004) and 'BYGG' (Wahlström (Ed.), 1969) in Section 3.3.2. See Appendix B and Appendix D.1 for calculations of analytical solutions and effective widths respectively.

Initially, the fixed-end slab model with distributed load effect was studied. It can be noted in Figure 5.16 and Figure 5.17 that the shell elements distribute the bending moment wider within the slab than what is recommended by BBK 04, thus resulting in lower design moments. The analytical bending moment distributed according to the recommendation in 'BYGG' agrees relatively well with the maximum bending moment in the slab model.

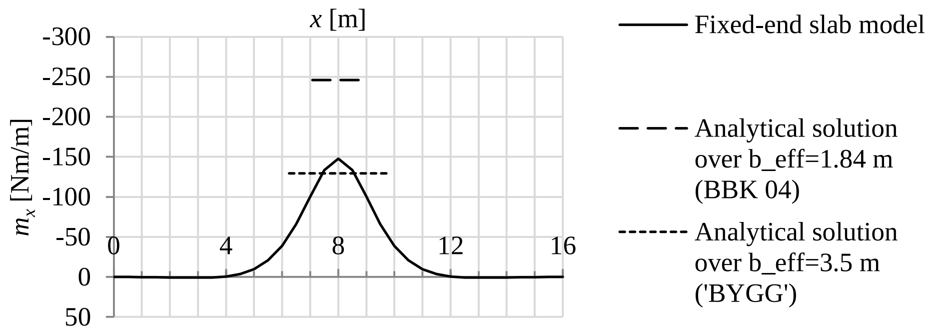

Figure 5.16 Bending moment distribution transverse to the load-carrying direction along the slab edge section based on shell elements in the fixed-end model and analytical values spread over effective widths.

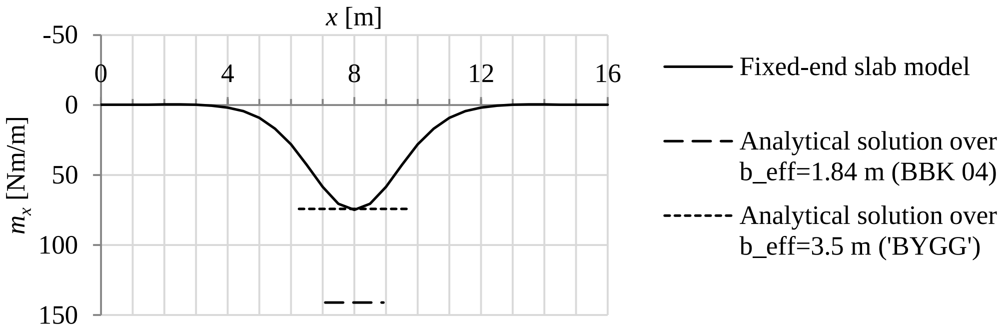

Figure 5.17 Bending moment distribution transverse to the load-carrying direction along slab mid-span section based on shell elements in the fixed-end model and analytical values spread over effective widths.

The shear force was only studied along the slab edge, since it equals zero at the mid-span section for the distributed load application. The distributions transverse to the load-carrying direction are presented in Figure 5.18 where it is apparent that the prescribed effective widths in both codes allow a transverse distribution that is too large in relation to the distribution in the slab model. This suggests that the recommendations result in an unsafe design shear force, if the result of the shell model is assumed to represent the real linear elastic solution.

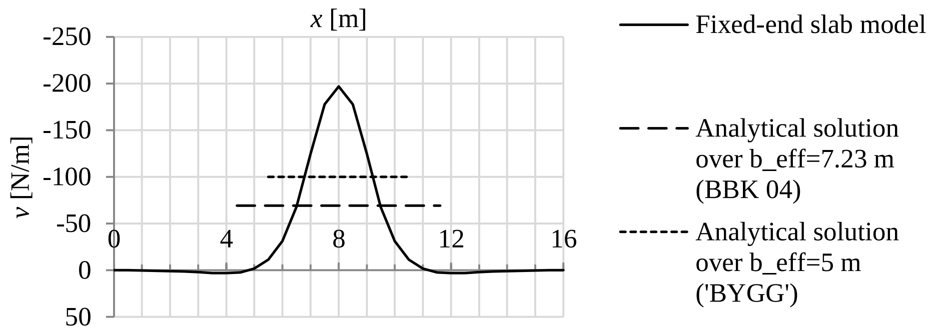

Figure 5.18 Shear force distribution transverse to the load-carrying direction along the slab edge section based on shell elements in the fixed-end model and analytical values spread over effective widths.

The simply supported model offers less possibility for comparison at the slab edge due to the local negative bending moment near the load application. As illustrated in Figure 5.19, the analytical values distributed over effective widths are all positive, while the slab model gives bending moments that vary in sign transversally.

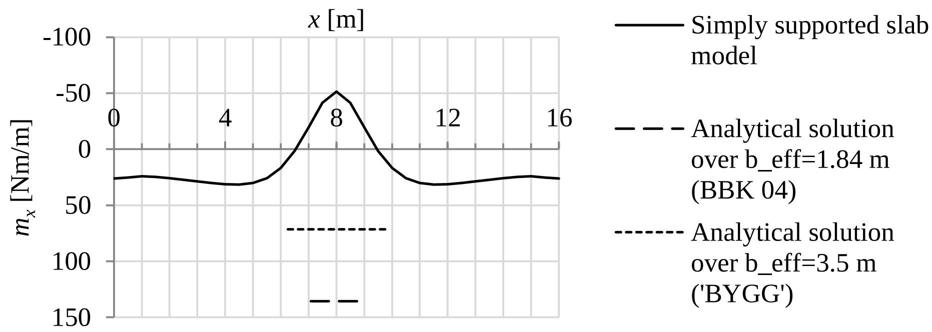

Figure 5.19 Bending moment distribution transverse to the load-carrying direction along the slab edge section based on shell elements in the simply supported model and analytical values spread over effective widths.

Along the mid-section the slab model shows the same behaviour as what the analytical model predicts, when it comes to the sign of the bending moment, see Figure 5.20. However, due to the extensive distribution transverse to the load-carrying direction the maximum bending moment is significantly smaller.

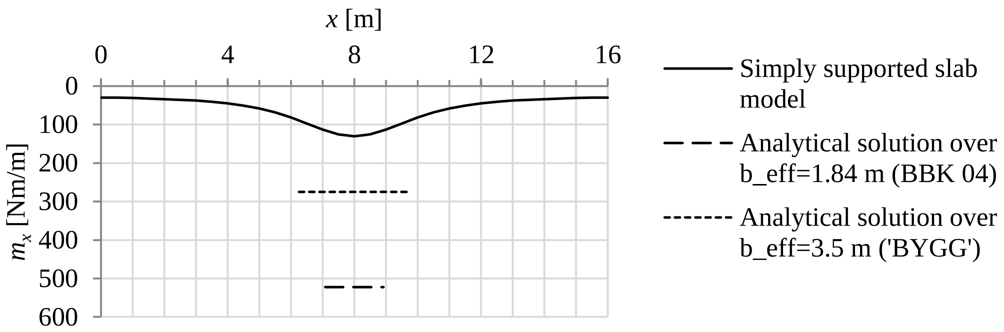

Figure 5.20 Bending moment distribution transverse to the load-carrying direction along slab mid-span section based on shell elements in the simply supported model and analytical values spread over effective widths.

The shear force distribution along the edge of the simply supported slab model is presented in Figure 5.21. As for the fixed-end model, the effective widths according to both codes result in design shear forces lower than what is found in the slab model.

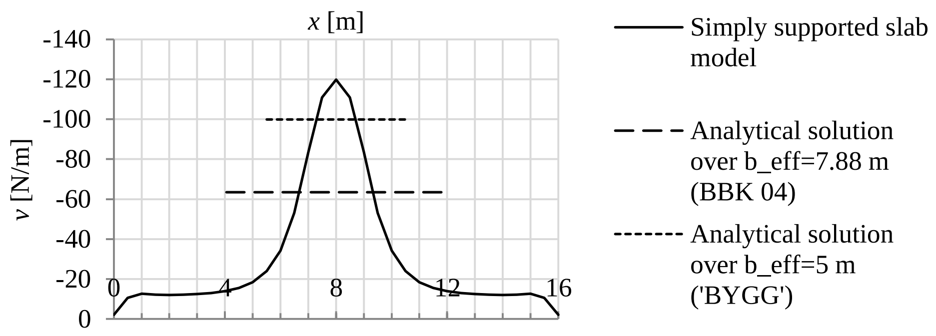

Figure 5.21 Shear force distribution transverse to the load-carrying direction along slab edge section based on shell elements in the simply supported model and analytical values spread over effective widths.

This study showed that shell elements generally distribute bending moments more than what is recommended in the codes, especially in the simply supported slab. Neither of the fixed-end and the simply supported slab models generated design shear forces that were on the safe side of the analytical value distributed over an effective width according to the codes. As the shell elements were assumed to describe a realistic linear elastic orthotropic response, all effective widths that result in sectional forces larger than those found in the slab model were considered to be safe to use in design.

In some cases the code prescribed values are conservative and it can be discussed whether the use of these values results in economic designs. However, if the design sectional forces were to be found without considering an effective width, corresponding to a 2D-beam, and thus neglecting the effect of transverse distribution of load effects the results would be even larger.

5.2 Sectional forces in the trough bridge FE-models

In this section the sectional response of the trough bridge FE-models is presented to help understanding of the analyses presented later in the report. The reader is referred to the thesis of the previous master's thesis project (Lundin & Magnander, 2012) for extensive analyses of the sectional response of trough bridges with various models. As the distributions of the total bending moment and shear force for the entire cross-section do not differ between the combined and the beam grillage model, these results are presented for the combined model only. The load was applied in accordance with the distributed load effect described in Section 4.1.2.

5.2.1 Bending moment distribution

The distributions of the bending moment for the entire cross-section are presented in Figure 5.22 and Figure 5.23, when the load was applied in either the mid support or mid-span section. Notice that the values are presented in reverse order on the vertical axis in accordance with general code of practice.

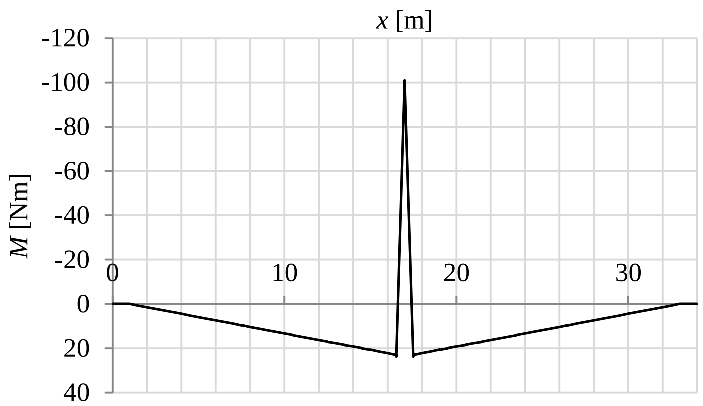

Figure 5.22 Distribution of total bending moment in the trough cross-section when load is applied at mid support section in the combined model.

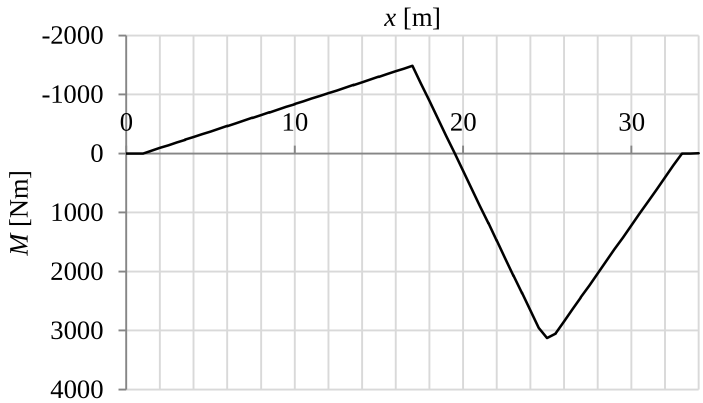

Figure 5.23 Distribution of total bending moment in the trough cross-section when load is applied at mid-span section in the combined model.

When load is applied at the mid-support section, the bending moment distribution obtains a peak of negative bending moment, large in comparison with the magnitude along the rest of the beam, but significantly smaller than the values in Figure 5.23. This negative support moment would not occur if a concentrated load had been applied and it arises due to the width of the load that extends slightly in both directions from the support section.

The shape of the bending moment distribution, when load is applied in the mid-span section, resembles that of a typical two span beam subjected to a concentrated load in the middle of the second span. One difference though is that the maximum peak is evened out due to the extension of the load in the longitudinal direction of the bridge. The bending moment is confined within the end supports and no bending moment occurs in the cantilevers that extend towards the end walls, which can be expected of a continuous beam.

5.2.2 Shear force distribution

Similarly to the bending moment distributions, the distributions of the total shear force are presented for the entire cross-section of the combined model, see Figure 5.24 and Figure 5.25 for the case of load in the mid support and mid-span section respectively.

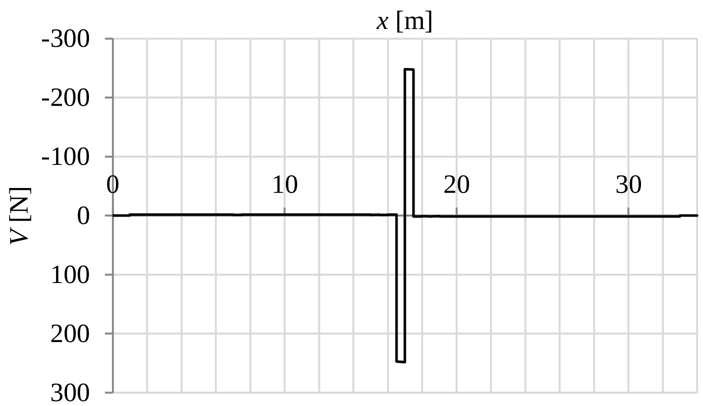

Figure 5.24 Distribution of total shear force in the trough cross-section when load is applied at mid support section in the combined model.

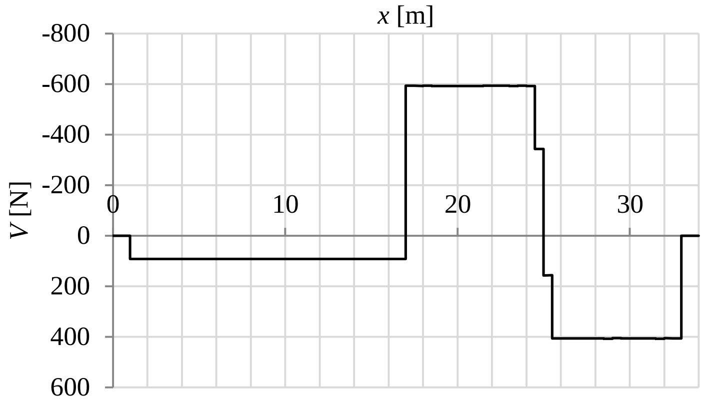

Figure 5.25 Distribution of total shear force in the trough cross-section when load is applied at mid-span section in the combined model.

When the load is applied directly above the mid support section shear force occurs in the loaded region only and the shear force along the rest of the bridge is therefore zero.

When the trough cross-section is subjected to load in the mid-span section, the majority of the load is resisted at the two adjacent supports, but some load is also transferred to the support furthest away. No shear force occurs however in the cantilevering parts between the end walls and the end supports. This is a typical distribution for a continuous beam.

5.2.3 Torsional moment distribution in one girder

The torsional moment distributions in the girders differ between the investigated models and results from both models are therefore presented in Figure 5.26 and Figure 5.27, where the load was applied in the mid support and mid-span section respectively.

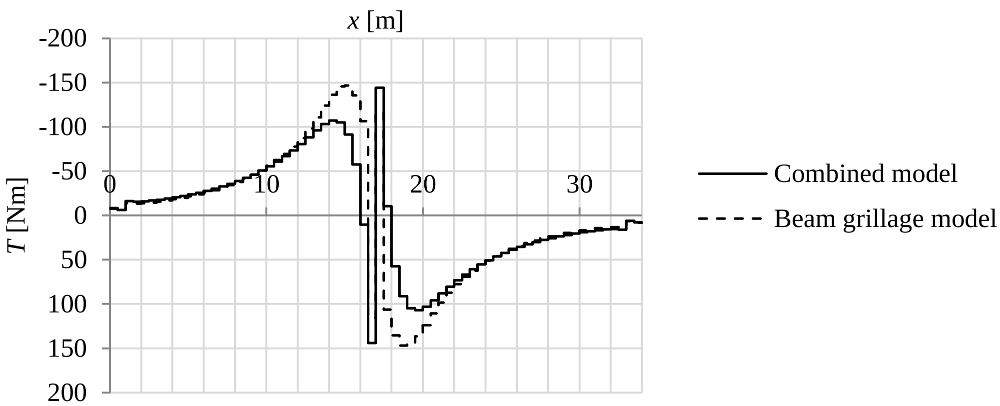

Figure 5.26 Torsional moment distribution in one girder for the combined and beam grillage model respectively, when load is applied at mid support section.

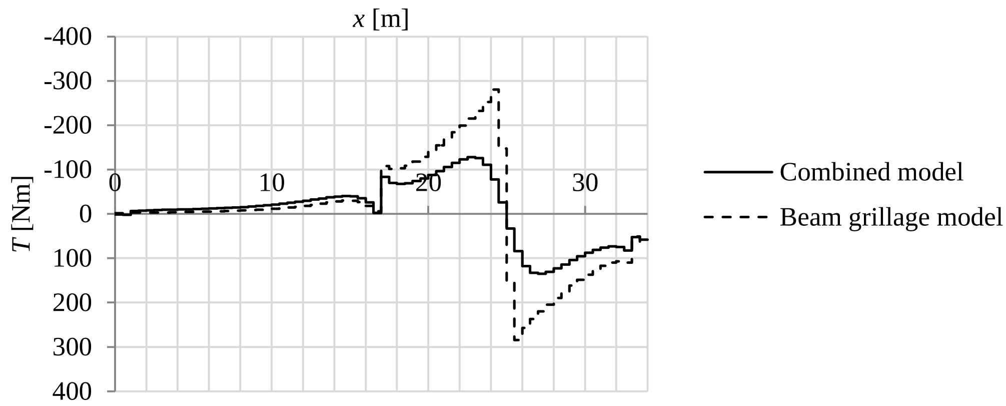

Figure 5.27 Torsional moment distribution in one girder for the combined and beam grillage model respectively, when load is applied at mid-span section.

Even though the torsional moment has opposite sign at each side of the load application, the girders are induced to twisting in the same direction along the entire bridge, in accordance with Figure 3.5 in Section 3.2.1.

It can be noticed in the figures above that all three supports influence the torsional moment distribution. The large variation at the mid-support section, when load is applied in this section, is treated further in Section 5.3.4. The disturbances of all supports have been investigated and the results are presented in Section 5.5.

5.3 Comparison with a concentrated load application

In the previous master's thesis project (Lundin & Magnander, 2012) the load from one wheel pair was simplified into one concentrated load acting on the slab centrically between the girders. One aim of this thesis was to investigate the effect of a more accurately modelled load application, where the distributions of load effects within rails, sleepers and ballast are taken into account. The load was therefore modelled as distributed over a certain area, as described in Section 4.1.2.

To enable a comparison with the simplified approach a new model was created, in which a concentrated load was applied centrically on the slab in accordance with the previous master's thesis project. This is specified in Section 4.3.3.1. Comparisons of the two models were carried out with respect to bending moment, shear force and normal force in the slab and torsional moment in the main girders. When producing graphs for the bending moment and shear force distributions it was necessary to account for the equivalent nodal forces and moments that are the result of distributed loading. Bending moments and shear forces are presented per meter in accordance with the procedure in Section 4.4.1.

5.3.1 Bending moment in slab

The longitudinal and transverse bending moment distributions were studied in the combined and beam grillage models when subjected to either distributed or concentrated load.

A beam will obtain different bending moment distributions both with regard to shape and maximum value depending on whether the applied load is distributed or concentrated. A concentrated load will generate higher support and field moments and the moment diagram will be linear between supports and mid-span. A load that is distributed over the entire span will instead cause a bending moment diagram with parabolic shape. The distributed load used in this study was only applied over a part of the span, which should generate a parabolic bending moment distribution over the loaded length of the beam and a linear variation over the rest of the beam.

The expected outcome for the bridge slab in the combined model is in general similar to that described for a beam above, but the slab also allows distribution of load effects transverse to the load-carrying direction. It was shown in the initial study of transverse distribution in shell elements in Section 5.1.2 that, although the field moment varied greatly between the models, the load type had little influence on the support moment and the bending moment distribution transverse to the load-carrying direction. As can be seen in Figure 5.28 the combined model also obtains different field moments while the support moments are similar between the two models with different load applications.

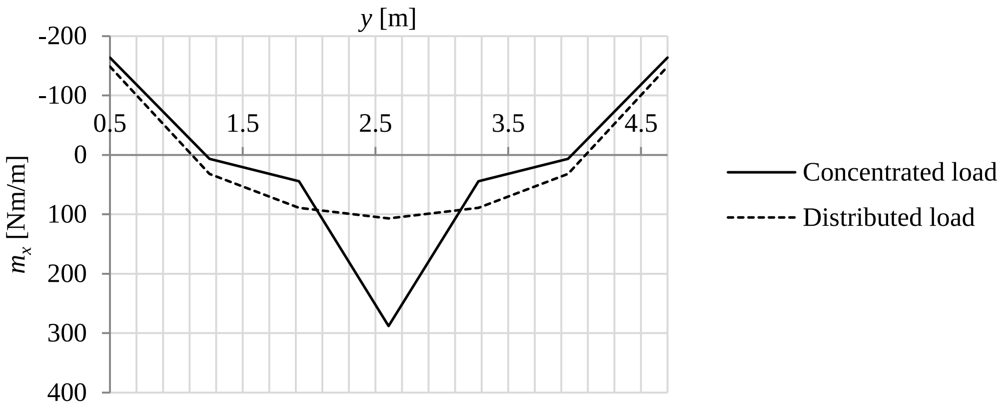

Figure 5.28 Bending moment distributions in the slab along mid support section of the combined model for the cases of concentrated and distributed load. Load at mid support section.

It can also be noted in the figure above that the bending moment distribution for the case of concentrated load is non-linear between support and field sections. This is assumed to depend on a variation in the amount of transverse distribution in different sections of the slab, i.e. the amount of transverse distribution along the slab edge is different from that of the mid-span section of the slab. A finer mesh would capture the distribution along the span better but the chosen mesh was considered to be sufficient to give a general description of the variation in sectional forces.

Figure 5.29 and Figure 5.30 show the bending moment distributions transverse to the load-carrying direction along the slab edge when the load is applied at mid support and mid-span respectively. The bending moments along the edge section generally agree very well between the two models. However, the model where the distribution of load effect within rails, sleepers and ballast is taken into account generates a slightly smaller bending moment in most sections.

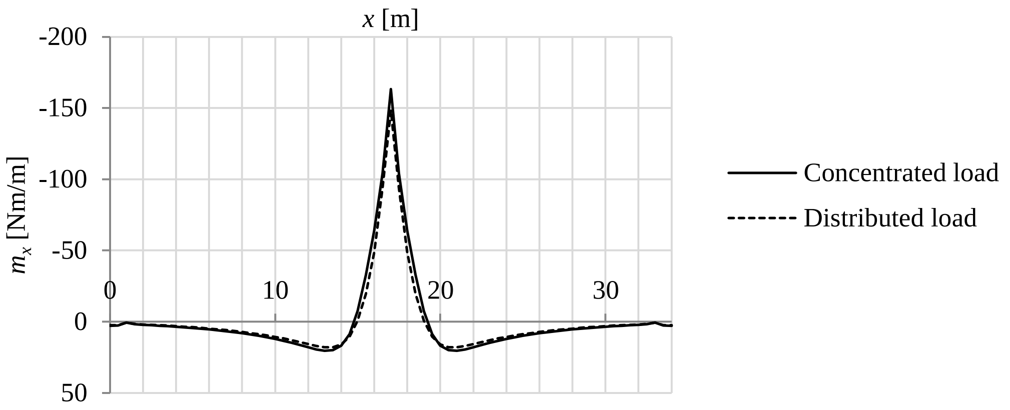

Figure 5.29 Bending moment distributions along the slab edge in the combined model for the cases of concentrated and distributed load. Load at mid support section.

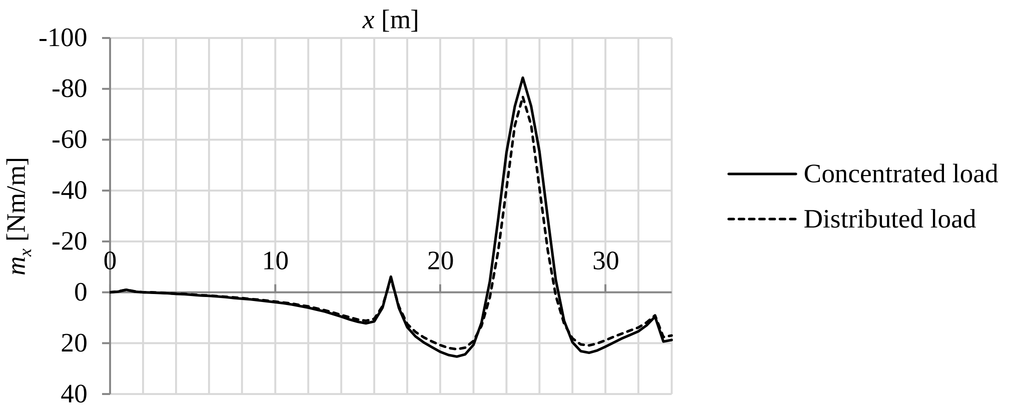

Figure 5.30 Bending moment distributions along the slab edge in the combined model for the cases of concentrated and distributed load. Load at mid-span section.

The bending moment distributions along the mid-span section of the slab are presented in Figure 5.31 and Figure 5.32, when the load is applied in the mid support and the mid-span section respectively. As could also be seen in Figure 5.28, the magnitude of the bending moment in the loaded section of the bridge differs greatly between the model subjected to a concentrated load and the model subjected to a distributed load. The distributed load generates significantly smaller field moments, which implies that this more accurate modelling of the load application enables a more economic design of the slab.

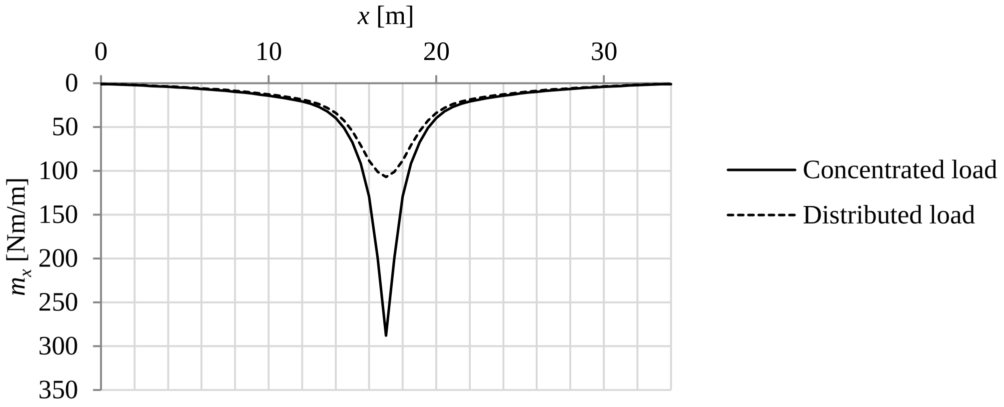

Figure 5.31 Bending moment distributions along the mid-span section of the slab in the combined model for the cases of concentrated and distributed load. Load at mid support section.

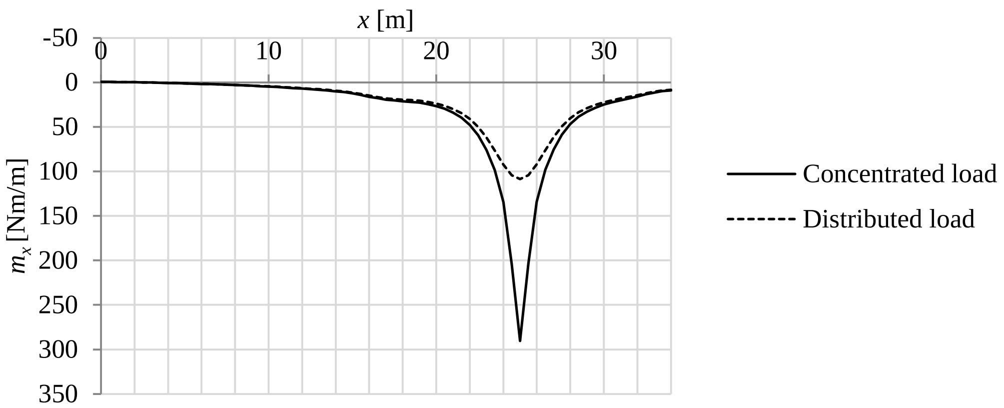

Figure 5.32 Bending moment distributions along the mid-span section of the slab in the combined model for the cases of concentrated and distributed load. Load at mid-span section.

The slab in the beam grillage model cannot distribute the bending moment transverse to the load-carrying direction, but transversal beams adjacent to those subjected to load will obtain bending moments induced by the torsion of the main girders. When the load is applied as a concentrated load onto one transversal beam, the bending moments in both the slab mid-section and slab edge are expected to increase drastically; both due to the analytical solution for a beam, presented in the beginning of this chapter, and due to lack of transverse distribution.

The shape of the transverse bending moment distributions along the transversal beams subjected to load naturally corresponds exactly to the analytical solution for a beam, see Figure 5.33. Note that the magnitude of the bending moment differs between the two load types. This depends on that only one transversal beam is loaded for the case with a concentrated load while three transversal beams share the distributed load, resulting in a load of half the size on the studied beam.

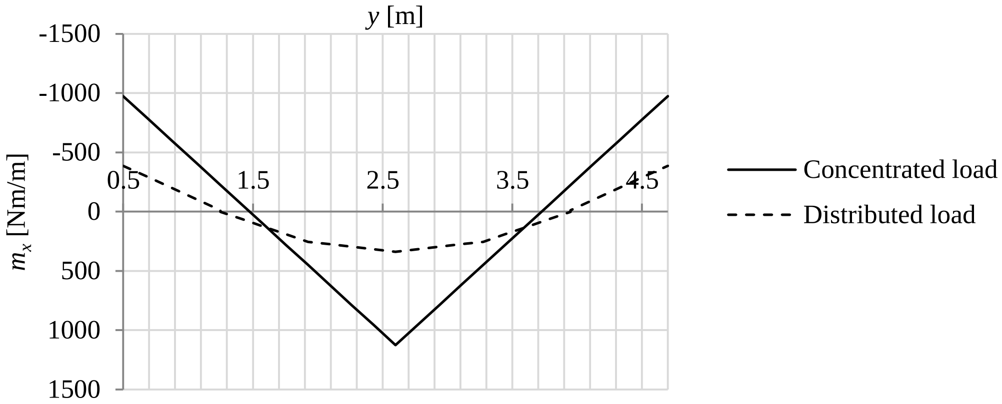

Figure 5.33 Bending moment distributions along the transverse mid-span section in the beam grillage model for the cases of concentrated and distributed load. Load at mid-span section.

Only the bending moments in the slab edge and slab mid-section were therefore assessed to be of interest and these are presented in Figure 5.34 and Figure 5.35 respectively. The figures show the distributions for load at the mid-span section, but the shapes and tendencies agree with those of the case of load at the mid support section. It is clear that a concentrated load induces maximum bending moments in both the mid and edge sections of the slab of more than twice the size compared with those induced by a distributed load.

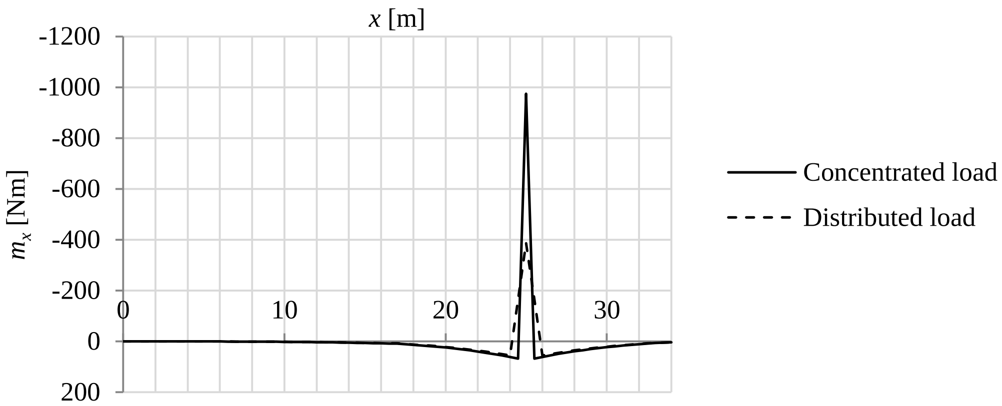

Figure 5.34 Bending moment distributions along the slab edge in the beam grillage model for the cases of concentrated and distributed load. Load at mid-span section.

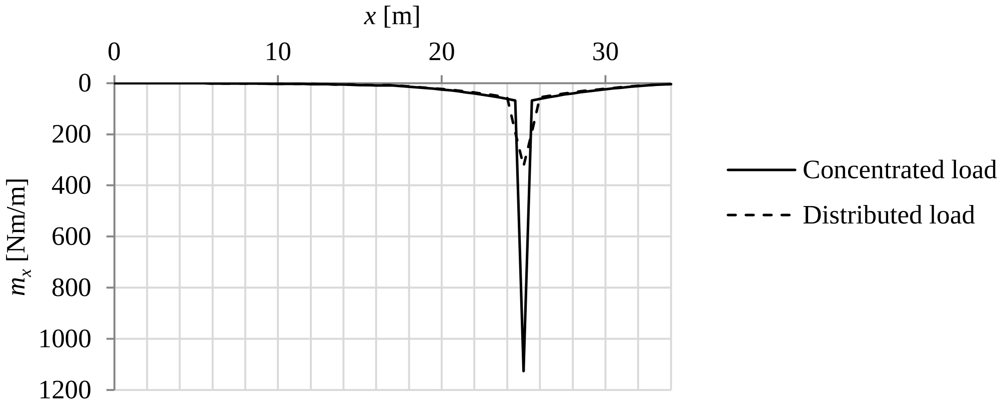

Figure 5.35 Bending moment distributions along the mid-section of the slab in the beam grillage model for the cases of concentrated and distributed load. Load at mid-span section.

The results in this study indicate that the type of load application in both models largely affects the bending moment distribution along the mid-span section of the slab. It was concluded that the choice of load application is of great importance when designing the slab of a trough bridge and that the design bending moments can be reduced a great deal, if the load is modelled more accurately with regard to the distribution of load effects within rails, sleepers and ballast.

Since the difference in bending moment distributions along the edge due to concentrated or distributed load is more or less negligible in the combined model, the choice of load application was assumed to be insignificant for the contribution to torsional moments in the main girders from the bending moment in the slab. In the beam grillage model however, a large difference between the two types of load could be noted along the slab edge too, which is assumed to result in a significant difference in the torsional moment of the girders.

5.3.2 Shear force in slab

The expected shear force distribution of a one-way slab strip subjected to a concentrated load is constant magnitude at each side of the load with positive and negative values respectively. An evenly distributed load along the span is instead expected to result in a linear variation of the shear force along the entire length of the slab strip. As the load applied in the FE-analyses of this project was distributed over a part of the span, the shear force distribution of a one-way slab strip subjected to this load would therefore be a combination of the two cases described above. The shear force would thus vary linearly under the load and be constant in unloaded parts.

Figure 5.36 presents the shear force distributions in the slab of the combined model along the mid support section of the bridge, when the load is applied in that section. The concentrated load generates the expected values at the loaded section, but then varies randomly. It can be noted that no transverse distribution occurs in the loaded section, which is consistent with what was found in the initial study. The variation of the shear force originating from the concentrated load is believed to depend on the variation of transverse distribution along the sections between the girders. The shear force distribution due to the distributed load is more alike the expected shape. Even though the shear force differs greatly in the mid-span section between the two types of load application the magnitudes at the slab edge are equal.

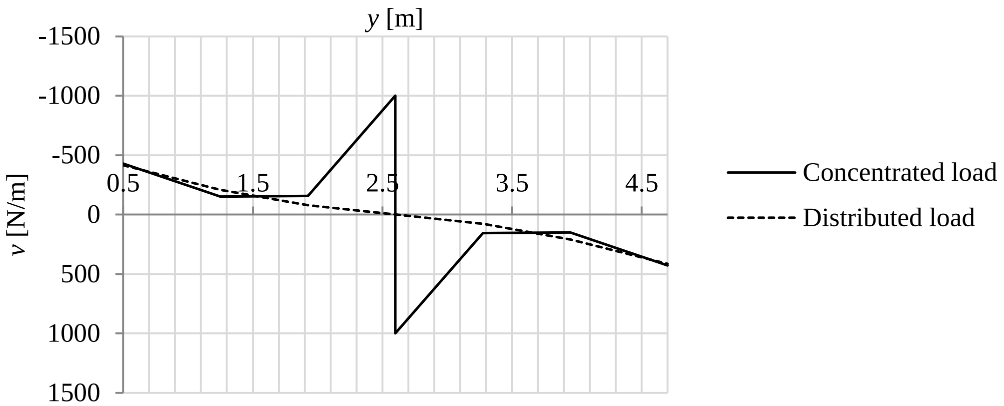

Figure 5.36 Shear force distributions in the slab along the mid support section of the combined model for the cases of concentrated and distributed load. Load at mid support section.

The shear force distribution along the mid-section of the slab in the combined model is presented in Figure 5.37 for when the load is placed in the mid support section. As was noted in the figure above and the results of the study of distribution within shell elements, no transverse distribution of shear force occurs in the mid-section of the slab for the concentrated load application.

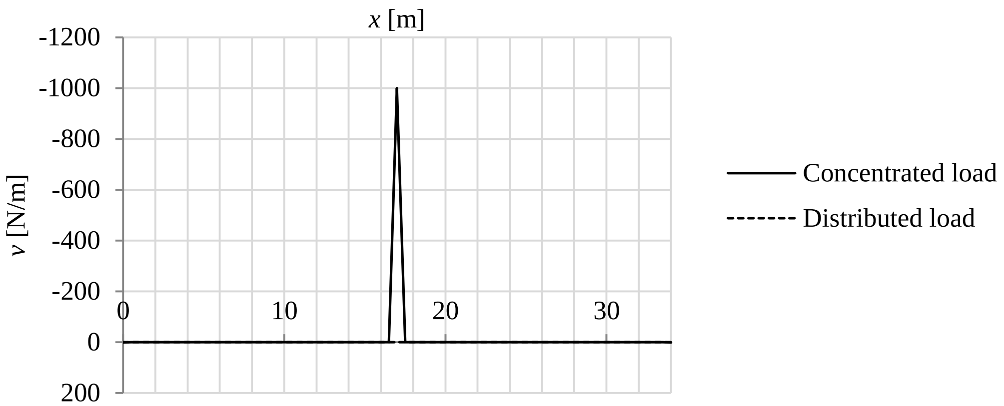

Figure 5.37 Shear force distributions along the mid-section of the slab in the combined model for the cases of concentrated and distributed load. Load at mid support section.

The distributions of shear force along the slab edge in the combined model are shown in Figure 5.38 and Figure 5.39 for the cases when the load is applied in the mid support and mid-span section respectively.

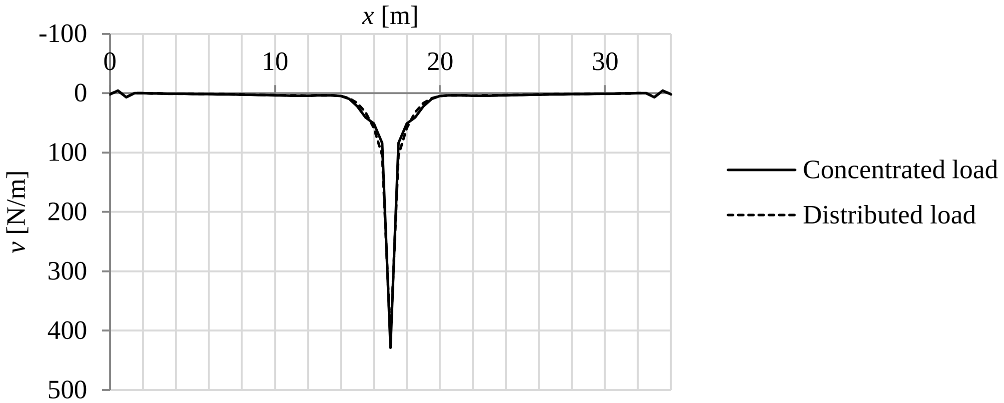

Figure 5.38 Shear force distributions along the slab edge in the combined model for the cases of concentrated and distributed load. Load at mid support section.

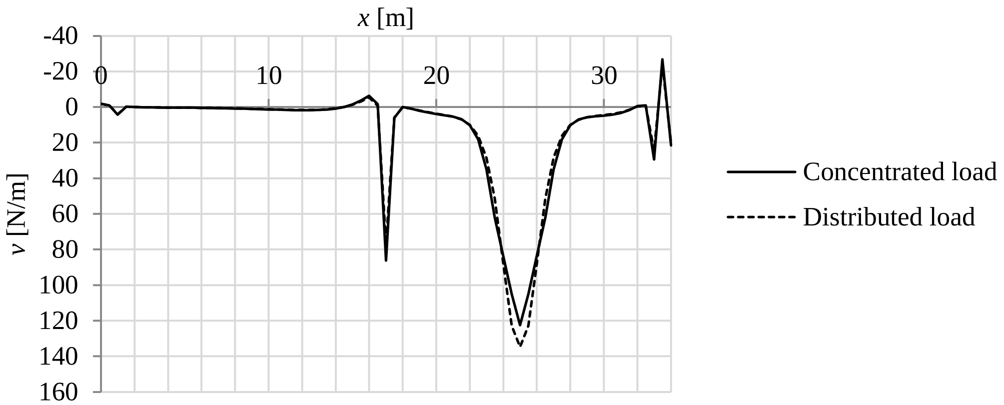

Figure 5.39 Shear force distributions along the slab edge in the combined model for the cases of concentrated and distributed load. Load at mid-span section.

The shear force distributions along the slab edge are more or less equal for the two models, except around the mid-span when the load is applied in that section, see Figure 5.39. In this case the shear force generated by the distributed load is approximately 10 % larger than that generated by the concentrated load application. This agrees with what was found in the initial study, where the concentrated load generally caused slightly larger shear forces than the distributed load application. Note that the distribution widths are equal for the two load applications, in line with what was found in Section 5.1.2. The distribution width refers to the width between sections with zero shear force.

The shear force distributions along the transverse mid-span section in the beam grillage model are presented in Figure 5.40. Similarly to the bending moment distributions, the shear force along the transversal beams subjected to load corresponds to the analytical solution for a beam. The difference in magnitude is explained by the different number of loaded beams in the cases of concentrated and distributed load.

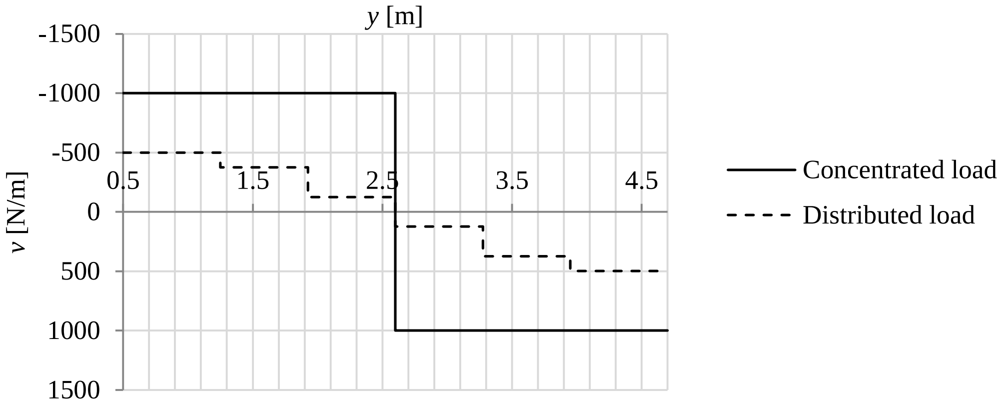

Figure 5.40 Distributions of shear force along the transverse mid-span section in the beam grillage model for the cases of concentrated and distributed load. Load at mid-span section.

Along the edge of the slab the shear force distribution is assumed to change in shape and magnitude as all shear force for the case of concentrated load is located to one transversal beam and no transverse distribution can occur. The distribution of shear force along the edge, when load is applied in the mid-span section, is presented in Figure 5.41, but the same relation can be seen for the case of load at mid support. It can be noted from the figure below that concentration of shear force to one transversal beam results in a peak of shear force of twice the magnitude along the edge.

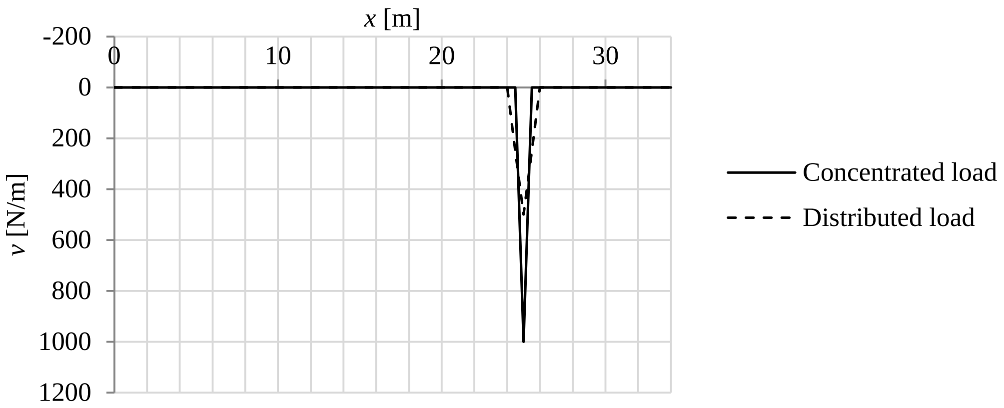

Figure 5.41 Distributions of shear force along the slab edge in the beam grillage model for the cases of concentrated and distributed load. Load at mid-span section.

5.3.3 Normal force in slab

The normal force in the transverse direction of the bridge due to concentrated and distributed loading was studied in both models. The distributions of normal force along the slab edge in the combined model is presented in Figure 5.43 and Figure 5.44 for the cases when the load is applied in the mid-span and mid support sections.

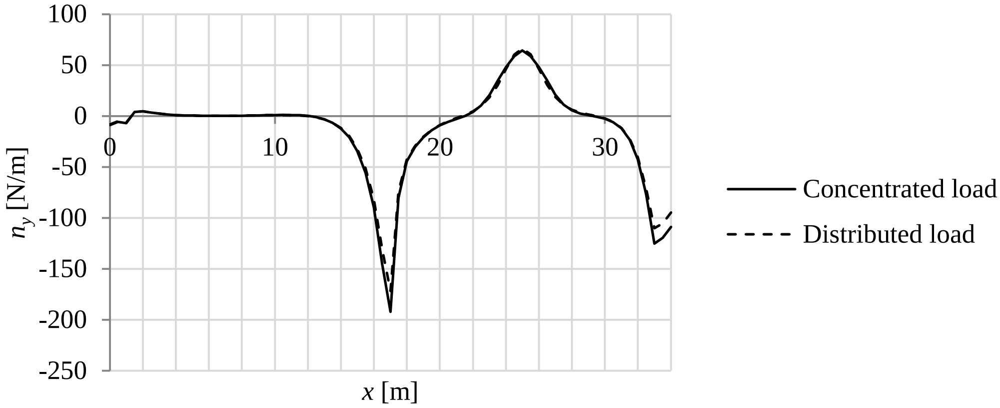

Figure 5.42 Normal force distributions along the slab edge in the combined model for the cases of concentrated and distributed load. Load at mid-span section.

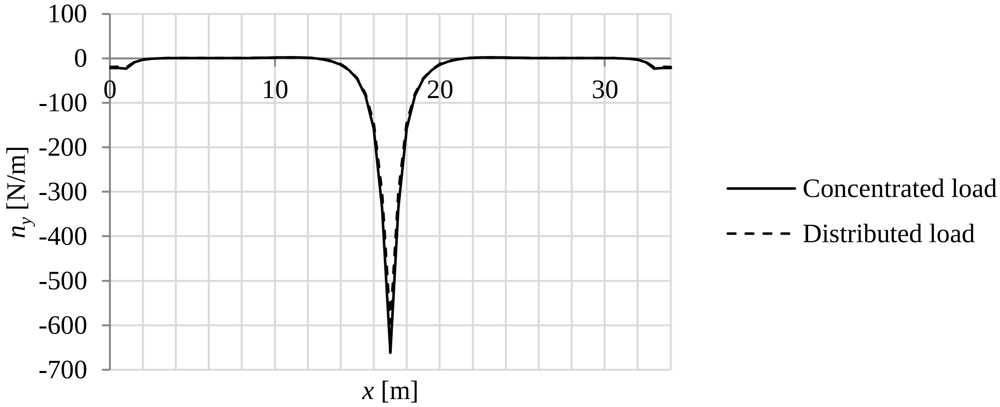

Figure 5.43 Normal force distributions along slab edge in the combined model for the cases of concentrated and distributed load. Load at mid support section.

The maximum values in the section where the load was applied were compared between the two different load applications. For the combined model it can be seen that the two distributions agree very well near the load application, when it was positioned in the mid-span section. However, the concentrated load gave rise to a slightly greater normal force.

Note that the normal force reached much larger values, when the load was applied in the mid support section than in the mid-span section. Since the normal force is caused by the need for deformation of the slab, it is naturally larger at supports due to the prevented deformation in these sections. In the mid-span section the slab has a smaller degree of fixation and is thus more free to deform, resulting in smaller normal force. The same tendency can be seen for the normal force distributions in the beam grillage model, which are presented in Figure 5.44 and Figure 5.45 for load positioned at mid-span and mid support respectively.

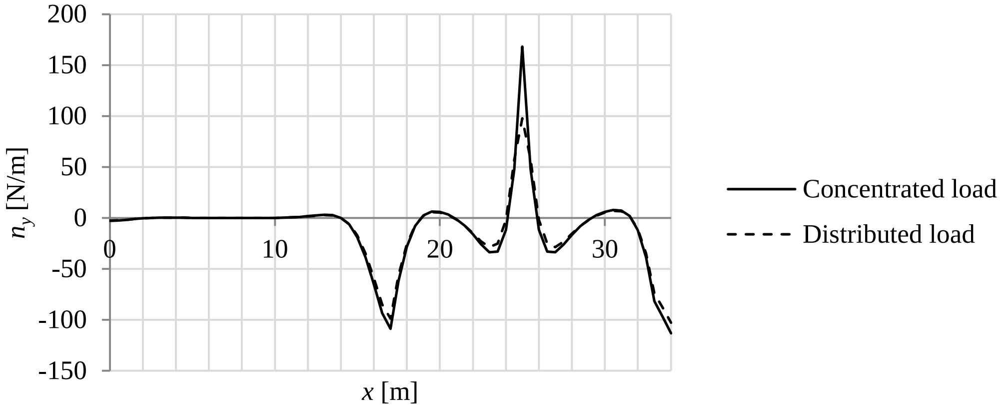

Figure 5.44 Normal force distributions along the slab edge in the beam grillage model for the cases of concentrated and distributed load. Load at mid-span section.

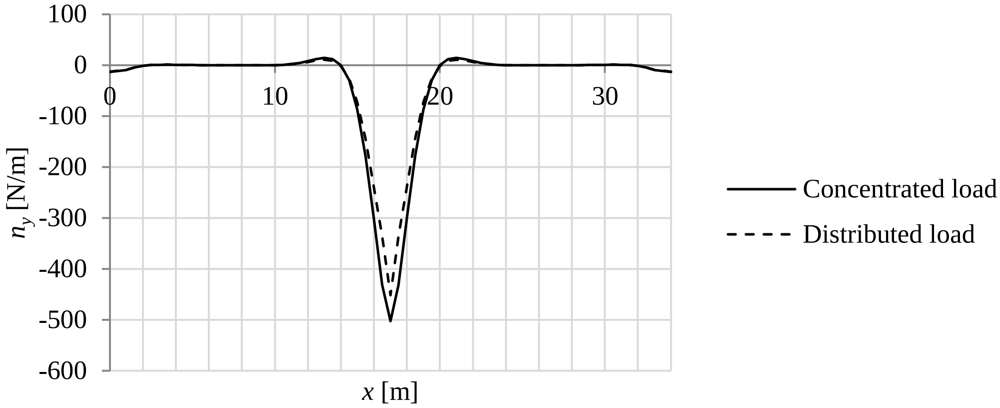

Figure 5.45 Normal force distributions along the slab edge in the beam grillage model for the cases of concentrated and distributed load. Load at mid support section.

The normal force in the slab in the beam grillage model differed more for the two types of load application than in the combined model. The concentrated load constantly generated larger normal forces than the distributed load. When loads were applied in the mid-span section the difference was as much as 72% of the distributed load, while a load application in the mid support section corresponded to what was found in the combined model as it resulted in a difference of 11%.

5.3.4 Torsional moment in girders

A comparison between the two load applications was also carried out with regard to torsional moment in the main girders. Figure 5.46 and Figure 5.47 present the torsional moment distributions in one girder for the combined model, when the load is applied in the mid support and the mid-span section respectively. For both load positions the concentrated load application resulted in a slightly larger torsional moment along the beam than the distributed load application. The differences in maximum torsional moment between the two load applications were about 12% and 14% of the maximum torsional moment using a distributed load, when the load was applied in the mid support section and the mid-span section respectively.

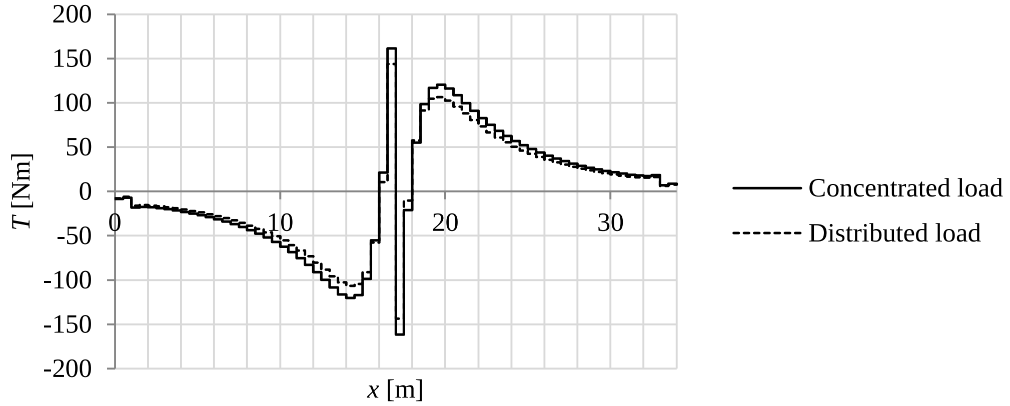

Figure 5.46 Torsional moment distributions in one girder in the combined model for the cases of concentrated load and distributed load. Load at mid support section.

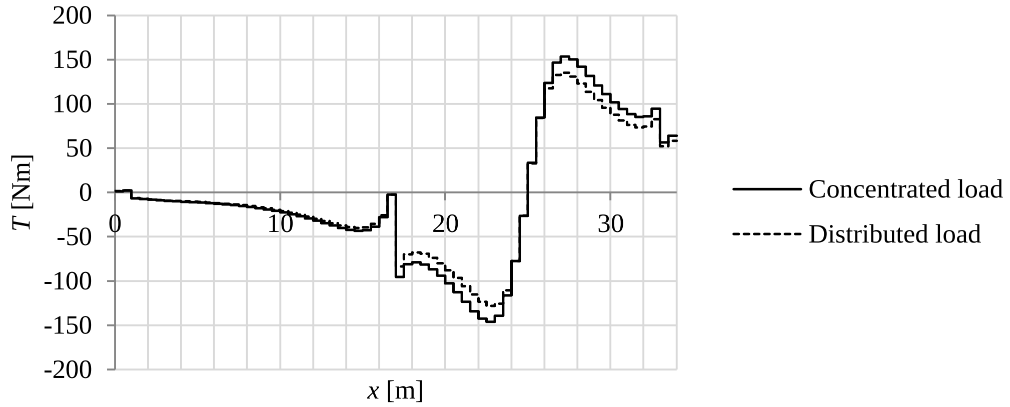

Figure 5.47 Torsional moment distributions in one girder in the combined model for the cases of concentrated load and distributed load. Load at mid-span section.

The torsional moment distributions in one girder in the beam grillage model are presented in Figure 5.48 and Figure 5.49. The beam grillage model also achieves a difference between the two load applications where the torsional moment in the model subjected to a distributed load is the smallest. The concentrated load generated a 4% larger maximum torsional moment than the distributed load, when the load was applied in the mid support section. In the mid-span section the difference amounted to approximately 25% of the torsional moment induced by a distributed load. As can be noted in the figures, the maximum value does not necessarily occur in the same section for both load applications.

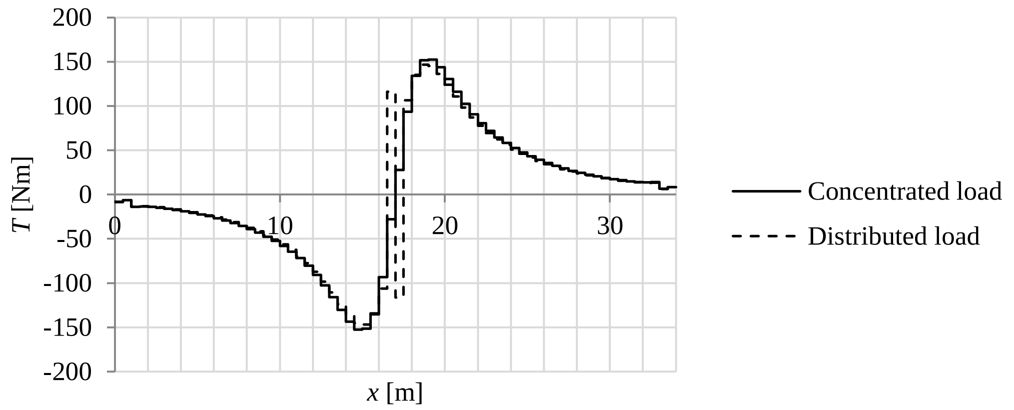

Figure 5.48 Torsional moment distributions in one girder in the beam grillage model for the cases of concentrated load and distributed load. Load at mid support section.

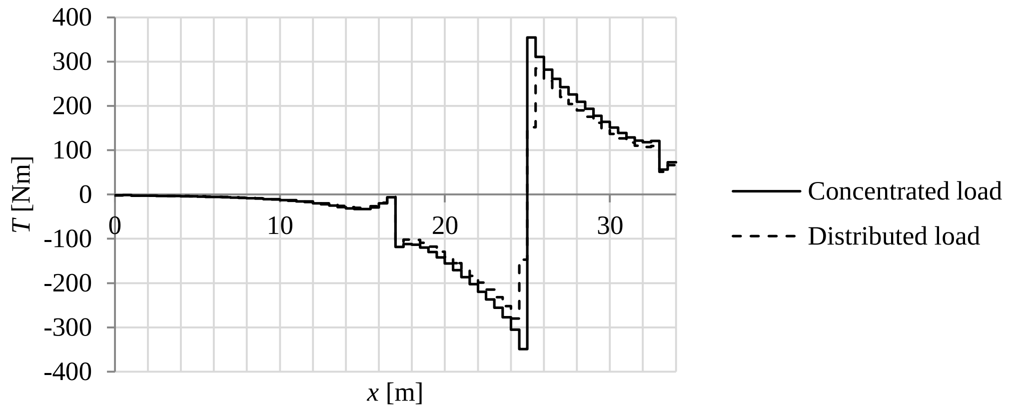

Figure 5.49 Torsional moment distributions in one girder in the beam grillage model for the cases of concentrated load and distributed load. Load at mid-span section.

A variation in torsional moment close to the mid support section can be noted in Figure 5.48, when the distributed load application is placed at the mid support. This effect is believed to arise due to the load being distributed over three beams, one at each side of the mid support section and one exactly at the mid support. The sectional forces at the ends of the loaded beams induce a positive torsional moments in the girder, but the horizontal reaction forces that occur at supports, and hence affect the middle beam, induce a large negative torsional moment. The influence of reaction forces on the torsional moment distribution is further explained in Section 5.5.

In general it can be concluded that the use of a distributed load application leads to reduced torsional moments in relation to using a concentrated load.

5.4 Adjustment of beam grillage model with regard to transverse distributions in the slab

The main difference between the beam grillage model and the combined model is that transverse distribution of sectional forces occurs within the slab in the model for the latter but not for the first. It is therefore this aspect of the beam grillage model that needs to be adjusted in order to obtain coupling between the transverse and longitudinal load-carrying systems and similar results as those from the combined model. It was discussed during the master's project whether to modify the beam grillage model, i.e. extend the area of the applied load further to also account for distributions within the slab, or to process its output. The latter approach was considered more applicable in practice as the number of FE-models that need to be created and consequently analyses that need to be performed is considerably smaller and was therefore studied further.

As mentioned and described in Section 4.4.5, unit sectional forces are of interest in design of reinforced concrete slabs. It was in the transformation into unit bending moment and shear force, i.e. from unit Nm and N to Nm/m and N/m, that the transverse distribution was accounted for in the beam grillage model.

The unit bending moment and shear force are presented in influence lines for the mid-span and mid support sections of the bridge as well as in envelope diagrams. In Section 3.3.2.1 a concern was raised that it might not be possible to use influence lines to superimpose several loads, if their respective transverse distributions coincide. It was therefore of interest to verify the influence lines obtained from one load application through comparison with a model with several loads. This is presented further in Section 5.4.3.

5.4.1 Influence lines for a single load application

Influence lines were created for both the combined and the beam grillage model when subjected to a single load application moving along the length of the bridge. Note that this load application refers to the distributed load effect from one single wheel axle through rails, sleepers and ballast. Thus, the load used in this section was defined in accordance with Section 4.3.1 for the combined model and Section 4.3.2 for the beam grillage model.

The unit bending moment and shear force of the beam grillage model were computed with regard to effective widths according to two different Swedish handbooks; BBK 04 (Boverket, 2004) and 'BYGG' (Wahlström (Ed.), 1969). This procedure is described in detail in Section 4.4.5. Note that the effective widths differ for bending moment and shear force respectively.

Influence lines of the bending moment along the mid-span and edge sections of the slab for the mid-span and mid support sections of the bridge are presented in Figure 5.50 to Figure 5.53. The unit bending moments from the beam grillage model were compared with those of the combined model, which acted as a reference.

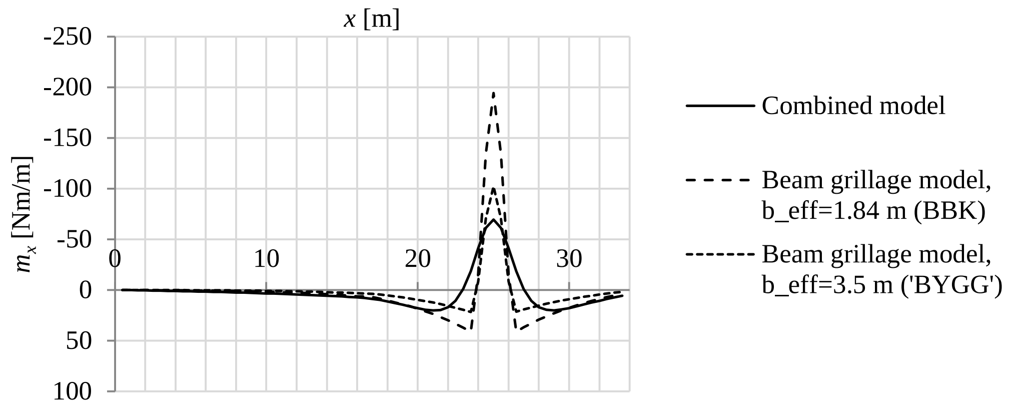

Figure 5.50 Influence lines for unit bending moment at the mid-span section at the slab edge for the combined model and the beam grillage model with different effective widths according to BBK 04 (b_{eff} = 1.84 m) and 'BYGG' (b_{eff} = 3.5 m).

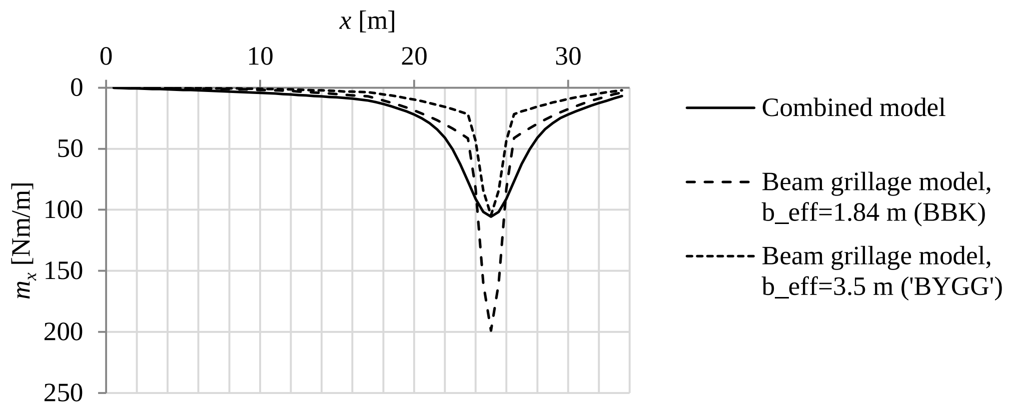

Figure 5.51 Influence lines for unit bending moment at the mid-span section at the slab mid-section for the combined model and the beam grillage model with different effective widths according to BBK 04 (b_{eff} = 1.84 m) and 'BYGG' (b_{eff} = 3.5 m).

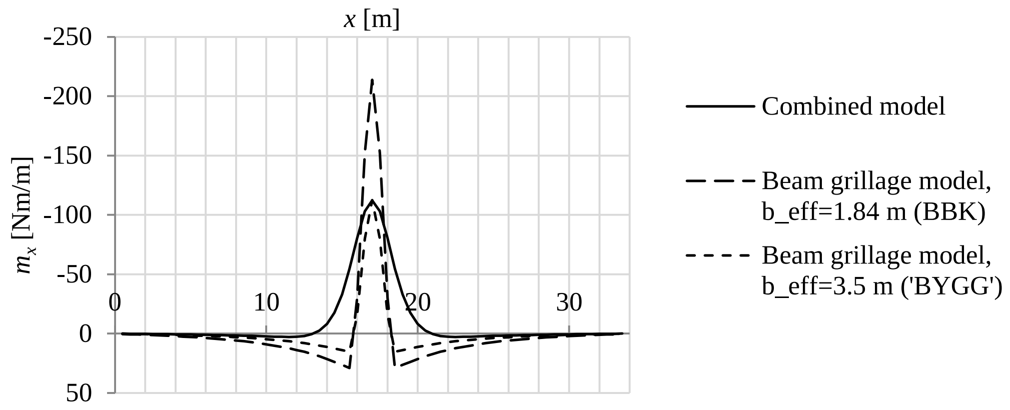

Figure 5.52 Influence line for unit bending moment at the mid support section at the slab edge for the combined model and the beam grillage model with different effective widths according to BBK 04 (b_{eff} = 1.84 m) and 'BYGG' (b_{eff} = 3.5 m).

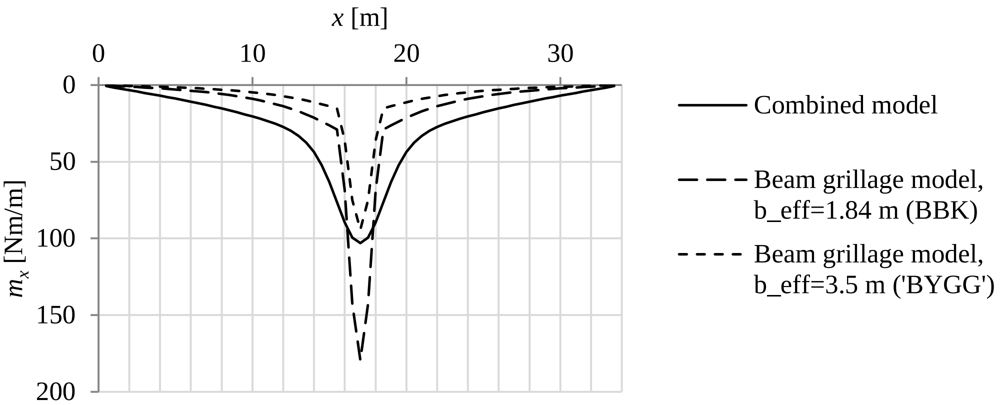

Figure 5.53 Influence lines for unit bending moment at the mid support section at the slab mid-section for the combined model and the beam grillage model with different effective widths according to BBK 04 (b_{eff} = 1.84 m) and 'BYGG' (b_{eff} = 3.5 m).

The beam grillage model that was adjusted with an effective width according to 'BYGG' achieves similar maximum bending moment to the reference model when the mid-span section of the bridge is studied. In fact, the unit bending moment at the slab mid-section for this load application exactly matches that of the combined model, as can be seen in Figure 5.51. The corresponding value in Figure 5.50 at the slab edge does not agree that well with the combined model, but is nonetheless on the safe side and more reasonable than the beam grillage model adjusted according to BBK 04. The latter approach results in greatly overestimated values, when the load is applied in the studied section, both at the mid and edge sections of the slab. In the mid support section the beam grillage model adjusted by the effective width recommended in 'BYGG' achieves a maximum bending moment that is slightly smaller than in the reference model in both sections of the slab. In accordance with the mid-span section of the bridge, the effective width of BBK 04 results in much greater values of almost twice the size of the combined model.

Load applications further away from the studied sections result in underestimated bending moments for both beam grillage models. This is insignificant when only considering a single load application, since the maximum bending moment occurs when the load is placed in the studied section. However, if the bridge is subjected to a combination of loads, superposition of the influence lines for the beam grillage models may result in too small bending moments. This was investigated further and the results are presented in Section 5.4.3.

Influence lines of the unit shear force at the slab edge are presented in Figure 5.54 and Figure 5.55 for the mid-span and mid support sections respectively. It is clear that the use of the effective widths specified in BBK 04 and 'BYGG' result in too small shear force along both sections and most significantly at the mid support section. This indicates that the shell elements distribute the shear force less in the transverse direction than what is assumed in code approaches, which is consistent with the findings of the study of distribution in shell elements presented in Section 5.1.3.

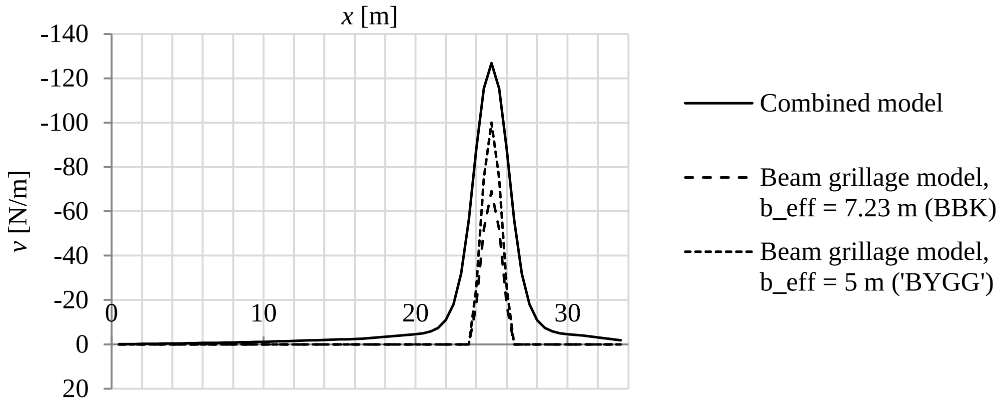

Figure 5.54 Influence lines for unit shear force at the mid-span section at the slab edge for the combined model and the beam grillage model with different effective widths according to BBK 04 (b_{eff} = 7.23 m) and 'BYGG' (b_{eff} = 5 m).

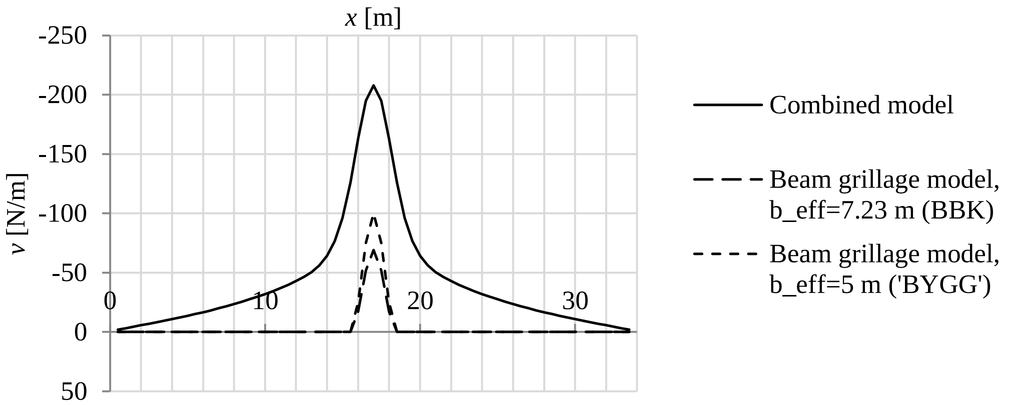

Figure 5.55 Influence lines for unit shear force at the mid support section at the slab edge for the combined model and the beam grillage model with different effective widths according to BBK 04 (b_{eff} = 7.23 m) and 'BYGG' (b_{eff} = 5 m).

As the effective widths regarding shear force recommended in Swedish handbooks clearly are too large, it was investigated what value of the effective width that would lead to the same maximum values in the beam grillage model as in the combined model. The sum of the shear forces at the edge of the three studied transversal beams, when the load is applied onto these beams, was therefore calculated. Naturally this value corresponds to the analytical solution for a beam subjected to the same load as the bridge. The total shear force was then divided by the maximum value of the unit shear force in the combined model, as shown in Equations (5-1) and (5-2).

$$b_{eff,v,\max,mid-span} = \frac{\left.\sum_{i=1}^{3} V_{bg,i}\right|_{mid-span}}{v_{comb,\max,mid-span}} = \frac{-499.50}{-126.82} = 3.94\,\mathrm{m} \tag{5-1}$$

$$b_{eff,v,\max,mid\ support} = \frac{\left.\sum_{i=1}^{3} V_{bg,i}\right|_{mid\ support}}{v_{comb,\max,mid\ support}} = \frac{-499.50}{207.74} = 2.40\,\mathrm{m} \tag{5-2}$$

The calculated effective widths in Equations (5-1) and (5-2) are significantly smaller than those prescribed by BBK 04 and ‘BYGG’. It is also apparent that the calculated effective width is much smaller for the mid support section, i.e. the transversal distribution of shear force in the combined model is less extensive in this section.

Table 5.2 presents a compilation of the effective widths required to obtain unit sectional forces in the beam grillage model that are equal to or on the safe side of the sectional forces found in the combined model. In some sections the effective width recommended by either BBK 04 or ‘BYGG’ was sufficient to obtain values on the safe side. When this was not the case the calculated effective width is listed. It is worth noting that the bending moment could constantly be computed using the code prescribed effective widths, while the shear force required a distribution width that was smaller than what was recommended in handbooks.

Table 5.2 Effective widths required to obtain unit bending moment and shear force in the beam grillage model equal to or on the safe side with regard to the combined model.

	Unit sectional force	Sufficient effective width	Calculated effective width
Slab mid-section	$m_{x,1Q}$, mid-span	3.5 m (‘BYGG’)	-
	$m_{x,1Q}$, mid support	1.84 m (BBK 04)	-
Slab edge	$m_{x,1Q}$, mid-span	3.5 m (‘BYGG’)	-
	$m_{x,1Q}$, mid support	3.5 m (‘BYGG’)	-
	v_{1Q}, mid-span	-	3.94 m
	v_{1Q}, mid support	-	2.40 m

5.4.2 Envelope diagrams for a single load application

Envelope diagrams were created for bending moment and shear force to assess how the maximum unit sectional forces vary along the structure in the two models and to verify if the mid-span and mid support sections are relevant for comparisons. The results regarding bending moment are presented in Figure 5.56 and Figure 5.57. It can be noted that when using the larger of the two recommended effective widths with respect to bending moment, the consistency between the maximum unit bending moments in the beam grillage and the combined model is very good. Use of the smaller effective width recommended by BBK 04 (Boverket, 2004) results in almost two times larger design moments.

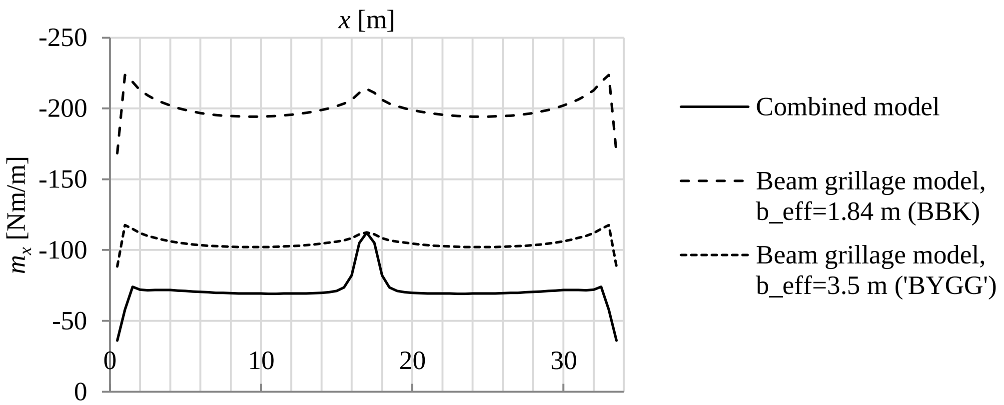

Figure 5.56 Envelope diagrams for unit bending moment along the slab edge for the combined model and the beam grillage model with different effective widths according to BBK 04 (b_{eff} = 1.84 m) and 'BYGG' (b_{eff} = 3.5 m).

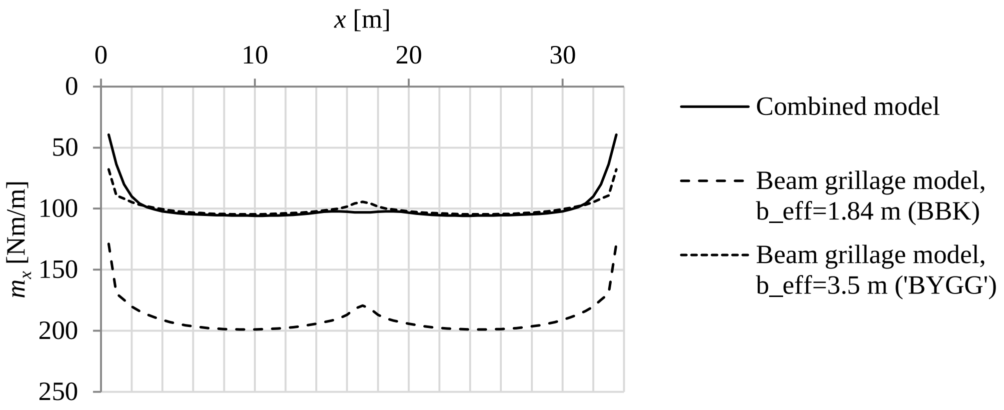

Figure 5.57 Envelope diagrams for unit bending moment along the slab mid-section for the combined model and the beam grillage model with different effective widths according to BBK 04 (b_{eff} = 1.84 m) and 'BYGG' (b_{eff} = 3.5 m).

It can be noted in Figure 5.56 that the unit bending moment along the edge of the slab increases drastically in sections close to and at the mid support in the combined model. Since the fixation degree of the slab-to-girder connection increases in those sections, the end moment at the slab edge increases too. However, only a small difference can be noted in the beam grillage model where the same relation exists. The main reason for the peak in the bending moment of the combined model is therefore assumed to depend on a smaller transverse distribution in the shell elements near support sections. This is consistent with the findings of Davidsson (2003), described in 3.3.2.1. In addition, it was found in the study of distribution of load effects in shell elements, presented in Section 5.1.1, that the transverse distribution of bending moment was much greater for a simply supported slab than a fixed-end slab. As the fixation degree increases near supports, it is therefore reasonable that the transverse distribution within the slab decreases.

The envelope diagrams in Figure 5.56 and Figure 5.57 have more or less constant values between support sections. This indicates that the fixation degree of the slab-to-girder connection and the rotational stiffness of the girder vary little in span sections. The rotational stiffness variation along the girder was therefore investigated in both the combined and the beam grillage model. Rotational stiffness diagrams were created according to the procedure described in Section 4.4.6 and can be found in Figure 5.58.

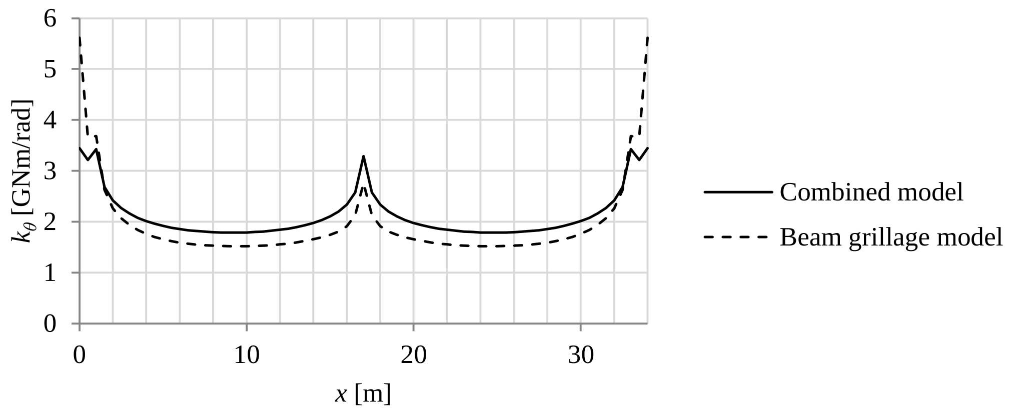

Figure 5.58 Distribution of rotational stiffness k_θ of one girder in the beam grillage and combined models respectively.

It is clear that the rotational stiffness is almost constant along the girder and that the stiffness increases some nearby and at support sections, which is consistent with the envelope diagrams presented above. The end walls have a significant influence on the rotational stiffness in the beam grillage model, which in end wall sections increases to almost three times the rotational stiffness in the mid-span. In the combined model the rotational stiffness in the end wall sections correspond to the rotational stiffness in the support sections. The large difference between the rotational stiffness of the end wall sections in the beam grillage and combined models is assumed to depend on a difference in structural response of the end walls and their connection with the trough cross-section in the two models. This was analysed further and the results are presented in Section 5.6.2.

The envelope diagrams for the unit shear force are presented in Figure 5.59. In the beam grillage model the envelope diagram is constant along the entire length of the bridge, except at end wall sections. This is reasonable as the shear force along the slab edge is independent of the fixation degree and no transverse distribution of load effects occurs in the transversal beams. In the combined model the unit shear force varies greatly near supports. Similarly to the reasoning regarding the envelope diagrams of unit bending moment and the finding regarding calculated effective widths in Section 5.4.1, this is believed to depend solely on the decreased transverse distribution near supports.

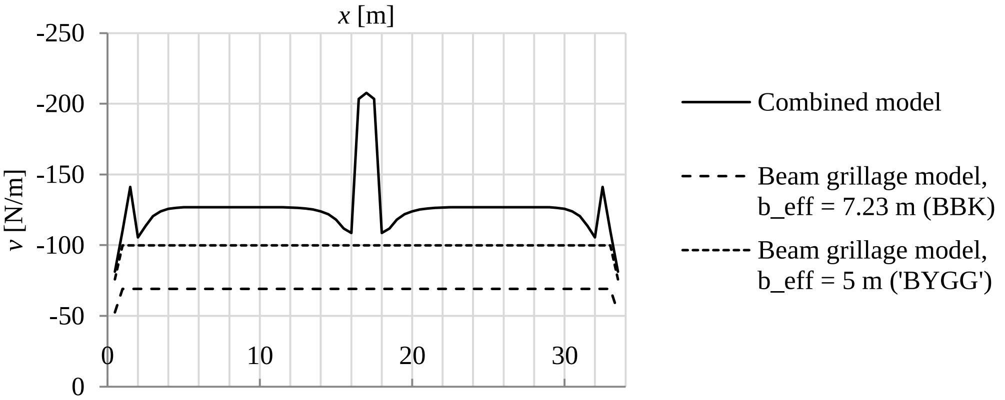

Figure 5.59 Envelope diagrams for unit shear force along the slab edge for the combined model and the beam grillage model with different effective widths according to BBK 04 (beff = 7.23 m) and 'BYGG' (beff = 5 m).

As expected, based on the influence lines for the mid-span section presented in Section 5.4.1, the effective widths prescribed in BBK 04 and 'BYGG' lead to much underestimated values of the beam grillage envelope diagrams along the entire bridge, and especially at the support sections, in relation to the combined model.

5.4.3 Use of influence lines for multiple load applications

As mentioned in Section 3.3.2 the effective width needs to be adjusted when multiple loads are applied adjacent to each other. This may affect the usability of the influence lines obtained from the application of a single load, since an influence line is based on a certain effective width. The sectional forces in one section calculated through superposition of influence line values were therefore compared with the values obtained from a model where the loads from four wheel axles were introduced, as described in Section 4.3.3.3. The influence line values were summed up as described in Section 4.4.5. The unit sectional forces that are superimposed from the influence lines of the load of one wheel axle are illustrated in Figure 5.60.

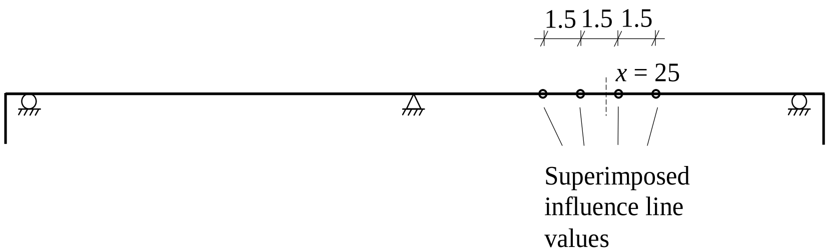

Figure 5.60 Values retrieved and superimposed from influence lines created for the load from one wheel axle. Distances in [m].

The bending moments collected from the models with four wheel pairs needed to be divided by a distance in order to obtain unit moments. For the combined model, this was executed in exactly the same way as for a single load application, i.e. by dividing the sum of the value of the studied section and the two nearby by $3h_{slab}$. In the beam grillage model the values of loaded beams were divided by adjusted effective widths as described below. It was therefore possible to account for the number and placement of the loads.

It is specified in 'BYGG' (Wahlström (Ed.), 1969) how to modify the effective width when two wheel loads are applied and this formula can be found in Equation (3-3) in Section 3.3.2.1. It was assumed that the same approach may be used for more than two wheel loads, if the number of loads and distances between the loads are adjusted. The formula was adjusted to fit for four load applications according to the procedure described in Appendix D.2. No specification regarding multiple loads is given in BBK 04 (Boverket, 2004) and it was therefore assumed that the effective width for multiple loads can be derived as the total distance between the loads plus the effective width for a single load application. The effective width for four wheel loads according to BBK 04 is illustrated in Figure 5.61.

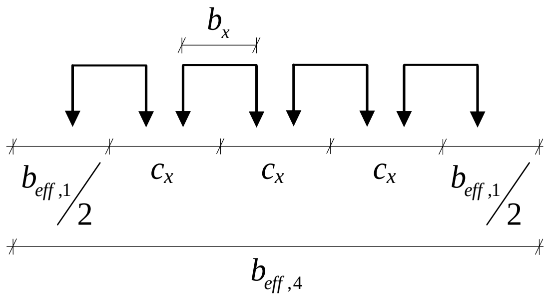

Figure 5.61 Assumed effective width for four wheel loads calculated as the total distance between the loads plus the effective width for one load application according to BBK 04.

For each choice of effective width, i.e. what is recommended in BBK 04 and 'BYGG' respectively, comparisons were performed in the mid-span and edge sections of the slab. The unit bending moment was compared with regard to model type, i.e. combined or beam grillage model, as well as to the mode of obtaining results, i.e. influence line superposition or model with four wheel loads. Results for the mid-span section of the bridge can be found in Table 5.3 and Table 5.4 and for the mid support section in Table 5.5 and Table 5.6.

Table 5.3 Unit bending moment $m_{x,4Q}$ [Nm/m] for the load from four wheel axles at mid-span of bridge (x=25) at slab edge.

	BBK 04		'BYGG'	
	Influence line superposition b_{eff} = 1.84 m	Four wheel loads b_{eff} = 6.34 m	Influence line superposition b_{eff} = 3.5 m	Four wheel loads b_{eff} = 8 m
Beam grillage model	-79.50	-106.91	-41.79	-84.73
Combined model	-91.95	-91.95	-91.95	-91.95

Table 5.4 Unit bending moment $m_{x,4Q}$ [Nm/m] for the load from four wheel axles at mid-span of bridge (x=25) at slab mid-section.

	BBK 04		'BYGG'	
	Influence line superposition b_{eff} = 1.84 m	Four wheel loads b_{eff} = 6.34 m	Influence line superposition b_{eff} = 3.5 m	Four wheel loads b_{eff} = 8 m
Beam grillage model	313.70	342.17	164.92	271.17
Combined model	305.63	305.63	305.63	305.63

Table 5.5 Unit bending moment $m_{x,4Q}$ [Nm/m] for the load from four wheel axles at mid support of bridge (x=17) at slab edge.

	BBK 04		'BYGG'	
	Influence line superposition b_{eff} = 1.84 m	Four wheel loads b_{eff} = 6.34 m	Influence line superposition b_{eff} = 3.5 m	Four wheel loads b_{eff} = 8 m
Beam grillage model	-131.85	-148.59	-69.318	-117.76
Combined model	-233.69	-233.69	-233.69	-233.69

Table 5.6 Unit bending moment $m_{x,4Q}$ [Nm/m] for the load from four wheel axles at mid support of bridge (x=17) at slab mid-section.

	BBK 04		'BYGG'	
	Influence line superposition b_{eff} = 1.84 m	Four wheel loads b_{eff} = 6.34 m	Influence line superposition b_{eff} = 3.5 m	Four wheel loads b_{eff} = 8 m
Beam grillage model	261.35	300.48	137.39	238.14
Combined model	304.31	304.31	304.31	304.31

As can be seen in the tables above, the combined model results in the same values independent of the modelling technique, i.e. if values are obtained from superposition of influence lines or a model with four loads. This is consistent with theory of linear elasticity and the possibility it entails to superimpose loads.

It can be noted that the influence lines obtained from a single load application in the beam grillage model generally result in underestimated values of the unit bending moments, when four wheel pairs are considered. This is clear both from comparisons with the combined model and the beam grillage four wheel model, where the bending moment found by superposition in the beam grillage model is much smaller in all sections except the slab mid-section at mid-span. The effective widths from both BBK 04 and 'BYGG' are clearly too large, which is reasonable as they are much greater than the load spacing of 1.5 m.

It is not realistic that a distribution further than the load spacing can occur between the loads, as this means that distributions from adjacent loads will overlap. Thus, when multiple loads are applied the distribution transverse to the load-carrying direction of the slab becomes smaller in comparison with the total load width and the effective width needs to be decreased. It was therefore investigated whether influence lines created with an effective width equal to the load spacing give unit bending moments closer to the combined reference model and the beam grillage models with four wheel loads. It was further studied whether the effective widths for four loads divided by the number of loads, i.e. four, could be a good estimation when creating the influence lines meant for superposition. The intention of using this assumed effective width is to avoid distributions of load effects within the slab from adjacent loads to overlap. The results are presented in Table 5.7 and Table 5.8 for the mid-span and mid support sections.

Table 5.7 Unit bending moment $m_{x,4Q}$ [Nm/m] at mid-span of bridge (x=25) for the load from four wheel axles obtained through superposition of influence line values. Effective widths for beam grillage model equal to load spacing and the total effective width for four wheel loads divided by number of loads.

	Combined model	Beam grillage model		
		b_{eff} = 1.5 m load spacing	b_{eff} = 6.34/4 m (BBK 04)	b_{eff} = 8/4 m ('BYGG')
$m_{x,4Q}$ *(slab edge)*	-91.95	-97.52	-92.29	-73.14
$m_{x,4Q}$ *(slab mid-section)*	305.63	384.81	364.17	288.61

Table 5.8 Unit bending moment $m_{x,4Q}$ [Nm/m] at mid support of bridge (x=17) for the load from four wheel axles obtained through superposition of influence line values. Effective widths for beam grillage model equal to load spacing and the total effective width for four wheel loads divided by number of loads.

	Combined model	Beam grillage model		
		b_{eff} = 1.5 m load spacing	b_{eff} = 6.34/4 m (BBK 04)	b_{eff} = 8/4 m ('BYGG')
$m_{x,4Q}$ *(slab edge)*	-233.69	-161.74	-153.07	-121.31
$m_{x,4Q}$ *(slab mid-section)*	304.31	320.59	303.40	240.44

It is evident from Table 5.7 that both the effective width equal to the load spacing and that derived from four wheel loads from BBK 04 achieve unit bending moments on the safe side in relation to the combined model for the mid-span section of the bridge. The recommendation according to 'BYGG' leads to underestimated values both at the slab edge and mid-section.

In the mid support section only the load spacing results in unit bending moments on the safe side at the slab mid-section. None of the investigated effective widths are sufficiently small to achieve a unit bending moment equal to or on the safe side of the unit bending moment at the slab edge in the combined model. An effective width that gives the same result in the beam grillage model as in the combined model was therefore calculated in Equation (5-3) with regard to the bending moment at mid support. It can be noted that this value is considerably smaller than the load spacing.

$$b_{eff,m,\max,mid\ support} = \frac{\sum_{i=1}^{4} M_{bg}(x_{Qi})\Big|_{mid\ support}}{m_{4Q,comb,mid\ support}} = \frac{-242.61}{-233.69} = 1.04\,\text{m} \tag{5-3}$$

The superposition of influence lines of unit shear force in the beam grillage model was investigated in the same manner as for unit bending moment, i.e. by comparison with the combined model and a beam grillage model subjected to load from four wheel axles. It was however evident from the influence lines created for the load of one wheel axle that the recommended effective widths in BBK 04 and 'BYGG' would be much too large to use in superposition for the load of four wheel axles. The comparison was therefore limited to the smaller effective widths derived from the load spacing and the effective widths for four wheel loads according to BBK 04 and 'BYGG'. As the shear force in the beam grillage model is independent of the fixation degree in the slab-to-girder connection, it will be constant at the edge of all loaded transversal beams. A comparison with a model with four wheel loads was therefore considered unnecessary in the edge section as the results are equal with those obtained by using the effective widths for four wheel loads divided by four.

The results for the mid-span section of the bridge are presented in Table 5.9 and indicate that the only unit shear force that is safe with regard to the reference value of the combined model originates from using the load spacing as effective width.

Table 5.9 Unit shear force v_{4Q} [N/m] for the load from four wheel axles at mid-span of bridge (x=25) at slab edge. Effective widths for beam grillage model equal to load spacing and the total effective width for four wheel loads divided by number of loads.

	Combined model	Beam grillage model		
		b_{eff} = 1.5 m load spacing	b_{eff} = 11.73/4 m (BBK 04)	b_{eff} = 9.5/4 m ('BYGG')
v_{4Q}	-252.98	-333.00	-170.33	-210.32
Δv_{4Q}	-	80.02	-82.65	-42.66

The envelope diagram for the shear force along the slab edge in the combined model, described in Section 5.4.2, indicates that the transverse distribution of shear force is much smaller near and at the support section. It was therefore estimated that the only effective width that might be sufficient in this section, and thus worth comparing, is the load spacing.

Table 5.10 presents the results and it is clear that even the load spacing, which is the smallest effective width studied in this project, exceeds the transverse distribution in the shell elements of the combined model.

Table 5.10 Unit shear force v_{4Q} [N/m] at mid-support of bridge (x=17) at slab edge. Effective widths for beam grillage model equal to load spacing.

	Combined model	Beam grillage model b_{eff} = 1.5 m (load spacing)
v_{4Q}	-530.31	-333.00
Δv_{4Q}	-	-197.31

A calculated effective width that can be used conservatively in relation to the combined model in superposition of four loads at the mid support section was computed as

$$b_{eff,v,\max,support} = \frac{\left.\sum_{i=1}^{4} V_{bg}(x_{Qi})\right|_{mid\ support}}{v_{4Q,comb,mid\ support}} = \frac{-499.50}{-530.31} = 0.94\,\mathrm{m} \tag{5-4}$$

The effective widths that were required to obtain consistency between the beam grillage and combined models with regard to both bending moment and shear force are compiled and presented in Table 5.11. As mentioned earlier, effective widths that result in equal maximum unit sectional forces in both models were calculated when none of the investigated effective widths were applicable.

Table 5.11 Effective widths required to obtain unit bending moment and shear force in the beam grillage model equal to or on the safe side with regard to the combined model.

	Unit sectional force	Sufficient effective width	Calculated effective width
Slab mid-section	$m_{x,4Q}$, mid-span	6.34/4=1.59 m (BBK 04)	-
	$m_{x,4Q}$, mid support	1.5 m (load spacing)	-
Slab edge	$m_{x,4Q}$, mid-span	6.34/4=1.59 m (BBK 04)	-
	$m_{x,4Q}$, mid support	-	1.04 m
	v_{4Q}, mid-span	1.5 m (load spacing)	-
	v_{4Q}, mid support	-	0.94 m

In some cases the load spacing or the effective width calculated for four loads according to recommendations in BBK 04 were sufficient to achieve values in the beam grillage model that were on the safe side in relation to the combined model. It can be noted that the calculated effective widths are more or less equal to the load width. This means that there will be no significant distribution of load effects at the mid support section.

5.5 Local effect on torsional moment at supports

A local variation of the torsional moment distribution is noted to occur near supports in both the combined and the beam grillage model. Figure 5.62 presents the torsional moment distribution in one girder, when the load is placed at mid-span. The local disturbance of the distribution is apparent at the mid support section (x=17 m) and a small effect can also be noticed at the end supports (x=1 m and x=33 m).

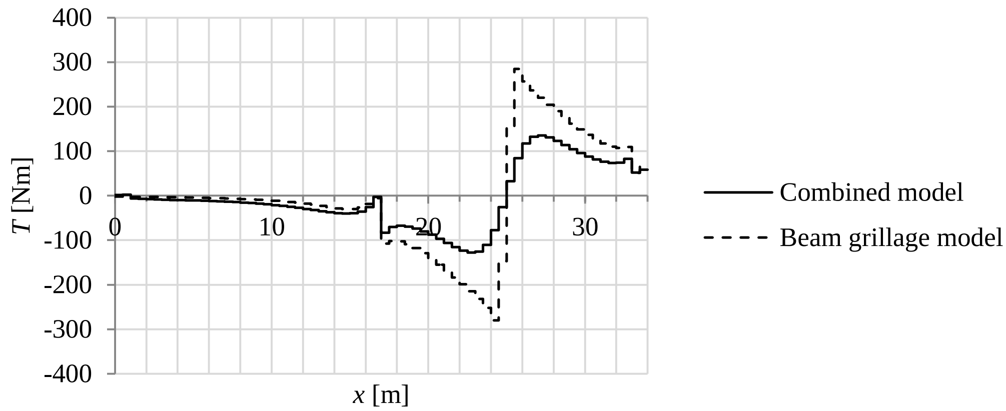

Figure 5.62 Torsional moment distributions in girder influenced by supports.

It was found that this local effect arises due to the horizontal reaction forces that are obtained at the fixed bearings in the *y*-direction, described in further detail in Section 3.2.4. The eccentric application of the horizontal reaction force in relation to the centre of twist of the girders introduces a concentrated torque in the main girders. This torque is of opposite direction to the torsional moment that is induced directly by the loading of the slab, thus resulting in a drastic change in the torsional moment distribution. All forces that induce torsion at support sections are presented graphically in Figure 5.63 and the torsional moment in the girder is derived in Equation (5-5).

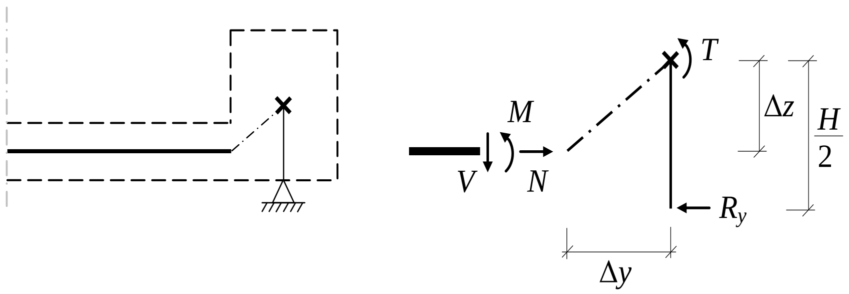

Figure 5.63 Forces that induce torsion of main girders at support sections, adapted from Lundin & Magnander (2012).

$$T = -V \cdot \Delta y - N \cdot \Delta z - M + R_y \cdot \frac{H}{2} \qquad (5\text{-}5)$$

where T = torsional moment [Nm] in girder at support section

V = shear force [N] at slab edge

N = axial force [N] at slab edge

M = bending moment [Nm] at slab edge

$\Delta y, \Delta z$ = lever arm [m] to shear and axial force respectively

H = height of girder

When both supports were fixed in the *y*-direction, equal horizontal reaction forces are obtained in the supports due to the prevented deformation of the cross-section. It can be expected that if one of the supports is free to move in the *y*-direction, no horizontal reaction force would occur. This assumption was investigated in the model created according to Section 4.3.3.4, i.e. that has pinned-roller supports in the *y*-direction. As can be seen in Figure 5.64 and Figure 5.65, the torsional moment clearly changes locally near the supports for the model where both supports are pinned in the *y*-direction, while the model with one pinned and one roller support generates a smoother curve. However, the horizontal reaction forces do not seem to affect the global distribution of torsional moment significantly, as the curve is smooth and continues along the same shape further away from the supports.

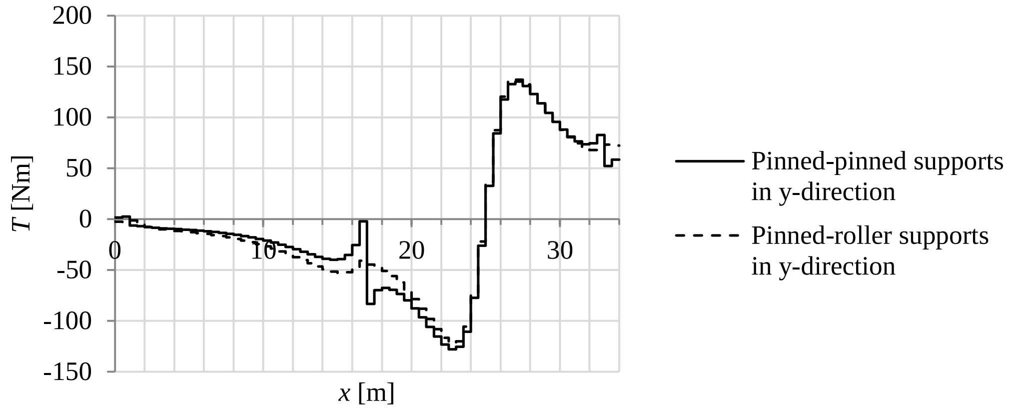

Figure 5.64 Torsional moment distributions in one girder for the combined model with either pinned-pinned or pinned-roller supports in y-direction.

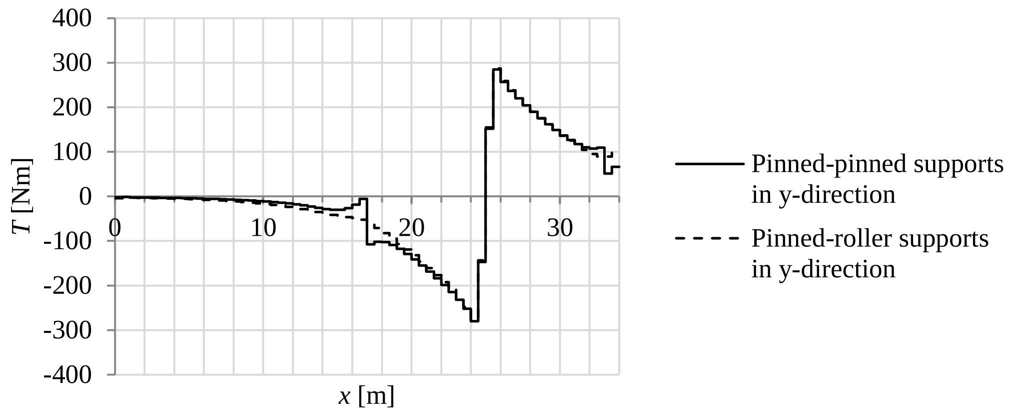

Figure 5.65 Torsional moment distributions in one girder for the beam grillage model with either pinned-pinned or pinned-roller supports in y-direction.

An unexpected deviation near the supports can still be noted for the combined model with free *y*-translation. This can be seen in greater detail in Figure 5.66, which shows a zoomed-in graph near one end support. The same effect can also be noticed at the other support sections, including those along the roller-side of the cross-section. Such deviations at support sections are not as easily distinguished in the beam grillage model, but there is a small local variation at all supports, which is illustrated for an end support in Figure 5.67. Note that the torsional moment decreases at the mid support but increases at end supports.

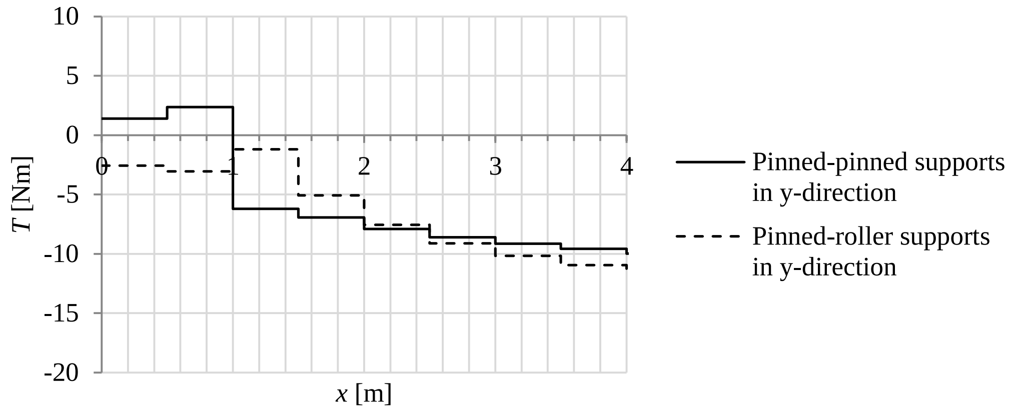

Figure 5.66 Zoomed-in region near end support at x=1 in the combined model.

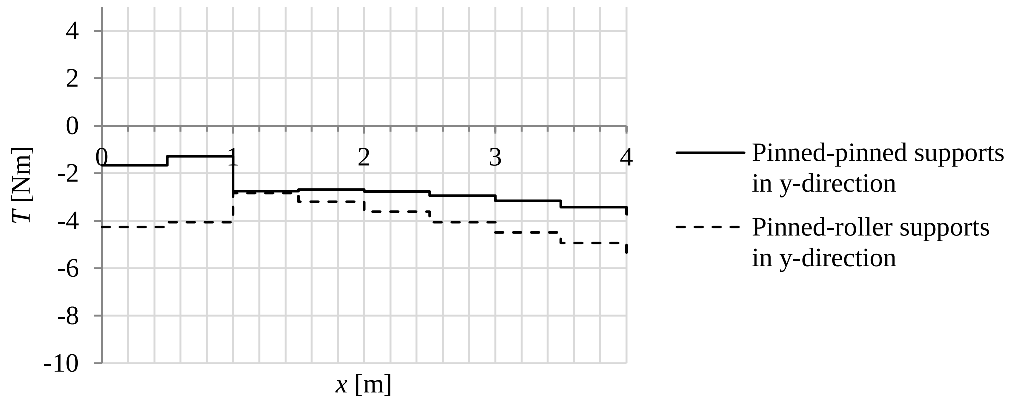

Figure 5.67 Zoomed-in region near end support at x=1 in the beam grillage model.

The reaction force at each support was studied in order to investigate the cause of the unexpected local variation of the torsional moment in the model with one free side. Influence lines for the horizontal reaction force in the *y*-direction at the pinned side of the mid and end supports are plotted in Figure 5.68 to Figure 5.71 for the combined and beam grillage models. The reaction force on the free side is constantly zero as expected and is not treated further.

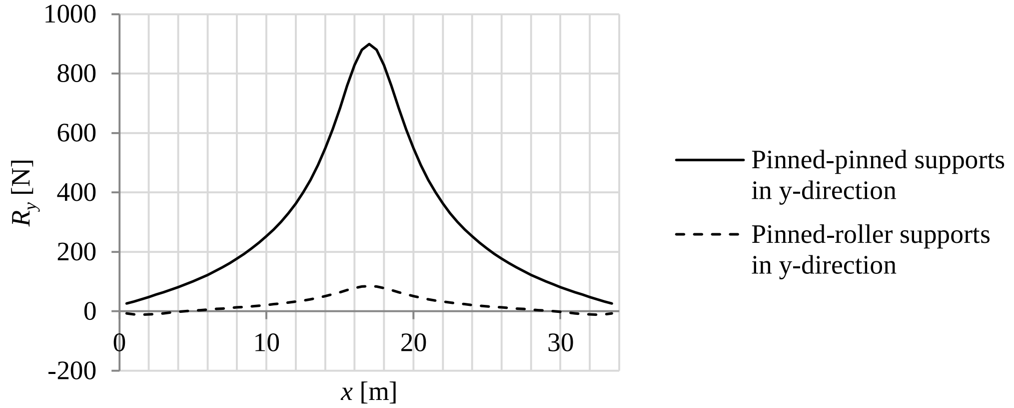

Figure 5.68 Influence lines for the reaction force in y-direction in the pinned node at the mid support in the combined model.

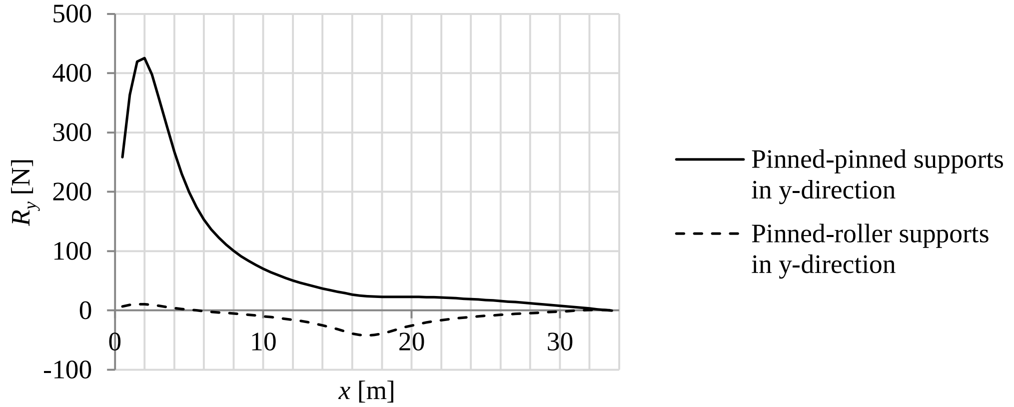

Figure 5.69 Influence lines for the reaction force in y-direction in the pinned node at one end support in the combined model.

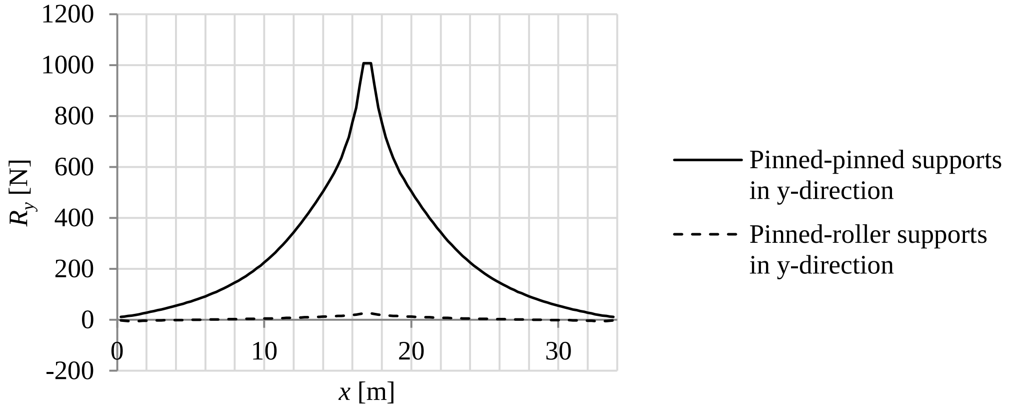

Figure 5.70 Influence lines for the reaction force in y-direction in the pinned node at the mid support in the beam grillage model.

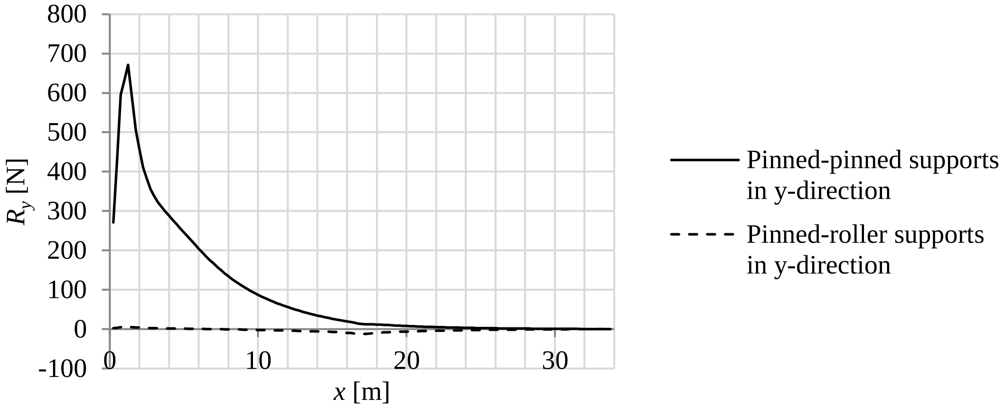

Figure 5.71 Influence lines for the reaction force in y-direction in the pinned node at one end support in the beam grillage model.

A comparison of these figures indicates that the horizontal reaction forces on the pinned side of the models balance each other. The reaction forces in *y*-direction on the pinned side at each support, when the load is placed in the mid support or mid-span section, are listed in Table 5.12.

Table 5.12 Reaction force in y-direction R_y [N] in the pinned supports in the combined and beam grillage models with pinned-roller supports in y-direction.

	Combined model		Beam grillage model	
	Load at mid support	Load at mid-span	Load at mid support	Load at mid-span
End support (x=1 m)	-42.4709	-9.12509	-12.2659	-2.151
Mid support (x=17 m)	84.9418	16.7031	24.5318	3.41349
End support (x=33 m)	-42.4709	-7.57804	-12.2659	-1.2625
Sum all supports	0	-0.00003	0	-0.00001

A summation of the horizontal reaction forces for each load application shows that the horizontal reaction forces at the pinned side of the bridge are balanced globally, as illustrated in Figure 5.72. This is valid for both the combined model and the beam grillage model. Note that the reaction forces in the beam grillage model are much smaller than those in the combined model, which is consistent with the barely noticeable deviations in the torsional moment distribution at support sections in Figure 5.65. It is also worth mentioning that the difference in sign of the reaction forces at mid and end supports respectively is consistent with the change in torsional moment seen at these sections.

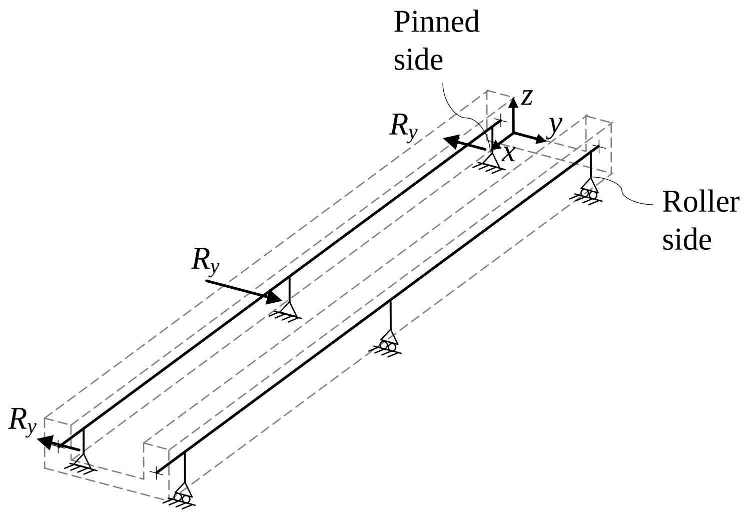

Figure 5.72 Horizontal reaction forces in the y-direction at the pinned side of the cross-section when the load is applied at the mid support section.

It can be noted in Figure 5.68 to Figure 5.71 that the magnitude of the horizontal reaction force differs greatly between the pinned-pinned and pinned-roller models. Also, the shape of the influence lines varies at the end support for the different boundary conditions. This indicates that the cause of the reaction forces differs between the two boundary situations. This was further investigated by a study of the rotational stiffness of one girder for the case of pinned-pinned and pinned-roller supports in *y*-direction. The rotational stiffness was computed as described in Section 5.4.2 and the results are presented in Figure 5.73.

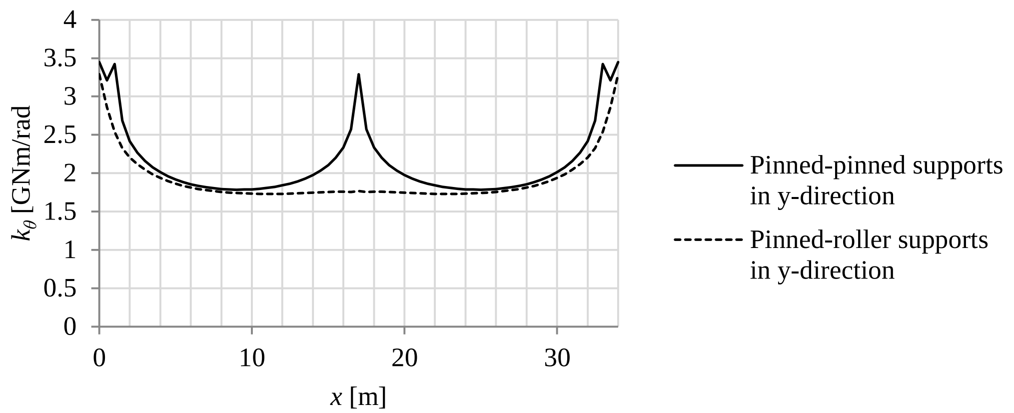

Figure 5.73 Rotational stiffness of one girder in the combined model with pinned-pinned or pinned-roller supports in y-direction.

Figure 5.73 confirms that the supports have no influence on the rotational stiffness when one side is free to translate in the transverse direction of the bridge. It is therefore reasonable to state that the horizontal reaction forces for this support condition occur due to the need for deformation in the girders at sections close to the load application, as a result of compatibility with the slab. The deformation of the girders is resisted by adjacent sections and balanced by reaction forces in the pinned supports of the bridge. This differs from the case of fully fixed supports in the transverse direction, where the reaction forces are instead consequences of the restrained need for deformation in the slab, as discussed in Section 3.2.4.

5.6 Modelling of end wall

A model feature that was developed from the previous master's thesis project is the end walls. In Lundin & Magnander (2012) the models were simplified by excluding the end walls. The torsional restraint was instead represented by fixed twisting in the girder centre at the end support sections. Different torsional restraints result in different torsional moment distributions and the modelling choices concerning the end walls of this and the previous master's thesis project were therefore studied and compared.

The modelling of the end walls also differ between the beam grillage and the combined models. It was shown in Section 5.4.2 that the rotational stiffness of sections close to the end walls varies greatly between the beam grillage and combined models. It was therefore investigated whether the use of beam and shell elements respectively results in different structural response of the end wall and if this might explain the difference in rotational stiffness. The bending moment in the end wall was also studied to compare with the theories regarding torsional restraint of the end walls presented in Section 3.2.4.

5.6.1 Comparison with prescribed fixed twisting

The models with and without end walls were compared with regard to the distribution of torsional moment in the girders. Figure 5.74 and Figure 5.75 show the torsional moment distribution in the combined model for load applied at mid support and mid-span section respectively.

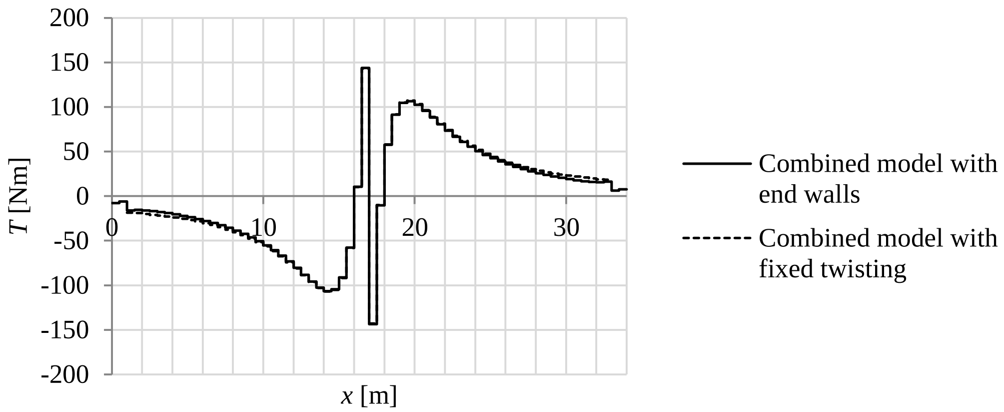

Figure 5.74 Torsional moment distributions for one girder in the combined model with either end walls or fixed twisting at end supports. Load is applied in mid support section.

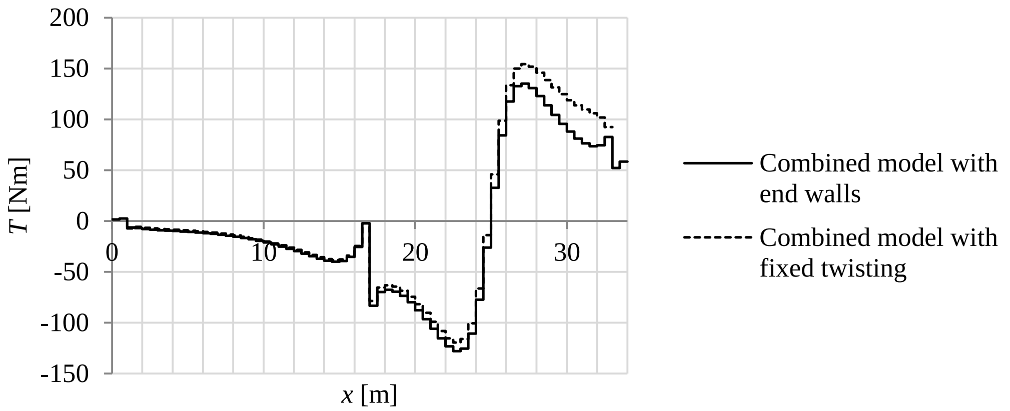

Figure 5.75 Torsional moment distributions for one girder in the combined model with either end walls or fixed twisting at end supports. Load is applied in mid-span section.

It can be noted that the difference between the two modelling choices is the greatest when load is applied in the mid-span section. This indicates that the difference increases with decreasing distance between load application and end support section. This tendency was investigated further by studying the torsional moment distribution in the girder for a load application closer to the end wall. The torsional moment distributions for the case of a load applied closer to the end wall, in x = 29 m, are presented in Figure 5.76. The difference between the distributions is even greater than when the load is applied in the mid-span section, which confirms the theory that the choice of modelling technique has the largest effect when the load approaches the end wall. It can also be seen that the difference between the two models generally is greater in sections closer to the end wall than to the mid support.

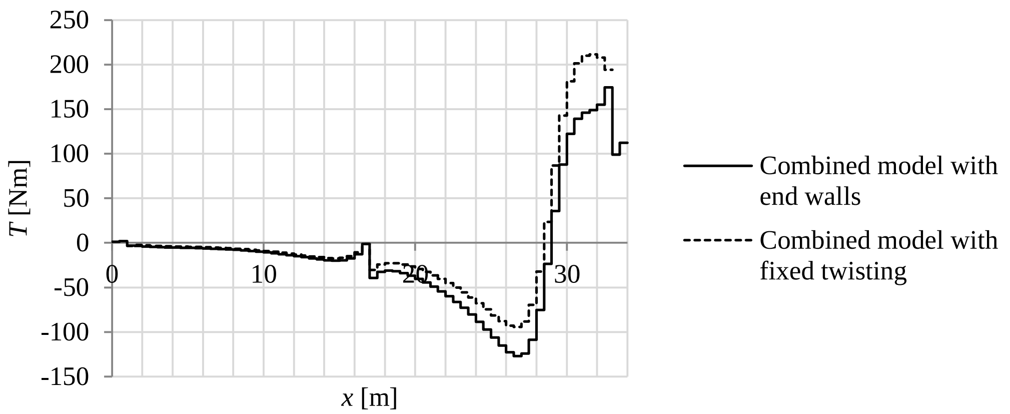

Figure 5.76 Torsional moment distributions for one girder in the combined model with either end walls or fixed twisting at end supports. Load is applied at x=29 m.

The beam grillage model showed the same tendencies as the combined model, with barely any difference between the two modelling options when the load was applied at the mid support and larger difference when the load was applied in mid-span, see Figure 5.77 and Figure 5.78. However, the difference in the beam grillage model was generally smaller in relation to the combined model.

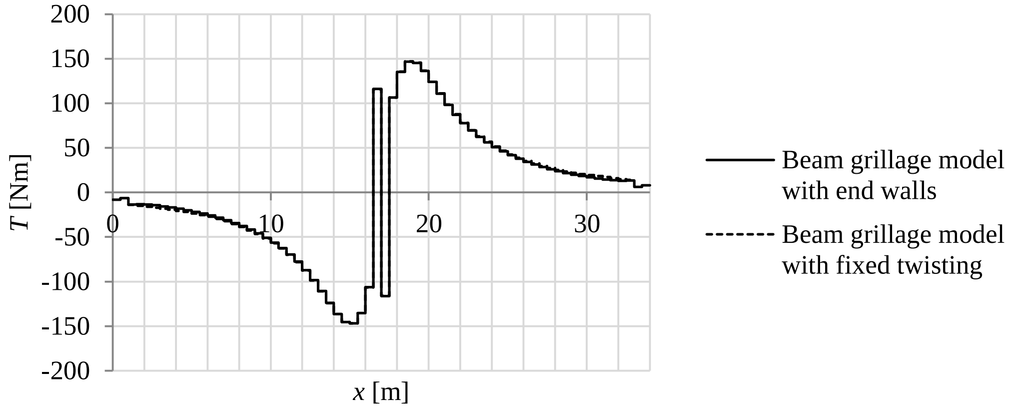

Figure 5.77 Torsional moment distributions for one girder in the beam grillage model with either end walls or fixed twisting at end supports. Load is applied in mid support section.

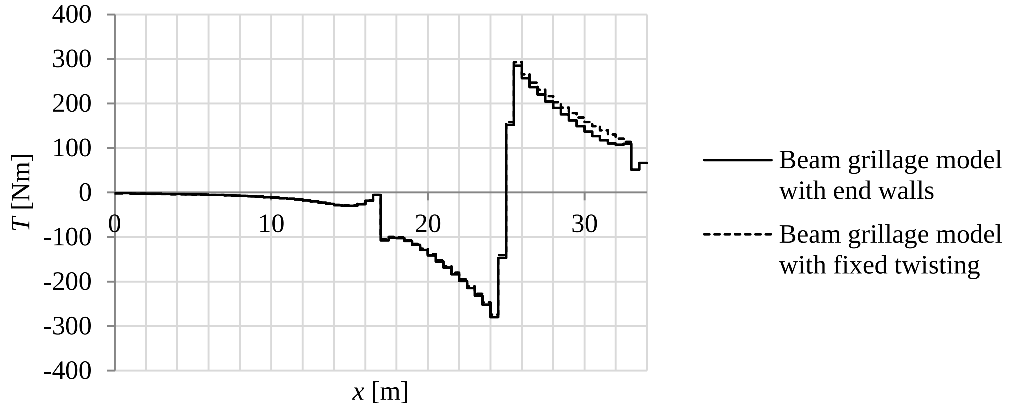

Figure 5.78 Torsional moment distributions for one girder in the beam grillage model with either end walls or fixed twisting at end supports. Load is applied in mid-span section.

The rotational stiffness of one girder was investigated in models with fixed twisting in accordance with the procedure explained in Section 5.4.2 and the results are presented and compared with the models with end walls in Figure 5.79 and Figure 5.80.

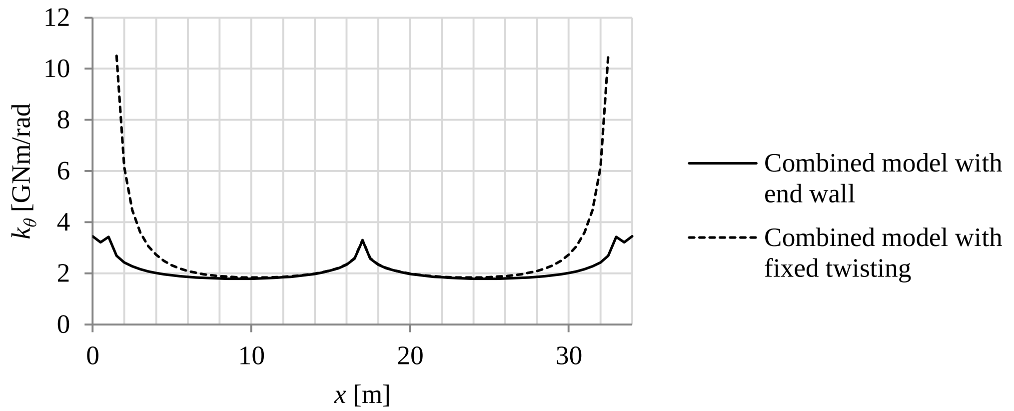

Figure 5.79 Rotational stiffness of one girder in the combined model with end wall or fixed twisting at end supports.

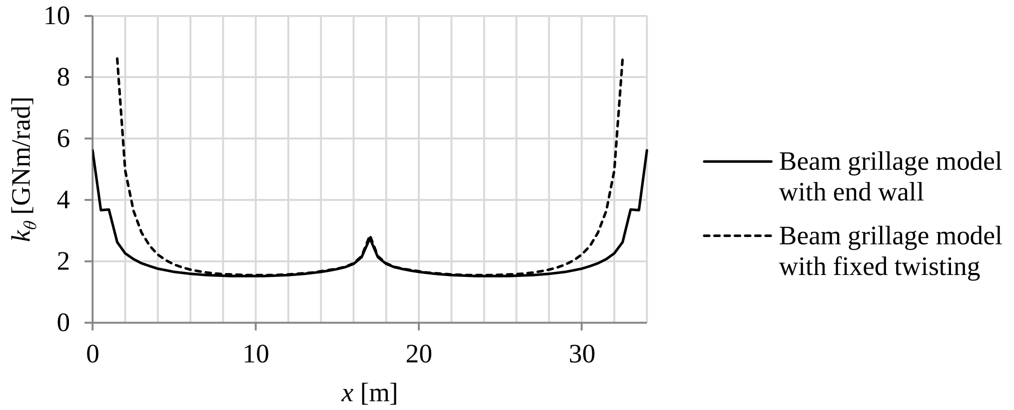

Figure 5.80 Rotational stiffness of one girder in the beam grillage model with end wall or fixed twisting at end supports.

It can be noted in the figures above that while the rotational stiffness approaches infinity at the end support sections when using fixed twisting, the values between mid-span and mid support sections correspond exactly to those of the models with end walls. This is valid for both the combined and the beam grillage model and indicates that it is sufficient to model the end walls as prescribed boundary conditions, if only the mid support and mid-span sections are of interest. If a realistic linear elastic response of the entire structure is desirable, it is however necessary to include the end walls in the model, as prescribed fixed twisting results in unrealistic values in the outer sections of the bridge.

5.6.2 Structural response of end walls

The structural response of the end walls is assumed to differ depending on the position of load application. Either the load is applied away from the end wall or at the end wall section so that the load is transferred to the end wall rather than to the main girders. In the first case the end wall in the model is subjected to torsion at girder centres. In reality, however, self-weight of ballast and the bridge itself will result in an additional load on the end wall. For the latter case the end wall in the model is mainly subjected to train load on top of the end wall but also a small amount of torsion at the girder centres, due to the transverse distribution of the load. In a real design case the torsion in this case is even larger due to multiple loads.

As described in Sections 4.3.1 and 4.3.2 the end walls were modelled with shell elements in the combined model and with beam elements in the gravity centre in the beam grillage model. In both cases the end walls were connected to both the slab and the girders, either directly or with rigid links. It was discussed during the master's thesis project whether beam elements, based on the Euler-Bernoulli beam theory, are appropriate for the end wall that has an aspect ratio smaller than the recommended limit and acts as a deep beam. It was however assumed that the margin of error would be small and that this modelling choice would not affect the torsional restraint significantly.

The bending moment distributions along the end walls were studied and the results for the case of load at mid-span are presented in Figure 5.81 for the beam grillage and combined model respectively. It is worth mentioning that the bending moment and shear force in both the combined and beam grillage model include the nodal moment and force contributions from the slab edge, as described in Section 4.4.3.

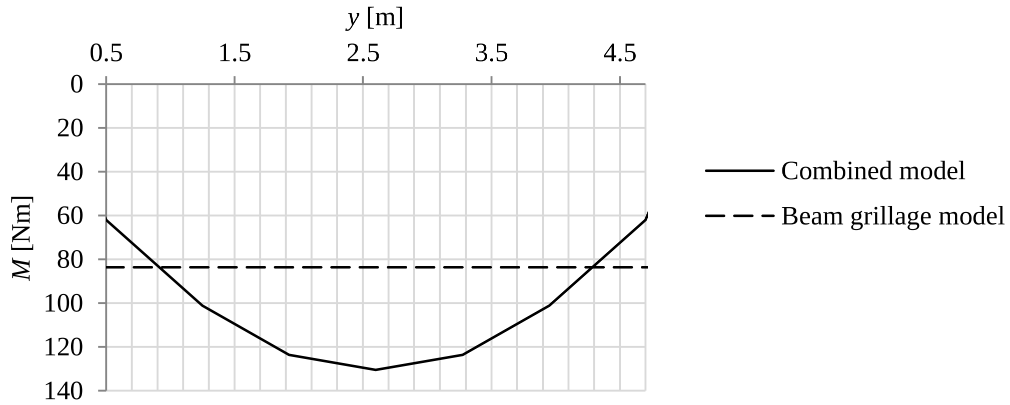

Figure 5.81 Bending moment distributions along the end wall for the combined and beam grillage model respectively. Load at mid-span of bridge.

It can be noted in the figure above that the bending moment distributions differ greatly between the two models. The end wall in the beam grillage model has constant bending moment, while the bending moment distribution in the end wall of the combined model has a parabolic shape. The shape of the bending moment distribution in the beam grillage model corresponds to what can be expected based on the strut-and-tie model presented in Section 3.2.4 where the a constant bending moment is a result of the constant force couple that restrains the torsion. However, the strut-and-tie model is not based on linear elastic analysis and assumes cracked reinforced concrete. It is therefore more likely that the end wall modelled with shell elements represent the real linear elastic bending moment distribution. It was investigated why the end wall of the two models obtains different structural responses with regard to bending moment. The bending moment in the end wall is highly influenced by the horizontal force resultant in the transverse direction of the bridge in the slab edge, as described in Section 4.4.2, and this normal force distribution was therefore studied further.

The normal force in the transverse direction of the bridge occurs due to the need for deformation, i.e. elongation, of the slab when subjected to load. The normal force was computed for the case of load at mid-span and is presented as a distribution per meter along the slab mid-section in Figure 5.82. It can be noted that both models obtain distinct peaks in the distribution at the mid support section, the loaded section and the end wall section located closest to the load. The force is generally larger in the combined model and especially at the end wall section, which explains the difference in magnitude in Figure 5.81.

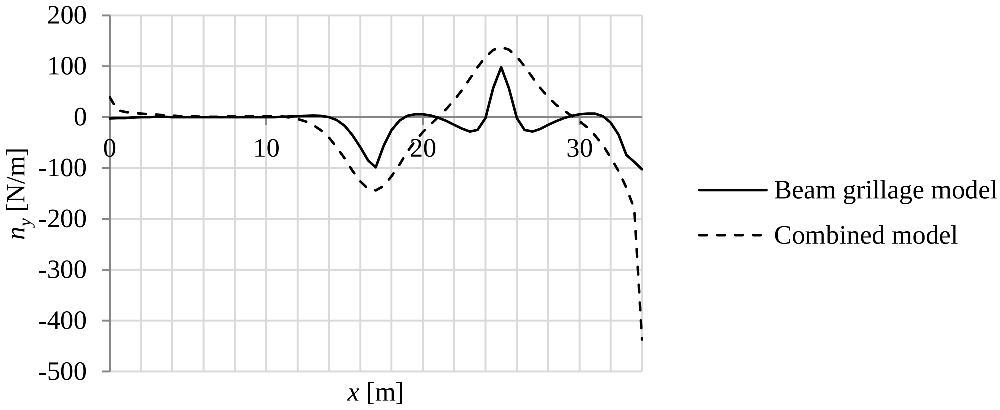

Figure 5.82 Normal force in the transverse direction of the bridge along the slab mid-section for the beam grillage and combined model respectively, when load is applied in the mid-span section.

It is worth noting in Figure 5.82 that the normal force is distributed over a larger width in the combined model due to the transverse distribution of load effects within the slab and compatibility between adjacent slab strips. In the beam grillage model only the three transversal beams subjected to load need to elongate. However, due to the torsion of the main girders normal forces of opposite sign are also found in adjacent transversal beams. Of the two models, the combined model is assumed to give the most correct distribution of normal force in the slab due to the transverse distribution in the slab that does not occur in the beam grillage model

In addition to the difference in magnitude, the shape of the normal force distributions along the bridge end, i.e. at the end wall section, also differs which is illustrated in Figure 5.83. In the combined model the normal force varies with a parabolic shape, while that of the beam grillage model is constant along the slab edge. It appears that the difference in magnitude and shape of the bending moment along the end wall originates from differences in the distributions presented in Figure 5.82 and Figure 5.83.

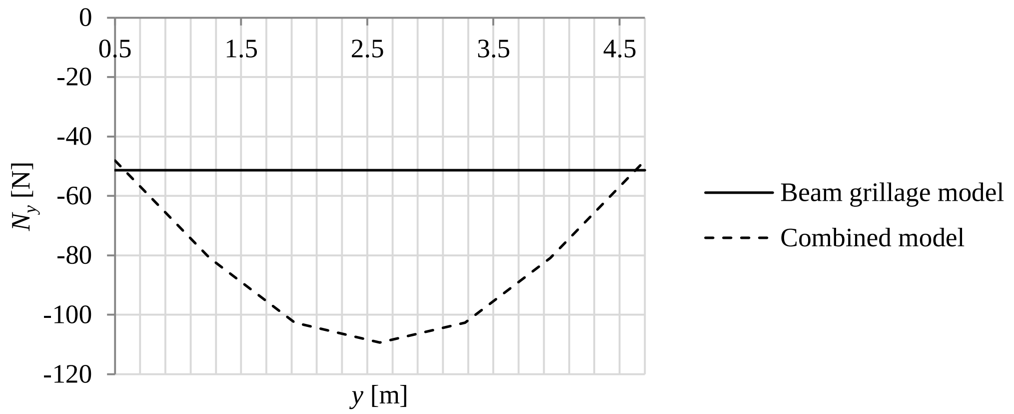

Figure 5.83 Normal force along the slab at the bridge end for the beam grillage and combined model respectively.

When studying the normal force distribution along the slab mid-section of the combined model in Figure 5.82, it is obvious that the end wall induces much larger normal forces within the slab than for example the constraint of the mid support. It also appears that the end supports have no significance on the distribution in the combined model. The latter statement was investigated through comparison between the original model and the model described in Section 4.3.3.4 where the supports are free to translate in the transverse direction on one side of the bridge. The results of this study are presented in Figure 5.84 and it is apparent that only the influence of the mid support changes significantly, when supports are defined as pinned-roller in the y-direction. The normal force distribution near the end walls is hardly affected at all, when the support conditions are modified. It was therefore concluded that the bending stiffness of the end wall modelled with shell elements constrains the slab deformation to a much larger extent than supports fixed for transverse translation.

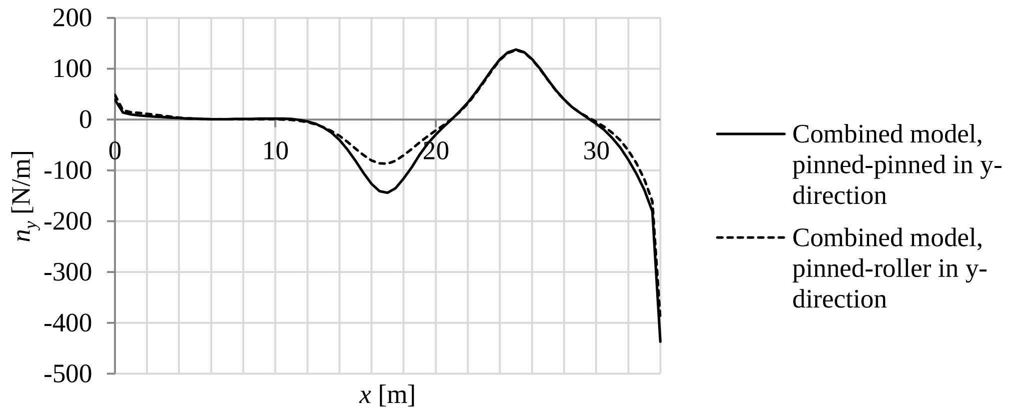

Figure 5.84 Normal force in the transverse direction of the bridge along the slab mid-section in the combined model for the cases of pinned-pinned and pinned-roller supports in y-direction respectively.

The shear force distributions along the nearest end wall for the case of load at mid-span are shown in Figure 5.85. As expected, considering that the bending moment was constant in the end wall of the beam grillage model, the shear force in the end wall of this model is constantly zero. However the shear force in the combined model varies, which indicates that there is non-zero shear force in the slab beyond the end support towards the end wall. Lundin and Magnander (2012) also noted this effect in models where the slab is represented by shell elements. This effect would naturally be eliminated if the supports extended below the entire cross-section.

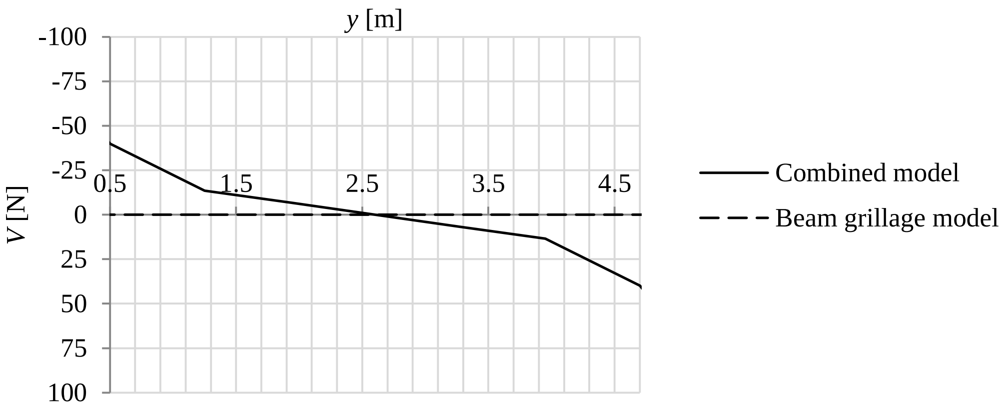

Figure 5.85 Shear force distributions along the end wall for the combined and beam grillage model respectively. Load at mid-span of bridge.

When load is applied at the end wall section of the bridge, the bending moment in the end wall is distributed according to Figure 5.86 in the beam grillage and combined model respectively.

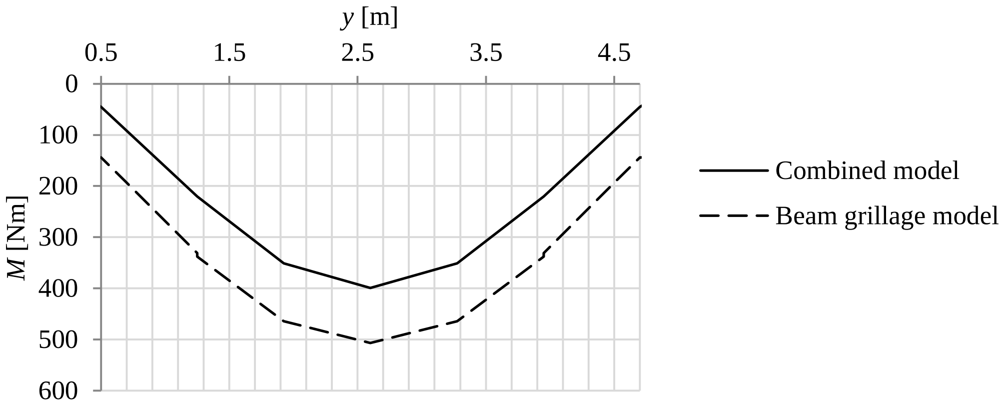

Figure 5.86 Bending moment distributions along the end wall for the combined and beam grillage model respectively. Load at end wall section.

For this load case the bending moments in the end walls of both models vary with a near parabolic shape and the difference in magnitude is smaller. This indicates that the end wall modelled with beam elements describes the real loading condition of the end wall better when the load is applied in the end wall section. This is naturally a result of the more accurate distribution of normal force in the slab edge of the beam grillage model when the end transversal beam is subjected to load. Further, if the results of the combined model are assumed to be correct, it is evident that the structural response of the end wall with regard to bending moment is similar for the cases of load applied in the span and load applied directly above the end wall.

Consequently, the shear force along the end wall is similar in shape and differs only slightly in magnitude between the two models, when load is applied at the end wall section, see Figure 5.87. The shear force distribution of the beam grillage obtains a jagged appearance due to constant shear force over each element, as described in Section 4.4.1.

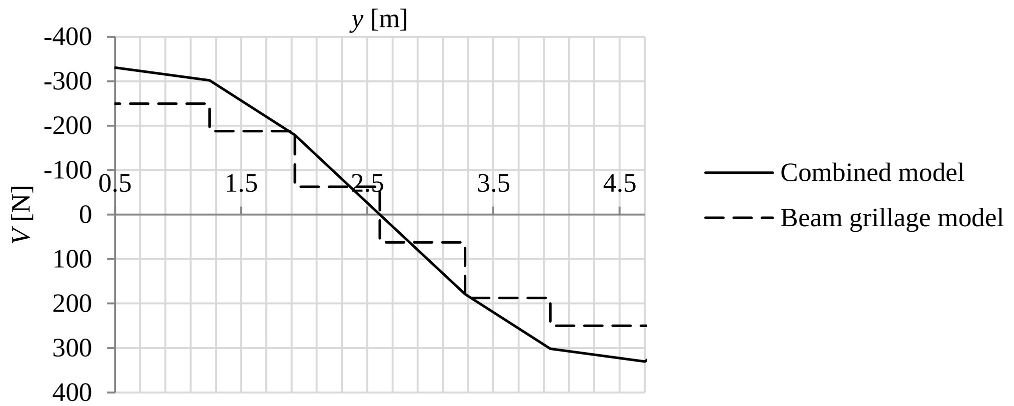

Figure 5.87 Shear force distribution along end wall for the combined and beam grillage model respectively. Load at end wall section.

Based on the bending stiffness relation between the end walls in the two models, it would have been more reasonable that the end wall modelled with shell elements in the combined model would induce higher rotational stiffness than the beam grillage model at end wall sections. However, the results of the rotational stiffness study disagree. It was therefore believed that the reason for the difference in rotational stiffness lies within the connections and interactions between the end walls and the rest of the bridge. This subject is however not studied further in this master's thesis project.

6 Evaluation of results

This section aims to put the findings in the project into a larger context and evaluate modelling choices in comparison with the simplified procedures that were used in the previous master's thesis project (Lundin & Magnander, 2012).

6.1 Modelling of load

One aim of this project was to examine whether if it can be motivated to model the load of one train wheel axle more accurately by considering the distribution of load effects within rails, sleepers and ballast. Sectional forces generated by a concentrated load and a load distributed according to handbook recommendations were compared. The study showed that the influence of load application varied between the beam grillage and combined models and between different parts within the models.

As could be expected, a large difference in bending moment was found in the mid-section of the slab in both the combined and beam grillage models where the models with distributed loading obtained considerably lower bending moments than those with concentrated load. These tendencies were also apparent in the study of distribution of load effects in shell elements. It is therefore essential to model with the distributed load to enable design and analyses of the slab and thus achieve coupling between the responses in transversal and longitudinal direction.

The transversal distributions of bending moment and shear force varied little along the slab edge of the combined model between the two load applications, as opposed to what was expected. A small difference in magnitude could however be noted, where the distributed load generated slightly larger shear forces and slightly smaller bending moments than the concentrated load in most sections. In the beam grillage model the differences in maximum bending moment and shear force along the slab edge were considerably larger as only one transversal beam was loaded and no transverse distribution could occur. The bending moment can be expected to differ in line with analytical solutions for a concentrated and distributed load.

The bending moment and shear force along the slab edge together with the normal force of the slab contribute to the torsion of the girders. Normal force arises due to the prevented deformation of the slab and varies in general little between a distributed and concentrated load application in the beam grillage and combined models. One significant difference is however evident in the mid-span section of the bridge in the beam grillage model, probably due to the need for a much larger deformation when subjected to a concentrated load.

It was found that the distributed load in the combined model resulted in approximately 12-14% smaller torsional moments than what was generated by the concentrated load. It is apparent that the generally small differences in bending moment, shear force and normal force in the combined model together achieve a considerable difference in torsion. The effects of the shear and normal force are however magnified due to the eccentric location of the slab edge in relation to the girder centre.

In the beam grillage model the difference in the maximum torsional moment varied greatly depending on where along the bridge the load was applied. The differences spanned between 4-25%, where the greatest difference was found when the model was subjected to load at the mid-span section. This larger difference in the mid-span section is reasonable as all forces at the slab edge that induce torsion are much greater for the case of concentrated load than for distributed load. When load is applied in the mid support section of the beam grillage model, the greatest torsional moment occurs in adjacent sections. Thus the considerably large differences in shear force and bending moment at the support section have smaller effect on the maximum torsional moment.

It was concluded to be preferable to model a distributed load, where the transverse and longitudinal distributions of load effects are accounted for, rather than a concentrated load, both with regard to the bending moment in the slab and torsion of the main girders.

6.2 Transverse distribution of load effects in FE-models

A method for how to treat the transverse distribution of load effects in the beam grillage model needed to be established to obtain results similar to those found in the combined model. Adjustment of the model output by distribution over an effective width was considered to be more general than to include the distribution width directly in the model when applying the load. The former approach saves time and computer resources as it leads to less computations and the result from one model can be adjusted to fit all cases rather than having to model each different case.

Analytical solutions distributed over an effective width were compared to the sectional forces in a slab model consisting of shell elements. This study suggested that the effective widths found in both BBK 04 and 'BYGG' obtain results that are well on the safe side in relation to the reference model. It can therefore be assumed that it should be acceptable to adjust the beam grillage model based on these widths. However, the usability of the results can be questioned as the computed values may be very conservative. Despite this it was concluded that even though the results may be well on the safe side, they would still be more accurate than if the transverse distribution was neglected.

Similarly, the adjusted output from the beam grillage model was compared to the sectional forces from the combined model. This study confirmed that the usage of the effective widths found in BBK 04 and 'BYGG' results in conservative sectional forces in most cases. It can however be discussed whether these recommendations are valid for other geometries and conditions. For example, the effective width recommended by 'BYGG' refers to the width of one traffic lane on a road bridge. It can be argued that this width should be adjusted to instead fit with the width of the track, if a railway bridge is studied.

In previous research (Davidsson, 2003) it has been shown that the transverse distribution of load effects in slabs is reduced in the vicinity of supports. It was noted that the combined model in this project takes account of this reduced distribution near supports as the average unit bending moment and shear force in these sections are larger than in other sections. This can be attributed to the natural distribution within shell elements and is closely related to the findings in the initial study of load effects in shell elements. The simply supported slab in the initial study distributed the load effects far more than the fixed-end model. This can be related to the varying rotational stiffness of the girders which results in a reduced distribution width near supports. None of the studied handbooks takes account of the support conditions when recommending a distribution width within the slab. This leads to a uniform transverse distribution of load effects in the slab along the entire bridge in the beam grillage model, independent of the difference in rotational stiffness of the girders in different sections of the bridge. As a result the beam grillage model did not obtain the same peaks in the average unit bending moment and shear force distributions at support sections as the combined model. It can be argued that this approach results in unsafe design values in support sections for the beam grillage model as this reduced transverse distribution is neglected.

Influence lines are suitable in design of structures subjected to moving loads. The possibility of superposition also decreases the amount of modelling required in design and analysis. A concern was however raised that superposition might not be applicable, if the transverse distribution of load effects was considered in the post-processing of the results. If the theoretical transverse distribution width would exceed the load spacing, the distributions would coincide between the loads and superposition would probably result in underestimated values.

This was consequently the result of the study in this master's thesis project. Using the recommended effective widths for one load, when creating influence lines of unit sectional forces, resulted in underestimated values after superposition. It was therefore investigated whether the load spacing or effective widths defined for several loads were better assumptions. It was shown that the usage of the load spacing as effective width resulted in values of the average unit bending moment and shear force well on the safe side in relation to the combined model in most cases, but allowed a too extensive distribution at the mid-support section.

Effective widths that give the same result as the combined model, when adjusting the beam grillage model, were computed in cases when the recommended values of b_{eff} resulted in too small sectional forces. The calculated effective width at the mid support section was more or less equal to the load width and in such cases no further distribution of load effects outside of the load application width can be included. As the transverse distribution of load effects varies along the bridge, both in the longitudinal direction and regarding of what section of the slab is studied, the procedure of choosing an effective width that can be used conservatively in design of all sections is difficult. The distribution width is also highly dependent on the number of load applications, which further complicates the choice of an effective width for general application.

In design and analysis the use of effective widths recommended in handbooks should always be acceptable. It is however questionable if the effective widths defined in 'BYGG' are applicable for railway bridges and whether both handbooks are allowed in combination with Eurocode. Calculations can be based on results from a beam grillage model adjusted according to handbook recommendations by distributing peak values over a certain effective width. In most cases the sectional forces found by this approach are very conservative and, if needed, a more detailed FE-analysis can be carried out to find new reduced design values. However, the reduced transverse distribution near support sections that has been shown both in this project and by Davidsson (2003) is not accounted for in the beam grillage model and the sectional forces in these sections should therefore be treated with caution. A combined model should preferably be created, if it is required to account for the difference in transverse distribution in different sections along the bridge.

6.3 Modelling and resistance of end wall and supports

It was assumed before the analyses that the torsional restraint of the model would primarily consist of the end walls and that the supports, if pinned-pinned in y-direction, should to some extent affect the torsional distribution. The results verified this assumption. It was however observed that the effect of supports was confined to nodes close to and at the support and that the torsional moment distribution continued along the unaffected shape further away from the support. It was also shown that horizontal reaction forces arise in the models also when the supports are pinned-roller in the y-direction. These unexpected reaction forces at various supports along the bridge balance each other and arise due to the girders need for deformation close to the load application and the restraint of this deformation along the rest of the girder. The horizontal reaction force at the mid support induces a torque of opposite sign and thus affects the torsional moment distribution, i.e. partially resists torsion at this support. This differs from the end supports where the horizontal reaction force contributes to the torsion induced by the slab edge forces.

It was investigated whether the torsional restraint of the bridge best was represented by end walls or if prescribed fixed twisting at the end supports was sufficient to achieve a similar response. It was found that the difference in torsional moment in the main girders between the two approaches was the greatest in sections close to the end wall and that the choice of modelling technique had more impact, when the load application approached the end wall. In the mid support and mid-span sections the differences were negligible. This indicates that it is sufficient to model the end walls as prescribed boundary conditions, if only the response in the mid support and mid-span sections is of interest. If a more realistic linear elastic response of the entire structure is desirable, it is however necessary to include the end walls in the model as prescribed fixed twisting results in unrealistic values in the outer sections of the bridge.

It was shown that the rotational stiffness of the girder close to the end walls varies greatly between the beam grillage and combined models. While the bending moment in the end wall of the combined model varies with a parabolic shape, the bending moment was constant in the end wall of the beam grillage model. It is believed that this difference occurs due to the modelling of the slab in each model rather than the choice of element types in the end walls. Normal forces arise in the slab due to the need for deformation that is restrained by the girders and end walls. Due to the compatibility between the shell elements in the combined model, the normal force distribution has a parabolic shape along all transverse sections of the slab, including the slab edge section that affects the bending moment distribution of the end wall. In the beam grillage model, non-loaded transversal beams, including the slab edge sections, obtains constant normal forces induced by the torsion of the girders. Only when the load is applied at the end wall section in the beam grillage model, does the shape of the normal force distribution, and thus also the bending moment distribution, become parabolic. It is therefore for this load application only that the real loading situation and the structural response of the end wall is represented correctly.

If the model is meant as a tool in design of the end wall or if a realistic linear elastic response of the entire bridge superstructure is desired, it is therefore assessed appropriate to model the bridge slab with shell elements as in the combined model. As is the case for fixed twisting, it is believed, based on the rotational stiffness diagrams, that the difference in torsional moment and rotational stiffness has little impact when design is solely based on the mid support and mid-span sections.

No evident conclusion regarding the difference in rotational stiffness could be identified during the Master's project. It was however assumed that the answer can be found in the connection and interaction between the end walls and the rest of the bridge if further studies would be performed on the subject.

6.4 Modelling choices

The two studied FE-models both have advantages and disadvantages regarding accuracy and the work effort required to build the model and process the results.

The greatest benefit of using a beam grillage model is the simplicity in both modelling and extraction of results in the FE-software. Sectional forces are easily accessed as they can be listed directly in the post-processor. However, if a coupling of the transverse and longitudinal response of the bridge is desired the output needs to be processed rather extensively. It is possible to standardise this procedure by creating general codes in e.g. MATLAB and in that way make the post-processing work more manageably. Influence lines can for example be created for a case without any transverse distribution and then be applied for different distribution widths by multiplication with a scale factor.

The definition of a suitable effective width may prove a difficult task as it has been shown that the transverse distribution varies along the bridge. An effective width derived to achieve conservative values along the whole bridge would result in sectional forces well on the safe side and thus not particularly cost-effective designs. On the other hand, a larger effective width may cause too small sectional forces in support sections and must therefore be used with caution. There is the possibility to use different effective widths in different sections, but this would also entail more extensive post-processing of results. The comparisons of superimposed influence lines and models subjected to four wheel loads imply that it is difficult to determine which recommended effective width gives a satisfactory result, if any of the recommendations hold. In fact, it may be hard to define an effective width that is known to be conservative without creating a reference model to compare with, thus losing the work effort saved by the easier modelling procedure.

Another disadvantage of the beam grillage model is the inability to connect the end wall with the transversal beams beyond the end transversal beams. When this coupling is lost, the normal forces that arise in the slab due to restrained deformation and to a large extent affect the bending moment of the end wall are inaccurately represented in unloaded transversal beams.

The combined model is considered to represent a sufficiently accurate linear elastic response of the bridge. The creation of the model involves roughly the same work effort as the beam grillage model, but the combined model demands more post-processing to obtain sectional forces in the slab.

7 Conclusions and suggestions for further studies

7.1 Conclusions

- Modelling with a distributed load that accounts for the distribution of load effects within rails, sleepers and ballast is appropriate as the maximum bending moment in the slab mid-section is drastically reduced in both models. Due to the transverse distribution, no or very small differences occur between the maximum bending moment, shear force and normal force along the slab edge in the combined model when subjected to either a concentrated or distributed load. Considerable differences can however be noted in the maximum torsional moment of the girder as both the shear force and normal force values at the slab edge are magnified with lever arms. In the beam grillage model that lacks the ability to distribute load effects within the slab the differences in bending moment, shear force and normal force between the two load applications are much greater. Hence, the torsional moment is considerably reduced, if distributions of load effects within the rails, sleepers and ballast are considered.
- The bending moment and shear force in the slab of the beam grillage model can always be distributed according to recommendations in handbooks by distributing peak values over a certain effective width. The codes do however not consider the support conditions of the slab or the distance to supports from the studied section although the FE-models of both this master's project and Davidsson (2003) indicate that no or a very small transverse distribution occurs close to and at support sections. The usage of recommended effective widths should therefore be used with caution at these sections.
- If more accurate bending moment and shear force distributions in the slab that account for the differences in transverse distribution near support sections, are desired, the combined model should be used.
- End walls restrain torsion by their bending stiffness. To include the end walls in the models results in more accurate linear elastic response near end wall sections compared to prescribing fixed twisting at end supports. It was however found that the difference is negligible at the mid support and mid-span sections which are often used in design.
- The modelling of the slab affects the structural response of the end wall as the bending moment distribution of the end wall depend on the normal forces in the transverse direction of the bridge in the slab. This interaction was lost in the beam grillage model in which loading of the end wall is only properly described when load is subjected at the end wall section. The slab should therefore be modelled with shell elements, if an accurate linear elastic response of the end wall is required.
- Supports that are fixed for translation in the transverse direction of the bridge affect the torsional distribution locally as horizontal restraint forces induce a torque of the opposite direction. Supports that are free to translate in the transverse direction of the bridge along one side also induce horizontal reaction forces along the fixed side due to the needed deformation of the girder. These

horizontal reaction forces balance each other and induce torques of that either partially resist or magnify the torsional moment at support sections.

7.2 Propositions for further studies

- This project studied the transversal distribution of bending moment and shear force in the slab. The next step may be to examine whether the torsional moment in the girder may be distributed over some effective width in the beam grillage model, to even out the peak in the torsional moment distribution in the sections of the girder where the sectional forces from the slab are introduced. As the torsion is induced by all sectional forces along the slab edge, where each has a specific distribution width in the transverse direction, it is not as straight-forward as effective widths in the slab.
- It was found that the distribution width within a slab represented by shell elements varies along the bridge. A future study may examine in detail why this occurs, how it relates to reality and possibly how it can be handled in a beam grillage model.
- The structural response of the end wall was studied in this project. The analyses were however not sufficient to describe the large difference in rotational stiffness in sections close to the end walls in the girders in the combined model and beam grillage model and this could be studied further.
- The findings and conclusions regarding the beam grillage model and the ability to modify its output are all based on the combined model, which was used as a reference model. It could be worth verifying the combined model and its response by a model constructed by solid elements.
- The recommended effective widths treated in this project were derived from Swedish handbooks as nothing it mentioned regarding effective widths in slabs in Eurocode. It would therefore be of interest to study other codes, such as the American or British codes.
- The concrete was assumed to be uncracked, as linear elastic analyses were performed. In reality, this would only be the case if the bridge was prestressed. How would the distribution of normal forces from prestressing differ in the two studied models?
- Restraint forces occur within the structure, for example due to thermal changes. How should these loads be treated in FE-modelling of trough bridges?

8 References

ADINA (2010): *Theory and Modelling Guide – Volume I: ADINA*. ADINA R & D, Watertown.

Banverket (2007): *Broprojektering, BVH 583.20* (Bridge design, BVH 583.20. In Swedish). Banverket, Borlänge.

Boverket (2004): *Boverkets handbok om betongkonstruktioner, BBK 04* (Boverket´s handbook on Concrete Structures BBK 04, In Swedish). Boverket, Karlskrona.

CEN (2003): *Eurocode 1: Actions on structures, Part 2: Traffic loads on bridges, EN 1991-2*. European Committee for Standardization, Brussels.

CEN (2005): *Eurocode 2: Design of concrete structures, Part 1-1: General rules and rules for buildings, EN 1992-1-1*. European Committee for Standardization, Brussels.

Collins, M., Mitchell, D. (1990): *Prestressed Concrete Structures*. Prentice Hall, New Jersey.

Davidsson, M. (2003): *Strukturanalys av brokonstruktioner med finita element-metoden – Fördelning av krafter och moment* (Structural analysis of bridge structures using the finite element method – Distribution of forces and moments. In Swedish). Brosamverkan Väst, Göteborg.

Ekström, J. (2009): *Structural Modelling with Different Finite Element Types - Comparison of Analytic and Numerical Solutions for a Simply Supported Beam*. Master Thesis. Department of Structural Engineering, Chalmers University of Technology, Publication no. 2009:44, Göteborg.

Engström, B. (Ed.) (2008): *Structural connections for precast concrete buildings*. International federation of structural concrete, Lausanne.

Lundh, H. (2000): *Grundläggande hållfasthetslära* (Fundamental solid mechanics. In Swedish). Department of Solid Mechanics, Royal Institute of Technology, Stockholm.

Lundin, K. & Magnander, A. (2012): *Structural Analysis of a Typical Trough Bridge Using FEM.* Master Thesis. Department of Structural Engineering, Chalmers University of Technology, Publication no. 2012:106, Göteborg.

Nilson, A., Winter, G. (1991): *Design of concrete structures (11th edition)*. McGraw-Hill.

Pacoste et al. (2012): *Recommendations for finite element analysis for the design of reinforced concrete slabs.* Division of Structural Engineering and Bridges, Royal Institute of Technology, Stockholm.

Trafikverket (2011): *TRVK Bro 11, Trafikverkets tekniska krav Bro* (TRVK Bro 11, technical bridge requirements from the Swedish Transport Administration. In Swedish). Trafikverket, Borlänge.

Trafikverket (2012): *BVS 583.11 – Bärighetsberäkning av järnvägsbroar, Utgåva 5* (BVS 583.11 – Calculation of bearing capacity of railway bridges, Edition 5. In Swedish). Trafikverket, Borlänge.

Wahlström, B. (Ed.) (1969): *Handboken 'BYGG' – Konstruktionsteknik, huvuddel 3 (*Construction handbook – Structural engineering, part 3. In Swedish). Byggmästarens förlag, Stockholm.

Wang, C. M. et al. (2000): *Shear Deformable Beams and Plates – Relationships with Classical Solutions.* Elsevier Science, Oxford.

Williams, A. (2009): *Structural Analysis: In Theory and Practice.* Butterworth-Heinemann, Burlington.

Oral reference:
Lidemar, P., Bridge engineer at REINERTSEN, interview 2013-01-30

Appendix A Influence lines

The methodology presented in this section is mainly based on Williams (2009). Simply supported structural members have linearly varying influence lines that can easily be determined. Influence lines of shear force and bending moment for a structure subjected to a concentrated load are determined according to Figure 8.1.

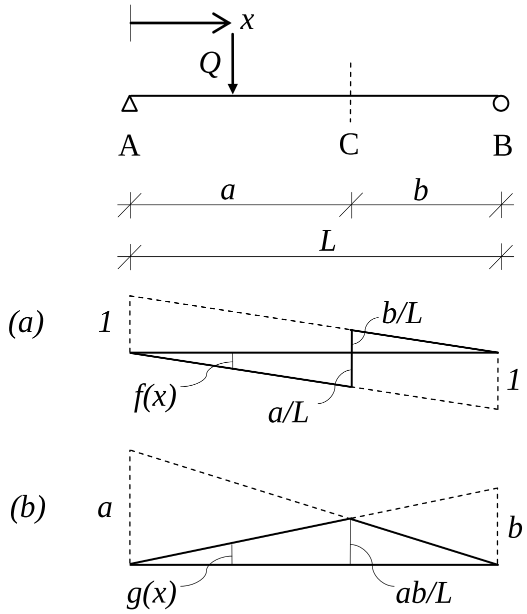

Figure 8.1 Influence lines for section C of a simply supported beam subjected to a concentrated load. a) Influence line for shear force. b) Influence line for bending moment.

When a single concentrated load is applied in an arbitrary section *x*, the shear force in the section C is obtained by multiplying the load with *f(x)* from the influence line diagram. The maximum positive shear force in section C is therefore obtained when the concentrated force is placed just to the right of the studied section and is calculated as

$$V_r = Q\frac{b}{L} \tag{8-1}$$

Similarly the maximum negative shear force in section C is found when the concentrated load is applied just to the left of the section and is given by

$$V_l = -Q\frac{a}{L} \tag{8-2}$$

The sectional bending moment in section C is obtained in a similar way as the shear force for each load position. Maximum bending moment occurs when the concentrated force is applied at $x = a$ and the maximum value is

$$M_{\max} = Q\frac{ab}{L} \tag{8-3}$$

Appendix B Derivations of analytical solutions

The analytical bending moment of a fixed end beam subjected to a centric concentrated load is obtained according to the fundamental case illustrated in Figure 8.2.

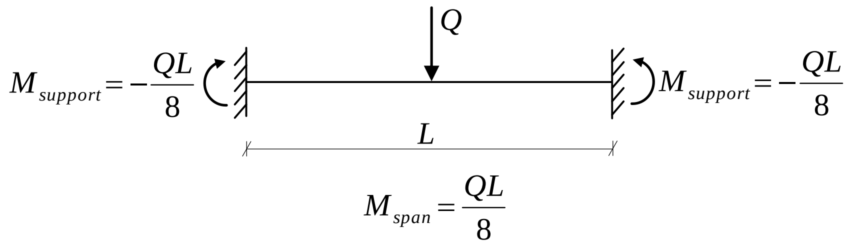

Figure 8.2 Fixed-end beam subjected to a centric concentrated load.

$$Q = 1000\,\text{N}$$

$$L = 4.2\,\text{m}$$

Support moment:

$$M_{support} = -\frac{QL}{8} = -\frac{1000 \cdot 4.2}{8} = -525 \text{ Nm} \tag{8-4}$$

Span moment:

$$M_{span} = \frac{QL}{8} = \frac{1000 \cdot 4.2}{8} = 525 \text{ Nm} \tag{8-5}$$

Other models were subjected to a distributed load over the length *b*, which represented the distributed load effect from one wheel pair through the ballast, see Figure 8.3.

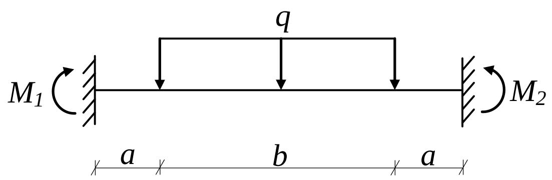

Figure 8.3 Fixed-end beam subjected to a distributed load q over the length b.

As there is no fundamental case for a fixed end beam with a distributed load applied along a certain length around the mid-span, the support moment is found by subtracting the support moment obtained from two distributed loads applied over length *a* from the support moment obtained from a load distributed over the entire span, see Figure 8.4, Figure 8.5 and Figure 8.6 respectively. In the preliminary study, the models were compared to analytical results for a beam of two different lengths; 4.2 m and 5.2 m.

$$q = 370\,\text{N/m}$$

$$a_{4.2m} = 0.75 \text{ m}$$

$$a_{5.2m} = 1.25 \text{ m}$$

$$b = 2.7\,\text{m}$$

$$M_1 = \frac{qa^2}{12}\left[6 - \frac{8a}{L} + \frac{3a^2}{L^2}\right]$$

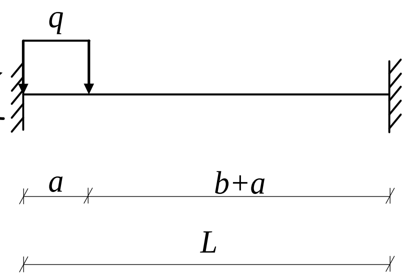

Figure 8.4 Fixed end beam subjected to a distributed load q over the length a on the left side of the span.

$$M_{1\_4.2m} = -\frac{370 \cdot 0.75^2}{12}\left[6 - \frac{8 \cdot 0.75}{4.2} + \frac{3 \cdot 0.75^2}{4.2^2}\right] = -80.94 \text{ Nm} \tag{8-6}$$

$$M_{1\_5.2m} = -\frac{370 \cdot 1.25^2}{12}\left[6 - \frac{8 \cdot 1.25}{5.2} + \frac{3 \cdot 1.25^2}{5.2^2}\right] = -204.77 \text{ Nm} \tag{8-7}$$

$$M_2 = \frac{qa^3}{12L}\left[4 - \frac{3a}{L}\right]$$

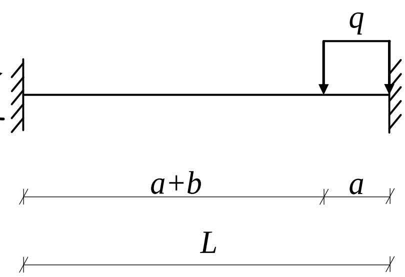

Figure 8.5 Fixed end beam subjected to a distributed load q over the length a on the right side of the span.

$$M_{2\_4.2m} = -\frac{370 \cdot 0.75^3}{12 \cdot 4.2}\left[4 - \frac{3 \cdot 0.75}{4.2}\right] = -10.73 \text{ Nm} \tag{8-8}$$

$$M_{2\_5.2m} = -\frac{370 \cdot 1.25^3}{12 \cdot 5.2}\left[4 - \frac{3 \cdot 1.25}{5.2}\right] = -37.97 \text{ Nm} \tag{8-9}$$

$$M_3 = \frac{qL^2}{12}$$

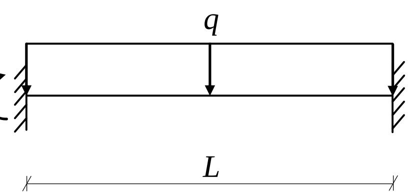

Figure 8.6 Fixed end beam subjected to a distributed load q over the entire span.

$$M_{3\_4.2m} = -\frac{370 \cdot 4.2^2}{12} = -543.9 \text{ Nm} \tag{8-10}$$

$$M_{3\_5.2m} = -\frac{370 \cdot 5.2^2}{12} = -833.73 \text{ Nm} \tag{8-11}$$

The support moment for a distributed load applied along the length 2.7 m on a beam of the length 4.2 m and 5.2 m respectively is found as

$$M_{edge} = M_3 - (M_1 + M_2) \tag{8-12}$$

$$M_{edge\_4.2m} = -543.9 - (-80.94 - 10.73) = -452.23 \text{ Nm} \tag{8-13}$$

$$M_{edge\_5.2m} = -833.73 - (-204.77 - 37.97) = -590.99 \text{ Nm} \tag{8-14}$$

In order to compare the analytical results of the 5.2 m long beam with the FE-model it was necessary to find the value corresponding to the slab edge, i.e. the analytical result 0.5 m from the support, and mid-span section. This was found by the use of the cut method. The sectional forces at the studied section $x = 0.5$ m are shown in Figure 8.7 and the bending moment in this section is derived in Equations (B-12) and (B-16).

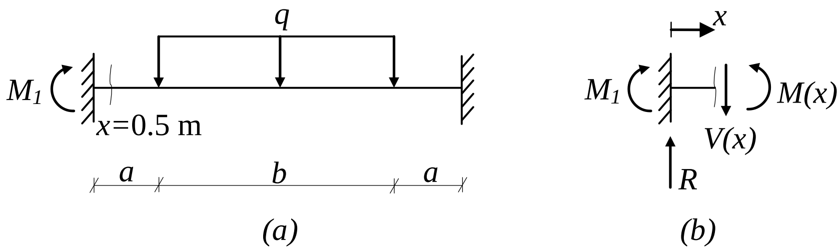

Figure 8.7 a) Cut at x=0.5 for a fixed-end beam subjected to a distributed load q over the length b and, b) Sectional forces at the studied section x.

$$M(x \le a) = M_1 + R \cdot x \tag{8-15}$$

$$M(x > a) = M_1 + R \cdot x + q \cdot \frac{(x-a)^2}{2} \tag{8-16}$$

$$M(0.5)_{5.2m} = -590.99 + 499.5 \cdot 0.5 = -341.25 \text{ Nm} \tag{8-17}$$

$$M(2.1)_{4.2m} = -452.23 + 499.5 \cdot 2.1 - 370 \cdot \frac{(2.1 - 0.75)^2}{2} = 259.55 \text{ Nm} \tag{8-18}$$

$$M(2.6)_{5.2m} = -590.99 + 499.5 \cdot 2.6 - 370 \cdot \frac{(2.6 - 1.25)^2}{2} = 371.01 \text{ Nm} \tag{8-19}$$

Similarly, the analytical values of bending moment at the edge and mid-span sections in a simply supported beam of 5.2 m length needed to be established as shown in Equations (B-17) to (B-20).

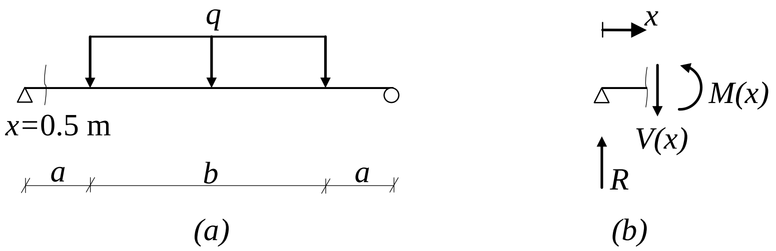

Figure 8.8 a) Cut at x=0.5 for a simply supported beam subjected to a distributed load q over the length b and, b) Sectional forces at the studied section x.

$$M(x) = R \cdot x \tag{8-20}$$

$$M(0.5)_{5.2m} = 499.5 \cdot 0.5 = 249.75 \text{ Nm} \tag{8-21}$$

$$M(x) = R \cdot x - q \cdot \frac{(x-a)^2}{2} \tag{8-22}$$

$$M(2.6)_{5.2m} = 499.5 \cdot 2.6 - 370 \cdot \frac{(2.6-1.25)^2}{2} = 961.54 \text{ Nm} \tag{8-23}$$

In the simply supported model of 4.2 m length the edge bending moment is zero and the bending moment of the mid-span section is calculated as

$$M(2.1)_{4.2m} = 499.5 \cdot 2.1 - 370 \cdot \frac{(2.1-0.75)^2}{2} = 711.79 \text{ Nm} \tag{8-24}$$

Appendix C Convergence studies

C.1 Study of distribution of load effects in shell elements

A convergence study was executed on the simplified slab model used in the preliminary study of the distribution of load effects in shell elements. As the model is mainly used to study the behaviour of the elements and not created to be used in design, the convergence study was simply focused on visual comparisons as well as comparison of a reference value.

Bending moment distributions along the slab edge and mid-sections are presented in Figure .1 and Figure A.2 and shear force distributions along the edge in Figure A.3.

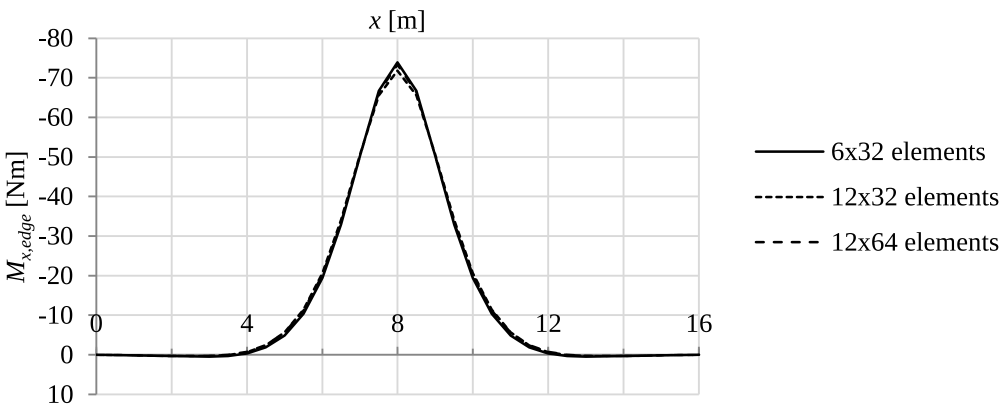

Figure .1 Bending moment distributions along the slab edge for different mesh densities of the slab.

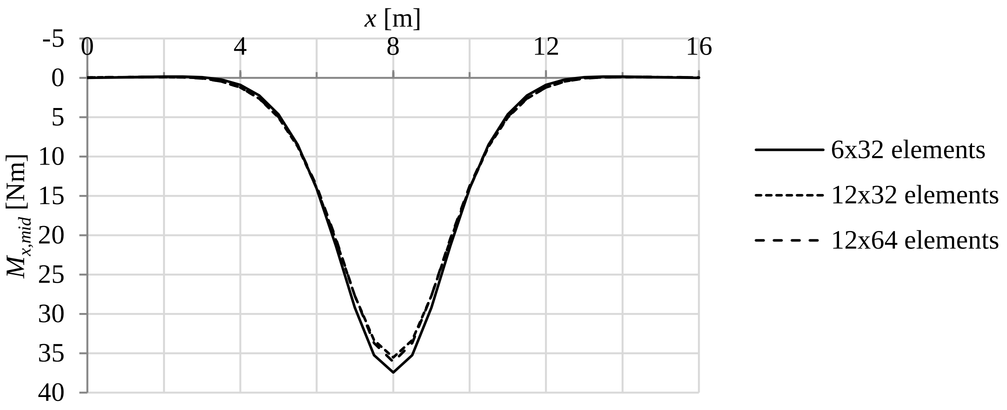

Figure A.2 Bending moment distributions along the mid-span section of the slab for different mesh densities of the slab.

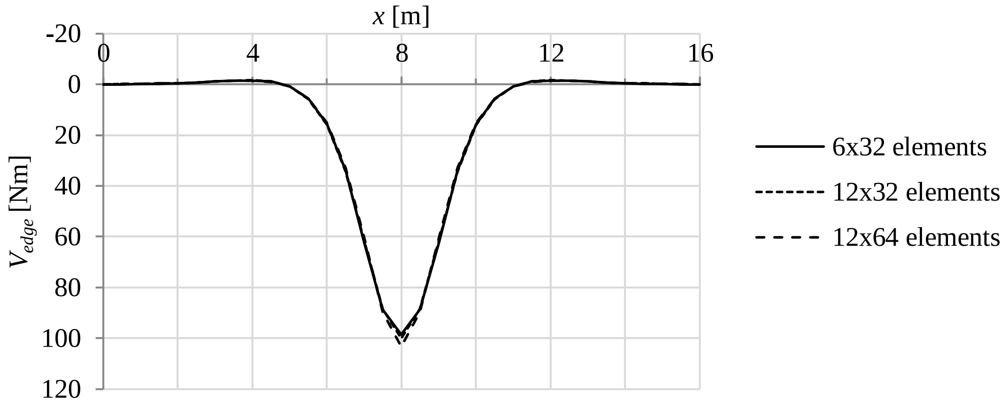

Figure A.3 Shear force distributions along the slab edge for different mesh densities of the slab.

The bending moment in the mid-point of the slab was compared for three different meshes with increased density, listed in Table A.1. Errors are calculated as the difference between the coarser meshes and the finest mesh divided by the finest mesh.

Table A.1 Bending moment [Nm] in mid-span of slab at x=6 m (3L/8).

Mesh	Number of elements	Bending moment in slab mid-point	Error
1	6x32	14.08	2.5 %
2	12x32	13.98	1.8 %
3	12x64	13.73	-

Based on the figures and table above, the mesh with 6x32 elements in the slab was concluded sufficiently good to use in the analyses of this project.

C.2 Combined model of the trough bridge

The bending moment for a specific load application was studied in the mid-span section of the bridge in the mid-span section of the slab in the combined model with three different mesh densities. Similarly, the torsional moment was studied in the mid-span section of the bridge in the girder to further verify the mesh of the model. The bending moments and torsional moments for the different mesh densities are presented in Table A.2. Errors are calculated as the difference between the coarser meshes and the finest mesh divided by the finest mesh.

Table A.2 Bending moment [Nm] and torsional moment [Nm] in chosen points of the slab and girder respectively for three meshes of increasing density.

Mesh	Number of elements	Bending moment in chosen point in slab	Error	Torsional moment in chosen point in girder	Error
1	6x68	54.2845	2.6 %	-26.0274	-1.3 %
2	12x68	53.0868	0.4 %	-26.2358	-0.6 %
3	18x68	52.8684	-	-26.3961	-

As the differences are all relatively small (less than 5 %), the mesh of 6x32 elements in the slab was assessed sufficiently dense to provide comparable results.

Appendix D Calculation of effective widths

D.1 Slab subjected to a single load application

Bending moment

The effective widths regarding the distribution of bending moment were derived from the formulas presented in Section 3.3.2. (D-1) and (D-2) represent the effective width based on BBK 04 (Boverket, 2004) and 'BYGG' (Wahlström (Ed.), 1969) respectively.

$$b_{eff.BBK,M} = b_x + 2 \cdot \min\left(3h, \frac{l}{10}\right) = 1 + 2 \cdot \min\left(3 \cdot 0.5, \frac{4.2}{10}\right) = 1.84\,\text{m} \qquad \text{(A-1)}$$

$$b_{eff.BYGG,M} = b_x + \min(0.75l, 2.5) = 1 + \min(0.75 \cdot 4.2, 2.5) = 3.5\,\text{m} \qquad \text{(A-2)}$$

Shear force

The effective width regarding the distribution of shear force according to BBK 04 was calculated as

$$b_{eff,BBK,V} = \max(7d + b_x, 10d + 1{,}3y)$$

$$= \max(7 \cdot 0.45 + 1{,}10 \cdot 0.45 + 1.3 \cdot 2.1) = 7.23\,\text{m} \qquad \text{(A-3)}$$

The effective width according to 'BYGG' was calculated in two steps.

$$b_{eff,BYGG,V} = \frac{1}{f}\left(\max(b_x + 2h_{\min}, 5h_{\min}) + 2y\right) \qquad \text{(A-4)}$$

where $f = \frac{4 + y/d}{8}$ for $y \leq 4d$ and $f = 1$ for $y > 4d$

The effective height of the cross-section is assumed to be equal to $0.9h$, i.e. $d = 0.45\,\text{m}$. The effective width differs at the slab mid-span and edge sections since $y = 2.1\,\text{m}$ at mid-span and $y = 0\,\text{m}$ at the edge. Thus, the factor f differs at these sections according to

$$f_{mid-span} = 1 \text{ since } 2.1 > 4d \qquad \text{(A-5)}$$

$$f_{edge} = \frac{4 + 0/0.45}{8} = 0.5 \text{ since } 0 < 4d \qquad \text{(A-6)}$$

The effective width at the mid-span and edge section respectively was calculated as

$$b_{eff,BYGG,V,mid-span} = \frac{1}{1}\left(\max(1 + 2 \cdot 0.5, 5 \cdot 0.5) + 2 \cdot 2.1\right) = 6.7\,\text{m} \qquad \text{(A-7)}$$

$$b_{eff,BYGG,V,edge} = \frac{1}{0.5}\left(\max(1 + 2 \cdot 0.5, 5 \cdot 0.5) + 2 \cdot 0\right) = 5\,\text{m} \qquad \text{(A-8)}$$

D.2 Slab subjected to four load applications

When the slab is subjected to several adjacent loads the distribution of load effects from each load might coincide. This was accounted for by calculating new effective widths for bending moment and shear force based on BBK 04 and 'BYGG'

Bending moment

BBK 04 does not give any recommendation for calculation of the effective width with regard to bending moment for multiple load applications. Instead, b_{eff} for four loads was found as the total distance between the loads plus the effective width that BBK 04 recommends for a single load application, see Figure A.4 and Equation (D-9).

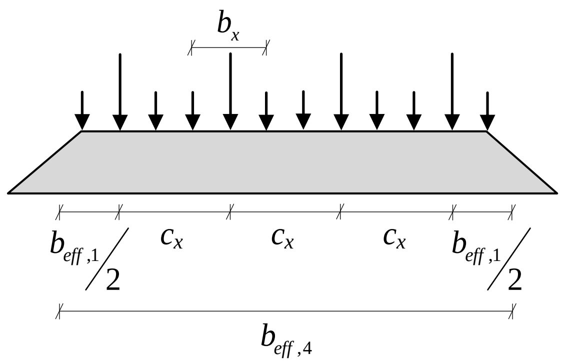

Figure A.4 Schematic drawing of the effective width for four wheel loads $b_{eff,4}$.

$$b_{eff,BBK,M,4} = 3c_x + b_{eff,BBK,M} = 3 \cdot 1.5 + 1.84 = 6.34\,\text{m} \tag{A-9}$$

An equation for deriving the effective width for two loads according to 'BYGG' was stated in 3.3.2.1. This equation was modified to fit for four applied loads and the effective width was then calculated as

$$\begin{aligned} b_{eff,BYGG,M,4} &= 4b_x + \min(1.5l, 2.5 + 3c_x - 3b_x, 0.75l + 3c_x - 3b_x) \\ &= 4 \cdot 1 + \min(1.5 \cdot 4.2, 2.5 + 3 \cdot 1.5 - 3 \cdot 1, 0.75 \cdot 4.2 + 3 \cdot 1.5 - 3 \cdot 1) = 8\,\text{m} \end{aligned} \tag{A-10}$$

Shear force

None of the codes contain any formula for how to calculate the effective width with regard to shear force for a slab subjected to multiple load applications. However, the effective widths based on each code were found using the same procedure as described for the distribution of bending moment according to BBK above.

$$b_{eff,BBK,V,4} = 3c_x + b_{eff,BBK,V} = 3 \cdot 1.5 + 7.23 = 11.73\,\text{m} \tag{A-11}$$

$$b_{eff,BYGG,V,4,mid-span} = 3c_x + b_{eff,BYGG,V,mid-span} = 3 \cdot 1.5 + 6.7 = 11.2\,\text{m} \tag{A-12}$$

$$b_{eff,BYGG,V,4,edge} = 3c_x + b_{eff,BYGG,V,edge} = 3 \cdot 1.5 + 5 = 9.5\,\text{m} \tag{A-13}$$

Note that the effective width in 'BYGG' differs between the mid-span and edge sections of the slab in line with what was found for a single load application.

Appendix E ADINA IN-files

E.1 Slab model in study of distribution of load effects

Example shown below: fixed-end slab model with distributed load, i.e. where the distribution of load effects within rails, sleepers and ballast are considered.

```
*************************************************
* GEOMETRY
*************************************************

COORDINATES

* Slab
1  0    0     0
2  7.5  0     0
3  8.5  0     0
4  16   0     0
5  0    0.75  0
6  7.5  0.75  0
7  8.5  0.75  0
8  16   0.75  0
9  0    3.45  0
10 7.5  3.45  0
11 8.5  3.45  0
12 16   3.45  0
13 0    4.2   0
14 7.5  4.2   0
15 8.5  4.2   0
16 16   4.2   0

* B.C. lines
17 0   -0.5   0
18 16  -0.5   0
19 0    4.7   0
20 16   4.7   0

* Auxiliary point
21 0    5     0

* Slab surfaces
SURFACE VERTEX NAME=1 P1=6 P2=5 P3=1 P4=2
SURFACE VERTEX NAME=2 P1=10 P2=9 P3=5 P4=6
SURFACE VERTEX NAME=3 P1=14 P2=13 P3=9 P4=10
SURFACE VERTEX NAME=4 P1=7 P2=6 P3=2 P4=3
SURFACE VERTEX NAME=5 P1=11 P2=10 P3=6 P4=7
SURFACE VERTEX NAME=6 P1=15 P2=14 P3=10 P4=11
SURFACE VERTEX NAME=7 P1=8 P2=7 P3=3 P4=4
SURFACE VERTEX NAME=8 P1=12 P2=11 P3=7 P4=8
SURFACE VERTEX NAME=9 P1=16 P2=15 P3=11 P4=12

* B.C. lines
LINE STRAIGHT NAME=25 P1=17 P2=18
LINE STRAIGHT NAME=26 P1=19 P2=20

* Cross-section beams (B.C. lines)
CROSS-SECTIO RECTANGULAR NAME=1 WIDTH=1,
   HEIGHT=1

*************************************************
* MATERIAL
*************************************************

* Concrete
MATERIAL ELASTIC NAME=1 E=3E+10 NU=0

*************************************************
* BOUNDARY CONDITIONS
*************************************************
FIXBOUNDARY LINES FIXITY=ALL
25
26

*************************************************
* LOAD APPLICATION
*************************************************

LOAD PRESSURE NAME=1 MAGNITUD=370

APPLY-LOAD BODY=0
1  'PRESSURE' 1  'SURFACE' 5 0 1 0 0 -1

*************************************************
* MESHING
*************************************************

* Element groups
* Slab
EGROUP SHELL NAME=1 MATERIAL=1,
   RESULTS=FORCES THICKNES=0.5

* Beams (B.C. lines)
EGROUP BEAM NAME=2 SUBTYPE=THREE-D,
   MATERIAL=1 RINT=5 RESULTS=SFORCES,
   DESCRIPT='BC LINES' SECTION=1 SPOINT=5

* Element sizes
SUBDIVIDE LINE NAME=1 MODE=LENGTH SIZE=0.5
3
5
8
11
12
14
16
18
19
21
23
25
26

SUBDIVIDE LINE NAME=2 MODE=LENGTH SIZE=0.75
4
9
10
13
17
20
24

SUBDIVIDE LINE NAME=6 MODE=LENGTH,
   SIZE=0.675
7
15
22

* Mesh generation
GSURFACE NODES=4 NCOINCID=BOUNDARIES,
   GROUP=1
```

```
1
2
3
4
5
6
7
8
9

GLINE NODES=2 AUXPOINT=21 GROUP=2
25
26

************************************************
* RIGID LINKS
************************************************

NODESET NAME=1 DESCRIPT='SLAB EDGES' ,
   OPTION=LINE-
3
8
12
16
19
23

NODESET NAME=2 DESCRIPT='BC LINES' ,
   OPTION=LINE-
25
26

RIGIDLINK NAME=1 SLAVETYP=NODESET,
   SLAVENAM=1 MASTERTY=NODESET,
   MASTERNA=2

************************************************
* ANALYSIS
************************************************
```

E.2 Combined model

```
***************************************************
* GEOMETRY
***************************************************

COORDINATES
*(number,x,y,z)

* Main girders
1    0    0     0
2    0    5.2   0
3    17   0     0
4    17   5.2   0
5    34   0     0
6    34   5.2   0
7    1    0     0
8    1    5.2   0
9    33   0     0
10   33   5.2   0

* Plate (slab)
11   0     1.25   -0.4
12   0     3.95   -0.4
13   0.5   1.25   -0.4
14   0.5   3.95   -0.4
15   0     0.5    -0.4
16   0     4.7    -0.4
17   0.5   0.5    -0.4
18   0.5   4.7    -0.4

* Auxiliary point, girders
19   0    7              0

* B.C. points
20   1    0     -0.65
21   1    5.2   -0.65
22   17   0     -0.65
23   17   5.2   -0.65
24   33   0     -0.65
25   33   5.2   -0.65

* Auxiliary points, stiff elements between girders and B.C.
26   35   0     -0.65
27   35   5.2   -0.65

* End walls
28  0   -0.5   -0.4
29  0   -0.5   -1.85
30  0   5.7    -0.4
31  0   5.7    -1.85
32  0   0.5    -1.85
33  0   1.25   -1.85
34  0   3.95   -1.85
35  0   4.7    -1.85
36  34  -0.5   -0.4
37  34  -0.5   -1.85
38  34  5.7    -0.4
39  34  5.7    -1.85
40  34  0.5    -1.85
41  34  1.25   -1.85
42  34  3.95   -1.85
43  34  4.7    -1.85

* Main girders
LINE STRAIGHT NAME=1 P1=1  P2=5
LINE STRAIGHT NAME=2 P1=2  P2=6


* Stiff elements between girder and B.C. points
LINE STRAIGHT NAME=3 P1=7  P2=20
LINE STRAIGHT NAME=4 P1=3  P2=22
LINE STRAIGHT NAME=5 P1=9  P2=24
LINE STRAIGHT NAME=6 P1=8  P2=21
LINE STRAIGHT NAME=7 P1=4  P2=23
LINE STRAIGHT NAME=8 P1=10 P2=25

* Plate (slab)
TRANSFORMATI TRANSLATION NAME=1,
   MODE=SYSTEM,
   DX=0.5 DY=0 DZ=0

* Mid (loaded) surfaces
SURFACE VERTEX NAME=101 P1=14 P2=12 P3=11
   P4=13

SURFACE TRANSFORMED NAME=102 PARENT=101,
   TRANSFOR=1 PCOINCID=YES PTOLERAN=1E-05,
   NCOPY=67

* End (unloaded) surfaces
SURFACE VERTEX NAME=201 P1=13 P2=11 P3=15,
   P4=17

SURFACE TRANSFORMED NAME=202 PARENT=201,
   TRANSFOR=1 PCOINCID=YES PTOLERAN=1E-05,
   NCOPY=67

SURFACE VERTEX NAME=301 P1=18 P2=16 P3=12,
   P4=14

SURFACE TRANSFORMED NAME=302 PARENT=301,
   TRANSFOR=1 PCOINCID=YES PTOLERAN=1E-05,
   NCOPY=67

* End wall at x=0
SURFACE VERTEX NAME=401 P1=12 P2=34 P3=33
   P4=11
SURFACE VERTEX NAME=402 P1=16 P2=35 P3=34
   P4=12
SURFACE VERTEX NAME=403 P1=11 P2=33 P3=32
   P4=15
SURFACE VERTEX NAME=404 P1=30 P2=31 P3=35
   P4=16
SURFACE VERTEX NAME=405 P1=15 P2=32 P3=29
   P4=28

* End wall at x=34
SURFACE VERTEX NAME=501 P1=42 P2=308 P3=311
   P4=41
SURFACE VERTEX NAME=502 P1=41 P2=311 P3=579
  P4=40
SURFACE VERTEX NAME=503 P1=43 P2=646 P3=308
  P4=42
SURFACE VERTEX NAME=504 P1=40 P2=579 P3=36
  P4=37
SURFACE VERTEX NAME=505 P1=39 P2=38 P3=646
  P4=43

* Cross-sections
* Main girders
CROSS-SECTIO RECTANGULAR NAME=1 WIDTH=1,
   HEIGHT=1.3

* Stiff elements
CROSS-SECTIO PROPERTIES NAME=2
   RINERTIA=1000 SINERTIA=1000 TINERTIA=1000,
   AREA=100


***************************************************
* MATERIAL
***************************************************
```

```
* Concrete
MATERIAL ELASTIC NAME=1 E=3E+10 NU=0,
    DENSITY=0 ALPHA=0 MDESCRIP='CONCRETE'

* Stiff elements
MATERIAL ELASTIC NAME=2 E=3E+10 NU=0,
    DENSITY=0 ALPHA=0 MDESCRIP='LINKS'


*************************************************
* BOUNDARY CONDITIONS
*************************************************

FIXITY NAME=MID_SUPPORT
 'X-TRANSLATION'
 'Y-TRANSLATION'
 'Z-TRANSLATION'
 'Z-ROTATION'

FIXITY NAME=END_SUPPORTS
 'Y-TRANSLATION'
 'Z-TRANSLATION'
 'Z-ROTATION'

FIXBOUNDARY POINTS FIXITY=ALL
20        'END_SUPPORTS'
22        'MID_SUPPORT'
24        'END_SUPPORTS'
21        'END_SUPPORTS'
23        'MID_SUPPORT'
25        'END_SUPPORTS'


*************************************************
* LOAD APPLICATION
*************************************************

read time_function_combined.in

LOAD PRESSURE NAME=1 MAGNITUD=370

APPLY-LOAD BODY=0
1 'PRESSURE' 1 'SURFACE' 101 0 1
2 'PRESSURE' 1 'SURFACE' 102 0 1
3 'PRESSURE' 1 'SURFACE' 102 0 2
4 'PRESSURE' 1 'SURFACE' 103 0 2
5 'PRESSURE' 1 'SURFACE' 103 0 3
6 'PRESSURE' 1 'SURFACE' 104 0 3
7 'PRESSURE' 1 'SURFACE' 104 0 4
8 'PRESSURE' 1 'SURFACE' 105 0 4
9 'PRESSURE' 1 'SURFACE' 105 0 5
10 'PRESSURE' 1 'SURFACE' 106 0 5
11 'PRESSURE' 1 'SURFACE' 106 0 6
12 'PRESSURE' 1 'SURFACE' 107 0 6
13 'PRESSURE' 1 'SURFACE' 107 0 7
14 'PRESSURE' 1 'SURFACE' 108 0 7
15 'PRESSURE' 1 'SURFACE' 108 0 8
16 'PRESSURE' 1 'SURFACE' 109 0 8
17 'PRESSURE' 1 'SURFACE' 109 0 9
18 'PRESSURE' 1 'SURFACE' 110 0 9
19 'PRESSURE' 1 'SURFACE' 110 0 10
20 'PRESSURE' 1 'SURFACE' 111 0 10
21 'PRESSURE' 1 'SURFACE' 111 0 11
22 'PRESSURE' 1 'SURFACE' 112 0 11
23 'PRESSURE' 1 'SURFACE' 112 0 12
24 'PRESSURE' 1 'SURFACE' 113 0 12
25 'PRESSURE' 1 'SURFACE' 113 0 13
26 'PRESSURE' 1 'SURFACE' 114 0 13
27 'PRESSURE' 1 'SURFACE' 114 0 14
28 'PRESSURE' 1 'SURFACE' 115 0 14
29 'PRESSURE' 1 'SURFACE' 115 0 15
30 'PRESSURE' 1 'SURFACE' 116 0 15
31 'PRESSURE' 1 'SURFACE' 116 0 16
32 'PRESSURE' 1 'SURFACE' 117 0 16
33 'PRESSURE' 1 'SURFACE' 117 0 17
34 'PRESSURE' 1 'SURFACE' 118 0 17
35 'PRESSURE' 1 'SURFACE' 118 0 18
36 'PRESSURE' 1 'SURFACE' 119 0 18
37 'PRESSURE' 1 'SURFACE' 119 0 19
38 'PRESSURE' 1 'SURFACE' 120 0 19
39 'PRESSURE' 1 'SURFACE' 120 0 20
40 'PRESSURE' 1 'SURFACE' 121 0 20
41 'PRESSURE' 1 'SURFACE' 121 0 21
42 'PRESSURE' 1 'SURFACE' 122 0 21
43 'PRESSURE' 1 'SURFACE' 122 0 22
44 'PRESSURE' 1 'SURFACE' 123 0 22
45 'PRESSURE' 1 'SURFACE' 123 0 23
46 'PRESSURE' 1 'SURFACE' 124 0 23
47 'PRESSURE' 1 'SURFACE' 124 0 24
48 'PRESSURE' 1 'SURFACE' 125 0 24
49 'PRESSURE' 1 'SURFACE' 125 0 25
50 'PRESSURE' 1 'SURFACE' 126 0 25
51 'PRESSURE' 1 'SURFACE' 126 0 26
52 'PRESSURE' 1 'SURFACE' 127 0 26
53 'PRESSURE' 1 'SURFACE' 127 0 27
54 'PRESSURE' 1 'SURFACE' 128 0 27
55 'PRESSURE' 1 'SURFACE' 128 0 28
56 'PRESSURE' 1 'SURFACE' 129 0 28
57 'PRESSURE' 1 'SURFACE' 129 0 29
58 'PRESSURE' 1 'SURFACE' 130 0 29
59 'PRESSURE' 1 'SURFACE' 130 0 30
60 'PRESSURE' 1 'SURFACE' 131 0 30
61 'PRESSURE' 1 'SURFACE' 131 0 31
62 'PRESSURE' 1 'SURFACE' 132 0 31
63 'PRESSURE' 1 'SURFACE' 132 0 32
64 'PRESSURE' 1 'SURFACE' 133 0 32
65 'PRESSURE' 1 'SURFACE' 133 0 33
66 'PRESSURE' 1 'SURFACE' 134 0 33
67 'PRESSURE' 1 'SURFACE' 134 0 34
68 'PRESSURE' 1 'SURFACE' 135 0 34
69 'PRESSURE' 1 'SURFACE' 135 0 35
70 'PRESSURE' 1 'SURFACE' 136 0 35
71 'PRESSURE' 1 'SURFACE' 136 0 36
72 'PRESSURE' 1 'SURFACE' 137 0 36
73 'PRESSURE' 1 'SURFACE' 137 0 37
74 'PRESSURE' 1 'SURFACE' 138 0 37
75 'PRESSURE' 1 'SURFACE' 138 0 38
76 'PRESSURE' 1 'SURFACE' 139 0 38
77 'PRESSURE' 1 'SURFACE' 139 0 39
78 'PRESSURE' 1 'SURFACE' 140 0 39
79 'PRESSURE' 1 'SURFACE' 140 0 40
80 'PRESSURE' 1 'SURFACE' 141 0 40
81 'PRESSURE' 1 'SURFACE' 141 0 41
82 'PRESSURE' 1 'SURFACE' 142 0 41
83 'PRESSURE' 1 'SURFACE' 142 0 42
84 'PRESSURE' 1 'SURFACE' 143 0 42
85 'PRESSURE' 1 'SURFACE' 143 0 43
86 'PRESSURE' 1 'SURFACE' 144 0 43
87 'PRESSURE' 1 'SURFACE' 144 0 44
88 'PRESSURE' 1 'SURFACE' 145 0 44
89 'PRESSURE' 1 'SURFACE' 145 0 45
90 'PRESSURE' 1 'SURFACE' 146 0 45
91 'PRESSURE' 1 'SURFACE' 146 0 46
92 'PRESSURE' 1 'SURFACE' 147 0 46
93 'PRESSURE' 1 'SURFACE' 147 0 47
94 'PRESSURE' 1 'SURFACE' 148 0 47
95 'PRESSURE' 1 'SURFACE' 148 0 48
96 'PRESSURE' 1 'SURFACE' 149 0 48
97 'PRESSURE' 1 'SURFACE' 149 0 49
98 'PRESSURE' 1 'SURFACE' 150 0 49
99 'PRESSURE' 1 'SURFACE' 150 0 50
100 'PRESSURE' 1 'SURFACE' 151 0 50
101 'PRESSURE' 1 'SURFACE' 151 0 51
102 'PRESSURE' 1 'SURFACE' 152 0 51
103 'PRESSURE' 1 'SURFACE' 152 0 52
```

```
104 'PRESSURE' 1 'SURFACE' 153 0 52
105 'PRESSURE' 1 'SURFACE' 153 0 53
106 'PRESSURE' 1 'SURFACE' 154 0 53
107 'PRESSURE' 1 'SURFACE' 154 0 54
108 'PRESSURE' 1 'SURFACE' 155 0 54
109 'PRESSURE' 1 'SURFACE' 155 0 55
110 'PRESSURE' 1 'SURFACE' 156 0 55
111 'PRESSURE' 1 'SURFACE' 156 0 56
112 'PRESSURE' 1 'SURFACE' 157 0 56
113 'PRESSURE' 1 'SURFACE' 157 0 57
114 'PRESSURE' 1 'SURFACE' 158 0 57
115 'PRESSURE' 1 'SURFACE' 158 0 58
116 'PRESSURE' 1 'SURFACE' 159 0 58
117 'PRESSURE' 1 'SURFACE' 159 0 59
118 'PRESSURE' 1 'SURFACE' 160 0 59
119 'PRESSURE' 1 'SURFACE' 160 0 60
120 'PRESSURE' 1 'SURFACE' 161 0 60
121 'PRESSURE' 1 'SURFACE' 161 0 61
122 'PRESSURE' 1 'SURFACE' 162 0 61
123 'PRESSURE' 1 'SURFACE' 162 0 62
124 'PRESSURE' 1 'SURFACE' 163 0 62
125 'PRESSURE' 1 'SURFACE' 163 0 63
126 'PRESSURE' 1 'SURFACE' 164 0 63
127 'PRESSURE' 1 'SURFACE' 164 0 64
128 'PRESSURE' 1 'SURFACE' 165 0 64
129 'PRESSURE' 1 'SURFACE' 165 0 65
130 'PRESSURE' 1 'SURFACE' 166 0 65
131 'PRESSURE' 1 'SURFACE' 166 0 66
132 'PRESSURE' 1 'SURFACE' 167 0 66
133 'PRESSURE' 1 'SURFACE' 167 0 67
134 'PRESSURE' 1 'SURFACE' 168 0 67


*************************************************
* MESHING
*************************************************

* Element groups
EGROUP SHELL NAME=1 MATERIAL=1,
   RESULTS=FORCES DESCRIPT='SLAB',
   THICKNES=0.5

EGROUP BEAM NAME=2 SUBTYPE=THREE-D,
   MATERIAL=1 RINT=5 RESULTS=SFORCES,
   DESCRIPT='GIRDERS' SECTION=1 SPOINT=5

EGROUP BEAM NAME=3 SUBTYPE=THREE-D,
   MATERIAL=2 RINT=5 RESULTS=SFORCES,
   DESCRIPT='STIFF ELEMENTS' SECTION=2,
   SPOINT=5

EGROUP SHELL NAME=4 MATERIAL=1,
   RESULTS=FORCES DESCRIPT='END WALL',
  THICKNES=0.5

* Element sizes
*Main girders
SUBDIVIDE LINE NAME=1 MODE=DIVISIONS,
   NDIV=68
2

* Stiff elements
SUBDIVIDE LINE NAME=3 MODE=DIVISIONS,
   NDIV=1
4
TO
8

* Slab
SUBDIVIDE SURFACE NAME=101,
   MODE=DIVISIONS  NDIV1=1 NDIV2=4
102
TO
168

SUBDIVIDE SURFACE NAME=201,
   MODE=DIVISIONS NDIV1=1 NDIV2=1
202
TO
268
301
TO
368

* End walls
SUBDIVIDE SURFACE NAME=401,
   MODE=DIVISIONS NDIV1=2 NDIV2=4
501

SUBDIVIDE SURFACE NAME=402,
   MODE=DIVISIONS NDIV1=2 NDIV2=1
403
502
503

SUBDIVIDE SURFACE NAME=404,
   MODE=DIVISIONS NDIV1=2 NDIV2=2
405
504
505

* Mesh generation

*Main girders
GLINE NODES=2 AUXPOINT=19 GROUP=2
1
2

* Stiff elements between girder and B.C. points
GLINE NODES=2 AUXPOINT=26 GROUP=3
3
TO
5

GLINE NODES=2 AUXPOINT=27 GROUP=3
6
TO
8

* Slab
GSURFACE NODES=4 GROUP=1
101
TO
168
201
TO
268
301
TO
368

*End walls
GSURFACE NODES=4 GROUP=4
401
TO
405
501
TO
505


*************************************************
* RIGID LINKS
*************************************************

* Between slab and girders
```

```
NODESET NAME=1 DESCRIPT='GIRDERS',
   OPTION=LINE-
1
2

NODESET NAME=2 DESCRIPT='SLAB EDGES',
   OPTION=LINE-
286
STEP 4 TO
546
555
STEP 4 TO
815

NODESET NAME=3,
   DESCRIPT='GIRDER END POINTS', OPTION=NODE
1
69
71
139

NODESET NAME=4,
   DESCRIPT='GIRDERS WITHOUT END POINTS',
   OPTION=SUBTR TARGET=1
3

RIGIDLINK NAME=1 SLAVETYP=NODESET,
   SLAVENAM=2 MASTERTY=NODESET,
   MASTERNA=4

* Between girder end points and end wall

RIGIDLINK NAME=2 SLAVETYP=LINE,
   SLAVENAM=835 MASTERTY=POINT,
   MASTERNA=1

RIGIDLINK NAME=3 SLAVETYP=LINE,
   SLAVENAM=832 MASTERTY=POINT,
   MASTERNA=2

RIGIDLINK NAME=4 SLAVETYP=LINE,
   SLAVENAM=843 MASTERTY=POINT,
   MASTERNA=5

RIGIDLINK NAME=5 SLAVETYP=LINE,
   SLAVENAM=847 MASTERTY=POINT,
   MASTERNA=6


*************************************************
* ANALYSIS
*************************************************
```

E.3 Time function (combined model)

```
* Time step definition, number of  *
steps and step size
TIMESTEP NAME=DEFAULT
@CLEAR
67 1

* Definition of each time step
TIMEFUNCTION NAME=1
@CLEAR
0 0
1 1
2 0
67 0

TIMEFUNCTION NAME=2
@CLEAR
0 0
1 0
2 1
3 0
67 0

TIMEFUNCTION NAME=3
@CLEAR
0 0
2 0
3 1
4 0
67 0

TIMEFUNCTION NAME=4
@CLEAR
0 0
3 0
4 1
5 0
67 0

TIMEFUNCTION NAME=5
@CLEAR
0 0
4 0
5 1
6 0
67 0

TIMEFUNCTION NAME=6
@CLEAR
0 0
5 0
6 1
7 0
67 0

TIMEFUNCTION NAME=7
@CLEAR
0 0
6 0
7 1
8 0
67 0

TIMEFUNCTION NAME=8
@CLEAR
0 0
7 0
8 1
9 0
67 0

TIMEFUNCTION NAME=9
@CLEAR
0 0
8 0
9 1
10 0
67 0

TIMEFUNCTION NAME=10
@CLEAR
0 0
9 0
10 1
11 0
67 0

TIMEFUNCTION NAME=11
@CLEAR
0 0
10 0
11 1
12 0
67 0

TIMEFUNCTION NAME=12
@CLEAR
0 0
11 0
12 1
13 0
67 0

TIMEFUNCTION NAME=13
@CLEAR
0 0
12 0
13 1
14 0
67 0

TIMEFUNCTION NAME=14
@CLEAR
0 0
13 0
14 1
15 0
67 0

TIMEFUNCTION NAME=15
@CLEAR
0 0
14 0
15 1
16 0
67 0

TIMEFUNCTION NAME=16
@CLEAR
0 0
15 0
16 1
17 0
67 0

TIMEFUNCTION NAME=17
@CLEAR
0 0
16 0
17 1
18 0
67 0

TIMEFUNCTION NAME=18
@CLEAR
0 0
17 0
18 1
19 0
67 0

TIMEFUNCTION NAME=19
@CLEAR
0 0
18 0
19 1
20 0
67 0

TIMEFUNCTION NAME=20
@CLEAR
0 0
19 0
20 1
21 0
67 0

TIMEFUNCTION NAME=21
@CLEAR
0 0
20 0
21 1
22 0
67 0

TIMEFUNCTION NAME=22
@CLEAR
0 0
21 0
22 1
23 0
67 0

TIMEFUNCTION NAME=23
@CLEAR
0 0
22 0
23 1
24 0
67 0

TIMEFUNCTION NAME=24
@CLEAR
0 0
23 0
24 1
25 0
67 0

TIMEFUNCTION NAME=25
@CLEAR
0 0
24 0
25 1
26 0
67 0

TIMEFUNCTION NAME=26
```

```
@CLEAR
0 0
25 0
26 1
27 0
67 0

TIMEFUNCTION NAME=27
@CLEAR
0 0
26 0
27 1
28 0
67 0

TIMEFUNCTION NAME=28
@CLEAR
0 0
27 0
28 1
29 0
67 0

TIMEFUNCTION NAME=29
@CLEAR
0 0
28 0
29 1
30 0
67 0

TIMEFUNCTION NAME=30
@CLEAR
0 0
29 0
30 1
31 0
67 0

TIMEFUNCTION NAME=31
@CLEAR
0 0
30 0
31 1
32 0
67 0

TIMEFUNCTION NAME=32
@CLEAR
0 0
31 0
32 1
33 0
67 0

TIMEFUNCTION NAME=33
@CLEAR
0 0
32 0
33 1
34 0
67 0

TIMEFUNCTION NAME=34
@CLEAR
0 0
33 0
34 1
35 0
67 0

TIMEFUNCTION NAME=35
@CLEAR
0 0
34 0
35 1
36 0
67 0

TIMEFUNCTION NAME=36
@CLEAR
0 0
35 0
36 1
37 0
67 0

TIMEFUNCTION NAME=37
@CLEAR
0 0
36 0
37 1
38 0
67 0

TIMEFUNCTION NAME=38
@CLEAR
0 0
37 0
38 1
39 0
67 0

TIMEFUNCTION NAME=39
@CLEAR
0 0
38 0
39 1
40 0
67 0

TIMEFUNCTION NAME=40
@CLEAR
0 0
39 0
40 1
41 0
67 0

TIMEFUNCTION NAME=41
@CLEAR
0 0
40 0
41 1
42 0
67 0

TIMEFUNCTION NAME=42
@CLEAR
0 0
41 0
42 1
43 0
67 0

TIMEFUNCTION NAME=43
@CLEAR
0 0
42 0
43 1
44 0
67 0

TIMEFUNCTION NAME=44
@CLEAR
0 0
43 0
44 1
45 0
67 0

TIMEFUNCTION NAME=45
@CLEAR
0 0
44 0
45 1
46 0
67 0

TIMEFUNCTION NAME=46
@CLEAR
0 0
45 0
46 1
47 0
67 0

TIMEFUNCTION NAME=47
@CLEAR
0 0
46 0
47 1
48 0
67 0

TIMEFUNCTION NAME=48
@CLEAR
0 0
47 0
48 1
49 0
67 0

TIMEFUNCTION NAME=49
@CLEAR
0 0
48 0
49 1
50 0
67 0

TIMEFUNCTION NAME=50
@CLEAR
0 0
49 0
50 1
51 0
67 0

TIMEFUNCTION NAME=51
@CLEAR
0 0
50 0
51 1
52 0
67 0

TIMEFUNCTION NAME=52
@CLEAR
0 0
51 0
52 1
53 0
67 0

TIMEFUNCTION NAME=53
@CLEAR
0 0
52 0
```

```
53 1
54 0
67 0

TIMEFUNCTION NAME=54
@CLEAR
0 0
53 0
54 1
55 0
67 0

TIMEFUNCTION NAME=55
@CLEAR
0 0
54 0
55 1
56 0
67 0

TIMEFUNCTION NAME=56
@CLEAR
0 0
55 0
56 1
57 0
67 0

TIMEFUNCTION NAME=57
@CLEAR
0 0
56 0
57 1
58 0
67 0

TIMEFUNCTION NAME=58
@CLEAR
0 0
57 0
58 1
59 0
67 0

TIMEFUNCTION NAME=59
@CLEAR
0 0
58 0
59 1
60 0
67 0

TIMEFUNCTION NAME=60
@CLEAR
0 0
59 0
60 1
61 0
67 0

TIMEFUNCTION NAME=61
@CLEAR
0 0
60 0
61 1
62 0
67 0

TIMEFUNCTION NAME=62
@CLEAR
0 0
61 0
62 1
63 0
67 0

TIMEFUNCTION NAME=63
@CLEAR
0 0
62 0
63 1
64 0
67 0

TIMEFUNCTION NAME=64
@CLEAR
0 0
63 0
64 1
65 0
67 0

TIMEFUNCTION NAME=65
@CLEAR
0 0
64 0
65 1
66 0
67 0

TIMEFUNCTION NAME=66
@CLEAR
0 0
65 0
66 1
67 0
67 0

TIMEFUNCTION NAME=67
@CLEAR
0 0
66 0
67 1
67 1
```

E.4 Beam grillage model

```
*************************************************
* GEOMETRY
*************************************************

COORDINATES
*(number,x,y,z)

* Main girders
1    0    0      0
2    0    5.2    0
3    17   0      0
4    17   5.2    0
5    34   0      0
6    34   5.2    0
7    1    0      0
8    1    5.2    0
9    33   0      0
10   33   5.2    0

* Transversal beams (slab)
11   0    1.25   -0.4
12   0    3.95   -0.4
13   0    0.5    -0.4
14   0    4.7    -0.4

* Auxiliary point, girders
15   0    7                 0

* B.C. points
16   1    0      -0.65
17   1    5.2    -0.65
18   17   0      -0.65
19   17   5.2    -0.65
20   33   0      -0.65
21   33   5.2    -0.65

* Auxiliary points stiff elements between girders and B.C.
22   35   0      -0.65
23   35   5.2    -0.65

* End walls
24   0    -0.5   -1.125
25   0    0.5    -1.125
26   0    1.25   -1.125
27   0    3.95   -1.125
28   0    4.7    -1.125
29   0    5.7    -1.125
30   34   -0.5   -1.125
31   34   0.5    -1.125
32   34   1.25   -1.125
33   34   3.95   -1.125
34   34   4.7    -1.125
35   34   5.7    -1.125

* Auxiliary points, transversal beams
36   -1   0.5    -0.4
37   -1   1.25   -0.4
38   -1   3.95   -0.4

* Auxiliary points, end walls
39   -1   -0.5   -1.125
40   -1   0.5    -1.125
41   -1   1.25   -1.125
42   -1   3.95   -1.125
43   -1   5.2    -1.125

* Auxiliary points, load
44   0    1.25   0
TO
112  34   1.25   0

* Main girders
LINE STRAIGHT NAME=1 P1=1  P2=5
LINE STRAIGHT NAME=2 P1=2  P2=6

* Stiff elements between main girders and B.C. points
LINE STRAIGHT NAME=3 P1=7  P2=16
LINE STRAIGHT NAME=4 P1=3  P2=18
LINE STRAIGHT NAME=5 P1=9  P2=20
LINE STRAIGHT NAME=6 P1=8  P2=17
LINE STRAIGHT NAME=7 P1=4  P2=19
LINE STRAIGHT NAME=8 P1=10 P2=21

* Transversal beams (slab)
TRANSFORMATI TRANSLATION NAME=1,
    MODE=SYSTEM DX=0.5 DY=0 DZ=0

* Mid (loaded) transversal beams
LINE STRAIGHT NAME=101 P1=11 P2=12

LINE TRANSFORMED NAME=102 PARENT=101,
    TRANSFOR=1 PCOINCID=YES,
    PTOLERAN=1E-05 NCOPY=68

* End (unloaded) transversal beams
LINE STRAIGHT NAME=201 P1=13 P2=11

LINE TRANSFORMED NAME=202 PARENT=201,
    TRANSFOR=1 PCOINCID=YES,
    PTOLERAN=1E-05 NCOPY=68

LINE STRAIGHT NAME=301 P1=12 P2=14

LINE TRANSFORMED NAME=302 PARENT=301,
    TRANSFOR=1 PCOINCID=YES,
    PTOLERAN=1E-05 NCOPY=68

* End wall at x=0
LINE STRAIGHT NAME=9  P1=24 P2=25
LINE STRAIGHT NAME=10 P1=25 P2=26
LINE STRAIGHT NAME=11 P1=26 P2=27
LINE STRAIGHT NAME=12 P1=27 P2=28
LINE STRAIGHT NAME=13 P1=28 P2=29

* End wall at x=34
LINE STRAIGHT NAME=14 P1=30 P2=31
LINE STRAIGHT NAME=15 P1=31 P2=32
LINE STRAIGHT NAME=16 P1=32 P2=33
LINE STRAIGHT NAME=17 P1=33 P2=34
LINE STRAIGHT NAME=18 P1=34 P2=35

* Cross-sections
* Main girders
CROSS-SECTIO RECTANGULAR NAME=1,
    WIDTH=1 HEIGHT=1.3

* Transversal beams (slab)
CROSS-SECTIO RECTANGULAR NAME=2,
    WIDTH=0.5 HEIGHT=0.5

* Stiff elements
CROSS-SECTIO PROPERTIES NAME=3,
    RINERTIA=1000 SINERTIA=1000,
    TINERTIA=1000 AREA=100

* End walls
```

```
CROSS-SECTIO RECTANGULAR NAME=4,
    WIDTH=0.5 HEIGHT=1.45
*************************************************
* MATERIAL
*************************************************
* Concrete
MATERIAL ELASTIC NAME=1 E=3E+10 NU=0,
    DENSITY=0 ALPHA=0,
    MDESCRIP='CONCRETE'

* Stiff elements
MATERIAL ELASTIC NAME=2 E=3E+10 NU=0,
    DENSITY=0 ALPHA=0 MDESCRIP='LINKS'


*************************************************
* BOUNDARY CONDITIONS
*************************************************

FIXITY NAME=MID_SUPPORT
 'X-TRANSLATION'
 'Y-TRANSLATION'
 'Z-TRANSLATION'
 'Z-ROTATION'

FIXITY NAME=END_SUPPORTS
 'Y-TRANSLATION'
 'Z-TRANSLATION'
 'Z-ROTATION'

FIXBOUNDARY POINTS FIXITY=ALL
16          'END_SUPPORTS'
18          'MID_SUPPORT'
20          'END_SUPPORTS'
17          'END_SUPPORTS'
19          'MID_SUPPORT'
21          'END_SUPPORTS'


*************************************************
* LOAD APPLICATION
*************************************************
read time_function_beam_grillage.in

LOAD LINE NAME=1 MAGNITUD=185

APPLY-LOAD BODY=0
1  'LINE'  1 'LINE'  101 0 1  0 0 -1 44
2  'LINE'  1 'LINE'  102 0 1  0 0 -1 45
3  'LINE'  1 'LINE'  102 0 2  0 0 -1 45
4  'LINE'  1 'LINE'  103 0 2  0 0 -1 46
5  'LINE'  1 'LINE'  103 0 3  0 0 -1 46
6  'LINE'  1 'LINE'  104 0 3  0 0 -1 47
7  'LINE'  1 'LINE'  104 0 4  0 0 -1 47
8  'LINE'  1 'LINE'  105 0 4  0 0 -1 48
9  'LINE'  1 'LINE'  105 0 5  0 0 -1 48
10 'LINE'  1 'LINE'  106 0 5  0 0 -1 49
11 'LINE'  1 'LINE'  106 0 6  0 0 -1 49
12 'LINE'  1 'LINE'  107 0 6  0 0 -1 50
13 'LINE'  1 'LINE'  107 0 7  0 0 -1 50
14 'LINE'  1 'LINE'  108 0 7  0 0 -1 51
15 'LINE'  1 'LINE'  108 0 8  0 0 -1 51
16 'LINE'  1 'LINE'  109 0 8  0 0 -1 52
17 'LINE'  1 'LINE'  109 0 9  0 0 -1 52
18 'LINE'  1 'LINE'  110 0 9  0 0 -1 53
19 'LINE'  1 'LINE'  110 0 10 0 0 -1 53
20 'LINE'  1 'LINE'  111 0 10 0 0 -1 54
21 'LINE'  1 'LINE'  111 0 11 0 0 -1 54
22 'LINE'  1 'LINE'  112 0 11 0 0 -1 55
23 'LINE'  1 'LINE'  112 0 12 0 0 -1 55
24 'LINE'  1 'LINE'  113 0 12 0 0 -1 56
25 'LINE'  1 'LINE'  113 0 13 0 0 -1 56
26 'LINE'  1 'LINE'  114 0 13 0 0 -1 57
27 'LINE'  1 'LINE'  114 0 14 0 0 -1 57
28 'LINE'  1 'LINE'  115 0 14 0 0 -1 58
29 'LINE'  1 'LINE'  115 0 15 0 0 -1 58
30 'LINE'  1 'LINE'  116 0 15 0 0 -1 59
31 'LINE'  1 'LINE'  116 0 16 0 0 -1 59
32 'LINE'  1 'LINE'  117 0 16 0 0 -1 60
33 'LINE'  1 'LINE'  117 0 17 0 0 -1 60
34 'LINE'  1 'LINE'  118 0 17 0 0 -1 61
35 'LINE'  1 'LINE'  118 0 18 0 0 -1 61
36 'LINE'  1 'LINE'  119 0 18 0 0 -1 62
37 'LINE'  1 'LINE'  119 0 19 0 0 -1 62
38 'LINE'  1 'LINE'  120 0 19 0 0 -1 63
39 'LINE'  1 'LINE'  120 0 20 0 0 -1 63
40 'LINE'  1 'LINE'  121 0 20 0 0 -1 64
41 'LINE'  1 'LINE'  121 0 21 0 0 -1 64
42 'LINE'  1 'LINE'  122 0 21 0 0 -1 65
43 'LINE'  1 'LINE'  122 0 22 0 0 -1 65
44 'LINE'  1 'LINE'  123 0 22 0 0 -1 66
45 'LINE'  1 'LINE'  123 0 23 0 0 -1 66
46 'LINE'  1 'LINE'  124 0 23 0 0 -1 67
47 'LINE'  1 'LINE'  124 0 24 0 0 -1 67
48 'LINE'  1 'LINE'  125 0 24 0 0 -1 68
49 'LINE'  1 'LINE'  125 0 25 0 0 -1 68
50 'LINE'  1 'LINE'  126 0 25 0 0 -1 69
51 'LINE'  1 'LINE'  126 0 26 0 0 -1 69
52 'LINE'  1 'LINE'  127 0 26 0 0 -1 70
53 'LINE'  1 'LINE'  127 0 27 0 0 -1 70
54 'LINE'  1 'LINE'  128 0 27 0 0 -1 71
55 'LINE'  1 'LINE'  128 0 28 0 0 -1 71
56 'LINE'  1 'LINE'  129 0 28 0 0 -1 72
57 'LINE'  1 'LINE'  129 0 29 0 0 -1 72
58 'LINE'  1 'LINE'  130 0 29 0 0 -1 73
59 'LINE'  1 'LINE'  130 0 30 0 0 -1 73
60 'LINE'  1 'LINE'  131 0 30 0 0 -1 74
61 'LINE'  1 'LINE'  131 0 31 0 0 -1 74
62 'LINE'  1 'LINE'  132 0 31 0 0 -1 75
63 'LINE'  1 'LINE'  132 0 32 0 0 -1 75
64 'LINE'  1 'LINE'  133 0 32 0 0 -1 76
65 'LINE'  1 'LINE'  133 0 33 0 0 -1 76
66 'LINE'  1 'LINE'  134 0 33 0 0 -1 77
67 'LINE'  1 'LINE'  134 0 34 0 0 -1 77
68 'LINE'  1 'LINE'  135 0 34 0 0 -1 78
69 'LINE'  1 'LINE'  135 0 35 0 0 -1 78
70 'LINE'  1 'LINE'  136 0 35 0 0 -1 79
71 'LINE'  1 'LINE'  136 0 36 0 0 -1 79
72 'LINE'  1 'LINE'  137 0 36 0 0 -1 80
73 'LINE'  1 'LINE'  137 0 37 0 0 -1 80
74 'LINE'  1 'LINE'  138 0 37 0 0 -1 81
75 'LINE'  1 'LINE'  138 0 38 0 0 -1 81
76 'LINE'  1 'LINE'  139 0 38 0 0 -1 82
77 'LINE'  1 'LINE'  139 0 39 0 0 -1 82
78 'LINE'  1 'LINE'  140 0 39 0 0 -1 83
79 'LINE'  1 'LINE'  140 0 40 0 0 -1 83
80 'LINE'  1 'LINE'  141 0 40 0 0 -1 84
81 'LINE'  1 'LINE'  141 0 41 0 0 -1 84
82 'LINE'  1 'LINE'  142 0 41 0 0 -1 85
83 'LINE'  1 'LINE'  142 0 42 0 0 -1 85
84 'LINE'  1 'LINE'  143 0 42 0 0 -1 86
85 'LINE'  1 'LINE'  143 0 43 0 0 -1 86
86 'LINE'  1 'LINE'  144 0 43 0 0 -1 87
87 'LINE'  1 'LINE'  144 0 44 0 0 -1 87
88 'LINE'  1 'LINE'  145 0 44 0 0 -1 88
89 'LINE'  1 'LINE'  145 0 45 0 0 -1 88
90 'LINE'  1 'LINE'  146 0 45 0 0 -1 89
91 'LINE'  1 'LINE'  146 0 46 0 0 -1 89
92 'LINE'  1 'LINE'  147 0 46 0 0 -1 90
93 'LINE'  1 'LINE'  147 0 47 0 0 -1 90
94 'LINE'  1 'LINE'  148 0 47 0 0 -1 91
95 'LINE'  1 'LINE'  148 0 48 0 0 -1 91
96 'LINE'  1 'LINE'  149 0 48 0 0 -1 92
97 'LINE'  1 'LINE'  149 0 49 0 0 -1 92
98 'LINE'  1 'LINE'  150 0 49 0 0 -1 93
99 'LINE'  1 'LINE'  150 0 50 0 0 -1 93
```

```
100 'LINE'  1 'LINE'  151 0 50 0 0 -1 94
101 'LINE'  1 'LINE'  151 0 51 0 0 -1 94
102 'LINE'  1 'LINE'  152 0 51 0 0 -1 95
103 'LINE'  1 'LINE'  152 0 52 0 0 -1 95
104 'LINE'  1 'LINE'  153 0 52 0 0 -1 96
105 'LINE'  1 'LINE'  153 0 53 0 0 -1 96
106 'LINE'  1 'LINE'  154 0 53 0 0 -1 97
107 'LINE'  1 'LINE'  154 0 54 0 0 -1 97
108 'LINE'  1 'LINE'  155 0 54 0 0 -1 98
109 'LINE'  1 'LINE'  155 0 55 0 0 -1 98
110 'LINE'  1 'LINE'  156 0 55 0 0 -1 99
111 'LINE'  1 'LINE'  156 0 56 0 0 -1 99
112 'LINE'  1 'LINE'  157 0 56 0 0 -1 100
113 'LINE'  1 'LINE'  157 0 57 0 0 -1 100
114 'LINE'  1 'LINE'  158 0 57 0 0 -1 101
115 'LINE'  1 'LINE'  158 0 58 0 0 -1 101
116 'LINE'  1 'LINE'  159 0 58 0 0 -1 102
117 'LINE'  1 'LINE'  159 0 59 0 0 -1 102
118 'LINE'  1 'LINE'  160 0 59 0 0 -1 103
119 'LINE'  1 'LINE'  160 0 60 0 0 -1 103
120 'LINE'  1 'LINE'  161 0 60 0 0 -1 104
121 'LINE'  1 'LINE'  161 0 61 0 0 -1 104
122 'LINE'  1 'LINE'  162 0 61 0 0 -1 105
123 'LINE'  1 'LINE'  162 0 62 0 0 -1 105
124 'LINE'  1 'LINE'  163 0 62 0 0 -1 106
125 'LINE'  1 'LINE'  163 0 63 0 0 -1 106
126 'LINE'  1 'LINE'  164 0 63 0 0 -1 107
127 'LINE'  1 'LINE'  164 0 64 0 0 -1 107
128 'LINE'  1 'LINE'  165 0 64 0 0 -1 108
129 'LINE'  1 'LINE'  165 0 65 0 0 -1 108
130 'LINE'  1 'LINE'  166 0 65 0 0 -1 109
131 'LINE'  1 'LINE'  166 0 66 0 0 -1 109
132 'LINE'  1 'LINE'  167 0 66 0 0 -1 110
133 'LINE'  1 'LINE'  167 0 67 0 0 -1 110
134 'LINE'  1 'LINE'  168 0 67 0 0 -1 111
135 'LINE'  1 'LINE'  168 0 68 0 0 -1 111
136 'LINE'  1 'LINE'  169 0 68 0 0 -1 112


************************************************
*MESHING
************************************************

* Element groups
EGROUP BEAM NAME=1 SUBTYPE=THREE-D,
   MATERIAL=1 RINT=5 RESULTS=SFORCES,
   DESCRIPT='GIRDERS' SECTION=1 SPOINT=5

EGROUP BEAM NAME=2 SUBTYPE=THREE-D,
   MATERIAL=1 RINT=5, RESULTS=SFORCES,
   DESCRIPT='SLAB' SECTION=2 SPOINT=5

EGROUP BEAM NAME=3 SUBTYPE=THREE-D,
   MATERIAL=2 RINT=5, RESULTS=SFORCES,
   DESCRIPT='STIFF ELEMENTS' SECTION=3,
   SPOINT=5

EGROUP BEAM NAME=4 SUBTYPE=THREE-D,
   MATERIAL=1 RINT=5 RESULTS=SFORCES,
   DESCRIPT='END WALLS' SECTION=4 SPOINT=5

EGROUP BEAM NAME=5 SUBTYPE=THREE-D,
   MATERIAL=1 RINT=5 RESULTS=SFORCES,
   DESCRIPT='END WALL OUTER LINES',
   SECTION=4 SPOINT=5

* Element sizes

* Main girders
SUBDIVIDE LINE NAME=1 MODE=DIVISIONS,
   NDIV=68
2

* Stiff elements, transversal beam end  and end wall ends
SUBDIVIDE LINE NAME=3 MODE=DIVISIONS,
   NDIV=1
4
TO
10
12
TO
15
17
18
201
TO
269
301
TO
369

* Mid transversal beams, mid end wall
SUBDIVIDE LINE NAME=11 MODE=DIVISIONS,
   NDIV=4
16
101
TO
169

* Mesh generation

* Main girders
GLINE NODES=2 AUXPOINT=15 GROUP=1
1
2

* Stiff elements between girder and B.C. points
GLINE NODES=2 AUXPOINT=22 GROUP=3
3
TO
5

GLINE NODES=2 AUXPOINT=23 GROUP=3
6
TO
8

* Transversal beams (slab)
GLINE NODES=2 AUXPOINT=36 GROUP=2
201
TO
269

GLINE NODES=2 AUXPOINT=37 GROUP=2
101
TO
169

GLINE NODES=2 AUXPOINT=38 GROUP=2
301
TO
369

* End walls
GLINE NODES=2 AUXPOINT=39 GROUP=5
9
14

GLINE NODES=2 AUXPOINT=40 GROUP=4
10
15

GLINE NODES=2 AUXPOINT=41 GROUP=4
11
16
```

```
GLINE NODES=2 AUXPOINT=42 GROUP=4
12
17

GLINE NODES=2 AUXPOINT=43 GROUP=5
13
18


**************************************************
* RIGID LINKS
**************************************************
* Between slab and girders

NODESET NAME=1 DESCRIPT='GIRDERS',
   OPTION=NODE
1
TO
69
71
TO
139

NODESET NAME=2,
   DESCRIPT='TRANSVERSAL ENDS' OPTION=NODE
148
151
STEP 2 TO
285
633
635
TO
702

RIGIDLINK NAME=1 SLAVETYP=NODESET,
   SLAVENAM=2 MASTERTY=NODESET,
   MASTERNA=1* Between end wall and bridge end

RIGIDLINK NAME=2 SLAVETYP=LINE,
   SLAVENAM=9 MASTERTY=POINT,
   MASTERNA=1

RIGIDLINK NAME=3 SLAVETYP=LINE,
   SLAVENAM=13 MASTERTY=POINT,
   MASTERNA=2

RIGIDLINK NAME=4 SLAVETYP=LINE,
   SLAVENAM=14 MASTERTY=POINT,
   MASTERNA=5

RIGIDLINK NAME=5 SLAVETYP=LINE,
   SLAVENAM=18 MASTERTY=POINT,
   MASTERNA=6

RIGIDLINK NAME=6 SLAVETYP=LINE,
   SLAVENAM=169 MASTERTY=LINE,
   MASTERNA=16

RIGIDLINK NAME=7 SLAVETYP=LINE,
   SLAVENAM=101 MASTERTY=LINE,
   MASTERNA=11


**************************************************
* ANALYSIS
**************************************************
```

E.5 Time function (Beam grillage model)

```
* Time step definition, number of *
steps and step size
TIMESTEP NAME=DEFAULT
@CLEAR
136 0.5


* Definition of each (whole) time step
TIMEFUNCTION NAME=1
@CLEAR
0 0
1 1
2 0
68 0

TIMEFUNCTION NAME=2
@CLEAR
0 0
1 0
2 1
3 0
68 0

TIMEFUNCTION NAME=3
@CLEAR
0 0
2 0
3 1
4 0
68 0

TIMEFUNCTION NAME=4
@CLEAR
0 0
3 0
4 1
5 0
68 0

TIMEFUNCTION NAME=5
@CLEAR
0 0
4 0
5 1
6 0
68 0

TIMEFUNCTION NAME=6
@CLEAR
0 0
5 0
6 1
7 0
68 0

TIMEFUNCTION NAME=7
@CLEAR
0 0
6 0
7 1
8 0
68 0

TIMEFUNCTION NAME=8
@CLEAR
0 0
7 0
8 1
9 0
68 0

TIMEFUNCTION NAME=9
@CLEAR
0 0
8 0
9 1
10 0
68 0

TIMEFUNCTION NAME=10
@CLEAR
0 0
9 0
10 1
11 0
68 0

TIMEFUNCTION NAME=11
@CLEAR
0 0
10 0
11 1
12 0
68 0

TIMEFUNCTION NAME=12
@CLEAR
0 0
11 0
12 1
13 0
68 0

TIMEFUNCTION NAME=13
@CLEAR
0 0
12 0
13 1
14 0
68 0

TIMEFUNCTION NAME=14
@CLEAR
0 0
13 0
14 1
15 0
68 0

TIMEFUNCTION NAME=15
@CLEAR
0 0
14 0
15 1
16 0
68 0

TIMEFUNCTION NAME=16
@CLEAR
0 0
15 0
16 1
17 0
68 0

TIMEFUNCTION NAME=17
@CLEAR
0 0
16 0
17 1
18 0
68 0

TIMEFUNCTION NAME=18
@CLEAR
0 0
17 0
18 1
19 0
68 0

TIMEFUNCTION NAME=19
@CLEAR
0 0
18 0
19 1
20 0
68 0

TIMEFUNCTION NAME=20
@CLEAR
0 0
19 0
20 1
21 0
68 0

TIMEFUNCTION NAME=21
@CLEAR
0 0
20 0
21 1
22 0
68 0

TIMEFUNCTION NAME=22
@CLEAR
0 0
21 0
22 1
23 0
68 0

TIMEFUNCTION NAME=23
@CLEAR
0 0
22 0
23 1
24 0
68 0

TIMEFUNCTION NAME=24
@CLEAR
0 0
23 0
24 1
25 0
68 0

TIMEFUNCTION NAME=25
@CLEAR
0 0
24 0
25 1
26 0
68 0
```

TIMEFUNCTION NAME=26
@CLEAR
0 0
25 0
26 1
27 0
68 0

TIMEFUNCTION NAME=27
@CLEAR
0 0
26 0
27 1
28 0
68 0

TIMEFUNCTION NAME=28
@CLEAR
0 0
27 0
28 1
29 0
68 0

TIMEFUNCTION NAME=29
@CLEAR
0 0
28 0
29 1
30 0
68 0

TIMEFUNCTION NAME=30
@CLEAR
0 0
29 0
30 1
31 0
68 0

TIMEFUNCTION NAME=31
@CLEAR
0 0
30 0
31 1
32 0
68 0

TIMEFUNCTION NAME=32
@CLEAR
0 0
31 0
32 1
33 0
68 0

TIMEFUNCTION NAME=33
@CLEAR
0 0
32 0
33 1
34 0
68 0

TIMEFUNCTION NAME=34
@CLEAR
0 0
33 0
34 1
35 0
68 0

TIMEFUNCTION NAME=35
@CLEAR
0 0
34 0
35 1
36 0
68 0

TIMEFUNCTION NAME=36
@CLEAR
0 0
35 0
36 1
37 0
68 0

TIMEFUNCTION NAME=37
@CLEAR
0 0
36 0
37 1
38 0
68 0

TIMEFUNCTION NAME=38
@CLEAR
0 0
37 0
38 1
39 0
68 0

TIMEFUNCTION NAME=39
@CLEAR
0 0
38 0
39 1
40 0
68 0

TIMEFUNCTION NAME=40
@CLEAR
0 0
39 0
40 1
41 0
68 0

TIMEFUNCTION NAME=41
@CLEAR
0 0
40 0
41 1
42 0
68 0

TIMEFUNCTION NAME=42
@CLEAR
0 0
41 0
42 1
43 0
68 0

TIMEFUNCTION NAME=43
@CLEAR
0 0
42 0
43 1
44 0
68 0

TIMEFUNCTION NAME=44
@CLEAR
0 0
43 0
44 1
45 0
68 0

TIMEFUNCTION NAME=45
@CLEAR
0 0
44 0
45 1
46 0
68 0

TIMEFUNCTION NAME=46
@CLEAR
0 0
45 0
46 1
47 0
68 0

TIMEFUNCTION NAME=47
@CLEAR
0 0
46 0
47 1
48 0
68 0

TIMEFUNCTION NAME=48
@CLEAR
0 0
47 0
48 1
49 0
68 0

TIMEFUNCTION NAME=49
@CLEAR
0 0
48 0
49 1
50 0
68 0

TIMEFUNCTION NAME=50
@CLEAR
0 0
49 0
50 1
51 0
68 0

TIMEFUNCTION NAME=51
@CLEAR
0 0
50 0
51 1
52 0
68 0

TIMEFUNCTION NAME=52
@CLEAR
0 0
51 0
52 1
53 0
68 0

TIMEFUNCTION NAME=53
@CLEAR
0 0

```
52 0
53 1
54 0
68 0

TIMEFUNCTION NAME=54
@CLEAR
0 0
53 0
54 1
55 0
68 0

TIMEFUNCTION NAME=55
@CLEAR
0 0
54 0
55 1
56 0
68 0

TIMEFUNCTION NAME=56
@CLEAR
0 0
55 0
56 1
57 0
68 0

TIMEFUNCTION NAME=57
@CLEAR
0 0
56 0
57 1
58 0
68 0

TIMEFUNCTION NAME=58
@CLEAR
0 0
57 0
58 1
59 0
68 0

TIMEFUNCTION NAME=59
@CLEAR
0 0
58 0
59 1
60 0
68 0

TIMEFUNCTION NAME=60
@CLEAR
0 0
59 0
60 1
61 0
68 0

TIMEFUNCTION NAME=61
@CLEAR
0 0
60 0
61 1
62 0
68 0

TIMEFUNCTION NAME=62
@CLEAR
0 0
61 0
62 1
63 0
68 0

TIMEFUNCTION NAME=63
@CLEAR
0 0
62 0
63 1
64 0
68 0

TIMEFUNCTION NAME=64
@CLEAR
0 0
63 0
64 1
65 0
68 0

TIMEFUNCTION NAME=65
@CLEAR
0 0
64 0
65 1
66 0
68 0

TIMEFUNCTION NAME=66
@CLEAR
0 0
65 0
66 1
67 0
68 0

TIMEFUNCTION NAME=67
@CLEAR
0 0
66 0
67 1
68 0
68 0

TIMEFUNCTION NAME=68
@CLEAR
0 0
67 0
68 1
68 1
```

E.6 Modified model with applied torque

Models used to obtain rotational stiffness. Changes are defined, unchanged variables refer to original models.

```
*************************************************
* GEOMETRY
*************************************************

COORDINATES
*(number,x,y,z)

* Main girders
1   0   0    0
2   0   5.2  0
3   17  0    0
4   17  5.2  0
5   34  0    0
6   34  5.2  0
7   1   0    0
8   1   5.2  0
9   33  0    0
10  33  5.2  0


* Load points
44    0.5    0     0
45    1.5    0     0
TO
75    16.5   0     0
76    17.5   0     0
TO
106   32.5   0     0
107   33.5   0     0
108   0.5    5.2   0
109   1.5    5.2   0
TO
139   16.5   5.2   0
140   17.5   5.2   0
TO
170   32.5   5.2   0
171   33.5   5.2   0


* Main girders
LINE STRAIGHT NAME= 401 P1= 1 P2= 44
LINE STRAIGHT NAME= 402 P1= 44 P2= 7
LINE STRAIGHT NAME= 403 P1= 7 P2= 45
LINE STRAIGHT NAME= 404 P1= 45 P2= 46
LINE STRAIGHT NAME= 405 P1= 46 P2= 47
LINE STRAIGHT NAME= 406 P1= 47 P2= 48
LINE STRAIGHT NAME= 407 P1= 48 P2= 49
LINE STRAIGHT NAME= 408 P1= 49 P2= 50
LINE STRAIGHT NAME= 409 P1= 50 P2= 51
LINE STRAIGHT NAME= 410 P1= 51 P2= 52
LINE STRAIGHT NAME= 411 P1= 52 P2= 53
LINE STRAIGHT NAME= 412 P1= 53 P2= 54
LINE STRAIGHT NAME= 413 P1= 54 P2= 55
LINE STRAIGHT NAME= 414 P1= 55 P2= 56
LINE STRAIGHT NAME= 415 P1= 56 P2= 57
LINE STRAIGHT NAME= 416 P1= 57 P2= 58
LINE STRAIGHT NAME= 417 P1= 58 P2= 59
LINE STRAIGHT NAME= 418 P1= 59 P2= 60
LINE STRAIGHT NAME= 419 P1= 60 P2= 61
LINE STRAIGHT NAME= 420 P1= 61 P2= 62
LINE STRAIGHT NAME= 421 P1= 62 P2= 63
LINE STRAIGHT NAME= 422 P1= 63 P2= 64
LINE STRAIGHT NAME= 423 P1= 64 P2= 65
LINE STRAIGHT NAME= 424 P1= 65 P2= 66
LINE STRAIGHT NAME= 425 P1= 66 P2= 67
LINE STRAIGHT NAME= 426 P1= 67 P2= 68
LINE STRAIGHT NAME= 427 P1= 68 P2= 69
LINE STRAIGHT NAME= 428 P1= 69 P2= 70
LINE STRAIGHT NAME= 429 P1= 70 P2= 71
LINE STRAIGHT NAME= 430 P1= 71 P2= 72
LINE STRAIGHT NAME= 431 P1= 72 P2= 73
LINE STRAIGHT NAME= 432 P1= 73 P2= 74
LINE STRAIGHT NAME= 433 P1= 74 P2= 75
LINE STRAIGHT NAME= 434 P1= 75 P2= 3
LINE STRAIGHT NAME= 435 P1= 3 P2= 76
LINE STRAIGHT NAME= 436 P1= 76 P2= 77
LINE STRAIGHT NAME= 437 P1= 77 P2= 78
LINE STRAIGHT NAME= 438 P1= 78 P2= 79
LINE STRAIGHT NAME= 439 P1= 79 P2= 80
LINE STRAIGHT NAME= 440 P1= 80 P2= 81
LINE STRAIGHT NAME= 441 P1= 81 P2= 82
LINE STRAIGHT NAME= 442 P1= 82 P2= 83
LINE STRAIGHT NAME= 443 P1= 83 P2= 84
LINE STRAIGHT NAME= 444 P1= 84 P2= 85
LINE STRAIGHT NAME= 445 P1= 85 P2= 86
LINE STRAIGHT NAME= 446 P1= 86 P2= 87
LINE STRAIGHT NAME= 447 P1= 87 P2= 88
LINE STRAIGHT NAME= 448 P1= 88 P2= 89
LINE STRAIGHT NAME= 449 P1= 89 P2= 90
LINE STRAIGHT NAME= 450 P1= 90 P2= 91
LINE STRAIGHT NAME= 451 P1= 91 P2= 92
LINE STRAIGHT NAME= 452 P1= 92 P2= 93
LINE STRAIGHT NAME= 453 P1= 93 P2= 94
LINE STRAIGHT NAME= 454 P1= 94 P2= 95
LINE STRAIGHT NAME= 455 P1= 95 P2= 96
LINE STRAIGHT NAME= 456 P1= 96 P2= 97
LINE STRAIGHT NAME= 457 P1= 97 P2= 98
LINE STRAIGHT NAME= 458 P1= 98 P2= 99
LINE STRAIGHT NAME= 459 P1= 99 P2= 100
LINE STRAIGHT NAME= 460 P1= 100 P2= 101
LINE STRAIGHT NAME= 461 P1= 101 P2= 102
LINE STRAIGHT NAME= 462 P1= 102 P2= 103
LINE STRAIGHT NAME= 463 P1= 103 P2= 104
LINE STRAIGHT NAME= 464 P1= 104 P2= 105
LINE STRAIGHT NAME= 465 P1= 105 P2= 106
LINE STRAIGHT NAME= 466 P1= 106 P2= 9
LINE STRAIGHT NAME= 467 P1= 9 P2= 107
LINE STRAIGHT NAME= 468 P1= 107 P2= 5

LINE STRAIGHT NAME= 501 P1= 2 P2= 108
LINE STRAIGHT NAME= 502 P1= 108 P2= 8
LINE STRAIGHT NAME= 503 P1= 8 P2= 109
LINE STRAIGHT NAME= 504 P1= 109 P2= 110
LINE STRAIGHT NAME= 505 P1= 110 P2= 111
LINE STRAIGHT NAME= 506 P1= 111 P2= 112
LINE STRAIGHT NAME= 507 P1= 112 P2= 113
LINE STRAIGHT NAME= 508 P1= 113 P2= 114
LINE STRAIGHT NAME= 509 P1= 114 P2= 115
LINE STRAIGHT NAME= 510 P1= 115 P2= 116
LINE STRAIGHT NAME= 511 P1= 116 P2= 117
LINE STRAIGHT NAME= 512 P1= 117 P2= 118
LINE STRAIGHT NAME= 513 P1= 118 P2= 119
LINE STRAIGHT NAME= 514 P1= 119 P2= 120
LINE STRAIGHT NAME= 515 P1= 120 P2= 121
LINE STRAIGHT NAME= 516 P1= 121 P2= 122
LINE STRAIGHT NAME= 517 P1= 122 P2= 123
LINE STRAIGHT NAME= 518 P1= 123 P2= 124
LINE STRAIGHT NAME= 519 P1= 124 P2= 125
LINE STRAIGHT NAME= 520 P1= 125 P2= 126
LINE STRAIGHT NAME= 521 P1= 126 P2= 127
```

```
LINE STRAIGHT NAME= 522 P1= 127 P2= 128
LINE STRAIGHT NAME= 523 P1= 128 P2= 129
LINE STRAIGHT NAME= 524 P1= 129 P2= 130
LINE STRAIGHT NAME= 525 P1= 130 P2= 131
LINE STRAIGHT NAME= 526 P1= 131 P2= 132
LINE STRAIGHT NAME= 527 P1= 132 P2= 133
LINE STRAIGHT NAME= 528 P1= 133 P2= 134
LINE STRAIGHT NAME= 529 P1= 134 P2= 135
LINE STRAIGHT NAME= 530 P1= 135 P2= 136
LINE STRAIGHT NAME= 531 P1= 136 P2= 137
LINE STRAIGHT NAME= 532 P1= 137 P2= 138
LINE STRAIGHT NAME= 533 P1= 138 P2= 139
LINE STRAIGHT NAME= 534 P1= 139 P2= 4
LINE STRAIGHT NAME= 535 P1= 4 P2= 140
LINE STRAIGHT NAME= 536 P1= 140 P2= 141
LINE STRAIGHT NAME= 537 P1= 141 P2= 142
LINE STRAIGHT NAME= 538 P1= 142 P2= 143
LINE STRAIGHT NAME= 539 P1= 143 P2= 144
LINE STRAIGHT NAME= 540 P1= 144 P2= 145
LINE STRAIGHT NAME= 541 P1= 145 P2= 146
LINE STRAIGHT NAME= 542 P1= 146 P2= 147
LINE STRAIGHT NAME= 543 P1= 147 P2= 148
LINE STRAIGHT NAME= 544 P1= 148 P2= 149
LINE STRAIGHT NAME= 545 P1= 149 P2= 150
LINE STRAIGHT NAME= 546 P1= 150 P2= 151
LINE STRAIGHT NAME= 547 P1= 151 P2= 152
LINE STRAIGHT NAME= 548 P1= 152 P2= 153
LINE STRAIGHT NAME= 549 P1= 153 P2= 154
LINE STRAIGHT NAME= 550 P1= 154 P2= 155
LINE STRAIGHT NAME= 551 P1= 155 P2= 156
LINE STRAIGHT NAME= 552 P1= 156 P2= 157
LINE STRAIGHT NAME= 553 P1= 157 P2= 158
LINE STRAIGHT NAME= 554 P1= 158 P2= 159
LINE STRAIGHT NAME= 555 P1= 159 P2= 160
LINE STRAIGHT NAME= 556 P1= 160 P2= 161
LINE STRAIGHT NAME= 557 P1= 161 P2= 162
LINE STRAIGHT NAME= 558 P1= 162 P2= 163
LINE STRAIGHT NAME= 559 P1= 163 P2= 164
LINE STRAIGHT NAME= 560 P1= 164 P2= 165
LINE STRAIGHT NAME= 561 P1= 165 P2= 166
LINE STRAIGHT NAME= 562 P1= 166 P2= 167
LINE STRAIGHT NAME= 563 P1= 167 P2= 168
LINE STRAIGHT NAME= 564 P1= 168 P2= 169
LINE STRAIGHT NAME= 565 P1= 169 P2= 170
LINE STRAIGHT NAME= 566 P1= 170 P2= 10
LINE STRAIGHT NAME= 567 P1= 10 P2= 171
LINE STRAIGHT NAME= 568 P1= 171 P2= 6

* Other geometry according to original model

* Cross-sections according to original model

*************************************************
* MATERIAL
*************************************************

* Materials according to original model

*************************************************
* BOUNDARY CONDITIONS
*************************************************

* Boundary conditions according to original model

*************************************************
* LOAD APPLICATION
*************************************************

LOAD MOMENT NAME=1 MAGNITUD=1000 MX=-1
MY=0 MZ=0

LOAD MOMENT NAME=2 MAGNITUD=1000 MX=1
MY=0 MZ=0

read time_function_applied_torque.in

APPLY-LOAD BODY=0
1  'MOMENT' 1  'POINT' 1 0 1
2  'MOMENT' 2  'POINT' 2 0 1

3  'MOMENT' 1  'POINT' 44 0 2
4  'MOMENT' 2  'POINT' 108 0 2

5  'MOMENT' 1  'POINT' 7 0 3
6  'MOMENT' 2  'POINT' 8 0 3

7  'MOMENT' 1  'POINT' 45 0 4
TO
37  'MOMENT' 1  'POINT' 75 0 34
38  'MOMENT' 2  'POINT' 109 0 4
TO
68  'MOMENT' 2  'POINT' 139 0 34

69  'MOMENT' 1  'POINT' 3 0 35
70  'MOMENT' 2  'POINT' 4 0 35

71  'MOMENT' 1  'POINT' 76 0 36
TO
101  'MOMENT' 1  'POINT' 106 0 66
102  'MOMENT' 2  'POINT' 140 0 36
TO
132  'MOMENT' 2  'POINT' 170 0 66

133  'MOMENT' 1  'POINT' 9 0 67
134  'MOMENT' 2  'POINT' 10 0 67

135  'MOMENT' 1  'POINT' 107 0 68
136  'MOMENT' 2  'POINT' 171 0 68

137  'MOMENT' 1  'POINT' 5 0 69
138  'MOMENT' 2  'POINT' 6 0 69


*************************************************
* MESHING
*************************************************

* Element groups according to original model

* Element sizes

* Main girders
SUBDIVIDE LINE NAME=401 MODE=DIVISIONS
NDIV=1
402
TO
468
501
TO
568

* Other element sizes according to original model

* Mesh generation according to original model


*************************************************
* RIGID LINKS
*************************************************

* Rigid links according to original model


*************************************************
* ANALYSIS
*************************************************
```

E.7 Time function (applied torque)

```
* Time step definition, number of *
steps and step size
TIMESTEP NAME=DEFAULT
@CLEAR
69 1

* Definition of each time step
TIMEFUNCTION NAME =1
@CLEAR
0      0
1      1
2      0
69     0

TIMEFUNCTION NAME =2
@CLEAR
0      0
1      0
2      1
3      0
69     0

TIMEFUNCTION NAME =3
@CLEAR
0      0
2      0
3      1
4      0
69     0

TIMEFUNCTION NAME =4
@CLEAR
0      0
3      0
4      1
5      0
69     0

TIMEFUNCTION NAME =5
@CLEAR
0      0
4      0
5      1
6      0
69     0

TIMEFUNCTION NAME =6
@CLEAR
0      0
5      0
6      1
7      0
69     0

TIMEFUNCTION NAME =7
@CLEAR
0      0
6      0
7      1
8      0
69     0

TIMEFUNCTION NAME =8
@CLEAR
0      0
7      0
8      1
9      0
69     0

TIMEFUNCTION NAME =9
@CLEAR
0      0
8      0
9      1
10     0
69     0

TIMEFUNCTION NAME=10
@CLEAR
0      0
9      0
10     1
11     0
69     0

TIMEFUNCTION NAME=11
@CLEAR
0      0
10     0
11     1
12     0
69     0

TIMEFUNCTION NAME=12
@CLEAR
0      0
11     0
12     1
13     0
69     0

TIMEFUNCTION NAME =13
@CLEAR
0      0
12     0
13     1
14     0
69     0

TIMEFUNCTION NAME =14
@CLEAR
0      0
13     0
14     1
15     0
69     0

TIMEFUNCTION NAME =15
@CLEAR
0      0
14     0
15     1
16     0
69     0

TIMEFUNCTION NAME =16
@CLEAR
0      0
15     0
16     1
17     0
69     0

TIMEFUNCTION NAME =17
@CLEAR
0      0
16     0
17     1
18     0
69     0

TIMEFUNCTION NAME =18
@CLEAR
0      0
17     0
18     1
19     0
69     0

TIMEFUNCTION NAME =19
@CLEAR
0      0
18     0
19     1
20     0
69     0

TIMEFUNCTION NAME =20
@CLEAR
0      0
19     0
20     1
21     0
69     0

TIMEFUNCTION NAME =21
@CLEAR
0      0
20     0
21     1
22     0
69     0

TIMEFUNCTION NAME =22
@CLEAR
0      0
21     0
22     1
23     0
69     0

TIMEFUNCTION NAME =23
@CLEAR
0      0
22     0
23     1
24     0
69     0

TIMEFUNCTION NAME =24
@CLEAR
0      0
23     0
24     1
25     0
69     0

TIMEFUNCTION NAME =25
@CLEAR
0      0
24     0
25     1
26     0
```

```
69	0

TIMEFUNCTION NAME=26
@CLEAR
0	0
25	0
26	1
27	0
69	0

TIMEFUNCTION NAME=27
@CLEAR
0	0
26	0
27	1
28	0
69	0

TIMEFUNCTION NAME =28
@CLEAR
0	0
27	0
28	1
29	0
69	0

TIMEFUNCTION NAME =29
@CLEAR
0	0
28	0
29	1
30	0
69	0

TIMEFUNCTION NAME =30
@CLEAR
0	0
29	0
30	1
31	0
69	0

TIMEFUNCTION NAME =31
@CLEAR
0	0
30	0
31	1
32	0
69	0

TIMEFUNCTION NAME =32
@CLEAR
0	0
31	0
32	1
33	0
69	0

TIMEFUNCTION NAME =33
@CLEAR
0	0
32	0
33	1
34	0
69	0

TIMEFUNCTION NAME =34
@CLEAR
0	0
33	0
34	1
35	0
69	0

TIMEFUNCTION NAME =35
@CLEAR
0	0
34	0
35	1
36	0
69	0

TIMEFUNCTION NAME =36
@CLEAR
0	0
35	0
36	1
37	0
69	0
TIMEFUNCTION NAME =37
@CLEAR
0	0
36	0
37	1
38	0
69	0

TIMEFUNCTION NAME =38
@CLEAR
0	0
37	0
38	1
39	0
69	0

TIMEFUNCTION NAME =39
@CLEAR
0	0
38	0
39	1
40	0
69	0

TIMEFUNCTION NAME =40
@CLEAR
0	0
39	0
40	1
41	0
69	0

TIMEFUNCTION NAME =41
@CLEAR
0	0
40	0
41	1
42	0
69	0

TIMEFUNCTION NAME =42
@CLEAR
0	0
41	0
42	1
43	0
69	0

TIMEFUNCTION NAME =43
@CLEAR
0	0
42	0
43	1
44	0
69	0

TIMEFUNCTION NAME =44
@CLEAR
0	0
43	0
44	1
45	0
69	0

TIMEFUNCTION NAME =45
@CLEAR
0	0
44	0
45	1
46	0
69	0

TIMEFUNCTION NAME =46
@CLEAR
0	0
45	0
46	1
47	0
69	0

TIMEFUNCTION NAME =47
@CLEAR
0	0
46	0
47	1
48	0
69	0

TIMEFUNCTION NAME =48
@CLEAR
0	0
47	0
48	1
49	0
69	0

TIMEFUNCTION NAME =49
@CLEAR
0	0
48	0
49	1
50	0
69	0

TIMEFUNCTION NAME =50
@CLEAR
0	0
49	0
50	1
51	0
69	0

TIMEFUNCTION NAME =51
@CLEAR
0	0
50	0
51	1
52	0
69	0

TIMEFUNCTION NAME =52
@CLEAR
0	0
51	0
52	1
53	0
69	0

TIMEFUNCTION NAME =53
@CLEAR
```

```
0	0
52	0
53	1
54	0
69	0

TIMEFUNCTION NAME =54
@CLEAR
0	0
53	0
54	1
55	0
69	0

TIMEFUNCTION NAME =55
@CLEAR
0	0
54	0
55	1
56	0
69	0

TIMEFUNCTION NAME =56
@CLEAR
0	0
55	0
56	1
57	0
69	0

TIMEFUNCTION NAME =57
@CLEAR
0	0
56	0
57	1
58	0
69	0

TIMEFUNCTION NAME =58
@CLEAR
0	0
57	0
58	1
59	0
69	0

TIMEFUNCTION NAME =59
@CLEAR
0	0
58	0
59	1
60	0
69	0

TIMEFUNCTION NAME =60
@CLEAR
0	0
59	0
60	1
61	0
69	0

TIMEFUNCTION NAME =61
@CLEAR
0	0
60	0
61	1
62	0
69	0

TIMEFUNCTION NAME =62
@CLEAR
0	0
61	0
62	1
63	0
69	0

TIMEFUNCTION NAME =63
@CLEAR
0	0
62	0
63	1
64	0
69	0

TIMEFUNCTION NAME =64
@CLEAR
0	0
63	0
64	1
65	0
69	0

TIMEFUNCTION NAME =65
@CLEAR
0	0
64	0
65	1
66	0
69	0

TIMEFUNCTION NAME =66
@CLEAR
0	0
65	0
66	1
67	0
69	0

TIMEFUNCTION NAME =67
@CLEAR
0	0
66	0
67	1
68	0
69	0

TIMEFUNCTION NAME =68
@CLEAR
0	0
67	0
68	1
69	0
69	0

TIMEFUNCTION NAME =69
@CLEAR
0	0
68	0
69	1
69	1
```

E.8 Modified models with fixed twisting

Models with fixed twisting instead of end walls. Changes are defined, unchanged variables refer to original models.

```
**************************************************
* GEOMETRY
**************************************************

* Geometry according to original, but with a
* length of 32 m (between x=1 and x=33) and no
* end walls


**************************************************
* MATERIAL
**************************************************

* Materials according to original


**************************************************
* BOUNDARY CONDITIONS
**************************************************
FIXITY NAME=MID_SUPPORT
 'X-TRANSLATION'
 'Y-TRANSLATION'
 'Z-TRANSLATION'
 'Z-ROTATION'

FIXITY NAME=END_SUPPORTS
 'Y-TRANSLATION'
 'Z-TRANSLATION'
 'Z-ROTATION'

FIXITY NAME=FIXED_TWISTING
 'X-ROTATION'

FIXBOUNDARY POINTS FIXITY=ALL
16      'END_SUPPORTS'
18      'MID_SUPPORT'
20      'END_SUPPORTS'
17      'END_SUPPORTS'
19      'MID_SUPPORT'
21      'END_SUPPORTS'
7   'FIXED_TWISTING'
8   'FIXED_TWISTING'
9   'FIXED_TWISTING'
10   'FIXED_TWISTING'

**************************************************
* LOAD APPLICATION
**************************************************

* Load application according to original, but
* with a length of 32 m (between x=1 and x=33)

**************************************************
* MESHING
**************************************************

* Meshing according to original, but with a
* length of 32 m (between x=1 and x=33) and no
* end walls

**************************************************
* RIGID LINKS
**************************************************

* Rigid links according to original, but with a
* length of 32 m (between x=1 and x=33) and no
* end walls


**************************************************
* ANALYSIS
**************************************************
```

E.9 Modified models with concentrated load

Models with concentrated load application instead of distributed over an area. Changes are defined, unchanged variables refer to original models.

Example below: beam grillage model

```
*************************************************
* GEOMETRY
*************************************************

COORDINATES

* Load points
44          0           2.6         0
TO
112         34          2.6         0

* Other geometry according to original model

*************************************************
* MATERIAL
*************************************************

* Material according to original model

*************************************************
* BOUNDARY CONDITIONS
*************************************************

* Boundary conditions according to original model

*************************************************
* LOAD APPLICATION
*************************************************

LOAD FORCE NAME=1 MAGNITUD=1000 FX=0 FY=0,
   FZ=-1

read time_function_point_load.in

APPLY-LOAD BODY=0
1  'FORCE' 1  'POINT' 45 0 1
TO
67  'FORCE' 1  'POINT' 111 0 67

*************************************************
* MESHING
*************************************************

GPOINT NODE=726
44
TO
112

* Other meshing according to original model

*************************************************
* RIGID LINKS
*************************************************

* Between load points and slab
NODESET NAME=3 DESCRIPT='LOAD POINTS' ,
   OPTION=NODE
727
TO
793

NODESET NAME=4,
   DESCRIPT='TRANSVERSAL BEAMS' ,
   OPTION=NODE
293
STEP 4 TO
557

RIGIDLINK NAME=8 SLAVETYP=NODESET,
   SLAVENAM=3 MASTERTY=NODESET,
   MASTERNA=4

* Other rigid links according to original model
```

Appendix F MATLAB command-files

F.1 Sectional forces in the entire cross-section in the combined model

MATLAB-code used in integration of the bending moment and shear force for the entire trough-cross-section in the combined model.

Example shown below: mid-span section

```
% -------------------------------------------------------------------------
% Creates sectional force diagrams for a trough structure made of shell
% and beam elements (combined model)
% -------------------------------------------------------------------------
%
% Load data from text-files indata_beam.txt and indata_slab.txt that
% contains nodal forces results from ADINA for half the section due to
% symmetry. The text files should have the following layout:
%
% indata_beam.txt:
% int_point x-coord shear_force-t bending_moment-s torsional_moment
% normal_force
%
% indata_slab.txt:
% local_node x-coord y-coord nodal_force-x nodal_force-z nodal_moment-y
%
% The data of the text-files should be limited to the studied time step
%
% -------------------------------------------------------------------------
% Created by: Andreas Magnander and Klas Lundin
% Date: 2012-04-17
% Modified by: Anna Werner and Jenny Axelsson
% Date: 2013-05-15
% -------------------------------------------------------------------------

clear all
close all
clc

in_girder=load('indata/sf_girder_span.txt');
in_slab=load('indata/sf_slab_span.txt');

% Integration points per beam element
n_int_b=max(in_girder(:,1));
% Elements in girder
nb=length(in_girder)/n_int_b;

% Local nodes per slab element
n_int_sl=max(in_slab(:,1));
% Division width (only half of the slab) and length for slab
npl_w=3;
npl_l=68;

% Centre of gravity of entire cross-section (from bottom)
zCG=0.471;

% Height of slab
Hpl=0.5;

% Location of girders
zGi=0.65;

% Length of structure
l=34;

% -------------------------------------------------------------------------
% GIRDERS
% -------------------------------------------------------------------------
```

```
girder_left=in_girder(n_int_b:n_int_b:end,[3:4 6]);
girder_right=in_girder(1:n_int_b:end,[3:4 6]);

shear_forces_gi=zeros(2*nb,1);
moments_gi=zeros(2*nb,1);

shear_forces_gi(1:2:end)=girder_right(:,1);
shear_forces_gi(2:2:end)=girder_left(:,1);

moments_gi(1:2:end)=girder_right(:,2)-girder_right(:,3)*(zGi-zCG);
moments_gi(2:2:end)=girder_left(:,2)-girder_left(:,3)*(zGi-zCG);

torsion=zeros(2*nb,1);
torsion(1)=in_girder(1,5);
torsion(end)=in_girder(end,5);
torsion(2:2:end-2)=in_girder(5:5:end-(1*5),5);
torsion(3:2:end-1)=in_girder(6:5:end-(1*5-1),5);

% -------------------------------------------------------------------------
% SLAB
% -------------------------------------------------------------------------

% Nodal forces slab
nodal_forces_slab=zeros(size(in_slab));

% Number of local points for one half slab section
npl_s=2*npl_w;

% Sorting sections
[~,poss]=sort(in_slab);
for i=1:length(in_slab);
   nodal_forces_slab(i,:)=in_slab(poss(i,2),:);
end

% First section
slab_first=nodal_forces_slab(1:npl_s,:);
% Sections in-between first and last
slab_main=nodal_forces_slab(npl_s+1:end-npl_s,:);
% Last section
slab_last=nodal_forces_slab(end-npl_s+1:end,:);

% Left and right section
slab_left=zeros(length(slab_main)/2,6);
slab_right=zeros(length(slab_main)/2,6);

% Section left and right
slab_left(1:6:end)=slab_main(1:12:end);
slab_left(2:6:end)=slab_main(2:12:end);
slab_left(3:6:end)=slab_main(3:12:end);
slab_left(4:6:end)=slab_main(4:12:end);
slab_left(5:6:end)=slab_main(9:12:end);
slab_left(6:6:end)=slab_main(10:12:end);

slab_right(1:6:end)=slab_main(5:12:end);
slab_right(2:6:end)=slab_main(6:12:end);
slab_right(3:6:end)=slab_main(7:12:end);
slab_right(4:6:end)=slab_main(8:12:end);
slab_right(5:6:end)=slab_main(11:12:end);
slab_right(6:6:end)=slab_main(12:12:end);

% Summarise sectional forces in the slab in the considered cross-section.
k=1;
shear_forces_sl=zeros(2*npl_l,1);
moments_sl=zeros(2*npl_l,1);
moments_sl_tot=zeros(2*npl_l,1);
for i=1:npl_s:length(slab_left)
   % Left
   k=k+1;
   shear_forces_sl(k)=sum(slab_left(i:i+npl_s-1,5));
   moments_sl(k)=-sum(slab_left(i:i+npl_s-1,6))...
                 +sum(slab_left(i:i+npl_s-1,4))*(zCG-Hpl/2);
   % Right
   k=k+1;
   shear_forces_sl(k)=-sum(slab_right(i:i+npl_s-1,5));
```

```
   moments_sl(k)=sum(slab_right(i:i+npl_s-1,6))...
                 -sum(slab_right(i:i+npl_s-1,4))*(zCG-Hpl/2);
end

% Adding first and last section
sum_first_sl=sum(slab_first((1:npl_s),5:6));
sum_last_sl=sum(slab_last((1:npl_s),5:6));
shear_forces_sl([1 end],:)=[-sum_first_sl(1); sum_last_sl(1)];
moments_sl([1 end],:)=[sum_first_sl(2); -sum_last_sl(2)];

% Since the input is only for half the section, this will be corrected for
% the slab
shear_forces_sl=2*shear_forces_sl;
moments_sl=2*moments_sl;

% -----------------------------------------------------------------------
% ENTIRE SECTION
% -----------------------------------------------------------------------

% Total sectional forces in entire section (one slab and two girders)
shear_force_tot=shear_forces_sl+2*shear_forces_gi;
moment_tot=moments_sl+2*moments_gi;

% -----------------------------------------------------------------------
% Saving outdata
% -----------------------------------------------------------------------

x=zeros(2*nb,1);
x(2:2:end)=1:(2*nb/2);
x(3:2:end)=1:(2*nb/2-1);

x=x*l/npl_l;

sf_out_combined_span=[x  shear_forces_gi shear_forces_sl shear_force_tot ...
                 moments_gi moments_sl moment_tot torsion];
save outdata/sf_outdata_combined_span.txt -ascii sf_out_combined_span
```

F.2 Influence lines of sectional forces in the slab of the combined model

Example shown below: bending moment

```
% --------------------------------------------------------------------------
% Creates influence lines for a slab made of shell elements (combined model)
% --------------------------------------------------------------------------
%
% Load data from text-files indata_slab_edge.txt and indata_slab_mid.txt
% that contains nodal forces results from ADINA with the following layout:
%
% local_node x-coord y-coord nodal_force-z nodal_moment-x time
%
% The data of the text-files should be limited to the studied nodes at
% x = 24.5, 25 and 25.5
%
% --------------------------------------------------------------------------
% Created by: Anna Werner and Jenny Axelsson
% Date: 2013-03-27
% --------------------------------------------------------------------------

clear all
close all
clc

indata_edge=load('indata/indata_il_slab_mid_span_edge_combined.txt');
indata_mid = load('indata/indata_il_slab_mid_span_mid_combined.txt');

n_node = 3;
h_el = 0.5;
n_time = max(indata_edge(:,6));

%Bending moment-x at edge
M_edge = indata_edge(:,5);
M_mean_edge = zeros(n_time,1);

for i = 1:n_time
       M_mean_edge(i) = -sum(M_edge(1+(i-1)*n_node*2:1+(i-1)*...
           n+5))/(h_el*3);
end

%Bending moment-x at mid-span
M_mid = indata_mid(:,5);
M_mean_mid = zeros(n_time,1);

for i = 1:n_time
    M_mean_mid(i) = -sum(M_mid(1+(i-1)*n_node*2:1+(i-1)*n_node*2+...
        (n_node*2-1)))/(h_el*3);
end

% --------------------------------------------------------------------------
% Saving outdata
% --------------------------------------------------------------------------

x = linspace(0.5,33.5,n_time);

outdata_il_slab_mid_span_combined=[x'  M_mean_edge M_mean_mid];
save outdata/outdata_il_slab_mid_span_combined.txt -ascii ...
    outdata_il_slab_mid_span_combined
```

F.3 Influence lines of sectional forces in the slab of the beam grillage model

Example shown below: bending moment, effective width according to BBK 04

```
% -----------------------------------------------------------------------
% Creates influence lines for a slab made of beam elements(beam grillage model)
% -----------------------------------------------------------------------
% Load data from text-files indata_slab_edge.txt and indata_slab_mid.txt that
% contains sectional forces results from ADINA with the following layout:
%
% int_point x-coord y-coord shear_force-t bending_moment-s time
%
% The data of the text-files should be limited to the studied nodes at x= 24.5, 25
% and 25.5 for the even time steps, i.e. when load is applied onto three transversal
% beams
% -----------------------------------------------------------------------
% Created by: Anna Werner and Jenny Axelsson
% Date: 2013-03-27
% -----------------------------------------------------------------------
clear all
close all
clc

indata_edge=load('indata/indata_il_slab_mid_span_edge_beam_grillage.txt');
indata_mid=load('indata/indata_il_slab_mid_span_mid_beam_grillage.txt');

n_node = 3;
b_eff = 1.84; % BBK 04
n_time = length(indata_edge)/n_node;

%Bending moment-x at edge
M_edge = indata_edge(:,5);
M_mean_edge = zeros(n_time,1);

for i = 1:n_time
       M_mean_edge(i) = sum(M_edge(1+(i-1)*n_node:1+(i-1)*n_node+2))/b_eff;
end

%Bending moment-x at mid-span
M_mid = indata_mid(:,5);
M_mean_mid = zeros(n_time,1);
q = 185;       L_el = 0.675;     M_Eq = q*L_el^2/12;

for i = 1:n_time
    if i < 48
    M_mean_mid(i) = sum(M_mid(1+(i-1)*n_node:1+(i-1)*n_node+2))/b_eff;
    elseif i == 48
        M_mean_mid(i) = (sum(M_mid(1+(i-1)*n_node:1+(i-1)*n_node+2))...
            -0.25*M_Eq/3)/b_eff;
    elseif i == 49
        M_mean_mid(i) = (sum(M_mid(1+(i-1)*n_node:1+(i-1)*n_node+2))...
            -0.75*M_Eq/3)/b_eff;
    elseif i == 50
        M_mean_mid(i) = (sum(M_mid(1+(i-1)*n_node:1+(i-1)*n_node+2))...
            -M_Eq/3)/b_eff;
    elseif i == 51
        M_mean_mid(i) = (sum(M_mid(1+(i-1)*n_node:1+(i-1)*n_node+2))...
            -0.75*M_Eq/3)/b_eff;
    elseif i == 52
        M_mean_mid(i) = (sum(M_mid(1+(i-1)*n_node:1+(i-1)*n_node+2))...
            -0.25*M_Eq/3)/b_eff;
    else
     M_mean_mid(i) = sum(M_mid(1+(i-1)*n_node:1+(i-1)*n_node+2))/b_eff;
    end
end

% Saving outdata
x = linspace(0.5,33.5,n_time);
outdata_il_slab_mid_span_beam_grillage=[x' M_mean_edge M_mean_mid];
save outdata/outdata_il_slab_mid_span_beam_grillage.txt -ascii...
    outdata_il_slab_mid_span_beam_grillage
```

F.4 Envelope diagrams of sectional forces in the slab of the combined model

Example shown below: bending moment

```
% -------------------------------------------------------------------------
% Creates envelope diagrams for a slab made of shell elements (combined
% model)
% -------------------------------------------------------------------------
%
% Load data from text-files indata_slab_edge.txt and indata_slab_mid.txt
% that contains nodal forces results from ADINA with the following layout:
%
% local_node x-coord y-coord nodal_force-z nodal_moment-x time
%
% The data of the text-files should include all nodes at all time steps
%
% -------------------------------------------------------------------------
% Created by: Anna Werner and Jenny Axelsson
% Date: 2013-03-27
% -------------------------------------------------------------------------
clear all
close all
clc

indata_edge=load('indata/indata_env_slab_edge_combined.txt');
indata_mid = load('indata/indata_env_slab_mid_combined.txt');

n_node = 3;
h_el = 0.5;
n_time = max(indata_edge(:,6));

%Bending moment-x at edge
M_edge = indata_edge(:,5);
M_mean_edge = zeros(n_time,1);

for i = 1:n_time
    if i == 1
       M_mean_edge(i) = -1*sum(M_edge(i:i+4))/h_el*3;
    elseif i < n_time
       M_mean_edge(i) = -1*sum(M_edge((n_time*2+4)*(i-1):...
           (n_time*2+4)*(i-1)+5))/b_dist;
    else
       M_mean_edge(i) = -1*sum(M_edge(end-4:end))/h_el*3;
    end
end

%Bending moment-x at mid-span
M_mid = indata_mid(:,5);
M_mean_mid = zeros(n_time,1);

for i = 1:n_time
    if i == 1
       M_mean_mid(i) = -1*sum(M_mid(i:i+4))/h_el*3;
    elseif i < n_time
       M_mean_mid(i) = -1*sum(M_mid((n_time*2+4)*(i-1):...
           (n_time*2+4)*(i-1)+(n_node*2-1)))/h_el*3;
    else
       M_mean_mid(i) = -1*sum(M_mid(end-4:end))/h_el*3;
    end
end

% -------------------------------------------------------------------------
% Saving outdata
% -------------------------------------------------------------------------

x = linspace(0.5,33.5,n_time);
outdata_env_slab_edge_combined=[x'  M_mean_edge M_mean_mid];
save outdata/outdata_env_slab_edge_combined.txt -ascii...
    outdata_env_slab_edge_combined
```

F.5 Envelope diagrams of sectional forces in the slab of the beam grillage model

Example shown below: bending moment, effective width according to BBK 04

```
% -------------------------------------------------------------------------
% Creates envelope diagrams for a slab made of beam elements (beam grillage
% model)
% -------------------------------------------------------------------------
%
% Load data from text-files indata_slab_edge.txt and indata_slab_mid.txt
% that contains nodal forces results from ADINA with the following layout:
%
% int_point x-coord y-coord shear_force-t bending_moment-s time
%
% The data of the text-files should include all nodes at all even time
% steps, i.e. when load is applied onto three transversal beams
%
% -------------------------------------------------------------------------
% Created by: Anna Werner and Jenny Axelsson
% Date: 2013-03-27
% -------------------------------------------------------------------------

clear all
close all
clc

indata_edge=load('indata/indata_env_slab_edge_beam_grillage.txt');
indata_mid = load('indata/indata_env_slab_mid_beam_grillage.txt');

n_el = 69;
n_time = length(indata_edge)/n_el;
b_eff = 1.84;

%Bending moment-x at edge
M_edge = indata_edge(:,5);
M_mean_edge = zeros(n_time,1);

for i = 1:n_time
    M_mean_edge(i) = sum(M_edge(1+(i-1)*(n_el+1):1+(i-1)*(n_el+1)+2))...
        /b_eff;
end

%Bending moment-x at mid-span
M_mid = indata_mid(:,5);
M_mean_mid = zeros(n_time,1);
q = 185;
L_el = 0.675;
M_Eq = q*L_el^2/12;

for i = 1:n_time
    M_mean_mid(i) = (sum(M_mid(1+(i-1)*(n_el+1):1+(i-1)*(n_el+1)+2))...
        -M_Eq/3)/b_eff;
end

% -------------------------------------------------------------------------
% Saving outdata
% -------------------------------------------------------------------------

x = linspace(0.5,33.5,n_time);

outdata_env_slab_edge_beam_grillage=[x'  M_mean_edge M_mean_mid];
save outdata/outdata_env_slab_edge_beam_grillage.txt -ascii...
    outdata_env_slab_edge_beam_grillage
```

F.6 Rotational stiffness diagrams

Example shown below: beam grillage model

```
% ------------------------------------------------------------------------
% Creates envelope diagrams for a girder made of beam elements (beam
% grillage model)
% ------------------------------------------------------------------------
%
% Load data from text-files indata_girder.txt that contains sectional
% forces results from ADINA with the following layout:
%
% int_point torsional_moment 1-rotation x-coord y-coord time
%
% ------------------------------------------------------------------------
% Created by: Anna Werner and Jenny Axelsson
% Date: 2013-04-05
% ------------------------------------------------------------------------

clear all
close all
clc

indata_girder=load('indata/indata_env_applied_torque_beam_grillage.txt');

n_el = 68;
n_int = max(indata_girder(:,1));       % Number of integration points
n_time = length(indata_girder)/(n_el*n_int);

T = 1000;

%Rotation around x
x_rot = indata_girder(:,3);
x_rot_env = zeros(n_time,1);

for i = 1:n_time
    if i == 1
        x_rot_env(i) = x_rot(i);
    elseif i < n_time
        x_rot_env(i) = sum(x_rot((i-1)*n_int*n_time:(i-1)*5*n_time+1))/2;
    else
        x_rot_env(i) = x_rot(end);
    end
end

% Rotational stiffness
EI_rot_env = zeros(n_time,1);

for i = 1:n_time
    EI_rot_env(i) = abs(T/x_rot_env(i));
end

% ------------------------------------------------------------------------
% Saving outdata
% ------------------------------------------------------------------------

x = linspace(0,34,n_time);

outdata_env_applied_torque_beam_grillage=[x' x_rot_env EI_rot_env];
save outdata/outdata_env_applied_torque_beam_grillage.txt -ascii...
    outdata_env_applied_torque_beam_grillage
```